Thesis reference number: XXXXX

University of Science and Technology of Hanoi

Doctoral School

Identifying PIK3CA, ESR1 gene mutations and their relationship with clinical outcome of breast cancer.

Dinh Thi Thao

Pharmacological, Medical and Agronomical Biotechnology

The thesis has been successfully defended in October 2025 in front of jury composed of:

Prof. Nguyen Huy Hoang, Institute of Biology, VAST, Chairman

Prof. Pascal RIHET, University of Aix Marseille, France, Reviewer

Assoc. Prof.Nguyen Thi Xuan, Institute of Biology, VAST, Reviewer

Dr. Duong Quoc Chinh, NIHBT, Reviewer

Assoc. Prof. Bui Khac Cuong, 108 Military Central Hospital, Member

Dr. Nguyen Thi Trang Huyen, USTH, Member

Dr. Nguyen Cam Linh, USTH, Member, Secretary

Hanoi, October 5th 2025

Thesis reference number: XXXXX

University of Science and Technology of Hanoi

Doctoral School

Identifying PIK3CA, ESR1 gene mutations and their relationship with clinical outcome of breast cancer.

Dinh Thi Thao

Pharmacological, Medical and Agronomical Biotechnology

The thesis has been defended in 2025 in front of jury composed of:

Prof. Nguyen Huy Hoang, Institute of Biology, VAST, Chairman

Prof. Pascal RIHET, University of Aix Marseille, France, Reviewer

Assoc. Prof.Nguyen Thi Xuan, Institute of Biology, VAST, Reviewer

Dr. Duong Quoc Chinh, NIHBT, Reviewer

Assoc. Prof. Bui Khac Cuong, 108 Military Central Hospital, Member

Dr. Nguyen Thi Trang Huyen, USTH, Member

Dr. Nguyen Cam Linh, USTH, Member, Secretary

Hanoi, October 5th 2025

Approval of supervisor(s) and co-supervisor(s):

1. Dr. Ngo Tat Trung, 108 Military Central Hospital, Hanoi

2. Assoc. Prof. Dong Van Quyen, Institute of Biology, VAST

KEYWORDS

Asymmetric PCR

Breast cancer

Cell-free DNA

Circulating tumor DNA

ESR1 mutations

Endocrine therapy

Endocrine therapy resistance

PIK3CA mutations

Liquid biopsies

Declaration

I hereby declare that the present thesis is my own work and that all the contents contained therein are my own original work unless otherwise explicitly indicated in the text. Moreover, affirm that I have not submitted this work for any other degree or professional qualification, except as specified. This declaration serves as a solemn confirmation of the authenticity and originality of the present thesis.

Ph.D. student

Dinh Thi Thao

Dedication

This dissertation is dedicated to my parents, my parents-in-law and my husband (Nguyen Van Nam). I owe my deepest gratitude to the support from my family.

Acknowledgments

I would like to express my deepest appreciation to my supervisors, Dr. Ngo Tat Trung and Assoc. Prof. Dong Van Quyen, for their tremendous support and guidance throughout the dissertation research.

I am incredibly grateful to Prof. Le Huu Song, Assoc. Prof. Hoang Van Tong and other members of Vietnamese-German Center for Medical Research (VGCARE) laboratory – 108 Military Center Hospital (108 MCH). I will never forget the invaluable suggestions in research and life offered by the lab members.

I would like to extend my sincere thanks to my committee members for their generous advice and guidance.

I would also thank to all members of the Center for Genetic Consultation and Cancer Screening – 108 MCH.

I would like to extend my appreciation to Assoc. Prof. Ly Tuan Khai and all other members of the Department of Hematology – 108 MCH.

I would thank to Dr Ngo Thi Minh Hanh and all other members of the Department of Pathology - Laboratory Center - 108 MCH.

I am grateful for the financial support provided by the Vingroup Innovation Foundation (VINIF), Vietnam.

Abstract

Breast cancer (BC) is the most frequently diagnosed malignancy and a major cause of cancer-related mortality among women. Approximately 70% of BCs are hormone receptor–positive (HR+), for which endocrine therapy (ET) remains the standard of care. However, about one-third of HR+ tumors exhibit primary resistance, and most eventually acquire resistance, leading to disease progression or relapse. Activating mutations in the *PIK3CA* and *ESR1* genes are recognized as key mechanisms underlying endocrine resistance. Consequently, the development of sensitive and clinically applicable assays for detecting these mutations through minimally invasive plasma testing is of considerable importance.

The *PIK3CA* gene encodes the catalytic subunit p110α of phosphatidylinositol 3-kinase (PI3K), a critical regulator of cell growth and survival. Hotspot mutations at E545K and H1047R activate the PI3K/AKT/mTOR pathway and are present in 30–50% of BCs, particularly within HR+ subtypes. Meanwhile, mutations in the *ESR1* gene, especially within the ligand-binding domain (LBD), result in ligand-independent activation of the estrogen receptor and are associated with acquired resistance to aromatase inhibitors (AIs). Common *ESR1* variants, including Y537S, Y537N, and D538G, arise in 20–40% of metastatic BCs after prolonged AI exposure.

This study aimed (1) to develop clinically relevant assays for deep identification of *PIK3CA* and *ESR1* hotspot mutations and (2) to evaluate the association between detected blood-circulating mutations and clinical presentation in BC patients. To achieve these goals, novel asymmetric real-time PCR assays were optimized using mutant-specific primers and wild-type blocking oligonucleotides to enhance detection sensitivity. The assays achieved a detection limit of 0.01–0.1% mutant allele frequency for both genes.

Plasma cell-free DNA (cfDNA) samples from 196 BC patients and 20 healthy controls were analyzed. Overall, 42.9% of all recruited patients carried

blood-circulating *PIK3CA* hotspot mutations. In the HR-positive early breast cancer (EBC) subgroup (n = 66), 19/66 (28.8%) had a *PIK3CA* mutation, 5/66 (7.6%) had an *ESR1* mutation, and 6/66 (9.1%) harbored co-mutations. Among HR-positive advanced breast cancer (ABC) patients (n = 82), 17/82 (20.7%) had a *PIK3CA* mutation, 21/82 (25.6%) had an *ESR1* mutation, and 28/82 (34.1%) carried both mutations. *PIK3CA* mutations were more frequent in patients with multiple metastatic sites—particularly those involving the lung, bone, or brain—and in cases with prior radiotherapy ($p < 0.05$). The *PIK3CA* E545K variant predominated in HR+ tumors with lung or bone metastases, whereas H1047R was more common in HER2-positive or brain-metastasized cases. Patients harboring *PIK3CA* or *ESR1* mutations exhibited shorter progression-free survival (PFS) than wild-type carriers ($p < 0.05$).

Overall, *PIK3CA* and *ESR1* alterations were associated with advanced disease stage, prior endocrine therapy, and less favorable outcomes. The coexistence of both mutations correlated with the poorest PFS, suggesting a possible additive effect on resistance mechanisms.

In conclusion, the newly developed asymmetric PCR assays demonstrated high analytical sensitivity and reliable performance for detecting *PIK3CA* and *ESR1* hotspot mutations from plasma cfDNA. The approach provides a practical and cost-effective tool for molecular profiling of HR+ BC and may complement existing methods for monitoring therapeutic response and resistance. Further prospective studies with larger, paired plasma–tumor cohorts are warranted to confirm the clinical relevance of these findings.

Tóm tắt

Ung thư vú (UTV) là bệnh ác tính phổ biến nhất và là một trong những nguyên nhân hàng đầu gây tử vong do ung thư ở phụ nữ. Khoảng 70% các trường hợp UTV là thể dương tính với thụ thể nội tiết (HR+), trong đó liệu pháp nội tiết (ET) được xem là phương pháp điều trị tiêu chuẩn. Tuy nhiên, khoảng một phần ba khối u HR+ biểu hiện kháng ET nguyên phát, và phần lớn các trường hợp còn lại xuất hiện kháng thuốc mắc phải trong quá trình điều trị, dẫn đến tiến triển hoặc tái phát bệnh. Trong đó, các đột biến hoạt hóa trên gen *PIK3CA* và *ESR1* được xác định là cơ chế phân tử quan trọng góp phần gây kháng thuốc. Việc phát hiện chính xác và kịp thời các đột biến này bằng những kỹ thuật nhạy, không xâm lấn có ý nghĩa lớn trong cá thể hóa điều trị và theo dõi đáp ứng của người bệnh.

Gen *PIK3CA* mã hóa tiểu đơn vị xúc tác p110α của enzym phosphatidylinositol 3-kinase (PI3K) – thành phần trung tâm điều hòa sự tăng sinh và sống sót của tế bào. Các đột biến điểm nóng tại vị trí E545K và H1047R làm hoạt hóa trục tín hiệu PI3K/AKT/mTOR, xuất hiện trong khoảng 30–50% trường hợp UTV, đặc biệt ở nhóm HR+. Bên cạnh đó, gen *ESR1* mã hóa thụ thể estrogen α; các đột biến tại vùng liên kết phối tử (ligand-binding domain, LBD) như Y537S, Y537N và D538G có thể gây hoạt hóa thụ thể độc lập với phối tử, dẫn đến kháng thuốc ức chế aromatase (AI) và tái phát ở giai đoạn di căn. Các đột biến *ESR1* này được ghi nhận xuất hiện ở khoảng 20–40% bệnh nhân UTV di căn đã điều trị AI kéo dài.

Nghiên cứu được tiến hành với hai mục tiêu: (1) phát triển các xét nghiệm PCR có độ nhạy cao nhằm phát hiện các đột biến điểm nóng của gen *PIK3CA* và *ESR1*; và (2) đánh giá mối liên quan giữa các đột biến lưu hành trong máu với đặc điểm lâm sàng của bệnh nhân UTV. Nhóm nghiên cứu đã tối ưu hóa kỹ thuật real-time PCR bất đối xứng, sử dụng mồi đặc hiệu alen kết hợp với đoạn oligonucleotide chặn trình tự kiểu dại, cho phép phát hiện đột biến ở mức tần suất thấp (0,01–0,1%) với độ chính xác cao.

Tổng cộng 196 mẫu huyết tương của bệnh nhân UTV và 20 mẫu đối chứng khỏe mạnh được phân tích. Kết quả cho thấy 42,9% bệnh nhân mang đột biến *PIK3CA* lưu hành trong máu. Ở nhóm HR+ giai đoạn sớm (EBC, n = 66), có 19 bệnh nhân (28,8%) mang đột biến *PIK3CA*, 5 bệnh nhân (7,6%) mang đột biến *ESR1*, và 6 bệnh nhân (9,1%) đồng mang cả hai đột biến. Trong nhóm HR+ giai đoạn tiến triển (ABC, n = 82), tỷ lệ tương ứng là 17 (20,7%), 21 (25,6%) và 28 trường hợp (34,1%). Đột biến *PIK3CA* xuất hiện thường xuyên hơn ở những bệnh nhân có nhiều vị trí di căn, đặc biệt tại phổi, xương và não, cũng như ở nhóm đã điều trị xạ trị ($p < 0,05$). Biến thể *PIK3CA* E545K phổ biến trong các trường hợp HR+ di căn phổi hoặc xương, trong khi H1047R thường gặp hơn ở thể HER2+ hoặc có di căn não. Các bệnh nhân mang đột biến *PIK3CA* E545K hoặc *ESR1* có thời gian sống không tiến triển (PFS) ngắn hơn so với nhóm không mang đột biến tương ứng ($p < 0,05$).

Nhìn chung, sự hiện diện của các đột biến *PIK3CA* và *ESR1* liên quan chặt chẽ đến giai đoạn bệnh tiến triển, tiền sử điều trị nội tiết và tiên lượng xấu hơn. Đáng chú ý, nhóm bệnh nhân đồng mang cả hai đột biến có thời gian PFS ngắn nhất, gợi ý khả năng tương tác cộng hưởng giữa hai cơ chế kháng thuốc.

Các kết quả trên cho thấy xét nghiệm real-time PCR bất đối xứng được phát triển trong nghiên cứu có độ nhạy và độ đặc hiệu cao, đồng thời có tiềm năng ứng dụng trong phát hiện các đột biến *PIK3CA* và *ESR1* từ cfDNA huyết tương. Phương pháp này có thể được xem như một công cụ hỗ trợ hữu ích cho việc theo dõi điều trị và quản lý bệnh nhân ung thư vú HR+. Tuy nhiên, các nghiên cứu tiến cứu với cỡ mẫu lớn hơn và có ghép cặp mẫu huyết tương – mô khối u vẫn cần được tiến hành để xác nhận thêm giá trị lâm sàng của các phát hiện này.

Table of Contents

List of Figures

List of Tables

Abbreviations

AJCC	American Joint Committee on Cancer
ASCO	College of American Pathologists
ASM	Asymmetric PCR
AI	Aromatase inhibitor
AKT	Protein kinase B
AS-PCR	Allele-specific amplification
ARMS-PCR	Amplification-refractory mutation system PCR
BC	Breast cancer
BRAF	B-Raf Proto-Oncogene, Serine/Threonine Kinase
cfDNA	Circulating cell-free DNA
ctDNA	Circulating tumor DNA
CDK	Cyclin-dependent kinase
CoA	Coactivator
COLD-PCR	Co-amplification at lower denaturation temperature
cfRNA	Circulating cell-free RNA
CTC	Circulating tumor cells
CNVs	Copy number variations
ddPCR	Droplet digital PCR
DFS	Disease-free survival
DRFS	Distant recurrence-free survival
ER	Estrogen receptor
EBC	Early breast cancer
ET	Endocrine therapy
ESR1	Estrogen receptor 1
ERE	Estrogen response elements
ERK	Extracellular signal-regulated kinase
EGFR	Epidermal growth factor receptor
EVs	Extracellular vesicles
FGFRs	Fibroblast growth factor receptors
FBS	Fetal bovine serum
PR	Progrestion receptor
HR	Hormone receptor
HER2	Human epidermal growth factor receptor 2
MBC	Metastatic breast cancer
MAPK	Mitogen-activated protein kinase
MAF	Mutant allele frequency
MRD	Minimal residual disease
PFS	Progression free survival

PIK3CA	Phosphatidylinositol 4,5-bisphosphate 3-kinase catalytic subunit alpha isoform
PCR	Polymerase chain reaction
OS	Overall survival
NCCN	National Comprehensive Cancer Network
NSCLC	Non-small cell lung cancer
NGS	Next generation sequencing
SERDs	Selective estrogen receptor degraders
SERMs	Selective estrogen receptor modulators
TTP	Time to progression
TNBC	Triple negative breast cancer
TEPs	Tumor-educated platelets
LBD	Ligand binding domain
LNA	Locked nucleic acid
LB	Liquid biopsy
IGF1R	Insulin-like growth factor-1 receptor
KRAS	Kirsten rat sarcoma virus
JAK2	Janus kinase 2
PNA	Peptide-nucleic-acid
WGS	Whole-genome sequencing
WES	Whole exome sequencing
ROR	Risk-of-relapse
gDNA	Genomic deoxyribonucleic acid
IHC	Immunohistochemical
SNV	Single-nucleotide variants

List of publications

1. Thao DT, Thanh NP, Quyen DV, Khai LT, Song LH, Trung NT. (2024) Identification of breast cancer-associated *PIK3CA* H1047R mutation in blood circulation using an asymmetric PCR assay. PLOS ONE 19(8): e0309209. https://doi.org/10.1371/journal.pone.0309209

2. Thao DT, Thanh NP, Quyen DV, Khai LT, Song LH, Trung NT. (2023). Investigation of exon20 *PIK3CA* gene mutation in plasma of hormone receptor positive breast cancer patients. Vietnam Medical Journal, 532(2). https://doi.org/10.51298/vmj.v532i2.7408.

3. Thao DT, Quyen DV, Khai LT, Song LH, Trung NT. Novel asymmetric real-time PCR assays for direct identification of *ESR1* mutations from periphery blood of breast cancer patients (manuscript).

4. **Thao DT**, Quyen DV, Khai LT, Song LH, Trung NT. Subtype-specific prognostic implications of plasma-detected *PIK3CA* mutations in Vietnamese breast cancer patients (accepted).

Chapter 1: Overview of cell-free DNA analysis and the clinical relevance of *PIK3CA* and *ESR1* mutations in breast cancer (Literature review)

1.1 Background

1.1.1 Breast cancer treatment

Globally, one of the most prevalent malignancies in women to be diagnosed is breast cancer (BC) [1]. In 2022, BC accounted for 23.8% of all new cases of cancer diagnosed in women [2]. Over 15% of female BC cases lead to death, making BC the leading cause of cancer-related mortality in women [2].

Histopathologic parameters that are established for pathology are used to diagnose BC. With invasive ductal carcinoma accounting for 50%-75% of cases, invasive lobular carcinoma follows with 5%-15% of cases [3]. The remaining patients have mixed ductal/lobular carcinomas and other less prevalent Histologies [3]. BC is a heterogeneous disease that is molecularly categorized by the expression of specific hormone receptors, as well as the overexpression of human epidermal growth factor receptor 2 (HER2) [4]. BC is commonly classified into four main subtypes: HER2, Luminal-A, Luminal-B, and Basal-like [4].

- Luminal-A, the most prevalent BC subtype, is defined by positivity for both estrogen receptor (ER+) and progesterone receptor (PR+).
- Luminal-B, is ER+ and PR+, just like LumA, however it differs from the latter due to its elevated expression of markers associated with proliferation, namely Ki67.
- HER2 BC is classified by the overexpression of the tyrosine kinase family HER2 receptor or overexpression of the *ERBB2* gene.
- Basal-like BC is classified as triple-negative (negative for PR, ER, and HER2 receptors).

Approximately 70% of invasive BC cells express estrogen receptor alpha (ERα), a transcription factor and steroid hormone receptor that triggers oncogenic growth pathways in BC cells when activated by estrogen [5].

Another indicator of ERα signaling is the expression of the closely related steroid hormone progesterone receptor (PR). According to American Society of Clinical Oncology/College of American Pathologists (ASCO/CAP) guidelines, hormone receptor positive (HR+) tumors are classified as those in which at least 1% of the tumor cells express either the ER or PR by Immunohistochemical (IHC) analysis [6]. Out of the four subtypes, the LumA subtype had the best prognosis [7]. The transmembrane receptor tyrosine kinase known as epidermal growth factor 2 (ERBB2, HER2, or HER2/neu), which is overexpressed or amplified in about 20% of BC cases and is connected to a poor prognosis in the absence of systemic therapy. Three molecular targets-ER, PR, and HER2-are not expressed in triple-negative breast cancers (TNBC), which account for 15% of all breast malignancies. In the first three to five years after diagnosis, TNBC patients are at a significant risk of experiencing a distant relapse [7].

BC is further classified based on its grade and stage. The stages for invasive BC recommended by the American Joint Committee on Cancer (AJCC) are stages I–III (non-metastatic) and stage IV (metastatic) [8]. Elston-Ellis grading system, which takes into account the tubule count, nuclear pleomorphism, and mitotic count, is used for pathological classification in BC grading [9].

Due to the heterogeneity of BC, the National Comprehensive Cancer Network (NCCN) guidelines recommend that medications and treatments will inevitably become more focused in order to address the subtype, stage, and grade of the disease [10].

* *Non-metastatic BC treatment [10]*

The primary objectives of treatment for non-metastatic BC are tumor elimination from the breast and the nearby lymph nodes as well as prevention of metastatic relapse. Surgical resection, axillary lymph node sampling or removal, and postoperative radiation therapy are the components of local therapy for non-metastatic BC. Systemic therapy can be taken either preoperative (neoadjuvant), postoperative (adjuvant), or in combination. The standard systemic therapy

provided depends on the subtype of BC and includes endocrine therapy (ET) to downregulate ER signaling for all HR+ tumors (with some patients requiring chemotherapy as well), *ERBB2*-targeted therapy, including anti-*ERBB2* antibodies (such as trastuzumab and pertuzumab) and small-molecule tyrosine kinase inhibitors (such as lapatinib and neratinib), plus chemotherapy for all HER2+ tumors (with endocrine therapy given in addition, if concurrent HR+), and chemotherapy alone for TNBC.

* *Metastatic BC treatment [10]*

Stage IV cancers have spread (metastasized) beyond the breast and nearby lymph nodes to other parts of the body (bones, liver, lungs, brain or other organs). The treatment objectives for metastatic BC (MBC) are life extension and symptom relief. For almost all affected individuals, MBC is still incurable at this time. For MBC, the same fundamental categories of systemic therapy—hormone therapy, chemotherapy, targeted therapy, and immunotherapy—are employed. Local therapy modalities (surgery and radiation) are typically used for palliation only in metastatic disease. Stage IV BC treatment options are determined by the cancer's HER2 status, HR status, and certain gene alterations that may allow for the use of targeted therapy.

Treatment for HR+ malignancies initially consists of ET (tamoxifen or aromatase inhibitors), which may thereafter be using exemestane go along with a targeted drug everolimus. If the initial ET shows ineffective, other options include selective estrogen receptor degraders (SERDs) like fulvestrant or elacestrant (if the cancer has a *ESR1* gene mutation), sometimes along with a targeted drug known as a CDK4/6 inhibitor. If the cancer cells show specific gene (*PIK3CA, AKT*, or *PTEN*) changes, fulvestrant is combined with either an AKT inhibitor (capivasertib) or a PI3K inhibitor (alpelisib).

Women with HER2+ BC are treated with trastuzumab and pertuzumab in addition to chemotherapy. Other alternatives, if the disease spreads, could be a kinase inhibitor combined with a chemotherapy or anti-HER2 therapy, or an

antibody-drug combination. If the tumor is also HR+, hormone therapy may be added to these therapeutic combinations.

Patients with advanced TNBC whose tumor produces the PD-L1 protein may get immunotherapy in addition to chemotherapy. The PARP inhibitors, such as olaparib or talazoparib, may be taken into consideration for women with TNBC with a *BRCA* mutation. Immune Checkpoint Inhibitors such as pembrolizumab might be an option for TNBC that has high levels of gene changes called microsatellite instability (MSI) or changes in any of the mismatch repair (MMR) genes (*MLH1, MSH2, MSH6*, or *PMS2*). Chemotherapy alone or the antibody-drug combination sacituzumab govitecan may be an option for TNBC without any specific gene or protein alterations.

1.1.2 Mechanism of Endocrine therapy resistance in breast cancer

The ER itself is a ligand-dependent transcription factor that is activated by the steroid hormone estrogen and promotes proliferation through genomic and non-genomic mechanisms [11]. The ligand-bound ER complex associates with DNA at estrogen response elements (ERE), generally recruiting coactivators in the process, and serves to mediate transcription of ER-controlled genes [11]. Among a myriad of functions, these genes induce production of growth factors such as transforming growth factor alpha (TGFα) and insulin-like growth factor-1 (IGF1), regulate the expression of membrane receptor tyrosine kinases (RTKs) that promote cell survival, and increase cyclin D1 and MYC expression which drive cell cycle progression [12]. Collectively, these functions can enhance pathologic breast cancer development when dysregulated. In response to estrogen, cytoplasm- and membrane-associated ER also stimulates growth signaling directly, which is considered to be a non-genomic mechanism of regulation [11]. ER interaction with growth factor-dependent RTKs, such as HER2, epidermal growth factor receptor (EGFR) and insulin-like growth factor-1 receptor (IGF1R), as well as other signaling molecules such as SRC kinase, activates downstream mitogen-activated protein kinase (MAPK) and

phosphoinositide 3-kinase (PI3K)/AKT oncogenic signal transduction pathways [13]. The MAPK and PI3K/AKT pathways are well characterized in cancer and play a role in tumor proliferation, invasive potential, and drug resistance [14].

ER+ BC are perfect candidates for ET including three types of agents: selective estrogen receptor modulators (SERMs), estrogen synthesis inhibitors (aromatase inhibitors-AI) and selective estrogen receptor down-regulators (SERDs). The main goal of endocrine targeted therapy is to remove the endogenous activating ligands of the estrogen receptors. SERMs, such as tamoxifen competitively bind the ER on cancer cells, preventing estrogen attachment, and have tissue-dependent antagonist or agonist properties. They potentiate an anti-estrogenic effect in breast tumors and prevent hormone-dependent proliferation [15]. SERM-bound ER binds ERE and downregulates transcriptional activity in breast tumors by associating with co-repressors [11]. SERDs, such as fulvestrant, both antagonize ER transcriptional activity and promote its degradation [16]. These agents bind ER causing immobilization and instability of the ER-SERD complex and facilitate ER degradation by the ubiquitin-proteasome pathway [17]. More recent research suggests that SERDs exert an effect by slowing ER nuclear translocation, increasing ER turnover as a consequence of limited intracellular mobility [18]. In addition, SERD-bound ER undergoes conformational changes that reduce transcription of ER-modulated genes [18]. Aromatase, the target of AI, is responsible for the conversion of androgens to estrogens in peripheral tissues and plays a key role in ER functions. In cases of BC, abnormally elevated levels of aromatase can be associated with local production of estrogens [19]. AI were developed in response to these findings, with the goal of treating ER+ BC patients by blocking the synthesis of estrogens, reducing their levels by more than 90% in postmenopausal women [19, 20].

Around 75% of patients with breast cancer have tumors expressing estrogen receptor α (ER) and are offered adjuvant endocrine therapy for 5–10 years, which reduces the risk of recurrence by almost 50% and the mortality by up to 30% [21].

However, *de novo* and acquired resistance appear in all cases of MBC and in approximately 25% of ER+ BC patients, limiting the efficiency of the treatment used to target the ER [22, 23]. Although the exact mechanisms that lead to endocrine resistance have not been identified, there are several theories revealing that altered expression and/or modification of several growth factor receptors and downstream signaling molecules correlate with ET resistance [12, 22].

Endocrine resistance can be broadly subdivided into two categories including ER-mediated and ER-independent signaling, shown in Figure 1.

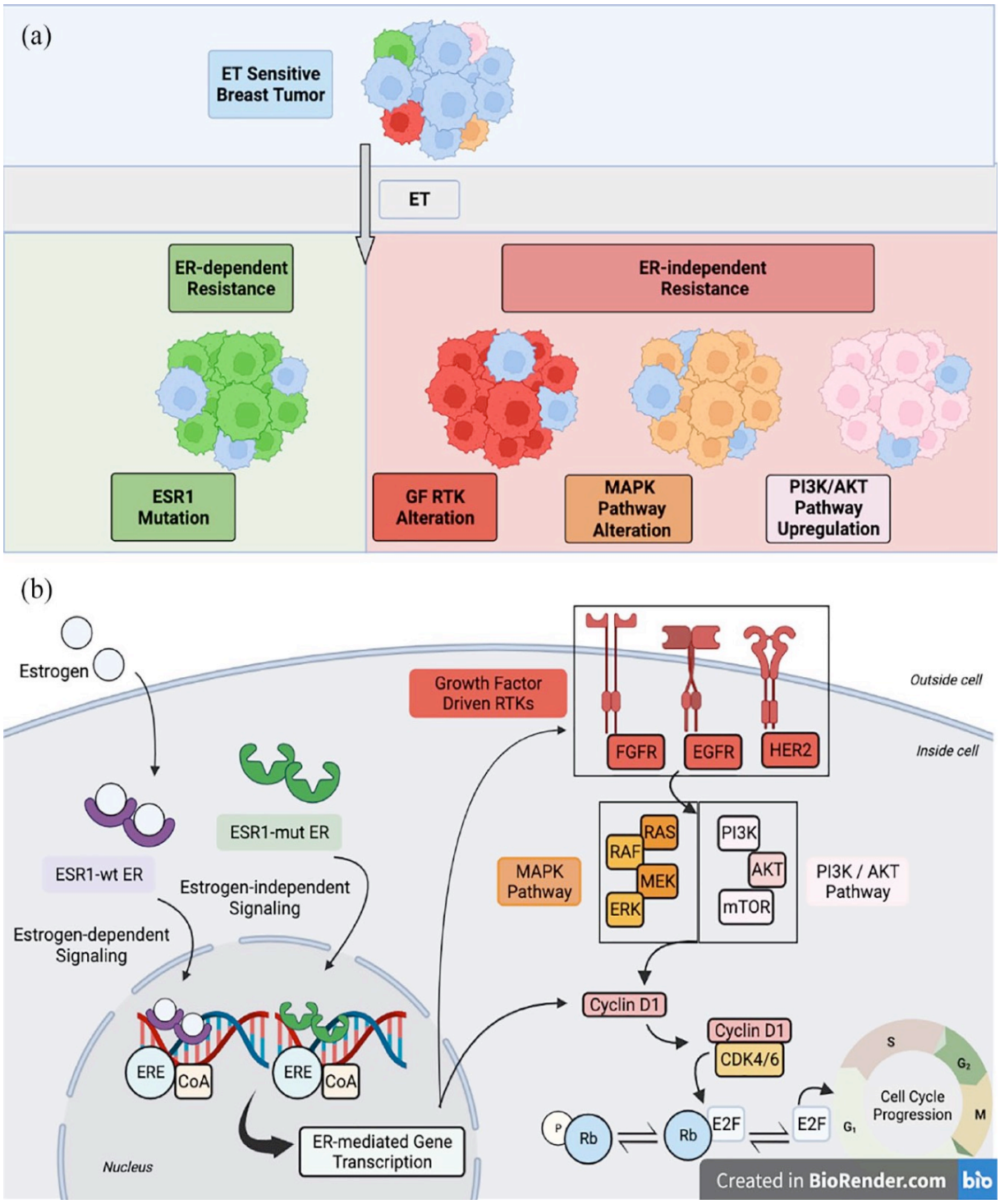

Figure 1. Drivers of ET resistance can be broadly subdivided into two categories of (i) ER-dependent and (ii) ER-independent mechanisms [56]. (a) Ligand binding domain Estrogen Receptor 1 (*ESR1*) mutations mediate ligand-independent ER signaling and promote ET resistance via constitutive ER activity, upregulated coactivator binding, and stability against proteolytic degradation; ER remains a viable therapeutic target in these tumors. ER-independent resistance

may be mediated by several mechanisms including mutations or amplifications in growth factor-driven RTKs (HER2, EGFR, and FGFR), alterations in MAPK pathway components including *KRAS, BRAF, MAP2K1*, and *NF1*, and upregulation in PI3K/AKT pathway signaling, though notably, *PIK3CA* and *AKT* mutations have not been shown to provoke resistance in the clinical setting. These alterations serve to upregulate mitogenic and survival signaling and promote cell cycle progression and drug resistance. (b) At the cellular level, depicted are select pathways implicated in response and resistance to ET in *ESR1*-mut and ESR1-wt metastatic breast cancer. Note, while ER-dependent and ER independent pathways are largely depicted separately for conceptualization, there is considerable intracellular crosstalk between these pathways. Purple factors are involved in estrogen-dependent signaling. Green factors facilitate estrogen-independent, ER-mediated signaling. Red, orange, and pink factors engage in ER crosstalk, and dysregulation in mitogenic signaling pathway components can contribute to ER-independent tumor growth and SERD resistance. AKT, protein kinase B; CDK, cyclin-dependent kinase; CoA, coactivator; EGFR, epidermal growth factor receptor; ER, estrogen receptor; ERE, estrogen response element; ERK, extracellular signal-regulated kinase; ESR1-mut, *ESR1* mutant; ESR1-wt, *ESR1* wild-type; ET, endocrine therapy; FGFR, fibroblast growth factor receptor; GF RTK, growth factor-driven receptor tyrosine kinase; HER2, human epidermal growth factor receptor 2; MAPK, mitogen-activated protein kinase; MEK, meiotic chromosome-axis-associated kinase; mTOR, mammalian target of rapamycin; *p*, phosphate; PI3K, phosphoinositide 3-kinase; Rb, retinoblastoma; SERD, selective estrogen receptor degrader.

1.1.2.1 ER-dependent resistance

*** ERα, ERβ, and receptor co-regulatory proteins**

Expression of ERα has long been considered the primary determinant of a clinical response to endocrine or antiestrogen therapy. The DNA binding domain of full-length ERβ1 shares 96% identity with that of ERα, and although the

affinity of this receptor for estrogen is similar to that of ERα, the response to antagonists like tamoxifen and fulvestrant is often different. Both receptors can modulate transcription, either directly from estrogen response elements (EREs), or indirectly through tethering to AP-1 and Sp1 binding sites [24]. However, although ERα perceives tamoxifen and fulvestrant as antagonists, it has been shown that ERβ can utilize these compounds as agonists when associated with AP-1 and Sp1 sites [25, 26]. The transcriptional activities of ERα, ERβ, and other steroid hormone receptors are modulated by coregulatory proteins in either a positive or negative fashion. The association of coactivators and corepressors with ER is regulated by conformational changes induced by ligand binding, with estrogen inducing coactivator recruitment and antiestrogens leading to association with corepressors [27-29].

*** ERα expression and downregulation**

In human breast tumors, the vast majority of ERα-negative tumors exhibit *de novo* or intrinsic resistance to tamoxifen and other antiestrogens; however, small numbers of ERα-negative but PR+ tumors respond to antiestrogen treatment [30]. One possible explanation for this finding is that PR+ tumors retain a functional ERα signaling pathway, particularly since expression of PR is an estrogen-regulated event, and that ERα is present in these tumors at levels that are below the limit of detection for ligand-binding or immunohistochemical assays. The importance of PR as a marker of antiestrogen response is substantiated by studies showing that 70% of ERα+/PR+ tumors effectively respond to tamoxifen, while only 34% of ERα+/PR- patients respond to tamoxifen therapy [31].

In the context of *de novo* antiestrogen resistance displayed by ERα-negative BC cells, several studies suggest that it may be possible to restore tamoxifen sensitivity through reexpression of ERα. Epigenetic silencing of the ER due to hypermethylation of the promoter region has been reported both *in vitro* and *in vivo* [32, 33].

Moreover, loss of ERα has been reported in a few models of acquired resistance to tamoxifen [34]. Loss or downregulation of ERα has the potential be

a viable mechanism for antiestrogen resistance in the context of acquired resistance to fulvestrant or other SERDs, but current evidence to this effect is contradictory [35, 36]. Clinical studies confirm that fulvestrant can reduce ERα levels following either 21 days or 6 months treatments, but that expression is not completely eliminated. Interestingly, patients who do not show a clinical response to fulvestrant treatment also do not show a decrease in ER expression [37].

*** ERα mutation**

Mutated ER can provoke estrogen-independent ER activity and mediate resistance to estrogen deprivation [38]. Activating mutations in the ligand binding domain (LBD) of *ESR1*, the gene that codes for ERα, are rare in primary BC but represent a commonly acquired mechanism of endocrine resistance in ER+ MBC [39].

There are several implicated mechanisms by which *ESR1*-mutant (*ESR1*-mut) ER mediates resistance to ET. Activating *ESR1* mutations affect the LBD and stabilize an active receptor conformation [40, 41]. This promotes binding of coactivators and upregulates ER signal transduction in the absence of estrogen [40, 41]. Biochemical changes at the LBD of *ESR1*-mut confer a decreased affinity for ligands, including SERMs and SERDs, and greater stability against proteolytic degradation [39-41]. Activity of *ESR1*-mut has neomorphic and hypermorphic regulatory effects as well, enhancing the transcription of genes not activated by *ESR1* wild-type (*ESR1*-wt) ER that promote a pro-metastatic phenotype [42, 43].

1.1.2.2. ER-independent resistance

Mutations and amplifications in oncogenic pathway components can drive ET resistance through upregulated mitogenic and survival pathway signaling. Laboratory and clinical data suggest that alterations in *RTK*s, *HER2* [44, 45], *EGFR* [46], and *fibroblast growth factor receptors* (*FGFR*s) [47], provoke ET resistance by facilitating downstream growth signaling. Similar resistance is seen with loss-of-function mutations in the tumor suppressor *NF1*, leading to uncontrolled RAS activity [48]. Activating alterations in other MAPK

components *KRAS, BRAF*, and *MAP2K1* have been demonstrated in pre- and post-treatment matched tumor samples that acquired ET resistance [48].

PI3K acts to phosphorylate proteins and lipid molecules and are overactive in a large proportion of BC [49]. PI3K triggers downstream activation of *AKT* (also known as protein kinase B) and mTOR, thus forming the PI3K/AKT/mTOR signaling pathway leading to cell growth, metabolism, proliferation, and survival [50, 51]. Alterations in *PIK3CA, AKT*, and *PTEN* are often observed in ER+ MBC [52]. The dysregulation of this pathway initiates bidirectional crosstalk and subsequent modulation of the ER to continue ER-dependent growth [12]. Moreover, activating mutations in *AKT* phosphorylates CDK4/6 and CDK2 inhibitors p21 and p27, moving them away from their cyclin/CDK targets and further promoting cell cycle progression [53, 54]. Loss of *PTEN* results in increased PI3K activity and may lead to clinical resistance to endocrine therapy and has been associated with shorter relapse-free survival following tamoxifen treatment [55]. Eventually these pathways will begin to act as ER-independent drivers of growth, thus leading to endocrine resistance.

Overall, intracellular communication between these pathways is important in the development of resistance and is exploitable therapeutically. Even in endocrine-resistant BC, the ER remains a promising target. This has led to considerable interest in novel ET, particularly those that will be active despite *ESR1* mutations [56].

1.1.3 PIK3CA mutation and its role in breast cancer

PI3K/AKT/mTOR signaling is involved in important physiological and pathophysiological functions that drive tumor progression such as metabolism, cell growth, proliferation, angiogenesis and metastasis [57, 58]. The PI3K/AKT/mTOR pathway is activated via point mutation of the *PIK3CA* gene or inactivation of the phosphatase (*AKT*) and tensin homolog (*PTEN*) gene [59]. Activation of this pathway occurs in approximately 30–50% human cancers and results in resistance to various anti-cancer therapies [12, 60-62].

Phosphatidylinositol 3-kinase is composed of an 85 kDa regulatory subunit and a 110 kDa catalytic subunit. The protein encoded by this gene represents the catalytic subunit, which uses ATP to phosphorylate PtdIns, PtdIns4P and PtdIns(4,5)P2 [63]. The 85-kD subunit lacks PI3-kinase activity and acts as an adaptor, coupling the 110-kD subunit (p110) to activated protein tyrosine kinases. The *PIK3CA* gene provides instructions for making the p110 alpha (p110α) protein, which is one piece (subunit) of an enzyme called phosphatidylinositol 3-kinase (PI3K). *PIK3CA* is a 34 kb gene located on chromosome 3q26. 3 that consists of 20 exons coding for 1068 amino acids yielding a 124 kDa size protein [63]. Like other kinases, PI3K adds a cluster of oxygen and phosphorus atoms (a phosphate group) to other proteins through a process called phosphorylation. PI3K phosphorylates certain signaling molecules, which triggers a series of additional reactions that transmit chemical signals within cells. PI3K signaling is important for many cell activities, including cell growth and division (proliferation), movement (migration) of cells, production of new proteins, transport of materials within cells, and cell survival [63]. Studies suggested that PI3K signaling may be involved in the regulation of several hormones and may play a role in the maturation of fat cells (adipocytes) [63].

The PI3K/AKT/mTOR pathway hyperactivation occurs mainly due to oncogenic mutations in phosphatidylinositol-4,5-bisphosphate 3-kinase catalytic subunit alpha or *PIK3CA* gene encoding the p110a catalytic subunit of the PI3Kα heterodimeric protein complex, observed in approximately 20%-40% of BC patients [64]. Although *PIK3CA* mutations can be detected across the entire coding sequence of the gene, 80% of the mutations are found in 3 major hotspot clusters in the helical domain (p.Glu542Lys and p.Glu545Lys in exon 9), and in the kinase domain (p.His1047Tyr in exon 20) (Table 1) [65-74].

Table 1. Prevalence of *PIK3CA* mutations in breast cancer

Publication	Sample	*PIK3CA* positive cases	*PIK3CA* variants (%)	Method
Julien Corné et al (2021) [66]	Plasma	74/123 HR+/HER2− metastatic BC	H1047R (27/74, 36.49%)	Droplet digital PCR
			E545K (25/74, 33.78%)	
			E542K (7/74, 9.46%)	
			H1047L (6/74, 8.11%)	
			C420R (3/74, 4.05%)	
			N345K (2/74, 2.70%)	
			Q546K (2/74, 2.70%)	
			Q546P (1/74, 1.35%)	
			Q546R (1/74, 1.35%)	
Alexandre Harlé et al (2013) [67]	Tissue	23/102 BC	H1047R (10/23, 43.5%)	An amplification refractory mutation system (ARMS-PCR) using allele-specific scorpion primers
			E545K (3/23, 13%)	
			E542K (6/23, 26.1%)	
			H1047L (4/23, 17.4%)	
Ruth E. Board et al (2008) [68]	Tissue	19/49 BC	H1047R (15/19, 78.9%)	An amplification refractory mutation system (ARMS) PCR
			E545K (3/19, 15.8%)	
			H1047L (1/19, 5.3%)	
Chiya Oshiro et al (2015) [69]	Serum	25/110 primary BC	H1047R (21/25, 84%)	Digital PCR
			E545K (3/25, 12%)	
			E542K (1/25, 4%)	
Leva Keraite et al (2020) [70]	Tissue	7/25 BC	H1047R (4/7, 57%)	The nuclease-assisted minor-allele enrichment PCR assay with overlapping probes
			E545K (1/7, 14.3%)	
			E542K (1/7, 14.3%)	
			H1047L (1/7, 14.3%)	
Kristin Reinhardt et al (2022) [65]	Tissue	300/1123 Non - metastatic BC	H1047R (174/300, 58%)	Real-time PCR
			E545K (85/300, 28%)	
			E542K (43/300, 14%)	
Zongbi Yi et al (2019) [71]	Plasma	10/120 metastatic BC	H1047R (6/10, 60%)	Real-time PCR
			H1047L (1/10, 10%)	
			H1047Y (1/10, 10%)	
			N345K (1/10, 10%)	
			E545K (1/10, 10%)	

Publication	Sample	*PIK3CA* positive cases	*PIK3CA* variants (%)	Method
Christoph Suppan et al (2022) [72]	Plasma	44/93 HR+/HER2− metastatic BC	H1047R (32.6%)	SiMSen-Seq
			E545K (7.5%)	
			E542K (9.7%)	
Chunni Fan et al (2019) [73]	Tissue	117/286 BC	H1047R/L (75/117, 64%)	Ion Torrent sequencing
			E545K (23/117, 19.6%)	
			E542K (13/117, 11.1%)	
			C420R (1/117, 0.8%)	
			E545G (1/117, 0.8%)	
			E545D (2/117, 1.7%)	
			Q546K (1/117, 0.8%)	
			Q546R (1/117, 0.8%)	
Takashi Takeshita et al (2015) [74]	Plasma	12/49 BC	H1047R (7/12, 58%)	Droplet digital PCR
			E542K (7/12, 58%)	
			E545K (0/12, 0%)	

ER+: estrogen receptor positive, HER2 -: human epidermal growth factor receptor-2 negative

The hotspot mutation such as *PIK3CA* E545K in exon 9 in the helical PI3K homology domain that suppresses inhibition of p110α by p85 regulatory subunit. Another mutation is *PIK3CA* H1047R present in the catalytic subunit in exon 20 which enhances the interaction of p110α with the lipid membrane [75, 76]. The *PIK3CA* E542K is another crucial PI3K mutation with significant oncogenic potential associated with elevated *in vitro* catalytic activity [63]. The helical and kinase mutations in p110α domain induce oncogenic activity based on different interaction between the PI3K regulatory subunit, p85 with RAS-GTP. The oncogenic activity induced by helical domain mutations is independent of binding to p85 subunit, requires interaction with RAS-GTP. However, the kinase domain mutations are active without RAS-GTP binding but dependent on their interaction with p85. In addition, co-existence of both the domain mutations increases the p110 function and tumorigenic activity synergistically [77].

The incidence of the *PIK3CA* mutations was reported to be higher in HR+/HER2- tumors compared to HER2-enriched or TNBC [78-80], and it was observed in patients carrying multiple variants of the *PIK3CA* gene [81]. The results obtained from 10,319 BC patients in a meta-analysis where *PIK3CA* mutations were present in 32% of patients and were increased with age, lower grade, and smaller size [80]. Li SY. et al. analyzed 250 primary breast tumors and detected that 35% of *PIK3CA* mutations were located in exon 9 and exon 20 which were associated with larger tumors and a significantly worse survival rate, especially in ER+/HER2- [82]. A total of 15–20% of BC cases present a HER2 overexpression associated with aggressive clinical behavior [83].

PIK3CA mutation*s* act as a prognostic biomarker and are associated with improved survival outcomes in patients with early-stage HR+/HER2− breast cancer [80]. In contrast, while the frequency of *PIK3CA* mutation*s* does not differ significantly between early stage and metastatic HR+/HER2− BC, patients with metastatic *PIK3CA* mutation*s* disease have been shown to have a poorer outcome and resistance to chemotherapy compared with *PIK3CA* wild-type tumors [84]. In the case of HER2+ BC, *PIK3CA* mutations seem to be associated with worse prognosis, either in the advanced and in the early setting [85, 86].

Beyond its high prevalence in BC, *PIK3CA* mutations exert variant-specific effects on tumor progression and clinical behavior. Helical-domain mutations such as E542K and E545K disrupt inhibitory interactions with the p85 regulatory subunit and promote RAS-dependent PI3K activation, whereas kinase-domain mutations such as H1047R enhance lipid–membrane association and drive strong, RAS-independent signaling through the PI3K/Akt/mTOR pathway [63, 75, 76]. Several clinical studies have suggested that these mechanistic differences may translate into distinct patterns of disease evolution, with exon 9 mutations being more frequently linked to earlier recurrence and less favorable outcomes, and exon 20 mutations associated with more invasive phenotypes or treatment resistance in specific subgroups [80, 82, 231, 235]. Taken together, these data

indicate that *PIK3CA* is not a uniform marker, but rather a family of functionally heterogeneous hotspot variants that can differentially influence tumor growth, metastatic potential, and response to systemic therapies.

Inhibition of PI3K/Akt/mTOR pathway has provided clinically meaningful improved outcomes, mostly in patients with HR + /HER2- metastatic disease who have developed endocrine resistance [87, 88]. Studies have shown that patients with *PIK3CA* mutations tend to have increased activation of PI3K pathway and may have increased sensitivity to PI3K inhibitors [89]. Based on randomized evidence showing significant progression-free and numerical clinically meaningful overall survival benefit when the oral PI3Kα-selective inhibitor alpelisib is combined with fulvestrant in patients with *PIK3CA*-mutated HR + /HER2- advanced or metastatic BC who progressed during or after endocrine therapy, this treatment combination has been approved from regulatory authoritie [90, 91].

Capivasertib/fulvestrant was recently assessed in the phase 3 CAPItello-291 investigation, demonstrating a markedly increased progression-free survival (PFS) for patients with changes in *PIK3CA/AKT1/PTEN* [92]. The FDA approved capivasertib in combination with fulvestrant for patients with HR+/HER2- locally advanced or MBC with one or more *PIK3CA/AKT1/PTEN* alterations and who had either a recurrence on or within 12 months of adjuvant therapy completion, or disease progression after treatment with at least one endocrine-based regimen in the metastatic setting.

Hence, PI3K/AKT inhibitor therapy candidates can be determined in part by using screening to identify *PIK3CA* mutations. The recommended testing employs breast tumor tissue and/or circulating tumor DNA taken from plasma specimens for BC patients with ET resistance [10]. The results have been identified by a PCR test reporting *PIK3CA* hotspot mutations, which are mainly observed in exon 9 (E542K, E545A, E545D, E545G, E545K, Q546E) and exon 20 (H1047L, H1047R, and H1047Y) [78]. It highlights the need of looking for

PIK3CA mutations in blood samples for the purpose of managing BC patients, including follow-up and personalized treatment. With a limit of detection ranging from 0.1% to 5% for the mutant allele fraction, the reported PCR-based methods were created to identify *PIK3CA* point mutations that are insufficient for ultra-low level ctDNA analysis [67, 68, 93-95].

1.1.4 ESR1 mutation and its role in breast cancer

Estrogen Receptor 1 gene (*ESR1*) encodes an estrogen receptor and ligand-activated transcription factor. The gene is more than 140 kb long. It contains 8 exons, and is located on chromosone 6q25.1-q25.2. The canonical protein contains an N-terminal ligand-independent transactivation domain, a central DNA binding domain, a hinge domain, and a C-terminal ligand-dependent transactivation domain [96]. The protein localizes to the nucleus where it may form either a homodimer or a heterodimer with estrogen receptor 2. The protein encoded by this gene regulates the transcription of many estrogen-inducible genes that play a role in growth, metabolism, sexual development, gestation, and other reproductive functions and is expressed in many non-reproductive tissues. The receptor encoded by this gene plays a key role in breast cancer, endometrial cancer, and osteoporosis [96]. This gene is reported to have dozens of transcript variants due to the use of alternate promoters and alternative splicing, however, the full-length nature of many of these variants remain uncertain [96]. The ERα is found in endometrium, BC cells, ovarian stromal cells, and hypothalamus. ERα is over-expressed in around 70% of BC cases. Two hypotheses have been proposed to explain why this causes tumorigenesis, and the available evidence suggests that both mechanisms contribute: (1) binding of estrogen to the ER stimulates proliferation of mammary cells, with the resulting increase in cell division and DNA replication leading to mutations; (2) estrogen metabolism produces genotoxic waste [96]. The result of both processes is disruption of cell cycle, apoptosis and DNA repair which increases the chance of tumor formation. ERα is certainly associated with more differentiated tumors, while evidence that ERβ is

involved is controversial. Different versions of the *ESR1* gene have been identified and are associated with different risks of developing breast cancer [96].

Although using ET can lower primary BC mortality by up to 40%, patients frequently become resistant to treatment, which increases the chance of metastasis and recurrence [23]. Moreover, the availability of multiple combination options for treatment, MBC-related drug resistance and eventual death continue to be a challenge. Numerous findings of *ESR1* missense mutations in BC samples have indicated that these changes have crucial role in ET resistance as well as disease progression in a significant number of MBC patients [97].

The *ESR1* mutations have been shown through *in vitro* experiments to produce a constitutively activated ER that is ligand-independent, which promotes proliferation and reduces sensitivity to ET [41]. *ESR1* mutations are constitutively active and unaffected by AI reduction of estrogen, in contrast to *ESR1* wild-type, which are bound by estrogen ligand to facilitate coactivator recruitment [39, 40, 98, 99]. Compared to *ESR1* wild-type, *ESR1* mutations exhibit enhanced stability of the active conformation, heightened binding to coactivators, and reduced proteolytic degradation in the absence of ligand [40, 98, 100, 101]. Hence, *ESR1* mutations require higher concentrations of tamoxifen and fulvestrant to suppress transactivation activity and cell proliferation, as their binding affinity can be lowered as much as 40 times (depending on the specific mutant variant) [39-41, 98, 99, 101-104].

The majority of *ESR1* mutations were found in the ligand-binding domain region (LBD); the most prevalent ones are D538G and Y537S; other variants include Y537N, Y537C, L536H, L536P, L536R, S463P, and E380Q (Table 2) [41, 105-109]. Polyclonal *ESR1* mutations were prominent (20–70%) [98, 107, 108]. Contributing to these common resistance mechanisms of *ESR1* mutations are differences specific for certain sub-clones and circumstances. Among the *ESR1* sub-clones, Y537S was identified as the one that most likely promoted the resistance to fulvestrant, tamoxifen [40, 41, 98, 99, 110]. On the other hand, D538G is more likely to metastasize, especially to the liver [99].

The frequency of these mutations varies from 6–55% in metastatic ET-resistant BC patients (Table 2), while they are seldom seen (0–3%) in primary cancers [39, 97-99, 105, 109, 111-113]. The hypothesis that mutant clones are selected over treatment duration is supported by the finding that metastatic patients treated with numerous lines of ET had a larger abundance of *ESR1* mutations (20–55%) compared to early metastatic patients (1-2%) [39, 97, 110, 114].

Table 2. Prevalence of *ESR1* hotspot mutations in metastatic breast cancer

Publication	Sample	*ESR1* positive cases	*ESR1* variants	Method
Jeselsohn et al. 2014 [39]	FFPE tissue	9/76 (12%) ER+ /HER2− MBC	E380Q, Y537N, Y537C, Y537S, D538G	Targeted NGS
Robinson et al. 2013 [41]	Blood and Tissue	6/11 (54%) ER+ MBC	L536Q, Y537S, Y537C, Y537N, D538G	Whole-exome NGS
Toy et al. 2013 [98]	FFPE tissue	84/616 (13.6%) HR+ MBC	Y537S, Y537N, Y537D, Y537C, V534E, V478L, V418E, S463P, S432L, S329Y, N532K, L536R, L536P, L536H, L466Q, G442R, G344D, F461V, E542G, E380Q, D538G, A546D	Targeted NGS (MSKIMPACT assay)
Schiavon et al. 2015 [97]	Plasma	HR+ ABC 16/44 (36.4%)	L536R, Y537C, Y537N, Y537S, D538G	Multiplex ddPCR
Clatot et al. 2020 [115]	Plasma	HR+ MBC 22/70 (31.4%)	D538G, Y537S, Y537N, Y537C, E380Q, S463P, L536R	ddPCR
Franken et al. 2020 [116]	Tissue	ER+ MBC 13/46 (28%)	G160C, K252R, N348S, E380Q, D426E, L507F, Y537C, Y537N, D538G, D541Q	Single-cell whole-genome sequencing
Zundelevich et al. 2020 [109]	FFPE tissue	5/41 (12%) newly diagnosed MBC 5/28 (18%), advanced MBC, 15/41 (36%) local recurrence	D538G, Y537C, Y537S	Targeted sequencing or ddPCR
Jeannot et al. 2020 [117]	Plasma	HR+/HER2− MBC 11/42 (26%)	E380Q, L536H, D538G, Y537N, Y537S, Y537C	Multiplex ddPCR

Publication	Sample	*ESR1* positive cases	*ESR1* variants	Method
Turner et al. 2020 [118]	Plasma	HR+ MBC 115/383 (30%)	D538G, Y537S, Y537N, Y537C, L536R, S463P, E380Q	Multiplex ddPCR
Spoerke et al. 2016 [105]	Plasma	ER+ MBC 57/153 (37%)	E380Q, S463P, P535H, L536Q, L536R, L536H, L536P, Y537C, Y537N, Y537S, D538G	ddPCR
Turner et al. 2020 [119]	Plasma	ABC 222/1051 (21%)	Y537S, D538G, E380Q	ddPCR and Targeted NGS
O'Leary et al. 2018 [120]	Plasma	ER+/HER2- MBC 49/195 (25.1%) pretreatment 61/195 (31.3%) posttreatment	Q75E, E380Q, S463P, L536H, L536I, L536P, L536R, L536V, Y537C, Y537N, Y537S, D538G, T553S	ddPCR
Lok et al. 2019 [121]	Plasma	ER+/HER2− MBC 10/33 (30%)	D538G, S463P, I514V, Y537C, E380Q, Y537S	ddPCR
Moore et al. 2020 [122]	FFPE tissue	ER+ MBC 89/338 (26%)	D538G, Y537S, Y537N, Y537C, E380Q, L469V, L536H, L536P	Targeted NGS

ER+: estrogen receptor positive, HER2-: human epidermal growth factor receptor-2 negative; MBC: metastatic breast cancer; ABC: advanced breast cancer
ddPCR: droplet digital PCR; NGS: next generation sequencing

ESR1 mutations are infrequent in primary and early BC but can be detected in approximately 1–7% of patients with recurrent disease following aromatase inhibitor (AI) therapy. Their prevalence increases substantially in the metastatic setting, where *ESR1* mutations are observed in about 20–40% of AI-treated metastatic breast cancer (MBC) patients, suggesting that these mutations are typically acquired and enriched under prolonged endocrine selective pressure [39, 97, 98, 113, 123, 124]. In other observation, all *ESR1* mutations were observed in advanced metastatic patients previously treated with both TAM and AI. Nonetheless, newly diagnosed metastatic individuals who had undergone TAM-monotherapy exhibited the majority of the *ESR1* mutations. Compared to *ESR1*-wild-type tumors, *ESR1*-mutant carriers' progression-free survival (PFS), disease-free survival (DFS), and distant recurrence-free survival (DRFS) were

significantly shorter [109]. Moreover, *ESR1* mutations in circulating tumor DNA were a more accurate indicator of how patients would respond with AI treatment than cancer antigen measurements or total amounts of cell-free DNA [115]. A nearly 5 times increase in the likelihood of progression at 3 months was observed in *ESR1*-mutant MBC patients, indicating that *ESR1* mutations can identify patients at a higher risk for AI resistance [115]. These studies suggest that not only do AIs enhance *ESR1* mutant acquisition in MBC, but *ESR1*-mutant patients also exhibit worse outcomes with AI therapy.

ESR1 ligand-binding–domain mutations represent a functionally diverse group of alterations that differentially shape endocrine resistance and metastatic behavior. Although all major hotspot variants promote ligand-independent activation of the estrogen receptor, experimental models and clinical observations have shown that they do so with varying strength and functional consequences. In particular, Y537S stabilizes the receptor in an agonist-like conformation and confers the most pronounced resistance to multiple endocrine agents, including tamoxifen and fulvestrant, often requiring higher drug exposure to achieve partial inhibition [39, 98–100, 102]. By contrast, D538G is consistently associated with enhanced proliferative and metastatic capacity, including a greater propensity for dissemination to visceral and bone sites, and induces a distinct ER-driven transcriptional program linked to tumor progression [99, 102, 109]. These findings highlight that *ESR1*-mutant BC comprises a spectrum of biologically distinct subclones, in which individual variants such as Y537S and D538G may confer different risks of progression and treatment failure, with important implications for mutation-specific monitoring and therapeutic tailoring [97, 113, 115].

Though, the preclinical study indicated that *ESR1*-mutant cells require significantly higher concentrations of SERDs than *ESR1*-wild-type cells to reduce ER activity [98], the role of *ESR1* mutations in therapeutic resistance to SERDs is controversial. *ESR1* mutation rate was considerably higher in fulvestrant-

treated patients who had a shorter PFS (0/6 vs. 6/10; Fisher's exact P = 0.03) [125]. While baseline *ESR1* mutation status may not predict the fulvestrant plus CDK4/6 inhibitor palbociclib therapy response, circulating *ESR1* mutation detection is intended to identify patients who are at risk of earlier disease progression [117]. Nonetheless, PFS for fulvestrant treatment has not been found to differ between *ESR1* mutant and WT patients in clinical trials [118, 119]. Regardless of mutational status, therapeutic resistance to fulvestrant that results in disease progression is still a significant problem for MBC, indicating the need for new SERDs and efficient combination therapies.

To improve the therapeutic response, the use of a CDK4/6 inhibitor in combination with first- or second-line ET is now recommended for MBC patients [10]. The current recommended ET for MBC is an AI in combination with one of three CDK4/6 inhibitors: ribociclib (MONALEESA-2) [126], palbociclib (PALOMA-2) [127] or abemaciclib (MONARCH-3) [128]. Each of these CDK4/6 inhibitors has been associated with improved PFS over an AI alone in women with ER+ advanced BC [126-128]. The use of these CDK4/6 inhibitors with fulvestrant is also more effective than fulvestrant alone in advanced BC [129-131].

Several targeted therapy candidates for MBC treatment have been investigated for the emergence of *ESR1* mutations and therapeutic efficacy, such as elacestrant (RAD1901), amcenestrant (SAR439859), camizestrant (AZD9833), giredestrant (GDC-9545), imlunestrant (LY3484356),...[56]. Among these, the oral SERDs elacestrant promotes ER turnover and interferes with downstream signaling by specifically blocking ER [132]. *In vitro* models of CDK4/6i resistance as well as ET-resistant BC cells and patient-derived xenograft (PDX) models expressing *ESR1* mutations [132, 133] show dose-dependent antitumor activity; efficacy is maintained in all of these models [134]. In the multicenter phase III EMERALD study, elacestrant demonstrated a significant and clinically meaningful improvement over fulvestrant or AI in *ESR1*-mutated ER+/HER2-MBC patients following progression on 1–2 prior

lines of ET (fulvestrant or AI) and prior exposure to a CDK4/6i [135], leading it the first FDA-approved oral SERDs [10].

It emphasizes how crucial it is to check for *ESR1* mutations in tissue or blood samples in order to manage BC patients, including follow-up and adjustments to treatment strategies. Certain PCR-based techniques were developed with rapid and straightforward steps that could identify 0.1% to 0.5% of *ESR1* mutations from a background of wild-type DNA [136-138]. However, because of a low prevalence of detectable mutations - which is even less than 0.1% of the total amount of available cfDNA from patient blood samples [139, 140] - the analytical sensitivity is unsatisfied with the requirements for detecting plasma circulating *ESR1* mutations.

1.2 The analysis of cell-free DNA from blood

1.2.1 Liquid biopsies

Solid biopsies are considered the gold standard for cancer management in oncology because they offer data on the histology of tumors and typical biomarkers for subtyping, prognosis, and strategizing treatment. However, they currently exhibit a number of drawbacks, such as a biopsy can only reveal a limited amount of molecular and genetic information about the tumor within the biopsy site due to the tumor heterogeneity or even between several metastatic sites [141]. Furthermore, tumor evolution must be considered when making therapy options. For this reason, repeated tissue biopsies provide molecular instantaneous images of the disease that would be ideal for guiding therapy. However, they require an invasive procedure, which makes them inconvenient and usually impossible [141]. Therefore, it is necessary to investigate novel strategies in order to overcome the aforementioned shortcomings.

The reasons given support the establishment of substitute strategies that can provide patients less invasive sampling procedures while yet yielding the same information as traditional methods. Liquid biopsy (LB), a minimally invasive method of analyzing bodily fluids like blood, can reveal insight about the entire

tumor's characteristics. Therefore, LB overcomes the challenges of acquired resistance and tumor heterogeneity by enabling surveillance of the BC individual and offering the potential of personalized BC management [141]. These days, LB makes it possible to gather and examine a wide range of circulating substances that are actively produced into the circulation by tumor cells, necrosis, or apoptosis [142]. This complex bodily fluid contains a variety of analytes known as the circulome, which can be further classified into extracellular vesicles (EVs), circulating cell-free RNA (cfRNA), tumor-educated platelets (TEPs), circulating cell-free DNA (cfDNA), circulating tumor cells (CTCs), and a wide range of proteins and metabolites, among other analytes [142, 143].

1.2.2 Circulating cell-free DNA

The term "circulating cell-free DNA" describes the massive DNA fragmentation that all human body cells release into the circulation [142]. Cell-free DNA (cfDNA) mostly originates from hematopoietic, non-neoplastic cells undergoing apoptotic cell death. The release of cfDNA can also occur through necrosis, other cell death processes, and active secretion [142]. Since cfDNA is mostly obtained from dying cells, it serves as a marker of cellular turnover. A portion of the cfDNA that originates from the tumor (ctDNA) in cancer patients is attributed to their increased cellular turnover. While the biological context and lifestyle factors—such as stress, chronic inflammation, physical activity, nutrition, and smoking—had a significant impact on the concentration of cfDNA, there has been increasing evidence over time that the amount of cfDNA and the mutant allele fraction were directly associated with tumor progression [144]. Research has demonstrated that the blood of cancer patients contained more cfDNA than that of healthy individuals, and the difference was considerably more pronounced in patients with metastatic tumors [144].

Stroun et al. extracted and described cfDNA from cancer patients in 1987 [145]. These authors demonstrated that cfDNA was double-stranded at that time and measured between 0.5 and 21 kb following the separation of the original

nucleoprotein complex, indicating that cfDNA of cancer origin is smaller than genomic DNA [144, 145]. Since then, it has been believed that cfDNA is composed of DNA fragments. The little fraction of cfDNA in the circulation that is made up of ctDNA which are short DNA fragments with a size range of 180-200 bp [144]. Its half-life is short, ranging from 15 minutes to approximately 2.5 hours. Two years later, Stroun et al. discovered some characteristics of the cfDNA of cancer origin, demonstrating that the double-stranded DNA of tumor origin is less stable than that from cells that are not tumors. It has been discovered that the amount of cfDNA in the circulation compartment increases with tumor cell number increase. More elevated amounts are found in blood from advanced and metastatic cancer patients than in early-stage cancer patients. Higher levels of cfDNA (5–1500 ng/mL) found in cancer patients as compared to healthy individuals (1–5 ng/mL) result from the release of cfDNA both by malignant and non-malignant cells since the germline cfDNA level deriving from normal cells stays constant [144]. Therefore, elevated cfDNA levels may account for the tumor burden. It is reasonable to postulate that the total mutant cfDNA concentration accounts for the cfDNA deriving from malignant cells. Thus, examination of the mutational load or the proportion of the mutant cfDNA within the total amount of cfDNA, first observed by Mouliere et al. and subsequently in various studies, demonstrated that their respective amount varies greatly (from 0.003 to 95 %), highlighting a strong interindividual heterogeneity [127, 130]. Thus, the length and concentration of the ctDNA fragment have potential as an indicator for cancer prognosis, diagnosis, and prediction [141].

Information on point mutations, copy number variations, loss of heterozygosity, structural rearrangements, gene fusions, methylation alterations, integrated viral sequences linked to the tumor, and other genomic signatures can be found in the ctDNA [146]. The ctDNA-derived information has already served to detect cancer, to monitor treatment response, therapeutic resistance, minimal residual disease after primary treatments, and/or risk-of-relapse determination for

many different solid tumors, for example, colorectal, endometrial, ovarian, breast, non-small cell lung cancer, oropharyngeal, pancreatic, prostate cancers, and melanoma [141, 146]. Currently, the ctDNA analyses is the preferred biomarker for mutation-targeted therapy. However, the extremely low amount of extractable cfDNA would not allow the extended use of liquid biopsy for downstream genetics analysis in clinical settings. A great number of technologies with excellent analytical sensitivity and accuracy have been developed to detect ctDNA, and numerous research have been conducted to explore the potential role of this biomarker [141, 146, 147].

1.2.3 Preanalytical variables effecting cell-free DNA analysis

1.2.3.1 Biological and physiological variables

Numerous physiological and biological factors can affect the cfDNA properties of biospecimens prior to collection. Significant variations exist both within and between individuals, and these characteristics are frequently related to one another [148]. A multitude of biological and physiological factors, such as age and gender differences, dietary habits, psychophysical states like obesity, physiological processes like pregnancy, infection, pathological diseases like cancer and inflammation, therapy, and surgery, are among the possible biological and physiological factors that could impact cfDNA characteristics [149-157].

As an illustration, consider cfDNA origin mechanisms and cfDNA in cancer. Apoptosis-related cfDNA fragments typically have a length of 160–180 bp or 360 bp [158]. On the other hand, necrotic cell cfDNA fragments are typically larger than 10,000 bp [159]. Furthermore, extracellular vesicles containing cfDNA fragments ranging in size from 150 to 6,000 bp can be actively secreted by living cells [160].

1.2.3.2 Blood collection

Studies indicate that plasma is preferred for cfDNA analysis because it mitigates the impact of genomic DNA (gDNA) generated by cell lysis on cfDNA purity and concentration [161]. Over time, cfDNA in plasma has shown to be

more stable, despite multiple studies reporting larger cfDNA quantities in serum than in plasma due to DNA breakdown and contamination of gDNA from white blood cells [162-164]. It is preferable to collect blood using collection tubes with greater performance. The quality and integrity of cfDNA can be impacted by anticoagulants, which are essential parts of blood collection tubes [165]. Due to its ability to inhibit DNase and provide superior preservation effects over heparin or citrate for delayed blood processing, EDTA tubes became known as the accepted standard for cfDNA analysis [166, 167].

Research indicates that the best plasma samples for ctDNA analysis are those that are extracted in EDTA tubes and processed in less than six hours [168]. These collection tubes might not effectively preserve samples, nevertheless, if blood processing is delayed because of long-distance transportation or unexpected circumstances. Blood is now frequently collected for cfDNA analysis using a variety of specialized collection tubes with unique characteristics. Within three days, these developed tubes preserve the quality of cfDNA samples just as well; but, beyond seven days, their storage effects seem to vary slightly [168].

1.2.3.3 Centrifugation

Centrifugation is the main method used to process whole blood samples in order to isolate cellular components and prevent gDNA from contaminating cfDNA [161]. Sample contamination may occur as a result of the variables that affect these processes, including centrifugal force, temperature, the number of centrifugations, and the centrifugation period. These days, an effective technique for separating plasma fractions without cells during blood processing consists of a lower centrifugation step first, then a higher centrifugation step later [169]. A slow centrifugal force, mainly between 380 to 3,000 ×g for 10 min, is employed in the first centrifugation step to separate a lot of cell components [170]. During the second stage of centrifugation, debris and remnants of cells are often removed by applying a stronger centrifugal force, typically between 12,000 and 20,000 ×g

for 10 minutes [171]. Usually, these centrifugation processes are done at room temperature or 4°C [158, 172].

1.2.3.4 Storage conditions

Most of the drawn blood samples were frozen at -80°C until DNA was extracted after centrifugation. After the plasma samples were centrifuged and left at room temperature for different durations, ranging from 0 to 4 hours, the concentration of cfDNA increased slightly [173]. Another study found that when centrifuged plasma was kept at −20°C for three months, cfDNA gradually fragmented [174]. Only nine months can be spent at -80°C for samples intended for quantitative analysis, but up to ten years can be spent at this temperature for plasma used to identify certain DNA sequences [175]. Because polypropylene tubes absorb less DNA, it is advised to store cfDNA in them before freezing [176]. No more than three freeze-thaw cycles should be performed on extracted cfDNA after freezing [177]. DNA deterioration is accelerated by more freeze-thaw cycles, with larger DNA fragments deteriorating more quickly [178].

1.2.3.5 Extraction methods

The precision and dependability of the outcomes of subsequent analyses depend on the effective extraction of cfDNA. Unfortunately, too little or too much fragmentation of the extracted cfDNA can result in poor analytical results or unsuccessful applications. One of the main concerns for researchers has been how to properly and economically extract cfDNA from samples. Many techniques have been used to extract cfDNA, including improved (methods for separating cfDNA primarily based on chromatographic columns or magnetic beads), novel (methods for separating cfDNA using new technologies or materials), and conventional (liquid-phase-based or solid-phase-based DNA isolation methods) [150, 179, 180].

Innovative technologies based on spin columns or magnetic particles are currently the most widely used techniques in specialized commercial kits for the extraction of cfDNA. Based on a spin column, the most stable kit was the Qiagen QIAamp circulating nucleic acid kit [181]. Yet, there is a major flaw with the kits:

the extraction and purification processes lose some short DNA fragments, which lowers the yield of cfDNA [182]. In contrast to silica membrane-based kits, magnetic particle-based kits for cfDNA isolation offer a greater recovery rate for short cfDNA fragments (50–250 bp) [148, 158].

1.2.4 Technologies for DNA mutation detection in liquid biopsies

Over the years, several methods have been developed with the goal of studying the genomic profile of tumors. Since ctDNA represents a limited portion of the total cell-free DNA (cfDNA), and ctDNA/cfDNA ratio strongly depends on tumor stage, histological type, and tissue of origin, making the analysis of ctDNA challenging in many cases, thus requiring ultra-sensitive strategies to be able to detect tumor alterations. Most commonly employed methods in cfDNA analysis include Next generation sequencing (NGS), ddPCR, and PCR-based.

1.2.4.1 Next generation sequencing

NGS for ctDNA analysis can be targeted or untargeted as well [183]. Targeted methods for ctDNA profiling typically involve gene panels or even the whole exome (WES). Targeted panels are recommended for clinical diagnosis due to their low cost, high analytical sensitivity, and specificity, which are achieved through the enrichment of certain regions of interest. Only point mutations and indels, nevertheless, are detectable by them. Given its ability to identify untargeted panels, NGS can be used to identify genome-wide DNA variation. The full genomic profile of tumor DNA, including point mutations, indels, rearrangements, and CNVs, is often obtained using whole-genome sequencing (WGS) [184]. While WGS offers an immense quantity of genomic data, it is more costly and less sensitive. Moreover, the high input sample volume requirement of both WGS and WES makes it difficult to use them for screening and early diagnosis in situations where the concentration of ctDNA is significantly low.

Tagged-amplicon deep sequencing (TAm-Seq) is a two-step amplification approach wherein regions of interest are initially amplified using specially designed primers, and then particular target sections are amplified using a

microfluidic technology [185]. Tam-seq was able to identify mutations of MAF as low as 2% with sensitivity and specificity over 97% [185]. The enhanced TAm-Seq (eTAm-Seq) can detect MAF as low as 0.25% with a sensitivity of 94%. It also utilizes revised bioinformatics analysis to identify single-nucleotide variants, short insertions/deletions (indels) and copy number variants [186].

One such NGS test is called Cancer Personalized Profiling by Deep Sequencing (CAPP-Seq), which combines a sophisticated bioinformatics methodology with a target-selection library preparation method [139]. Among patients with stage II–IV NSCLC, MAF ~ 0.02% can be found by CAPP-Seq with a sensitivity of nearly 100% [139].

Many companies are creating assays for NGS ctDNA testing. Now, CancerSEEK is a NGS blood test that looks for ctDNA mutations along with protein biomarkers to enable early diagnosis of different types of cancer [187]. Two NGS-based liquid biopsy ctDNA testing methods have already received FDA approval: the FoundationOne CDx assay and the Guardant360 CDx assay, which can sequence 311 and 55 genes, respectively [147].

Together with increased depth of coverage as well as decreasing cost, NGS may be the dominant technology for the future liquid biopsy ctDNA testing assays [188]. Even though some of them have already been validated in clinical settings, the greater complexity and cost of these approaches provide an obstacle to their widespread application in clinical laboratories. In order to effectively identify actionable genetic variations in solid cancers, there is still a need for less expensive and easier screening techniques.

1.2.4.2 Digital PCR

The numerous advantages of digital PCR have led to its widespread use in clinical diagnostics and precision medicine since the 1990s [189, 190]. Multiple platforms have been established, and currently, several commercialized digital PCR platforms are available. Based on the partitioning techniques, there are two main types of commercial digital PCR platforms: (1) chamber-based digital PCR

(cdPCR), also known as chip-based digital PCR or microwell digital PCR and (2) droplet digital PCR (ddPCR) [190]. The formulation of the surfactant and oil is an essential part of this procedure since it ensures the stability of the droplets and their compatibility with PCR reactions. This method permits continuous flow for droplet formation, offers control over size dispersity, and can be used to manipulate small partition volumes [190].

Currently, ddPCR is the most widely used digital PCR method for analyzing cfDNA, particularly for copy number variation and mutation detection [191]. Based on the fluorescence amplitude, the number of droplets containing positives and negatives is calculated following PCR. Target molecules are enriched inside the isolated drops as a result of sample partitioning, and this enrichment effect reduces template competition. This makes it possible to detect rare variants when there is an abundance of wild-type sequences. The concentration of the target nucleic acid is calculated by Poisson statistical analysis without the need for a standard curve [190]. ddPCR offers a lot of advantages, e.g., greater precision and analytical sensitivity for the detection of low copy variants (0.1% and lower) and high tolerance to inhibitors [190, 192].

1.2.4.3 PCR-based

Since real-time PCR amplification of nucleic acids is inexpensive and quick, it is now extensively used in many applications [193, 194]. There are several PCR-based methods that have been used in routine clinical practice, including allele-specific amplification (AS-PCR), amplification-refractory mutation system PCR (ARMS-PCR), PNA-LNA (peptide-nucleic-acid-locked nucleic acid) Clamp PCR and co-amplification at lower denaturation temperature (COLD-PCR).

Point mutations can be found using allele-specific primers in ARMS-PCR (amplification-refractory mutation system PCR). The assay's detection limit has been variable across different studies, with relatively high false positive rates with a detection limit ranging from 0.5 to nearly 0.01% in plasma DNA [136, 195-197].

Peptide nucleic acids are used as clamps in PNA-LNA (peptide-nucleic-acid-locked nucleic acid) Clamp PCR, a different technique that promotes the selection of variant alleles by blocking the amplification of wild-type DNA. A PNA clamp specifically designed to detect mutations at codons 12 and 13 in *KRAS* gene. The sample containing mutant DNA amplified by PCR with the PNA clamp probe [198, 199]. This technique has also been applied to the detection of *EGFR* T790M mutations, *PIK3CA* hotspot mutations, *ESR1* mutations [138, 196, 200, 201].

COLD-PCR (co-amplification at lower denaturation temperature PCR) is a single-step amplification method that preferentially enriches low-abundance variant alleles from a combination of wild-type and variation-containing DNA, regardless of mutation type and position. A crucial step in distinguishing variant alleles is to use the critical denaturation temperature, which is the point at which a mutant allele preferentially melted over a wild type. The method allows for the enrichment of mutant alleles to increase mutation detection sensitivity up to 0.1% [202].

In conclusion, the PCR-based method provides a reliable, sensitive, affordable, straightforward and clinically relevant tool for the detection of gene hotspot mutations, particularly in limited-resource healthcare settings. One of the drawbacks of most PCR-based methods is that their multiplexing ability is limited.

Chapter 2: Optimization of *PIK3CA* hotspot mutant detection assays for plasma circulating cell free DNA

This section was previously published by PlosOne, a peer-reviewed, open access journal of science and medicine, published by the Public Library of Science (PLOS), and by Frontiers in Oncology, a leading peer-reviewed open-access journal in the field of cancer research.

2.1 Introduction

Breast cancer (BC) remains the most common malignancy among women worldwide, with hormone receptor–positive (HR^+) tumors representing approximately 70% of all cases [2]. Endocrine therapy (ET) is the standard first-line treatment for this subgroup; however, resistance eventually develops in up to 20% of patients, leading to disease recurrence, distant metastasis, and poor clinical outcomes [203]. One of the most important molecular mechanisms underlying endocrine resistance is the dysregulation of the PI3K/Akt/mTOR signaling pathway, which promotes tumor cell survival, proliferation, and treatment escape [4–9].

Activating mutations in the *PIK3CA* gene are among the most frequent genetic events driving PI3K pathway hyperactivation in breast cancer. These somatic alterations, typically clustered in exons 9 and 20—most commonly at codons E542K, E545K, and H1047R—occur in about 30–40% of $HR^+/HER2^-$ tumors and are strongly associated with endocrine resistance and metastatic progression [64, 78]. Identifying such mutations has direct therapeutic relevance, as patients harboring *PIK3CA* alterations may benefit from targeted inhibitors such as alpelisib or inavolisib, often in combination with endocrine agents [204–206]. Additionally, patients with *PIK3CA/AKT1/PTEN* alterations who experience progression after endocrine therapy have shown favorable responses to capivasertib, an AKT kinase inhibitor [92]. Therefore, accurate detection of *PIK3CA* mutations plays a crucial role in guiding precision treatment, particularly in $HR^+/HER2^-$ advanced or metastatic BC [207].

While tumor tissue has traditionally served as the main source for genomic testing, tissue biopsies are invasive, sometimes infeasible in metastatic settings, and represent only a static snapshot of a heterogeneous disease. In contrast, cell-free DNA (cfDNA) analysis from plasma—commonly referred to as *liquid biopsy*—offers a minimally invasive alternative for real-time assessment of tumor-derived mutations [210]. However, cfDNA-based genotyping poses analytical challenges due to the very low abundance of mutant alleles, often representing less than 0.1% of total cfDNA in plasma [139, 140]. Hence, highly sensitive and cost-effective detection methods are required for reliable mutation identification.

Conventional sequencing methods such as Sanger sequencing lack the analytical sensitivity needed for cfDNA analysis, whereas next-generation sequencing (NGS) and digital PCR can detect mutations at low frequencies but are often expensive and technically demanding for routine diagnostics [69, 139, 210, 211]. Asymmetric real-time PCR (ASM-PCR), when combined with mutation-specific primers and wild-type blocking oligonucleotides, represents a promising alternative due to its simplicity, specificity, and adaptability for low-resource settings [194, 197, 199, 212, 213].

In this study, we aimed (1) to develop and optimize a clinically applicable asymmetric real-time PCR assay capable of ultra-sensitive detection of *PIK3CA* hotspot mutations (E545K and H1047R) in plasma cfDNA, and (2) to evaluate the association between blood-circulating *PIK3CA* mutations and the clinical characteristics of breast cancer patients. To achieve these objectives, we designed a novel blocker-mediated allele-specific asymmetric PCR platform that selectively suppresses wild-type amplification while enriching mutant signals, thereby improving analytical sensitivity to as low as 0.01–0.1%. This optimized assay offers a robust, low-cost, and highly sensitive tool for molecular stratification and therapeutic monitoring of breast cancer in clinical practice.

Table 3. The detection limit of various PCR-based approaches for detecting the *PIK3CA* hotspot mutations

Methods	LOD (%)	Sample types	Tumor types	Authors (Year)
An amplification refractory mutation system (ARMS) PCR	1.0%-0.1%	Tissue	Breast cancer	Ruth E. Board et al. (2008) [68]
Lock Nucleic Acid (LNA) PCR Sequencing	1.3% - 1.0%	Tissue	Breast cancer	Daphne Ang et al. (2012) [95]
An amplification refractory mutation system (ARMS-PCR) using allele-specific scorpion primers	0.5%	Tissue	Breast cancer	Alexandre Harlé et al. (2013) [67]
The combination of allele-specific, melting analysis and asymmetric rapid PCR	0.05%	Plasma	Breast cancer	Athina Markou et al. (2014) [203]
Digital PCR	0.01%	Serum	Breast cancer	Chiya Oshiro et al. (2015) [69]
Peptide Nucleic Acid (PNA) PCR Sequencing	0.2% - 0.1%	Plasma	Colorectal carcinoma	Qian Zeng et al. (2017) [200]
Allele-specific competitive blocker-PCR	10% - 5%	Tissue	Breast cancer	Virginia Alvarez-Garcia et al. (2018) [93]
The nuclease-assisted minor-allele enrichment PCR assay with overlapping probes	0.6% - 0.3%	Plasma	Breast cancer	Ieva Keraite et al. (2020) [70]
Droplet digital PCR	0.25% - 0.1%	Plasma	Breast cancer	Julien Corné et al. (2021) [66]
LNA-modified hairpin-shaped primers	0.1%	Plasma	Colorectal carcinoma	Junsoo Park et al. (2022) [94]

LOD: limit of detection

2.2 Material and methods

2.2.1 Study population and clinical specimen collection

This study enrolled 196 female breast cancer patients over the age of 18 (stages I-IV) from 108 Military Central Hospitals (108 MCH) between June 2021 and June 2023. Individual patients were given written consent to participate in the study right after being admitted to the hospital; blood samples, clinical and paraclinical variables were also collected.

Pathologic tissues were examined by designated breast pathologists at the Department of Pathology, Laboratory Center, 108 MCH. Immunohistochemical analysis determined the status of estrogen receptor and progesterone receptor. Nuclear staining ≥ 1% for estrogen receptor and/or progesterone receptor was considered positive. HER2 status was determined by immunohistochemical analysis or FISH if available or if needed for 2+ IHC. Positive HER2 status was determined by immunohistochemical analysis score of 3+ or positive FISH.

The time to progression (TTP) or progression-free survival (PFS) was calculated from the date of blood collection to the date of first progression following enrollment. Documentation in the medical record was used to collect the patients' clinical characteristics

2.2.2 Plasma separation, DNA extraction, and storage conditions

Peripheral blood samples were drawn in EDTA K2 tubes that were centrifuged at 2,000 g for 10 minutes at room temperature; then the separated plasma was collected and stored until DNA extraction was required. The MagMAX™ Cell-Free DNA Isolation Kit (Thermo Fisher Scientific, USA; Cat. No. A29319) was used for individual cfDNA extraction from 500 µL aliquots of plasma. The isolated cfDNA samples were kept at -80 °C until further utilization.

We bought the human breast cancer cell lines, MCF7 or T-47D, from Thermo Fisher Scientific Inc. RPMI 1640 media (Invitrogen, Carlsbad, CA; Cat. No. 11875-093) supplemented with 7.5% fetal bovine serum (FBS, Gibco, USA; Cat. No. 16000-044) and 100 units/ml penicillin-streptomycin (Sigma-Aldrich,

USA; Cat. No. P4333) was used to maintain MCF7 or T-47D cells. Cells were cultured and grown in an air-carbon dioxide (95:5) environment at 37 °C. Thermo Fisher Scientific's genomic DNA purification kit (Cat. No. K0512) was used to extract genomic DNA from MCF7 cells, T-47D cells, and 20 healthy donors' white blood cells in an elution volume of 100 µl, according to the manufacturer's instructions. The electrophoresis images, concentration, and purity (A260/A280 ratios) of total genomic DNA extracted from 20 healthy individuals are presented in Table 4 and Figure 2. After extraction, the DNA was aliquoted and kept at -20 °C until it was needed.

Table 4. Concentration and purity of total genomic DNA extracted from peripheral blood of 20 healthy individuals

Sample ID	DNA concentration (ng/µL)	A260/A280	Sample ID	DNA concentration (ng/µL)	A260/A280
HC 1	72.4	1.83	HC 11	71.4	1.87
HC 2	68.9	1.81	HC 12	66.7	1.92
HC 3	75.6	1.85	HC 13	82.6	2.01
HC 4	66.7	1.79	HC 14	59.3	1.85
HC 5	55.8	1.82	HC 15	74.8	1.85
HC 6	102	1.85	HC 16	70.5	1.79
HC 7	88.2	1.84	HC 17	79.6	1.82
HC 8	69.8	1.87	HC 18	73.9	1.85
HC 9	58.3	1.81	HC 19	68.3	1.84
HC10	74.6	1.85	HC 20	82.6	1.87

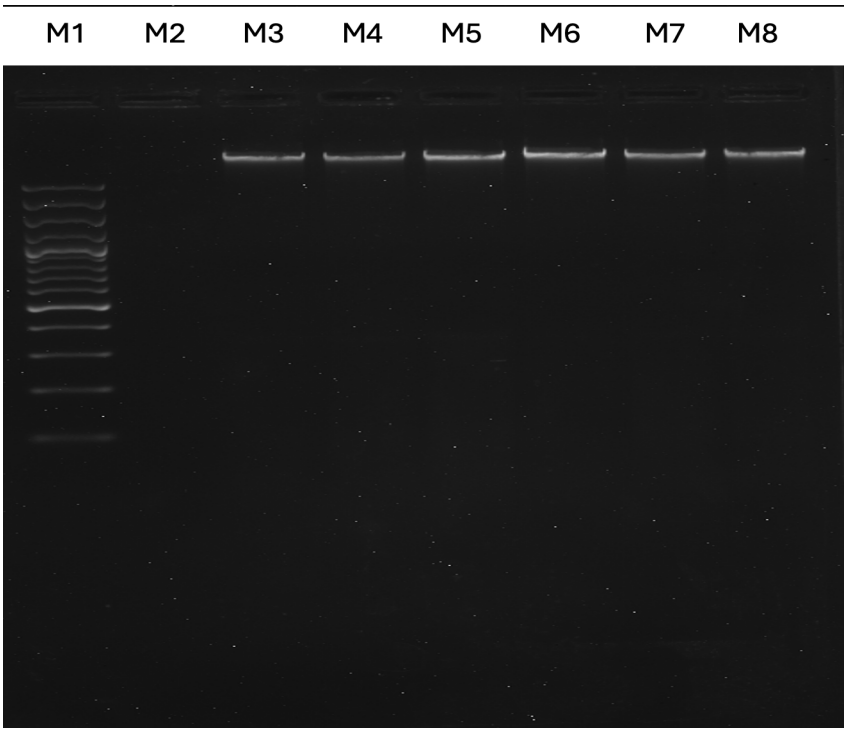

Figure 2. Electrophoresis image of PCR amplification from representative gDNA samples of healthy individuals. Agarose gel electrophoresis showing successful PCR amplification using genomic DNA (gDNA) extracted from peripheral blood of 6 healthy individuals. The selected samples (lanes M3–M8) demonstrate clear, single DNA bands of the expected amplicon size (~200 bp), confirming the integrity and amplifiability of extracted gDNA. Lane M1: 100 kb DNA ladder; Lane M2: no-template control (NTC).

2.2.3 Preparation of positive and negative control DNAs

White blood cells from healthy donors were combined with a specific MCF7 cell line number (which contains 30% *PIK3CA* E545K mutant allele) or T-47D cell line number (which contains 50% *PIK3CA* H1047R mutant allele) to create a so-called positive cell line dilution series that contains 10%, 1%, 0.1%, 0.01%, 0.001%, and 0% of MCF7 or T-47D cells, respectively. The whole genomic DNA was then extracted using these positive cell line dilution series. For additional assay adjustment, the genomic DNA that was taken out of the positive dilution series was then utilized as both positive and negative controls.

2.3 Optimization of *PIK3CA* hotspot mutant detection assays

2.3.1 Primers and oligonucleotide design

While blockers were chosen to bone-finely complementarily clamp and inhibit the amplification of particular wild-type alleles, primers were created to amplify amplicons of 125 bp encompassing the studied E545K mutant and 86 bp flanking around the studied H1047R mutant (detailed sequences of primers and blockers have been provided in Table 5).

Table 5. Oligo sequences for the Real-time PCR assays

Primer name	Sequence (5'-3')	Tm (°C)	Final concentration
PIK3CA H1047R mt F	ACAAATGAATGATGCACG	58.5	40 nM
PIK3CA H1047R R	CAGTTCAATGCATGCTGTTTAATT	64.1	40 nM
PIK3CA H1047R wt BL	TGATGCACATCATGG TG/PO4	59	1.2 µM
PIK3CA E545K mt F	CCTCTCTCTGAAATCACGA	58.6	40 nM
PIK3CA E545K R	CTGAGATCAGCCAAATTCAGTTA	62.5	40 nM
PIK3CA E545K wt BL	TGAAATCACTGAGCAGGAG/PO4	59.7	1.2 µM

mt F – mutant specific forward primer, R – common reverse primer, wt BL: wild-type blocker

The IDT Company (USA) provided all of the oligonucleotides. dNTPs, 6 x loading buffer, nuclease-free water, and master mix were acquired from Thermo Fisher Scientific Inc. (USA).

2.3.2 cfDNA quantification and evaluation of PCR input volume

Because the unavailability of Qubit fluorometric quantification in our laboratory and the known inaccuracy of Nanodrop for low-concentration cfDNA, we assessed cfDNA yield and quality using a qPCR-based approach. Plasma-derived cfDNA samples with Ct values less than 35 were considered adequate for downstream mutation analysis, while samples with Ct values above 35 were re-extracted from stored plasma aliquots to ensure sufficient cfDNA quality. Given the typically low abundance of cfDNA, the DNA volume used for PCR can influence reaction efficiency; therefore, we assessed the potential effect of cfDNA input volume by conducting wild-type–specific PCR

reactions on both *PIK3CA* mutation–negative and mutation–positive samples. The resulting Ct values were comparable between the two groups, indicating that using 2 μL of cfDNA as PCR input did not introduce amplification bias and was suitable for low-concentration cfDNA samples. The summarized results are presented in the newly added **Table 6.**

Table 6. Evaluation of Wild-Type–Specific PCR Amplification (Ct Values) in *PIK3CA* Mutation–Positive and –Negative Samples

Samples	***PIK3CA* mutation (Ct value of wild-type-specific PCR amplification)**	
	H1047R	E545K
Negative (n = 15)	28.66	28.11
Positive (n = 15)	30.22	29.95
p-value	0.351	0.221

2.3.3 To optimize the condition of Asymmetric PCR assays for PIK3CA mutation detection

Optimizations of the reaction conditions were then conducted for Asymmetric PCR assays (ASM-PCR). To determine the optimum conditions, the temperature and concentration of primers as well as blockers were examined. The annealing temperature was investigated between 52˚C and 64˚C, and Ct was monitored. Because the activities of enzymes and the hybridization efficiency were highly dependent upon the reaction temperature, the effect of temperature was investigated using both wild-type and mutant templates. The highest efficiency for ASM-PCR to amplify the mutant was achieved at 55˚C. The influence of primers' concentration was also studied, and primers' concentration of 40 nM was obtained as the optimum for the amplification (Table 4).

The blocker-mediated PCR clamping system is schematically presented in Figure 2A. A 3′ phosphorylated, unextended oligonucleotide sequence (wild-type blocker) that is perfectly complementary to the wild-type sequence on the same strand

was employed as the blocker to prevent the polymerase-mediated amplification of the wild-type allele, whereas a forward primer (mutant-specific primer) is perfectly matched to the mutant allele. In order to assess the clamping effect on the amplification of wild-type versus mutant alleles, several blocker concentrations (0, 0.8μM, 1.2μM, and 1.6μM) were investigated. The blocker has its strongest inhibitory effect on the amplification of the wild-type allele at 1.2μM, while the mutant allele remains nearly unaltered. Therefore, the optimal parameter for additional downstream analysis was determined to be 1.2μM of blocker (Figure 2B).

The analytical sensitivity of the ASM-PCR assays was significantly impacted by the activity of the PCR polymerase and the additional reagents in the master mix. Using several commercial master mixes, it was discovered that there was a difference in the ability to distinguish between the target mutant and the wild-type templates (Data not shown).

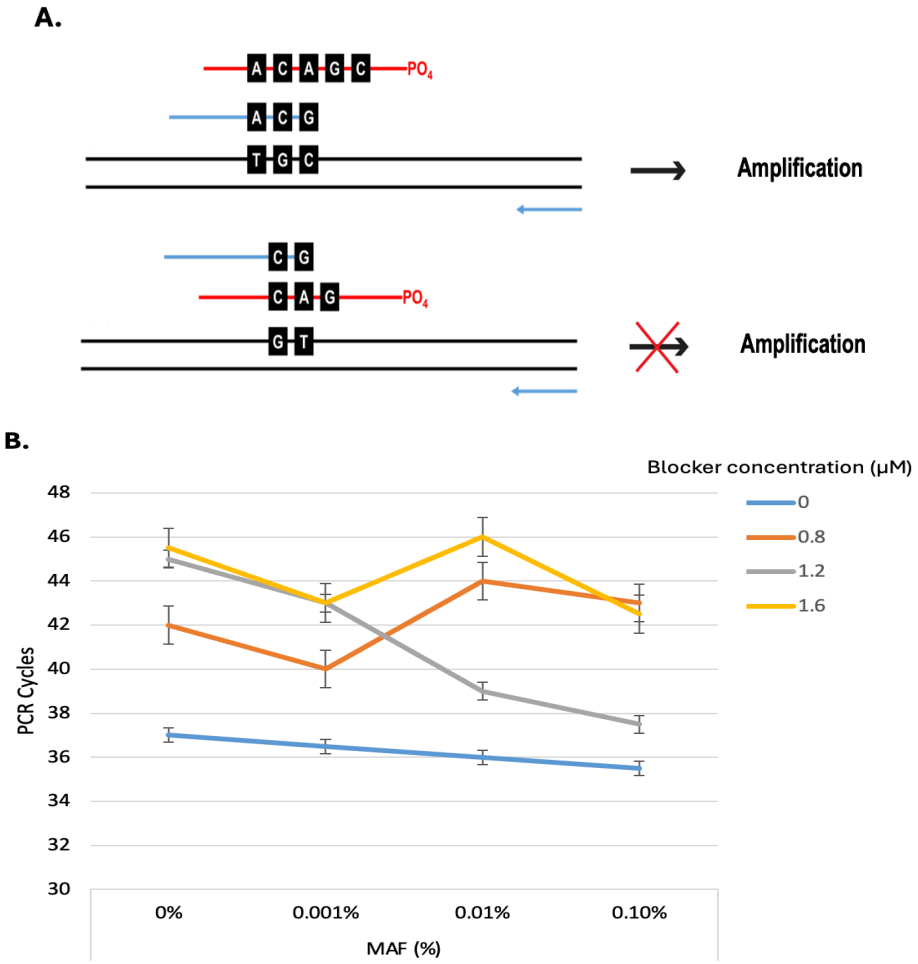

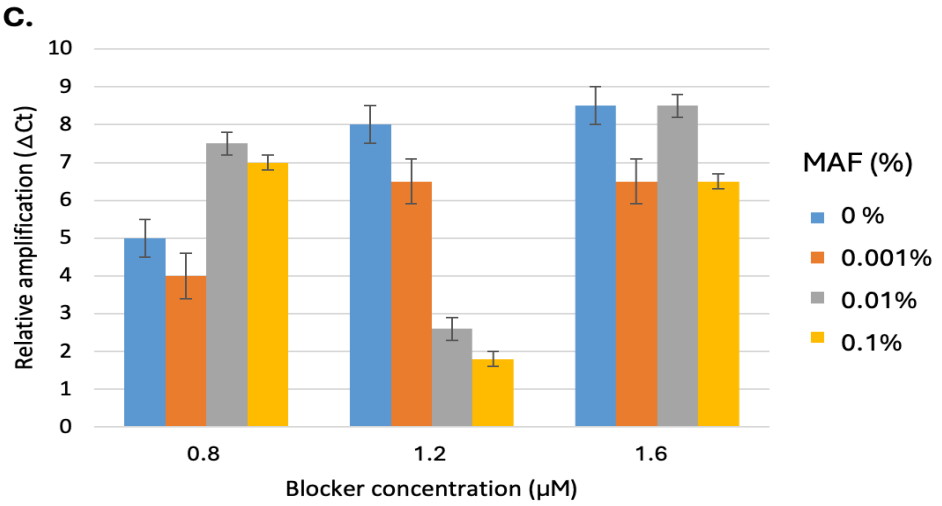

Figure 3. The impact of Blocker on the polymerase-mediated amplification of targeted amplicons. (A): The blocker oligomer (red line) was designed to perfectly match the wild-type allele, while the forward primer (mutant-specific primer or blue line) partially overlapped the blocker binding site, and its 3' end exactly matched the H1047R mutation site. A perfect blocker/wild-type allele hybrid prevents the forward primer from annealing to its target during the PCR reaction, hence inhibiting the wild-type sequence's amplification (lower panel). A blocker/mutant allele hybrid, on the other hand, is poorly created and barely suppresses the amplification of the mutant allele because the designed blocker has a nucleotide that is mismatched to the mutant allele (upper panel). (B, C): To assess the clamping effect on the amplification of wild-type vs mutant alleles, various amounts of blockers were examined. At specified blocker concentrations (0, 0.8µM, 1.2µM, and 1.6µM), real-time PCR reactions were carried out in triplicate. Cycle threshold-Ct values (Fig B) were noted, and ΔCt values (Fig C) were calculated as the difference in Ct of the corresponding target assays with and without blocker (CTB, CTNB), respectively. It was determined that the best-optimized parameter for further downstream analysis was the 1.2µM blocker. MAF: mutant allele frequency.

2.3.4 Allele-specific asymmetric PCR assay for PIK3CA mutation detection

Allele-specific amplification targeting the *PIK3CA* point mutations were performed using a real-time PCR system (LightCycler 96, Roche, Switzerland).

Primers, blocker, and 2 µl DNA sample were mixed with 2X Universal PCR Master Mix (no UNG) TM (SYBR™ Green; Applied Biosystems, Thermo Fisher Scientific, USA; Cat. No. 4344463) in a reaction were used: 10 min. at 95°C, 50 cycles of 15 sec. at 95°C, 20 sec. at 55°C, and 20 sec. at 72°C.

2.3.5 Validation of the assays for PIK3CA mutation detection

For further confirmation, the amplicons were sequenced with the use of a Big Dye Terminator v3.1 Cycle Sequencing kit (Applied Biosystems, Thermo Fisher Scientific, USA; Cat. No. 4337455) and a 3130 XL Genetic analyser (Applied Biosystems) according to the manufacturer's instructions. Confirmation of *PIK3CA* hotspot mutations by Sanger sequencing shown in Figure 4. Table 7 shows the sequencing primers that were designed to amplify amplicons of 169 bp and 188 bp around the targeted mutant variants.

Table 7: Sequencing primers for determining *PIK3CA* hotspot mutations

Primer name	Sequence (5'-3')	Tm (°C)	Final concentration	Amplicon
H1047F	GATGACATTGCATACATTCG	57.0	0.4 µM	188 bp
H1047R	AGTGAGCTTTCATTTTCTCAG	58.4	0.4 µM	
E545F	GGGAAAATGACAAAGAACAGC	59.9	0.4 µM	169 bp
E545R	CTGAGATCAGCCAAATTCAGTTA	60.6	0.4 µM	

A. H1047R

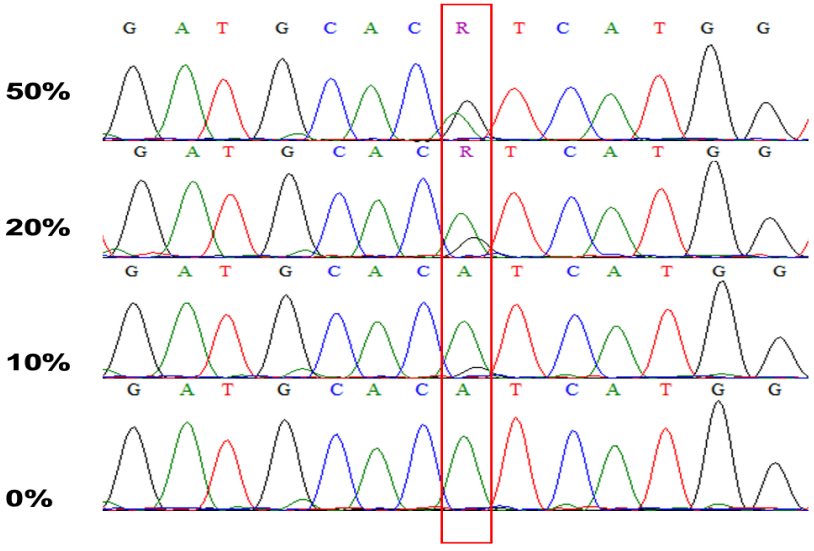

B. E545K

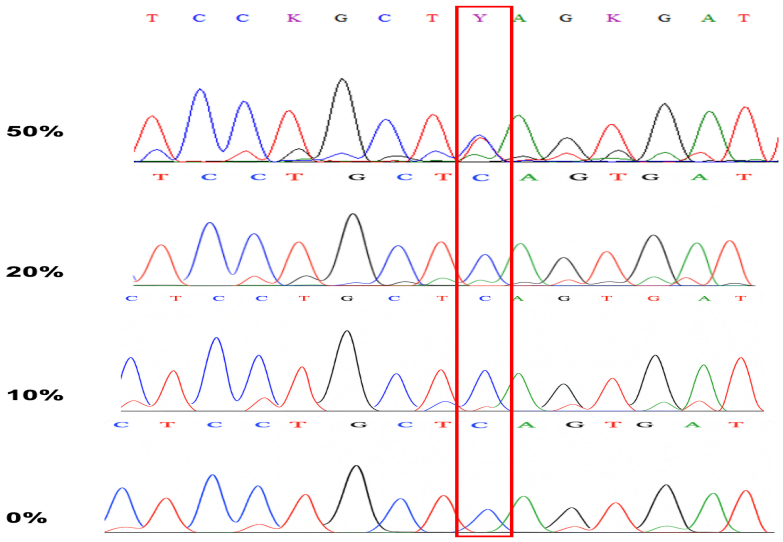

Figure 4: Confirmation of *PIK3CA* hotspot mutations by Sanger sequencing

(A): Sanger sequencing results of dilution series control samples with H1047R (A>G) mutant concentrations of 0%, 10%, 20%, 50%. (B): Sanger sequencing results of dilution series control samples with E545K (C>T) mutant concentrations of 0%, 10%, 20%, 50%.

2.3.6 Statistical analysis

Statistical analysis was performed via SPSS version 25.0 (IBM SPSS Statistics, Armonk, NY, USA). The $\chi 2$ and Fisher's tests were used to determine associations between *PIK3CA* gene mutation and clinicopathological features of BC patients. Progression-free survival (PFS) was calculated as the time from enrollment to any recurrence, progression event. The Kaplan-Meier method was used to estimate the PFS, followed by a log-rank or Wilcoxon test for comparison among subgroups; variables associated with PFS were also assessed by Cox proportional hazard model. A p-value of < 0.05 was judged significant. Graphics were created using MS Excel 2010 (Microsoft Corporation, USA), Prism 10.0.0 (GraphPad) software.

2.4 Results

2.4.1 Analytical sensitivity and specificity of the PIK3CA mutant detection assays

The total genomic DNA extracted from MCF7 or T-47D cell positive cell line dilution series that bear 10%, 1%, 0.1%, 0.01%, 0.001% and 0%, were used

as input templates of corresponding real-time PCR assays. At each dilution point, the real-time PCR was performed in four conditions (i- wild-type template without blocker (blocker free), ii- wild-type template with blocker, iii- mutant template (0.001%, 0.01%, 0,1%, 1%, 10%) without blocker and iv- mutant template (0.001%, 0.01%, 0,1%, 1%, 10%) with blocker and was repeated 15 times with primers and blocker to determine assay's technical sensitivity (or the limit of detection - LOD) (Figure 5). The obtained ΔCt value distance was 7.74 ($p = 0.569$) at the lowest concentration of the E545K mutant allele (0.001%), and it linearly dropped to 2.32 ($p < 0.001$) at the greatest dilution point of 10% E545K mutant allele. At the lowest concentration of the H1047R mutant allele (0.001%), the acquired ΔCt value distance was 5.19 ($p = 0.714$) and the ΔCt distance linearly decreased to 1.22 ($p = 0.001$) at the highest dilution point of 10% H1047R mutant allele (Figures 5-7). Because only assay with a p-value lower than 0.05 is considered statistically significant [204], the 0.1% and 0.01% mutant alleles were concluded to be the LOD of our newly established technique for detecting E545K and H1047R point mutations, respectively. The assays' accuracy was maintained at the LOD or higher of these variants.

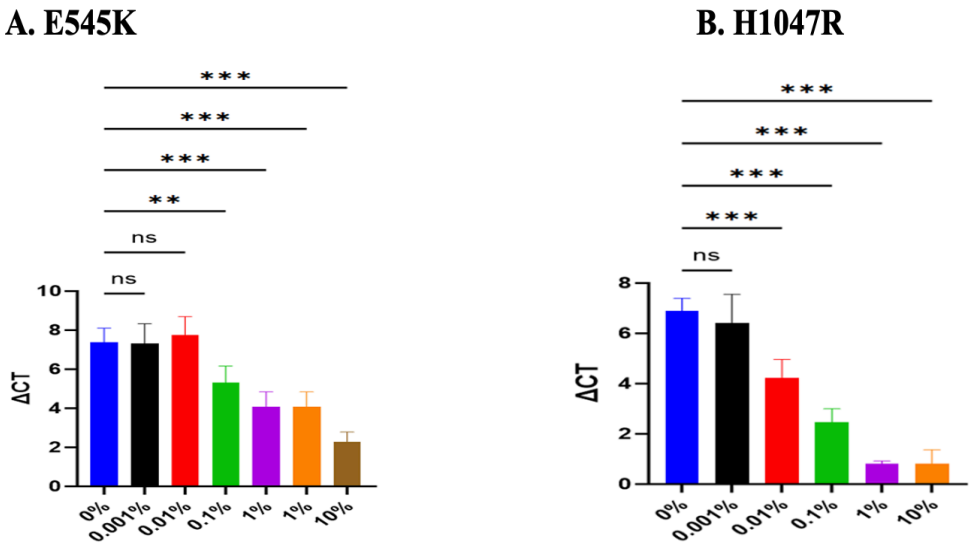

Figure 5. The detection limit of real-time PCR assays for *PIK3CA* mutation detection. Real-time PCR assays with or without blocker were performed fifteen

times on dilution series of 10%, 1%, 0.1%, 0.01%, 0.001% and 0% mutant (or wild-type DNA). Acquired ΔCt value distance and statistical p-values were recorded. ***P < 0.001, **P < 0.01, and *P < 0.05 compared to 0% mutant load (or wild-type DNA).

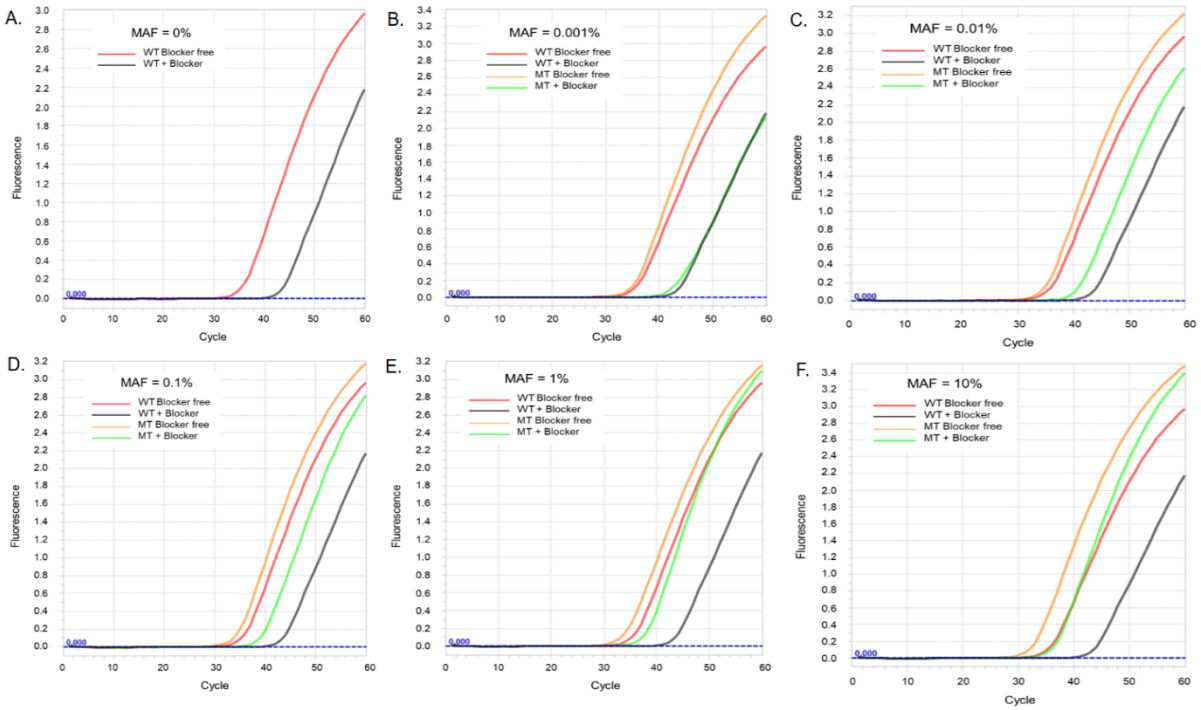

Figure 6. Real-time PCR assays to determine the LOD for the *PIK3CA* E545K mutation detection. Total genomic DNA was isolated from MCF7 cell positive cell line dilution series with mutant allele frequency (MAF) values of 10%, 1%, 0.1%, 0.01%, 0.001%, and 0% (or wild-type DNA) and utilized as input templates for corresponding real-time PCR tests. The real-time PCR was performed in four conditions at each dilution point (i- wild-type template without blocker (blocker free), ii- wild-type template with blocker, iii- mutant template (0.001%, 0.01%, 0,1%, 1%, 10%) without blocker, and iv- mutant template (0.001%, 0.01%, 0,1%, 1%, 10%) with blocker).

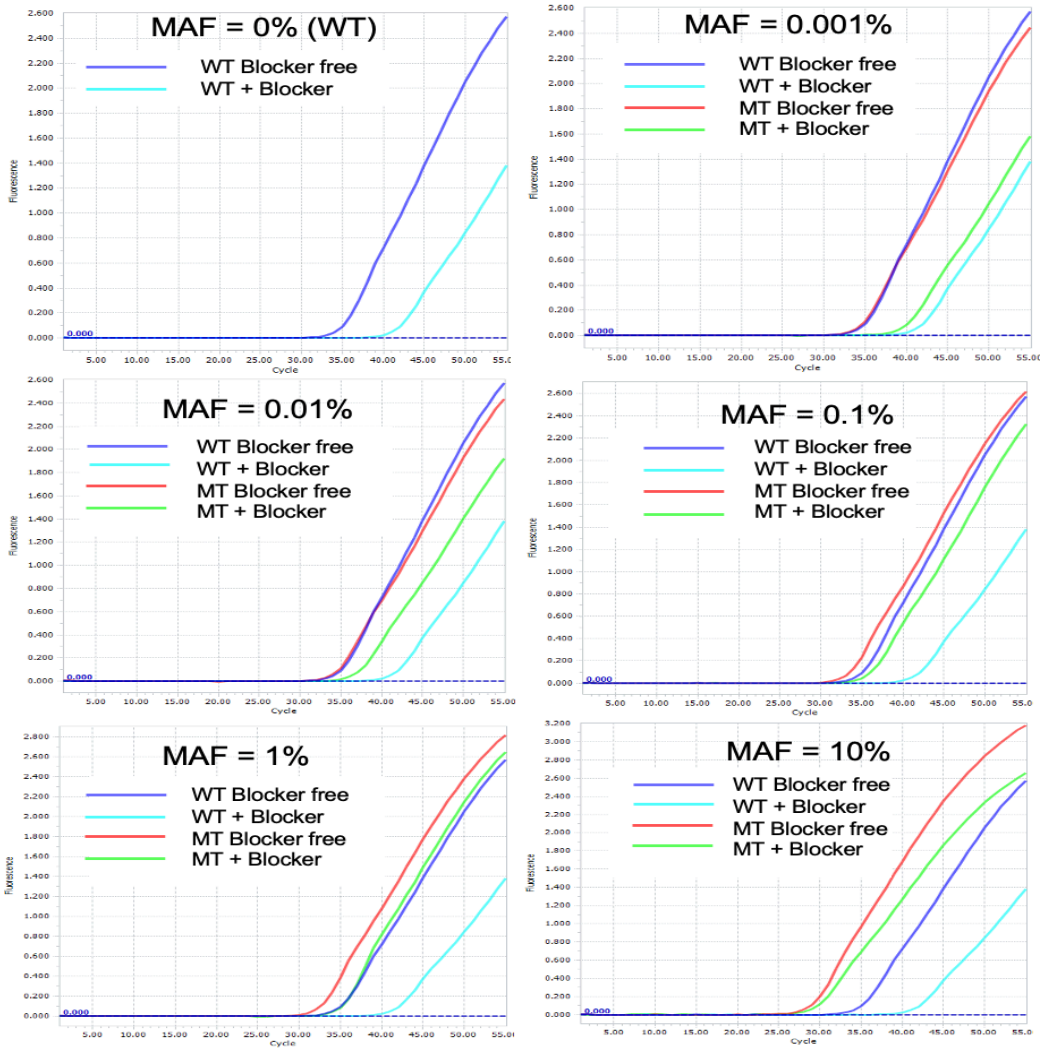

Figure 7. Real-time PCR assays to determine the LOD for the *PIK3CA* H1047R mutation detection. The input templates for the associated real-time PCR experiments were the entire genomic DNA isolated from T-47D cell positive cell line dilution series that have mutant allele frequencies (MAF) of 10%, 1%, 0.1%, 0.01%, 0.001%, and 0% (or wild-type DNA). Four conditions were used for the real-time PCR at each dilution point: i) wild-type template without blocker (blocker free); ii) wild-type template with blocker; iii) mutant template (0.001%, 0.01%, 0,1%, 1%, 10%) without blocker; and iv) mutant template (0.001%, 0.01%, 0,1%, 1%, 10%) with blocker.

2.4.2 Application of PIK3CA mutation detection assays on clinical samples

By applying the newly established assay on 196 institutionally recruited BC patient's plasma samples, 84 cases (42.9% of total recruited cases) had at least one mutation, either E545K or H1047R, 62 cases (31.6%) had *PIK3CA* H1047R mutation and 30 cases (15.3%) carried *PIK3CA* E545K mutation (Table 8). Eight of them (4.1%) were positive with both E545K and H1047R mutation and 112 of them were both negative (Table 9). *PIK3CA* mutations occur early in the process of tumor development, in which the H1047R mutation was more frequently found than the E545K mutation. The majority of early breast cancer (EBC) patients had a single *PIK3CA* mutation, and its status did not change in the patients who develop recurrent or progressive breast cancer (Table 10).

Among the studied cohort, 43 cases (21.9%) suffered recurrence, 54 out of 196 (27.6%) patients were classified as stage IV, and 116 out of 196 (59.2%) patients bear at least one invasive location, either lymph nodes and/or metastases to other organs, as summarized in Table 8 (the patients' characteristics).

An increasing trend of *PIK3CA* mutation detection was observed across disease stages, with higher proportions in stages III–IV compared with stages I-II. This trend reached statistical significance in our cohort ($p = 0.024$). However, there was no relationship between *PIK3CA* mutations and the patient's age family history, menopausal status, HR or HER2 expressions, or tumor histopathology (Table 8).

Our data revealed that *PIK3CA* mutation rates are higher in metastatic patients ($p = 0.032$), particularly those with multiple metastatic locations ($p = 0.032$) or liver metastases ($p = 0.044$) or brain metastatic disease ($p = 0.032$) (Table 8). Especially, *PIK3CA* H1047R mutation was more prevalent in females who were at late stage ($p = 0.025$), having recurrence ($p = 0.045$), having metastasis ($p = 0.049$) or those with liver metastatic disease ($p = 0.034$) or brain metastases ($p = 0.009$) (Table 8).

The finding also found that *PIK3CA* mutation carriers were strongly associated with patients who are radiation-treated BC ($p = 0.009$) (Table 8,

Figures 8-9, 11-12). Compared to patients received other therapies, *PIK3CA* mutations were more common in BC patients who had received radiation treatment. Interestingly, *PIK3CA* E545K mutation was frequently observed in radiation-treated HR+BC women ($p = 0.022$), meanwhile *PIK3CA* H1047R mutation was much more prevalent in radiation-received HER2+BC women ($p = 0.004$) (Figure 9, Figure 12).

To find out whether hormone treatment affects the occurrence of *PIK3CA* mutations, we observed the distribution of the gene mutant frequency in HR+ advanced BC patients treated with various endocrine agents. We evaluated the HR+ advanced BC patients since only the group received SERDs or fulvestrant. We realized that while *PIK3CA* H1047R mutation were frequently observed in patients receiving SERMs or SERDs, a lower rate was found in the AI-received group. It was found that SERDs-recipients had a greater incidence of *PIK3CA* gene alterations, particularly the H1047R variant ($p < 0.05$) (Figure 10).

Of the patients who underwent testing, 94 (48%) were ≤ 50 years old (age range 26–50) and 102 (52%) > 50 years old (age range 51–81). ctDNA *PIK3CA* mutations were found in 46.8% of young patients and in 39.2% of older patients. The majority of *PIK3CA* mutation carriers who were younger than 50 years old had metastatic disease ($p = 0.047$), and there was a significant difference between the presence of the *PIK3CA* mutated gene and the sites of metastatic disease in the study's population, with the majority (100%) of patients having liver disease at the time of ctDNA testing ($p = 0.02$) (Figure 13). There was no significant difference between the *PIK3CA* mutations and the sites of metastatic disease in the study's population, with the majority of patients having brain disease at the time of ctDNA testing (≤ 50 years old: 100%; > 50 years old: 100%), followed by bone metastasis (≤ 50 years old: 63.2%; > 50 years old: 50%), lymph node metastasis (≤ 50 years old: 54.7%; > 50 years old: 41.2%), and lung metastasis (≤ 50 years old: 53.3%; > 50 years old: 54.5%). In group under the age of 50, *PIK3CA* H1047R mutant carriers were strongly associated with liver-metastasized ($p = 0.044$) or brain metastases ($p = 0.037$) or lymph node-invaded

($p = 0.03$), while no correlation was observed between *PIK3CA* H1047R mutated and lung metastatic disease or bone metastatic disease (Figure 15). In patients over 50, there was no correlation ($p > 0.05$) between metastatic status and the presence of H1047R, or E545K mutation (Figures 14-15).

Table 8. Characteristics of the study population according to circulating *PIK3CA* hotspot mutation status

Variable	Total	*PIK3CA*		P-value[#]	E545K		P-value[#]	H1047R		P-value[#]
	n = 196 (100%)	Mutant n = 84 (42.9 %)	WT n = 112 (57.1 %)		Mutant n = 30 (15.3%)	WT n = 166 (84.7%)		Mutant n = 62 (31.6 %)	WT n = 134 (68.4 %)	
Age ($\bar{X}$±SD, years)	52.43 ± 12.38	50.45 ± 12.46	53.92 ± 12.16	0.052	48.9 ± 19.92	53.07 ± 12.21	0.089	50.32±11.97	53.41±12.49	0.105
Family history										
Yes	38 (19.4)	18 (21.4)	20 (17.9)	0.586	7 (23.3)	31 (18.7)	0.553	11 (17.7)	27 (20.1)	0.846
No	158 (80.6)	66 (78.6)	92 (82.1)		23 (76.7)	135 (81.3)		51 (82.3)	107 (79.9)	
Disease stages										
I	18 (9.2)	4 (4.8)	14 (12.5)	**0.024**[*]	2 (6.7)	16 (9.6)	0.184	2 (3.2)	16 (11.9)	**0.025**[*]
II	71 (36.2)	24 (28.6)	47 (42.0)		8 (26.7)	63 (38)		17 (27.4)	54 (40.3)	
III	53 (27)	28 (33.3)	25 (22.3)		13 (43.3)	40 (24.1)		20 (32.3)	33 (24.6)	
IV	54 (27.6)	28 (33.3)	26 (23.2)		7 (23.3)	47 (28.3)		23 (37.1)	31 (23.1)	
Tumor histology										
Ductal	191 (97.4)	83 (98.8)	109 (96.4)	0.394	29 (96.7)	162 (97.6)	0.568	62 (100)	129 (96.3)	0.181

Variable	Total	*PIK3CA*		P-value[#]	E545K		P-value[#]	H1047R		P-value[#]
	n = 196 (100%)	**Mutant n = 84 (42.9 %)**	**WT n = 112 (57.1 %)**		**Mutant n = 30 (15.3%)**	**WT n = 166 (84.7%)**		**Mutant n = 62 (31.6 %)**	**WT n = 134 (68.4 %)**	
Lobular	5 (2.6)	1.0 (1.2)	4 (3.6)		1 (3.3)	4 (2.4)		0 (0)	5 (3.7)	
Grade										
1	12 (6.1)	3.0 (3.6)	9 (8.0)	0.395	0 (0)	12 (7.2)	0.305	3 (6.1)	9 (6.7)	0.797
2	108 (55.1)	49 (58.3)	59 (52.7)		17 (56.7)	91 (54.8)		36 (58.1)	72 (53.7)	
3	76 (38.8)	32 (38.1)	44 (39.3)		13 (43.3)	63 (38)		23 (37.1)	53 (39.6)	
Menopausal status										
Post-menopausal	109 (55.6)	41 (48.8)	68 (60.7)	0.111	11 (36.7)	98 (59)	**0.023**[*]	31 (50)	78 (58.2)	0.354
HR status										
Positive	148 (75.7)	68 (81)	80 (71.4)	0.125	24 (80)	124 (74.7)	0.534	50 (80.6)	98 (73.1)	0.255
Negative	48 (24.5)	16 (19)	32 (28.6)		6 (20)	42 (25.3)		12 (19.4)	36 (26.9)	
HER2 status										
Positive	120 (61.2)	53 (63.1)	68 (60.7)	0.734	18 (60)	103 (62)	0.832	42 (67.7)	78 (58.2)	0.212

Variable	Total	*PIK3CA*		P-value[#]	E545K		P-value[#]	H1047R		P-value[#]
	n = 196 (100%)	**Mutant n = 84 (42.9 %)**	**WT n = 112 (57.1 %)**		**Mutant n = 30 (15.3%)**	**WT n = 166 (84.7%)**		**Mutant n = 62 (31.6 %)**	**WT n = 134 (68.4 %)**	
Negative	76 (38.8)	31 (36.9)	44 (39.3)		12 (40)	63 (38)		20 (32.3)	56 (41.8)	
Recurrence										
Yes	43 (21.9)	24 (28.6)	19 (17.0)	0.052	6 (20)	37 (22.3)	0.78	19 (30.6)	24 (17.9)	**0.045**[*]
No	153 (78.1)	60 (71.4)	93 (83.0)		24 (80)	129 (77.7)		43 (69.4)	110 (82.1)	
Metastatic disease										
Yes	116 (59.2)	57 (67.9)	59 (52.7)	**0.032**[*]	21 (70)	95 (57.2)	0.19	43 (69.4)	73 (54.5)	**0.049**[*]
No	80 (40.8)	27 (32.1)	53 (47.3)		9 (30)	71 (42.8)		19 (30.6)	61 (45.5)	
The number of metastasis lesion										
0	80 (40.8)	27 (32.1)	53 (47.3)	**0.032**[*]	9 (30)	71 (42.8)	0.176	19 (30.6)	61 (45.5)	0.131
≤ 2	94 (48)	43 (51.2)	51 (45.5)		15 (50)	79 (47.6)		34 (54.8)	60 (44.8)	
≥ 3	22 (11.2)	14 (16.7)	8 (7.1)		6 (20)	16 (9.6)		9 (14.5)	13 (9.7)	
Metastatic sites										

Variable	Total	*PIK3CA*		P-value[#]	E545K		P-value[#]	H1047R		P-value[#]
	n = 196 (100%)	**Mutant n = 84 (42.9 %)**	**WT n = 112 (57.1 %)**		**Mutant n = 30 (15.3%)**	**WT n = 166 (84.7%)**		**Mutant n = 62 (31.6 %)**	**WT n = 134 (68.4 %)**	
Lymph nodes	104 (53.1)	50 (59.5)	54 (48.2)	0.148	19 (63.3)	85 (51.2)	0.221	38 (61.3)	66 (49.3)	0.126
Lung	26 (13.3)	14 (16.7)	12 (10.7)	0.224	6 (20)	20 (12)	0.246	9 (14.5)	17 (12.7)	0.821
Liver	7 (3.6)	6 (7.1)	1 (0.9)	**0.044**[*a]	1 (3.3)	6 (3.6)	1.00	5 (8.1)	2 (1.5)	**0.034**[*]
Brain	4 (2.0)	4 (4.8)	0 (0.0)	**0.032**[*a]	0 (0)	4 (2.4)	1.00	4 (6.5)	0 (0)	**0.009**[*a]
Bone	29 (14.8)	17 (20.2)	12 (10.7)	0.063	7 (23.3)	22 (13.3)	0.165	12 (19.4)	17 (12.7)	0.279
Treatment										
Surgical therapy	161 (82.1)	49 (79)	112 (83.6)	0.431	22 (73.3)	139 (83.7)	0.171	49 (79)	112 (83.6)	0.431
Hormone therapy	98 (50)	43 (51.2)	55 (49.1)	0.885	16 (53.3)	82 (49.4)	0.692	32 (51.6)	66 (49.3)	0.878
Chemotherapy	175 (89.3)	78 (92.9)	97 (86.6)	0.243	29 (96.7)	146 (88)	0.209	57 (91.9)	118 (88.1)	0.469
Radiotherapy	60 (30.6)	34 (40.5)	26 (23.2)	**0.009** [*]	13 (43.3)	47 (28.3)	0.1	25 (40.3)	35 (26.1)	**0.045** [*]

"*", $p < 0.05$; p-value[#] Mutant versus Wild type (WT); a, Fisher's Exact Test.

Table 9. Circulating *PIK3CA* mutations in 196 BC patients'plasma

		Number of H1047R mutation (n)		Total
		Negative	Positive	
Number of E545K mutation (n)	Negative	112	54	166
	Positive	22	8	30
Total		134	62	196

Table 10. Distribution of the circulating *PIK3CA* mutations based on BC stages

Stages	**Number of *PIK3CA* mutations** (n=84)			
	E545K n=30	H1047R n=62	Monoclonal n=76	Polyclonal n=8
Early BC (n = 89)	10	19	27	1
Locally advanced BC (n = 53)	13	20	23	5
Metastatic BC (n = 54)	7	23	26	2

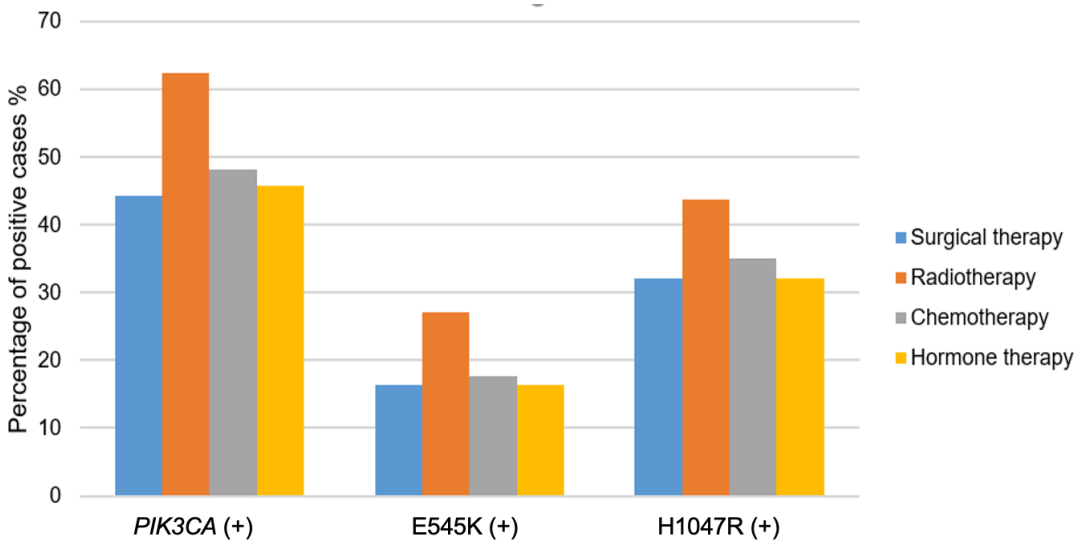

Figure 8. The distribution of *PIK3CA* mutations and variants E545K or H1047R in HR+ BC subtypes treated with different therapies

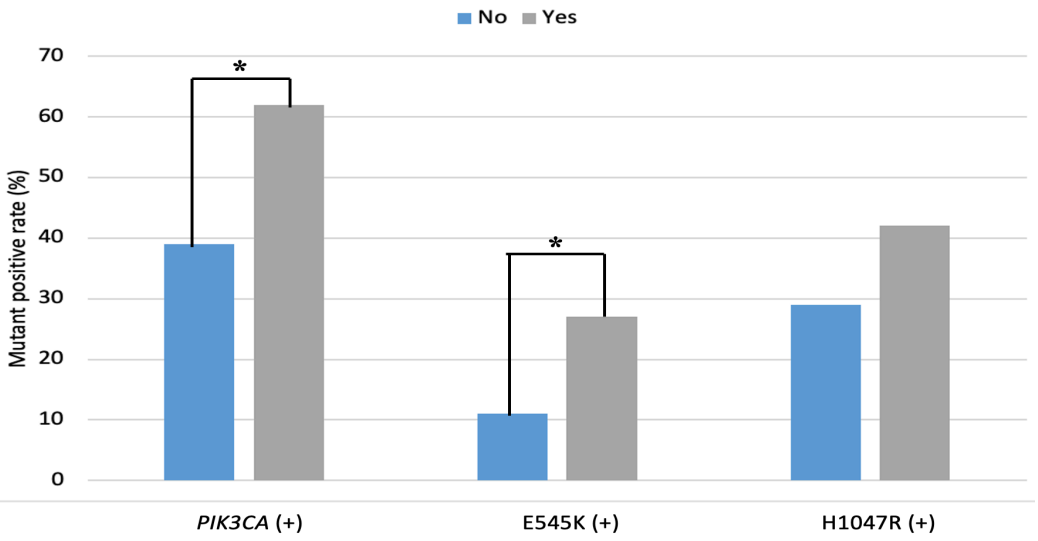

Figure 9. The distribution of *PIK3CA* mutations and variants E545K or H1047R in radio-received HR+ Breast cancer. "*"Statistically significant value, $p < 0.05$; p-value: comparation of mutation positive rate between HR+BC treated with (grey) and without radio therapy (blue). P values were derived from Fisher's exact.

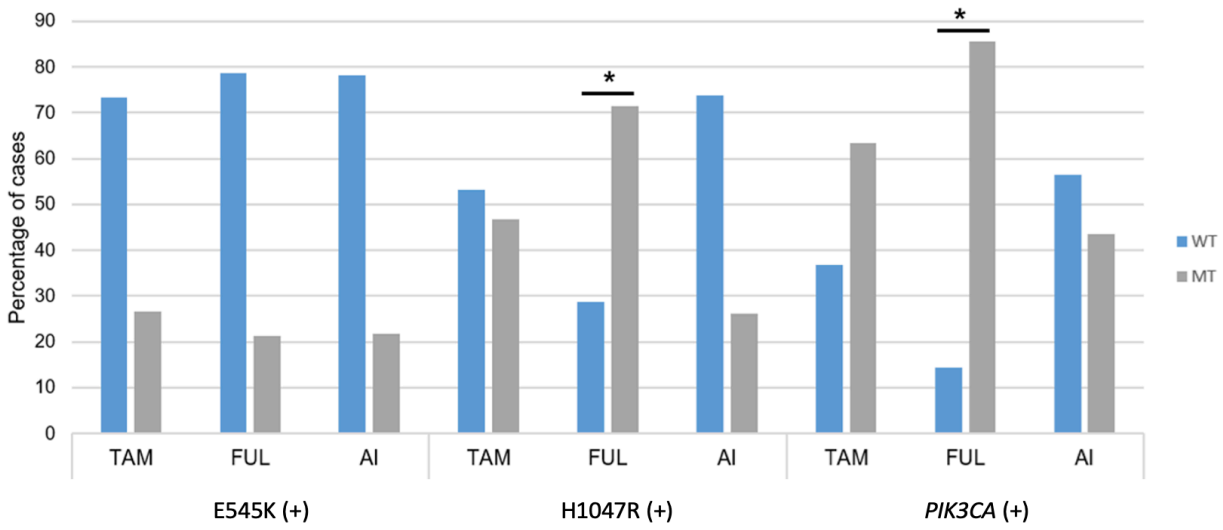

Figure 10. Distribution of the circulating *PIK3CA* mutations in HR-positive advanced breast cancer (ABC) based on treated hormone therapies. Prevalence of the circulating E545K, H1047R, and *PIK3CA* mutations in HR-positive ABC treated with different endocrine regimens: TAM: tamoxifen, FUL: fulvestrant, AI: aromatase inhibitors, WT: wild-type, MT: mutant. * $p < 0.05$; p-value: mutant versus wild-type. P values were derived from Fisher's exact.

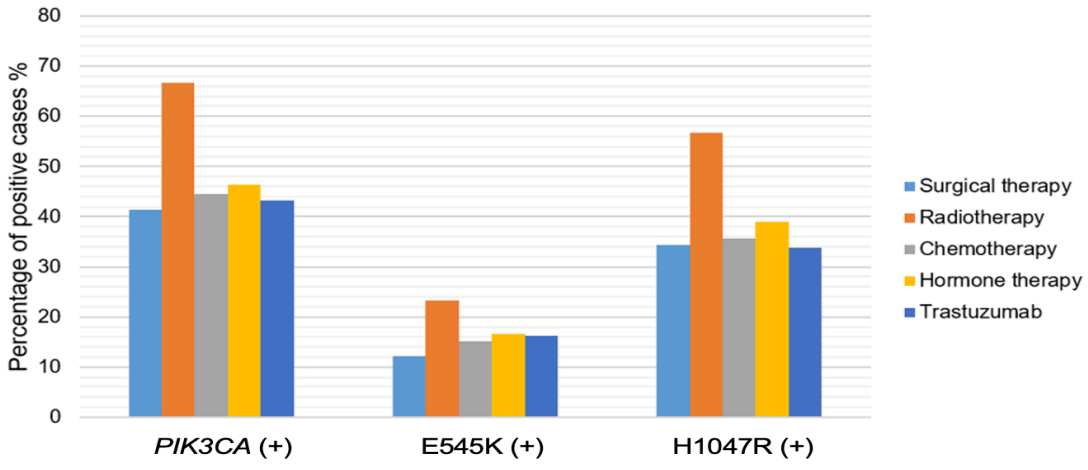

Figure 11. The distribution of *PIK3CA* mutations and variants E545K or H1047R in HER2+ BC treated with different therapies.

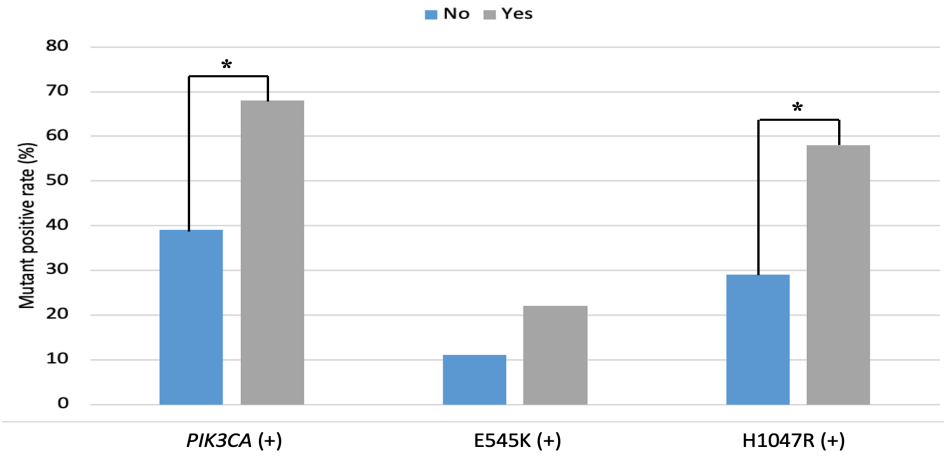

Figure 12. The distribution of *PIK3CA* mutations and variants E545K or H1047R in radio-received HER2+ Breast cancer. "*"Statistically significant value, p < 0.05; p-value: comparation of mutation positive rate between HR+BC treated with (grey) and without radio therapy (blue). P values were derived from Fisher's exact.

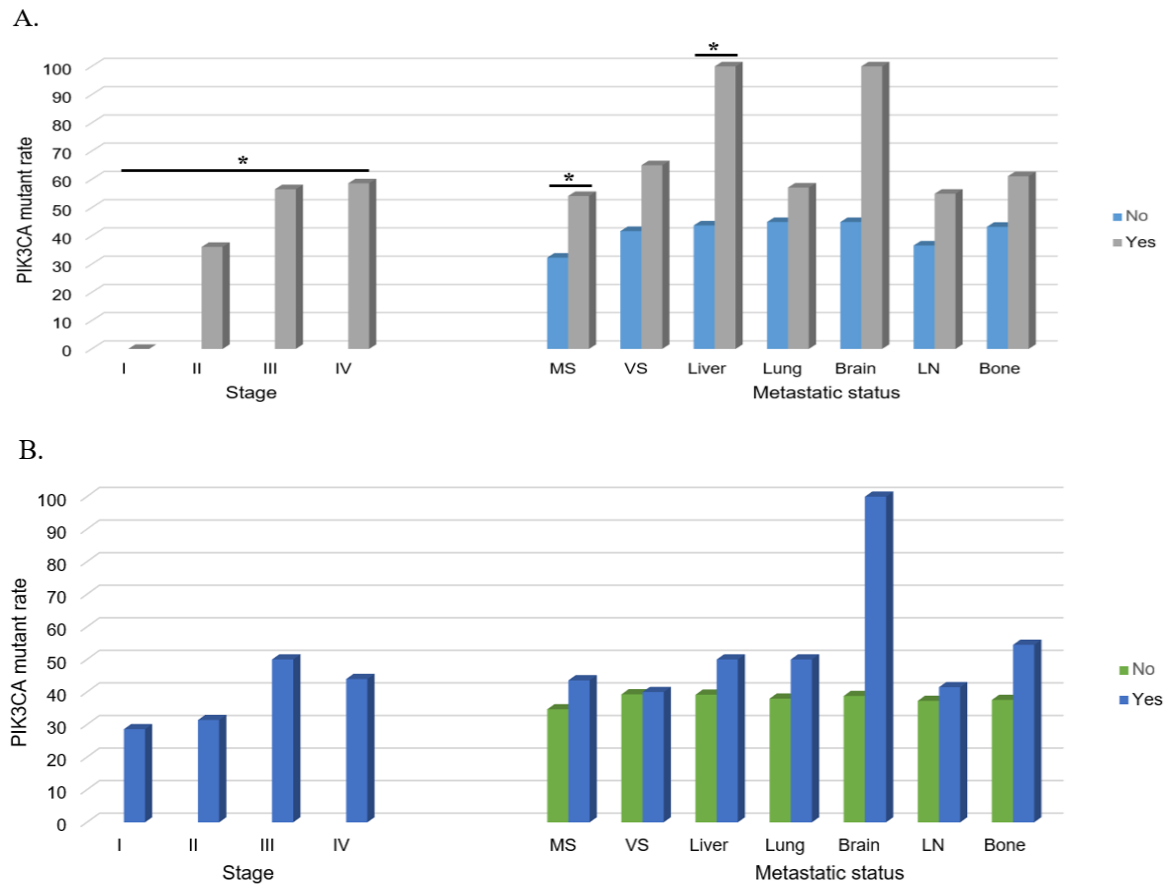

Figure 13. Distribution of the circulating *PIK3CA* mutations by age groups

The *PIK3CA* mutant frequency in groups ≤ 50 years old (A) and > 50 years old (B), respectively. MS: metastatic disease; VS: visceral metastasis; LN: lymph node invasion;

Liver: liver metastasis; Lung: lung metastasis; Brain: brain metastasis; Bone: bone metastasis. "*" $p < 0.05$, comparation of mutation positive rate between metastatic BC (A: grey/B: dart blue) and non-metastatic BC (A: blue/B: green). P values were derived from Fisher's exact.

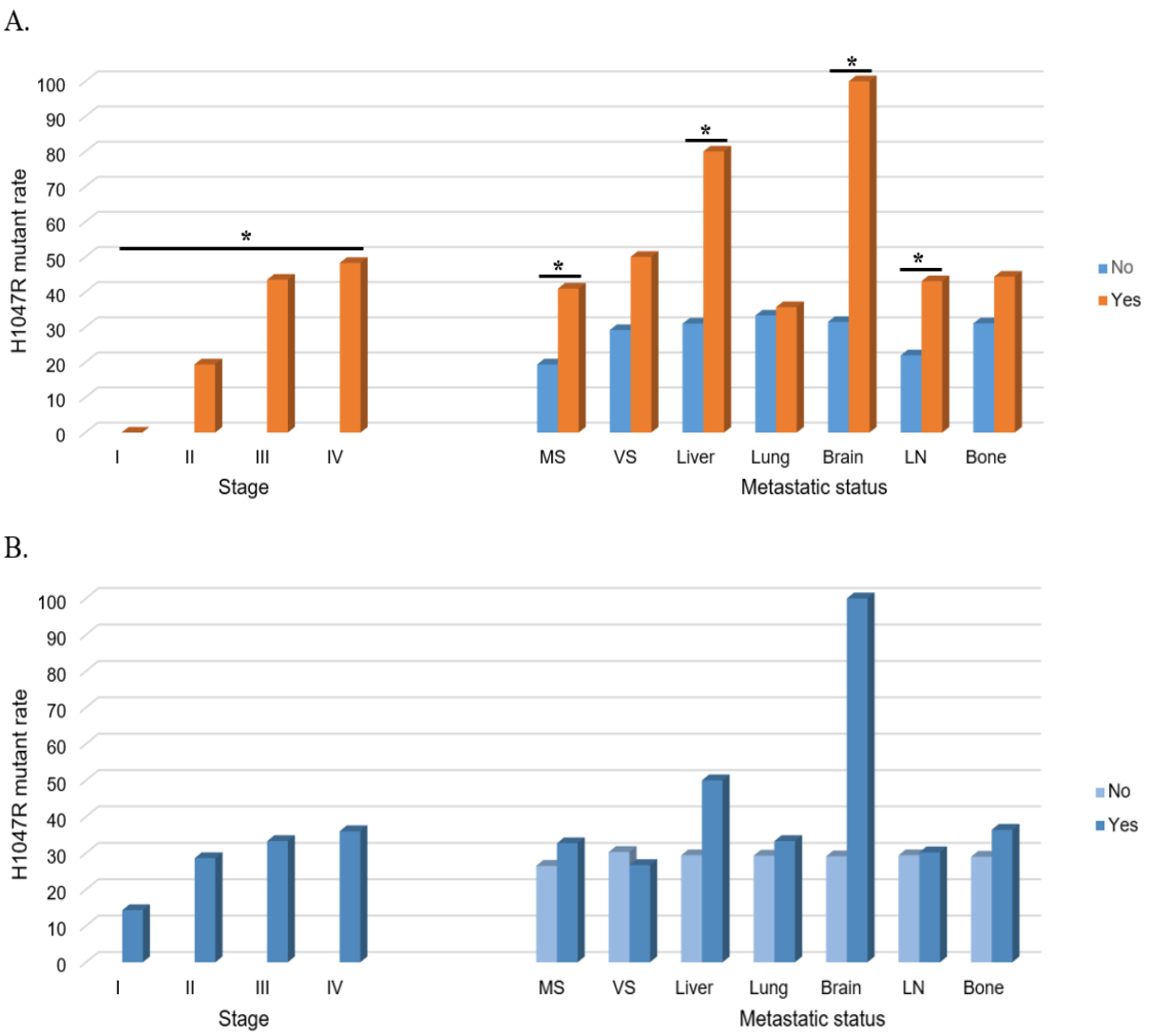

Figure 14. Distribution of the circulating *PIK3CA* H1047R mutation by age groups. The *PIK3CA* mutant frequency in groups ≤ 50 years old (A) and > 50 years old (B), respectively. MS: metastatic disease; VS: visceral metastasis; LN: lymph node invasion; Liver: liver metastasis; Lung: lung metastasis; Brain: brain metastasis; Bone: bone metastasis. * $p < 0.05$, comparation of mutation positive rate between metastatic HR+BC (A: orange/B: dart blue) and non-metastatic BC (A: blue/B: light blue). P values were derived from Fisher's exact.

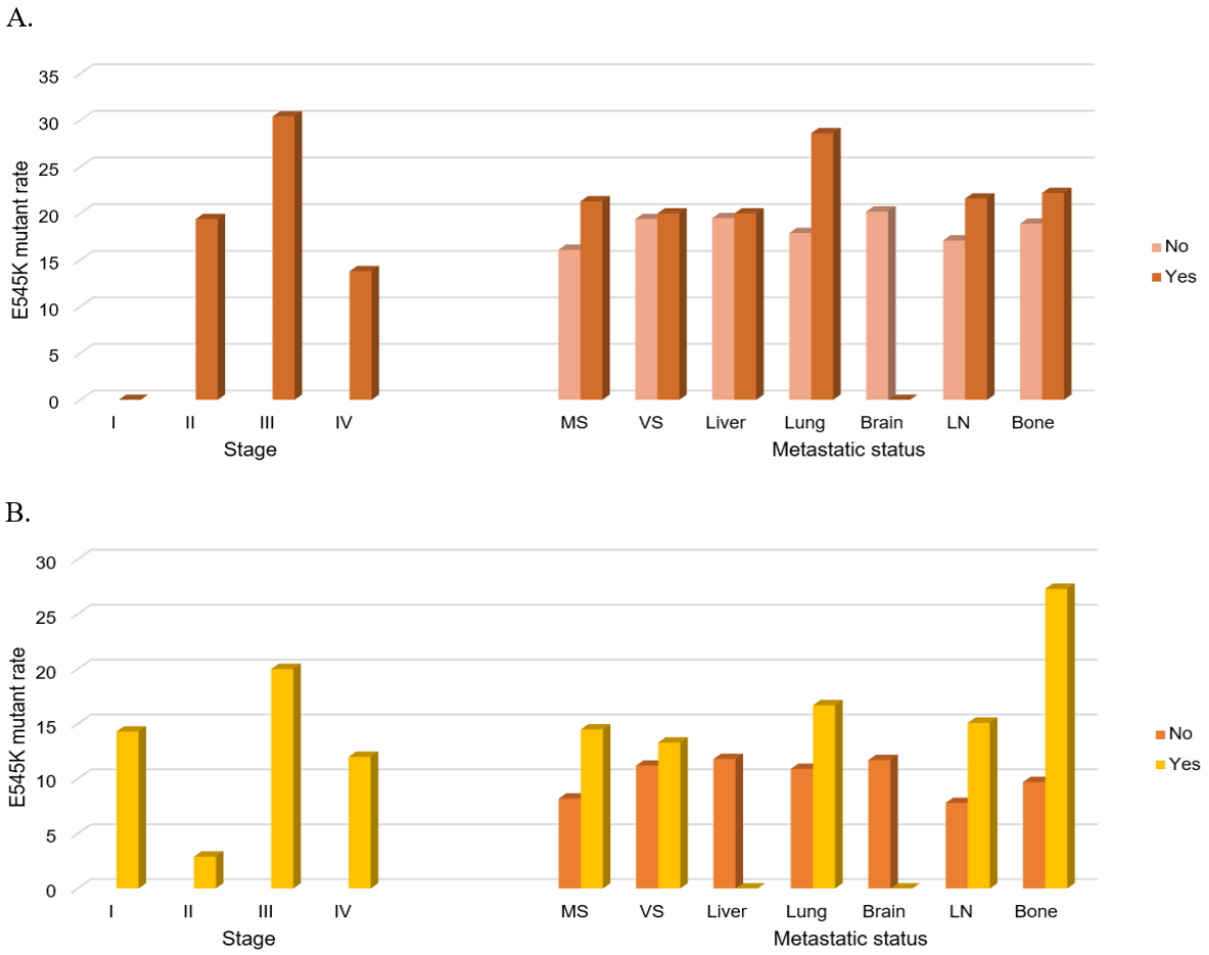

Figure 15. Distribution of the circulating *PIK3CA* E545K mutation by age groups. The E545K mutant frequency in groups ≤ 50 years old (A) and > 50 years old (B), respectively. MS: metastatic disease; VS: visceral metastasis; LN: lymph node invasion; Liver: liver metastasis; Lung: lung metastasis; Brain: brain metastasis; Bone: bone metastasis. $p > 0.05$, comparation of mutation positive rate between metastatic BC (A: red/B: yellow) and non-metastatic BC (A: pink/B: orange). P values were derived from Fisher's exact.

2.4.3 Circulating PIK3CA mutant status and outcomes of metastatic breast cancer

2.4.3.1 Association between PIK3CA hotspot mutations and metastatic breast cancer patients' characteristics

Table 11 displays the results of our clinical analysis of all 54 MBC (stage IV). *PIK3CA* mutation rate was higher in patient with recurrence as well as individuals with multiple metastases than those with single metastases (78.6% vs 21.4%, p = 0.28, and 85.7% vs 14.3%, p = 0.081). There was no association between *PIK3CA* mutation prevalence and baseline clinical variables. As shown in Table 9, the E545K mutation rate was as high as 85.7% (6/7) in MBC with lung metastasis (p = 0.047) and reached 100% (7/7) in MBC with bone metastasis (p = 0.012). Furthermore, patients with brain metastases had a greater prevalence (4/4, 100%) of H1047R mutation (p = 0.028).

Table 11. Characteristics of the circulating *PIK3CA* hotspot mutation in 54 metastatic breast cancers (stage IV BC)

Variable	Total n = 54 (100%)	*PIK3CA*		P-value[#]	E545K		P-value[#]	H1047R		P-value[#]
		Mutant n = 28 (51.9%)	WT n = 26 (48.1%)		Mutant n = 7 (13%)	WT n = 47 (87%)		Mutant n = 23 (42.6%)	WT n = 31 (57.4%)	
Age ($\bar{X}$±SD, years)	53.15 ± 11.68	51.07 ± 13.33	55.38 ± 9.35	0.178	47.86 ± 15.76	53.94 ± 10.95	0.202	51.74 ± 12.36	54.19 ± 11.24	0.45
HR status										
Positive	40 (74.1)	22 (78.6)	18 (69.2)	0.434	6 (85.7)	34 (72.3)	0.451	18 (78.3)	22 (71)	0.545
Negative	14 (25.9)	6 (21.4)	8 (21.4)		1 (14.3)	13 (27.7)		5 (21.7)	9 (29)	
HER2 status										
Positive	31 (57.4)	17 (60.7)	14 (53.8)	0.61	5 (71.4)	26 (55.3)	0.685	14 (60.9)	17 (54.8)	0.658
Negative	23 (42.6)	11 (39.3)	12 (46.2)		2 (28.6)	21 (44.7)		9 (39.1)	14 (45.2)	
Recurrence										
Yes	39 (72.2)	22 (78.6)	17 (65.4)	0.28	5 (71.4)	34 (72.3)	0.96	18 (78.3)	21 (67.7)	0.393
No	15 (27.8)	6 (21.4)	9 (34.6)		2 (28.6)	13 (27.7)		5 (21.7)	10 (32.3)	
The number of metastasis lesion										
< 2	13 (24.1)	4 (14.3)	9 (34.6)	0.081	0 (0)	13 (27.7)	0.11	4 (17.4)	9 (29)	0.322
≥ 2	41 (75.9)	24 (85.7)	17 (65.4)		7 (100)	34 (72.3)		19 (82.6)	22 (71)	
Metastatic sites										
Lymph nodes	44 (81.5)	24 (85.7)	20 (76.9)	0.406	6 (85.7)	38 (80.9)	0.757	20 (87)	24 (77.4)	0.372
Lung	26 (48.1)	14 (50)	12 (46.2)	0.777	6 (85.7)	20 (42.6)	**0.047**[*a]	9 (39.1)	17 (54.8)	0.253
Liver	7 (13)	6 (21.4)	1 (3.8)	0.102[a]	1 (14.3)	6 (12.8)	0.911	5 (21.7)	2 (6.5)	0.122[a]
Brain	4 (7.4)	4 (14.3)	0 (0)	0.112[a]	0 (0)	4 (8.5)	1.00[a]	4 (100)	0 (0)	**0.028**[*a]
Bone	29 (53.7)	17 (60.7)	12 (46.2)	0.284	7 (100)	22 (46.8)	**0.012**[*a]	12 (52.2)	17 (54.8)	0.846

Variable	Total n = 54 (100%)	*PIK3CA*		P-value[#]	E545K		P-value[#]	H1047R		P-value[#]
		Mutant n = 28 (51.9%)	WT n = 26 (48.1%)		Mutant n = 7 (13%)	WT n = 47 (87%)		Mutant n = 23 (42.6%)	WT n = 31 (57.4%)	
Treatment										
Hormone therapy	39 (72.2)	21 (75)	18 (69.2)	0.636	6 (85.7)	33 (70.2)	0.393	17 (73.9)	22 (71)	0.811
Chemotherapy	47 (87)	25 (89.3)	22 (84.6)	0.699[a]	7 (100)	40 (85.1)	0.274	20 (87)	27 (87.1)	1.00
Radiotherapy	23 (42.6)	15 (53.6)	8 (30.8)	0.09	4 (57.1)	19 (40.4)	0.443[a]	13 (56.5)	10 (32.3)	0.075

*Statistically significant value, $p < 0.05$; p-value[#] Mutant versus Wild type (WT); a, Fisher's Exact Test; HER2 - human epidermal growth factor receptor-2; HR - hormone receptor.

2.4.3.2 PIK3CA mutant variants and outcome of metastatic breast cancer

We investigated whether there might be a relationship between progression and detectable plasma *PIK3CA* mutations that were tested by Kaplan-Meier analysis and verified by the log-rank test. There was a tendency toward a shorter time to progression after enrollment (TTP) or PFS in patients with the presence of *PIK3CA* E545K mutation [median TTP: 4.0 months (95% CI 0.0 – 8.8) vs 9.0 months (95% CI 6.3 – 11.7), p = 0.104] (Figure 16B), or in patients with H1047R mutation compared to wild-type participants [median TTP: 7.0 months (95% CI 4.9 – 9.0) vs 13 months (95% CI 4.3 – 21.7), p = 0.085] (Figure 16A). Due to the limited number of genetic alteration events in *PIK3CA* mutant variant, clinical significance analysis was not concluded. In addition, the MBC patients with *PIK3CA* mutation in their cfDNA showed numerically shorter PFS compared to those without the factor [median TTP: 7 months (95% CI 5.0 – 9.0) vs. 15 months (95% CI 7.3 – 22.6), p = 0.022] (Figure 16C). Patients had more *PIK3CA* mutations shown shorter PFS time [median TTP: 15 months (95% CI 7.3 – 22.6) vs. 7 months (95% CI 4.4 – 9.6) vs 4 months (95% CI 0.0 – 8.8), p = 0.049] (Figure 16D).

Univariate Cox regression revealed a significant association between *PIK3CA* mutation and progression-free survival (HR = 2.16; 95% CI 1.07–4.35; p = 0.031). However, after multivariate adjustment, the association weakened and was not statistically significant (HR = 1.58; 95% CI 0.73–3.43; p = 0.245; Table 12), suggesting that *PIK3CA* mutation may not be an independent predictor of progression.

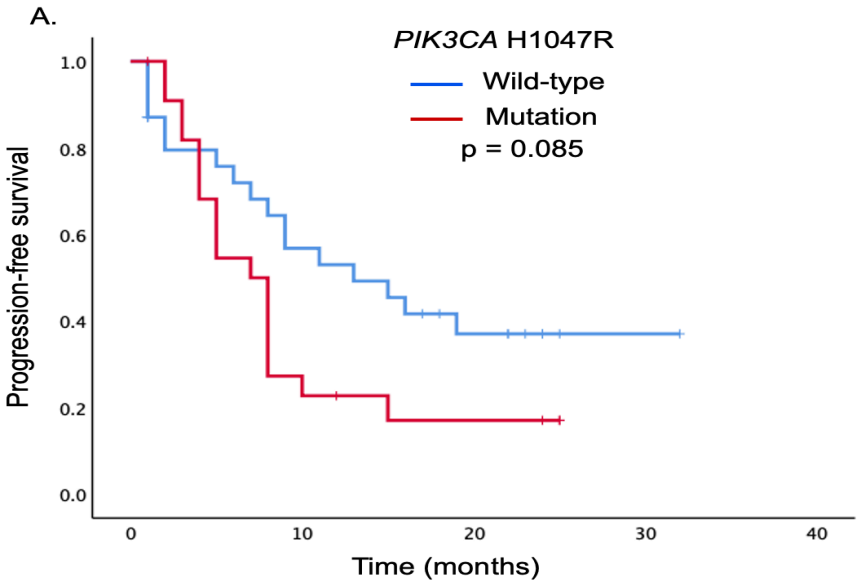
A.
PIK3CA H1047R
Wild-type
Mutation
p = 0.085
Progression-free survival
1.0
0.8
0.6
0.4
0.2
0.0
0
10
20
30
40
Time (months)

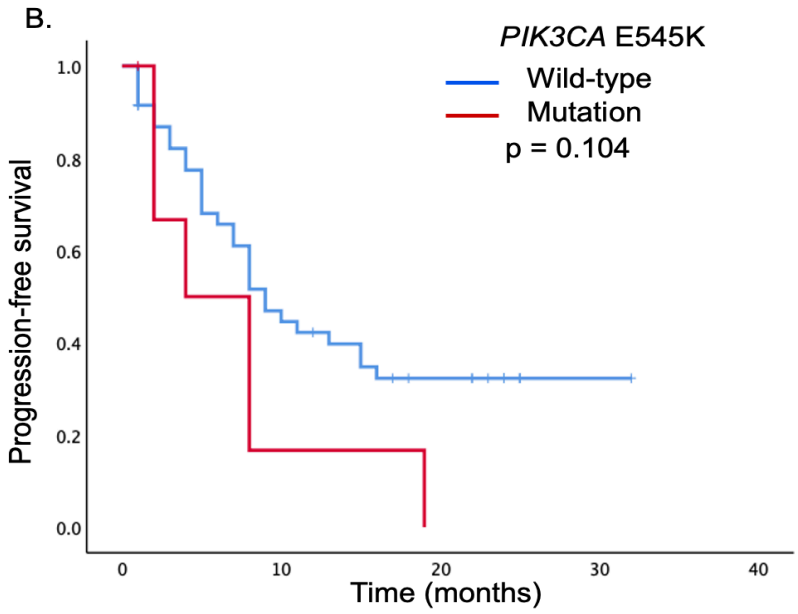
B.
PIK3CA E545K
Wild-type
Mutation
p = 0.104
Progression-free survival
1.0
0.8
0.6
0.4
0.2
0.0
0
10
20
30
40
Time (months)

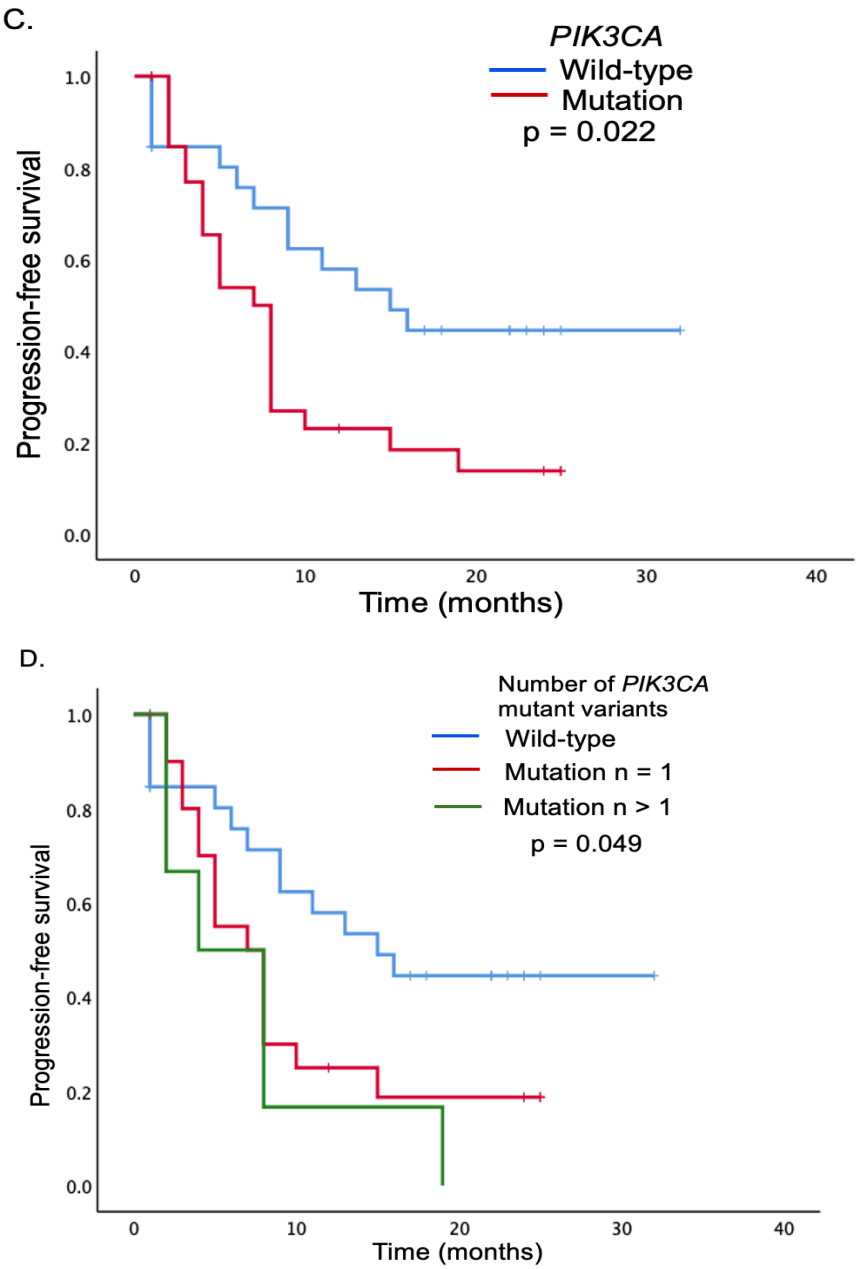

Figure 16. Time to progression after enrollment according to *PIK3CA* mutational status. (A) Time to progression after enrollment according to the presence of *PIK3CA* H1047R mutation, (B) Time to progression after enrollment according to the presence of *PIK3CA* E545K mutation, (C) Time to progression after enrollment according to the presence of *PIK3CA* mutations, (D.) Time to progression after enrollment according to the number of *PIK3CA* mutations.

Table 12. Univariate and multivariate analyses of predictors of progression-free survival among patients with metastatic breast cancer (n=54)

Variables	Univariate analysis		Multivariate analysis	
	HR (95%CI)	**p-value**	**HR (95%CI)**	**p-value**
PIK3CA mutation (mutant vs. wild-type)	2.16 (1.07 – 4.35)	**0.031**	1.58 (0.73 – 3.43)	0.245
Age (≤ 50 vs. > 50 years)	-	-	0.95 (0.41 – 2.18)	0.895
HER2 status (positive vs. negative)	-	-	0.86 (0.41 – 1.85)	0.709
Metastatic number (< 2 vs. ≥ 2)	-	-	0.55 (0.14 – 2.15)	0.387
Lymph node invasion (Yes vs. No)	-	-	1.58 (0.47 – 5.27)	0.458
Visceral invasion (Yes vs. No)	-	-	3.59 (1.36 – 9.51)	**0.010**
Bone invasion (Yes vs. No)	-	-	1.94 (1.79 – 4.77)	0.150
Prior ET (Yes vs. No)	-	-	1.46 (0.60-3.55)	0.41

Abbreviations: HR, hazard ratios; HER2, human epidermal growth factor receptor-2; Statistically significant values ($p < 0.05$) are shown in bold.

2.5 Discussion

Clinical samples are normally heterogeneous in terms of having both tumor and normal cells, or both wild-type and mutant DNA alleles. The mutation load may occasionally be below the detection threshold of diagnostic tools when the disease is at an early stage. Therefore, it is necessary to establish high analytical sensitivity diagnostic tools suitable for deployment in routine diagnostic conditions, especially for patient samples with low DNA quantities obtained from plasma.

Despite using primers specific to mutant sequences, the main disadvantage of allele-specific PCR is that it may result in false positive results due to the generating amplicons of wild-type DNA background or inadequate priming on the wild-type sample. An enhanced method for detecting gene mutations is asymmetric PCR, which employs competitive oligonucleotides and allele-specific priming to prevent the amplification of wild-type alleles used to detect different mutation targets [199, 205, 206]. Over the last decade, nucleic acids have undergone significant modification by substituting different neutral or charged structures for the sugar-phosphodiester backbone or the phosphodiester linker. A few of these modified oligonucleotides exhibit enhanced binding and affinity for DNA and RNA. Locked nucleic acids (LNA), often referred to as bridging nucleic acids (BNA), and peptide nucleic acids (PNA) are two important examples of this novel class of oligomers [207]. Synthetic DNA analogs known as PNAs have a methyl carbonyl linker connecting the purine and pyrimidine bases to repeating units of N-(2-aminoethyl) glycine, which take the role of the phosphodiester backbone. Because of their flexible and uncharged polyamide backbone, PNAs have an exceptionally high affinity and specificity for hybridizing with complementary DNAs. Compared to DNA–DNA hybridization, PNA–DNA hybridization is far more impacted by base mismatches. This significant degree of discriminating at the single base level suggests that great specificity may be possible with short PNA probes [207]. The monomer nucleotides that make up

LNAs are connected by a 2′–4′ methylene bridge. The binding affinity of LNAs for complementary nucleic acids is increased by the entropic constraint provided by the 2′–4′ linker. The LNA bases have improved duplex formation, increased mismatch discrimination, and a better binding strength for complementary sequences according to this changed state. These characteristics improve amplification success when LNAs are added to oligonucleotides and raise duplex melting temperatures, which allow for shorter probes and primers and provide higher specificity [208]. Detection techniques for *PIK3CA* mutations have used PNA/LNA due to their strong affinity for mismatch discrimination [94, 95, 200]. With respect to cost, availability, or enrichment efficiency, each process has advantages and disadvantages of its own. In this study, we examine the use of mutant enrichment with 3′-modified oligonucleotides, a straightforward and useful enrichment approach, for the identification of *PIK3CA* mutations in medical specimens. Similar in principle to PNA/LNA-mediated PCR clamping, this approach substitutes 3′-modified oligonucleotides, which are significantly easier to design and far less expensive than the PNA or LNA. However, in some cases, the blocking of wild-type alleles is not specific enough to generate a significant signal amplification difference between the targets and unwanted alleles. In the case of the *PIK3CA* mutations model, most of the previously reported asymmetric PCR assays hardly acquired enough analytical sensitivity to be robustly implemented in routine clinical diagnostics, especially to detect circulating *PIK3CA* mutations in patients' blood samples. We tactfully designed asymmetric PCR assays with optimized blockers to weakly inhibit the PCR signal of the mutant target while strongly clamping amplification of wild-type sequences, hence leading to the acquisition of 0.1% and 0.01% mutant allele detection limits (LOD) for determining *PIK3CA* E545K and *PIK3CA* H1047H mutations in a DNA cell line model. Most earlier studies did not reveal any methods that were superior to the novel technique mentioned here (Table 3).

With the use of the newly established assay, we identified 42.9% (84/196) of recruited BC patients carrying at least one *PIK3CA* mutation detectable in their plasma. This mutation rate was in accordance with previous findings from other ethnicities [66, 68, 78]. Our *PIK3CA* mutation rate is lower than that of Zongbi Yi 's research (62.5%), Ben Rekaya' s research (61%), Violette Allouchery 's research (55 %), as well as greater than that of Lefebvre C 's research (37%), Kristin Reinhardt 's research (26.7%), Chiya Oshiro' research (22.7%), and results from Takashi Takeshita 's research (24.6%) [65, 69, 71, 107, 209-211]. This appears to be primarily explained by different PCR platforms with varying detection limit, racial genetic differences and sample types, such as tumor tissue, serum, or plasma.

The variation in *PIK3CA* mutation frequencies across studies can be attributed to multiple biological and methodological factors. Across populations, mutation prevalence in BC has been reported to range from 22% to 62%, with higher frequencies typically seen in European cohorts—for example, Ben Rekaya (61%), Violette Allouchery (55%), and Lefebvre C (37%)—compared with Asian studies such as Chiya Oshiro (22.7%) and Takashi Takeshita (24.6%) [65, 69, 71, 107, 209–211]. This discrepancy may reflect genetic and ethnic background differences, as previously observed between Asian, European, and African cohorts [8, 9, 78], as well as differences in clinical stage and subtype composition among study populations.

Sample type also plays a significant role. Studies analyzing tumor tissue DNA generally report higher mutation rates (approximately 35–60%) than those based on plasma or serum cfDNA (typically 20–45%), likely due to the higher tumor DNA fraction in tissue and the dilution of ctDNA in plasma [66, 68, 78, 203]. Nonetheless, plasma cfDNA offers distinct clinical advantages for real-time, noninvasive monitoring and reflects tumor heterogeneity better than single-site biopsies [21, 32–34].

Regarding assay analytical sensitivity, differences in the limit of detection (LOD) directly influence reported prevalence. Conventional PCR-based methods, such as ARMS-PCR or LNA-PCR, typically achieve LODs of 0.5–1%, whereas ddPCR and NGS reach 0.01–0.1%, resulting in a 10–20% increase in detection rates in cfDNA cohorts [69, 139, 194, 203]. Indeed, studies utilizing ddPCR or NGS platforms—such as Julien Corné et al. (60.2%) and Ben Rekaya et al. (61%)—consistently report higher mutation frequencies compared with PCR-only studies (typically 25–40%) [66, 69, 211, 217].

In addition, treatment exposure and disease stage markedly affect observed frequencies. In our cohort, *PIK3CA* mutation rates were significantly higher among fulvestrant-treated HR^+ advanced breast cancer and radiotherapy-exposed patients; specifically, *PIK3CA* E545K was enriched in HR^+ cases receiving radiotherapy, while *PIK3CA* H1047R was more frequent in $HER2^+$ patients undergoing radiation ($p < 0.05$) [1, 2]. Similar enrichment after endocrine therapy or radiation has been described in previous studies, suggesting that therapeutic selection pressure promotes clonal expansion of *PIK3CA*-mutated cells during disease progression [218, 222–225].

Among all samples, *PIK3CA* H1047R mutation was more frequently detected than *PIK3CA* E545K mutation; most *PIK3CA*-mutated patients had monoclonal, and the gene mutations occurred early in the process of tumor development as well as in the patients who develop recurrent or progressive BC, which was consistent with earlier investigations [66, 69, 209, 210, 212, 213]. An analysis by Mariem Ben Rekaya, on the other hand, revealed that *PIK3CA* mutations were more prevalent in exon 9 than in exon 20 in Tunisian women's BC [211].

In our study cohort, the *PIK3CA* mutations were linked to disease progression or worse illness in patients, which is consistent with prior research [84, 213]. The high frequency of *PIK3CA* mutations we observed among stage IV BC with different metastatic sites, especially those with lung invasion, brain metastases, or bone disease ($p < 0.05$). The percentages of *PIK3CA* H1047R and *PIK3CA* E545K

mutations varied according on the metastatic site. *PIK3CA* H1047R mutation was more frequent among brain metastatic disease (100%), and *PIK3CA* E545K was more common among MBC with lung (85.7%) or bone disease (100%). A study reported by Takashi Takeshita et al., the existence of *PIK3CA* mutations in PBC patients was not connected to any particular clinicopathological variables, however *PIK3CA* mutations were linked to visceral invasion in MBC ($p = 0.029$) but not to other clinical features [210].

Our results showed that the *PIK3CA* mutation rates were higher in younger BC with liver invasion (more specifically, the *PIK3CA* H1047R mutation rate in younger patients with liver, brain, or lymph node metastases) than in those without metastatic disease, but they did not differ significantly between metastasized and non-metastasized older individuals. Previous studies revealed that while the *PIK3CA* mutation rate was common in both young and old BC patients, older women had more gene somatic alterations than younger patients [214-217].

In BC, the molecular abnormalities of the PI3K pathway, such as somatic mutations in *PIK3CA*, have significant therapeutic implications. Patients with such *PIK3CA* mutations were believed to be resistant to endocrine, anti-HER2 treatments, chemotherapy [84, 218, 219]. *PIK3CA* mutations have been reported by Doudou Huang et al. to be not only less sensitive to fulvestrant but also to increase cell migration and proliferation [61]. Kristin Reinhardt et al. found that *PIK3CA* mutations had a significantly negative prognostic effect on HR-positive, HER2-negative BC if aromatase inhibitors were the only adjuvant therapy given (adjusted HR 4.44, 95% CI 1.385–13.920), yet no impact was observed in tamoxifen-treated patients [65]. Others discovered that if *PIK3CA* mutations were present, there was a markedly increased endocrine sensitivity to tamoxifen [220]. In a phase 1 study, the hotspot mutation *PIK3CA* H1047R showed to be connected to greater clinical effect from alpelisib than helical domain variants [221]. Double *PIK3CA* mutations in cis (on the same allele) than single mutations have shown increased sensitivity to PI3Kα inhibitor [222]. Additionally, our data

showed that *PIK3CA* mutation rates were significantly higher in FUL-treated HR-positive ABC patients as well as in those who underwent radiotherapy; radio-received HR-positive BC had a higher prevalence of *PIK3CA* E545K, whereas radio-received HER2-positive BC had a higher frequency of the *PIK3CA* H1047R mutation ($p < 0.05$). Our findings support the potential use of cfDNA *PIK3CA* mutations as a tumor marker to inform decisions about treatment.

Kaplan–Meier survival analysis was attempted to estimate whether *PIK3CA* mutations were associated with PFS in MBC patients. Kaplan–Meier curves displayed that the E545K-mutated or H1047R-mutated BC had a tendency for unfavorable PFS when compared to the *PIK3CA*-wildtype; however, the sample size in our study was too small to meet statistical significance ($p > 0.05$). On the other hand, we observed a significant difference in PFS between *PIK3CA*-wild-type and *PIK3CA*-mutanted BC ($p = 0.047$). Thus, the *PIK3CA* mutation might be a poor predictive factor for MBC. Our finding was compatible with the results of a previous study that only *PIK3CA* mutation was independently associated with early recurrence [223].

Although *PIK3CA* mutation was significantly associated with shorter PFS in the univariate analysis, this association was not retained after multivariate adjustment for other clinical factors (HR = 1.58; 95% CI 0.73–3.43; $p = 0.245$). This suggests that *PIK3CA* mutation alone may not serve as an independent prognostic marker in metastatic BC, and its apparent association with disease progression could be confounded by tumor subtype or treatment-related variables. Nevertheless, the observed trend toward poorer outcomes among *PIK3CA*-mutated patients is consistent with previous studies reporting that *PIK3CA* alterations activate the PI3K/Akt/mTOR signaling pathway, leading to enhanced tumor proliferation, survival, and therapy resistance [5-9]. Several clinical trials have further demonstrated that this pathway contributes to endocrine resistance in $HR^+/HER2^-$ advanced BC [17, 113]. From a clinical standpoint, these findings suggest that *PIK3CA* mutation may hold predictive rather than purely prognostic

value, particularly in identifying patients likely to benefit from PI3K inhibitors such as alpelisib [9, 10]. The approval of alpelisib in combination with fulvestrant for *PIK3CA*-mutated $HR^+/HER2^-$ metastatic BC highlights the translational importance of *PIK3CA* testing in guiding treatment selection. Altogether, the current findings indicate that while *PIK3CA* mutation reflects a biologically relevant oncogenic driver, its prognostic effect is context-dependent and may be overshadowed by other clinical and molecular factors in multivariate analyses. Future studies with larger cohorts and integrated molecular profiling will be necessary to refine the prognostic versus predictive implications of *PIK3CA* mutation in BC.

Studies have shown conflicting results about the impact of *PIK3CA* mutational status on survival outcome and relapse free survival (RFS) or PFS in BC. One analysis showed that *PIK3CA* mutations confer a better prognosis in MBC treated with everolimus combined with fulvestrant ($p < 0.05$) [71]. Kalinsky et al. analysis also reported a significant improvement in overall survival ($p = 0.03$) and breast cancer-specific survival ($p = 0.004$) in *PIK3CA*-mutant detected individuals compared with *PIK3CA*-wild-type carriers [220]. There is also evidence showing that *PIK3CA* mutations were associated with considerably longer metastasis-free survival in the overall population ($P = 0.0056$), and especially in the PR-positive and ERBB2-positive subgroups [224]. Similarly, in patients with *PIK3CA*-mutated, HR+/HER2- advanced or MBC, PFS was significantly longer when alpelisib was added to fulvestrant (median PFS 11 months vs. 5.7 months, HR 0.65, $p < 0.0001$) [91]. Recently, a phase 3 trial demonstrated that the addition to palbociclib plus fulvestrant, increased the median PFS (15.0 vs. 7.3 months, HR 0.43, $p < 0.001$) in patients with *PIK3CA*-mutated, HR+/HER2- locally advanced or MBC [225]. Other studies have shown that the detectable circulating *PIK3CA* mutations were highly correlated with a worse PFS ($p < 0.05$) [84, 213, 226]. Yoon Ah Cho et al. also found that *PIK3CA* mutations together inavolisib with c-Met or dMMR/MSI status might be relevant to poor prognosis in BC subsets, especially in Asian women [227]. Important therapeutic

implications result from Flavia R. Mangone et al.'s discovery that *PIK3CA* exon 20 mutation was linked to more aggressive BC and poor outcomes, regardless of treatment approach [228]. Barbareschi and colleagues, on the other hand, found that exon 20 mutation was linked to favorable outcomes, while only *PIK3CA* exon 9 mutation was independently linked to early recurrence and mortality [223]. Nevertheless, research by Violette Allouchery et al. revealed no prognostic or predictive value of *PIK3CA* mutations at the diagnosis of nonmetastatic Inflammatory breast cancer (IBC) [209]. Similarly, several teams have not discovered any noticeable effect of *PIK3CA* mutations on patient outcomes [79, 229]. A meta-analysis [230] of BC in 21 countries in Latin America identified the most studied mutations in the *TP53* and *PIK3CA* genes. *PIK3CA* H1047R was the *PIK3CA* mutation that was most prevalent. Research has shown that resistance to chemotherapy has been related to mutations in the *PIK3CA* gene. Reduced complete tumor regression (pCR) rates in TNBC have been associated with the *PIK3CA* H1047R mutation when treated with anthracycline and taxane neoadjuvant chemotherapy. A less favorable response to neoadjuvant anti-HER2 therapy is caused by a mutation in *PI3KCA* in HER2+ BC diseases. In preclinical research, *PIK3CA* H1047R mutation in *PIK3CA* in HER2+ disease is specifically associated with resistance to HER2-targeted treatments (trastuzumab and lapatinib) and metastatic risk. In HR+/HER2-metastasized cancers, *PI3KCA* mutations had no noticeable impact on clinical outcomes.

PIK3CA and other co-mutations that could be correlated with either increased responses or resistance to PI3Kα inhibitors [222, 231]. In a phase Ib Study of Alpelisib (BYL719), clinical benefit was not seen in ER+/HER2- MBC patients with *PIK3CA* mutations and concomitant alterations in *TP53, KRAS* or *FGFR1* [221]. Concomitant mutations between *PIK3CA* and *TP53*—the most frequent genomic alterations (occurring from 15% to 85%) in different BC subtypes—not only suggested unfavorable features and poor prognosis in BC but also conferred less benefit to neoadjuvant systemic therapy than *TP53* mutations alone [232-234]. Notably, the *PIK3CA* mutated implication on outcome and

responsiveness to PI3K inhibitors was assessed in combination with other gene interactions, including mutations in PI3K pathway members such as *PTEN* and *AKT1* genes. Since the prevalence of *AKT1* mutation is low in BC patients, the impact of AKT1 mutations on the prognosis remains unclear [79, 235, 236]. *PIK3CA* and *PTEN* mutations have been reported to be mutually exclusive in BC [237]. In Stemke-Hale and colleagues' research [79] conducted on 547 human BC tumors and 41 cell lines, *PIK3CA* and *PTEN* mutations were more common than *AKT1* mutations. In the BC cell lines and tumors analyzed herein, *PIK3CA*, *AKT1*, and *PTEN* mutations were also mutually exclusive. *AKT1* mutations may be associated with a favorable outcome, although their small number impeded this from reaching statistical significance. They discovered that an integration of *PIK3CA* mutation and *PTEN* protein loss in HER2-positive BC is an even stronger predictor of the adverse effect on trastuzumab efficacy than either *PIK3CA* mutation or *PTEN* loss alone [79]. Another team found that in the HER2-positive BC population, *PIK3CA* activating mutations and *PTEN* loss were associated with shorter TTP ($p = 0.004$) and with decreased survival ($p = 0.008$) [238]. However, Pérez-Tenorio et al. shown that *PTEN* loss and *PIK3CA* mutations were connected to comparable prognostic variables and were not mutually exclusive occurrences. Furthermore, radiosensitivity was often conferred by *PTEN* loss alone or in conjunction with mutated *PIK3CA* [239]. In a study [240] that sequenced 173 genes in 2,433 primary breast tumors, *PIK3CA* (40.1%) and *TP53* (35.4%) dominated the mutant landscape, followed by five other genes—*MUC16, AHNAK2, SYNE1, KMT2C*, and *GATA3*—had coding mutations in at least 10% of the cases. Mutations in *PIK3CA* and *AKT1* were mutually exclusive (OR=0.017, CI=0.00044–0.1), and there was concomitant mutation between *CDH1* and *PIK3CA* (OR=2.1, CI=1.6–2.9). For patients with ER− tumors, mutations in *PIK3CA* were predictive of outcome (HR=1.4, CI=1.1–1.9), but not for those with ER+ tumors (HR=1.1, CI=0.9–1.3). *PIK3CA* mutations in both the helical and kinase domains were linked to poorer survival in ER-patients. According to Barakeh and

partners [241], *PIK3CA* (12.9%), *BRCA2* (11.7%), and *BRCA1* (10.2%) had the highest mutation rates out of the 51 genes examined. Survival analysis based on the four most common mutations (*BRCA1, BRCA2*, and *PIK3CA*) showed lower survival in *BRCA1* ($p = 0.004$) and *BRCA2*-mutant patients ($p = 0.003$) compared to total patients, despite the fact that there was no difference in survival between patients with and without *PIK3CA* mutations (76.9% vs. 77.3%).

Overall, it seems that the *PIK3CA* mutation is important to predict clinical outcomes in an endocrine-resistant HR-positive metastatic setting, making them valuable for detecting more aggressive BC tumors and predicting how a patient would respond to treatment.

Building on these data, the newly developed cfDNA PCR assay for *PIK3CA* mutations offers a feasible and clinically relevant tool for precision oncology. By enabling minimally invasive genotyping, it provides real-time molecular information that can refine prognostic assessment and assist in identifying patients eligible for PI3K-targeted therapy. In clinical practice, *PIK3CA* testing is recommended for $HR^+/HER2^-$ advanced breast cancer to determine eligibility for PI3K inhibitors such as alpelisib or inavolisib. The integration of cfDNA-based testing into diagnostic workflows can therefore complement tissue genotyping, particularly for patients with inaccessible or insufficient tumor samples.

In Vietnam and other resource-limited healthcare settings, where NGS remains costly and not widely available, the implementation of this optimized PCR-based approach could bridge a critical diagnostic gap. Its low equipment demands, rapid turnaround, and high analytical sensitivity (LOD 0.01–0.1%) make it suitable for routine hospital laboratories. With appropriate clinical validation and quality control, this assay could be incorporated into molecular diagnostic pipelines for therapy selection and disease monitoring, ultimately supporting the personalized treatment of BC patients.

The absence of matched plasma–tumor samples limits the direct validation of cfDNA analysis as a surrogate for tissue genotyping. Nevertheless, prior studies have reported strong concordance between plasma- and tissue-based genotyping in breast cancer [32–34], and plasma-based *PIK3CA* testing is now recognized as a clinically acceptable alternative when tumor tissue is unavailable [21]. Despite this, additional validation in prospectively collected, paired plasma–tumor cohorts remains warranted.

We conducted a cross-sectional study of the *PIK3CA* mutational landscape of patients with BC, whose plasma specimens were analyzed at a single institution. We evaluated the association between the presence of the *PIK3CA* mutation and clinical outcomes in MBC settings. To our knowledge. On the other hand, the current study embeds a number of limitations, including a small patient size in a cross-sectional design and being a single-institute study. Additionally, we only tested for the present of *PIK3CA* gene mutation in blood, this is the first study that has been conducted on plasma samples from Vietnamese BC women *PIK3CA* gene's hotspot mutations, and the method does not provide a quantitative evaluation of initial mutant allele frequency, which is important for quantitative monitoring of patients' responses during a given treatment.

2.6. Conclusion

We successfully established and optimized highly sensitive asymmetric PCR assays integrated with wild-type-specific oligo blockers for the detection of *PIK3CA* hotspot mutations (E545K and H1047R) in plasma cfDNA from breast cancer patients. This method achieved a remarkable LOD, with limits of detection as low as 0.01% for *PIK3CA* H1047R mutation and 0.1% for *PIK3CA* E545K mutation, which is remarkable LOD compared to several previously reported PCR-based approaches. Important enhancements included the careful design of mutant-specific primers and wild-type blockers, the adjustment of annealing temperatures, and the fine-tuning of primer and blocker concentrations. Validation using serial dilutions of positive control DNA demonstrated excellent specificity and reproducibility. Further confirmation through Sanger sequencing reinforced the reliability of the developed assays. Applying the optimized assays to plasma samples from 196 breast cancer patients revealed that 42.9% of cases harbored at least one *PIK3CA* mutation. Notably, the *PIK3CA* H1047R mutation was more prevalent than the *PIK3CA* E545K, aligning with global mutational profiles in BC. Our findings also indicated that *PIK3CA* mutations were significantly associated with advanced disease stages, metastatic burden (particularly liver and brain metastases), and a history of radiation therapy. Furthermore, among hormone receptor-positive patients, those receiving SERDs exhibited higher frequencies of *PIK3CA* mutations, suggesting potential links between therapeutic pressure and mutational selection. Importantly, this method offers several advantages: (1) ultra-high analytical sensitivity allowing detection of low-abundance mutations in cfDNA; (2) relatively simple and cost-effective setup compared to digital PCR or NGS; and (3) potential suitability for routine monitoring of breast cancer progression and treatment response in resource-limited settings. However, despite these promising results, certain limitations remain. The assay currently targets only two major hotspots and may miss rare *PIK3CA* mutations outside of these loci.

In addition, while analytic validation was robust, clinical validation involving longitudinal monitoring of mutation dynamics during therapy is needed to fully establish the clinical utility of this method. In conclusion, the development of this enhanced asymmetric PCR assay represents a meaningful step forward in the non-invasive molecular profiling of breast cancer. It holds significant promise for broader clinical implementation, particularly for real-time surveillance of *PIK3CA* mutations to guide personalized therapeutic strategies. Future work will aim to expand mutation coverage, further validate clinical applicability across different treatment regimens, and integrate this technique into multiplexed platforms for simultaneous detection of multiple relevant genomic alterations.

Chapter 3: Optimization of *ESR1* hotspot mutant detection assays for plasma circulating cell free DNA

3.1 Introduction

Almost two-thirds of initial breast cancers (BC) express hormone receptors (or are HR-positive); endocrine therapy (ET) is the primary method of care for breast cancers in either the early or late stages [242]. A significant obstacle to controlling the growth and metastasis of BC is the fact that most cancers initially respond to treatment but eventually develop resistance (acquired resistance), and about 30% of HR-positive breast tumors do not respond to endocrine treatment (*de novo* resistance) [3]. Endocrine resistance-related mutations have been associated to modifications in the *ESR1* gene, which codes for the ER alpha [41, 243]. In an adjuvant condition, *ESR1* mutations were associated with primary endocrine resistance, especially in patients exposed to aromatase inhibitors, and were detected in 25% to 40% of HR-positive BC patients who underwent relapse and/or metastases [5, 6]. Elacestrant, the first authorized oral selective estrogen receptor degraders (SERDs), may be effective in treating patients with the *ESR1* mutation, despite their poor prognosis [244, 245]. Thus, searching for *ESR1* mutations in advanced BC could assist with personalized endocrine therapy, predicting treatment response, and identifying individuals who are likely to exhibit early ET resistance [245].

In clinical research and molecular analysis, solid biopsies are the conventional method for extracting DNA. However, advanced-stage patients can benefit from plasma cell-free DNA (cfDNA) as a noninvasive diagnostic method that is effortless to repeat, allows for the real-time identification of *ESR1* mutants, and may reveal signs of ongoing metastases along with details about the aggressive disease state [8-10]. Digital PCR (dPCR) and next-generation sequencing (NGS) are the two most widely used laboratory techniques for detecting ctDNA mutations. While dPCR is exceptional in its analytical

sensitivity for detecting hotspot mutations, NGS is a preferred method that may detect broader regions without prior knowledge of the alterations [106, 246-250]. The high cost and complexity of the tests make it challenging to get them to be widely used in clinical practice, despite their value in *ESR1* gene mutation detection. Asymmetric PCR can be used to determine the hotspots mentioned above because codons 538, 537, and 380 contain the majority of the identified *ESR1* gene mutations (more than 80%) [251].

Amplification refractory mutation system PCR (ARMS-PCR) used higher-affinity primers specific to *ESR1*, known as "Super-ARMS" or integrated of Nuclease-assisted Minor Allele Enrichment utilizing Probe Overlap (NaME-PrO) with the ARMS to produce a NAPA (NaME-PrO-assisted ARMS) PCR [136, 137]. Furthermore, a peptide nucleic acid (PNA)-based PCR was designed to boost the analytical sensitivity of detecting polyclonal *ESR1* mutations in cfDNA, yielding a PNA-LNA PCR clamp [138]. These asymmetric PCR techniques have a limit of detection (LOD) of 0.1% to 0.5% and were straightforward to use to detection *ESR1* mutations.

The small proportion of detectable mutations, which is even less than 0.1% of the total amount of cfDNA that can be obtained from patient blood samples, means that the analytical sensitivity is much below the requirements for detecting plasma circulating *ESR1* mutations [139, 140]. Therefore, in order for these tests to be widely used in clinical practice, it is crucial to develop a highly analytical specific and enhanced the LOD as well as reduce their cost.

In the present study, we described ARMS PCR tests that use wild-type blocking to identify plasma circulating *ESR1* hotspot mutations, which are extremely sensitive and specific. We showed that employing an improved method to find *ESR1* gene mutations in clinical samples is both feasible and reliable. These results could assist in establishing a reliable method for identifying ctDNA *ESR1* mutations to inform decisions about personalized therapies.

3.2 Material and methods

3.2.1 Patient enrollment and clinical samples

196 women diagnosed with breast cancer who were recruited from the 108 Military Central Hospital (MCH) between June 2021 and June 2023 were included in this study. Eligible were 148 HR-positive BC individuals who had received ET at any point during the treatment course (66 early BC and 82 advanced BC).

Pathologic specimens were reviewed by designated breast pathologists at the Department of Pathology, Laboratory Center, 108 MCH. Immunohistochemical analysis determined the status of estrogen receptor and progesterone receptor. Nuclear staining ≥ 1% for estrogen receptor and/or progesterone receptor was considered positive. HER2 status was determined by immunohistochemical analysis or FISH if available or if needed for 2+ IHC. Positive HER2 status was determined by immunohistochemical analysis score of 3+ or positive FISH.

Patients who gave written informed consent during the research's enrollment process promptly had their venous blood and clinical or paraclinical data collected. After obtaining venous blood samples using vacuum blood collection and EDTA anticoagulation; the samples were then centrifuged at 2,000 g for 10 minutes at room temperature. The supernatants were collected and frozen prior to cfDNA extraction.

To determine the time to progression (TTP) or progression-free survival (PFS), the period between the date of blood collection and the first progression after enrollment was utilized. Treatment progress was evaluated and recorded either radiographically or clinically by the treating physician. Documentation in the patient's medical file provided the test results.

3.2.2 Plasma processing, DNA isolation, and sample storage

Plasma aliquots of 500 µL were used for getting individual cfDNA using the MagMAX™ Cell-Free DNA Isolation Kit (Thermo Fisher Scientific, USA;

Cat. No. A29319) in accordance with the protocol. The cfDNA samples were extracted and stored in a refrigerator at -80 °C until usage.

Wild-type genomic DNA was isolated from the white blood cells of healthy volunteers using genomic DNA purification kit (Thermo Fisher Scientific, USA; Cat. No. K0512), following the manufacturer's protocol. The isolated DNA was aliquoted and kept at -20°C until needed.

3.2.3 Preparation of control samples for assay validation

Each synthetic gene fragment sequence, known as gBlock® Gene Fragments (gBlock) (Integrated DNA Technologies), was designed to include each specific mutation, which served as positive control for each individual variant. We chose the four most common variants of the *ESR1* gene for breast carcinoma tumor samples from the Catalogue of Somatic variants in Cancer database (COSMIC): D538G, Y537S, Y537N, and E380Q.

Positive samples were blended with 20 ng of genomic DNA from healthy volunteers to provide a set of reference samples with mutation allelic frequencies (MAF) of 10%, 1%, 0.1%, 0.01%, 0.05%, and 0.001%, respectively.

3.3 Optimization of *ESR1* hotspot mutant detection assays

3.3.1 Primers and oligonucleotide design

Based on conventional ARMS primers, we offer the following modifications to enhance the primer's identifying capability and specificity. While the final base at the 3' end of the primer precisely matches the mutant sequence, the subsequent bases from the 5' end of the primer are completely attached to the template sequence. The adjacent base from the 3' end was altered to enhance the detection of the mutant sequence and decrease the primer's affinity for wild-type DNA.

Furthermore, the target sequence was overlapped with oligo clamping (blocker), which has a middle base that exactly fits the wild-type DNA and a 3' end that is phosphorylated to stop polymerase extension in wild-type DNA amplification. Table 13 lists the primers and blockers that were designed.

Table 13. The oligo sequences of clamping-mediated ARMS PCR assays

Oligo name	Sequence (5'-3')	Tm (°C)	Amplicon size (bp)
537/538 wtF	5'-AGCATGAAGTGCAAGAACGTG-3'	63.4	144
537/538 wtR	5'-AGTAGAGCCCGCAGTGG-3'	63	
D538G mtF	5'-AACGTGGTGCCCCTCTAT**TG-3'**	64.1	129
D538G wtR	5'-AGTAGAGCCCGCAGTGG-3'	63	
Y537S mtF	5'-AACGTGGTGCCCCTCT**C-3'**	63.6	129
Y537S wtR	5'-ACGGCTAGTGGGCGCATGTA-3'	67	
Y537N wtF	5'-TCCTTTCTGTGTCTTCCCACCTACA-3'	66.7	98
Y537N mtR	5'-TCCAGCAGCAGGTCA**CT**-3'	62.7	
380 wtF	5'-TGTGGATTTGACCCTCCATG-3'	66.2	120
380 wtR	5'-TTAGGAGCAAACAGTAGCTTCCCTG-3'	67.5	
E380Q mtF	5'-CATGATCAGGTCCACCTTCTA**C**-3'	61.7	72
E380Q wtR	5'-CATGGAGCGCCAGACGAGA-3'	65.9	
537/538 wtBL	5'-TGCCCCTCTATG**A**CCTGCTG-3'	67.1	-
E380Q wtBL	5'-TCCACCTTCTA**G**AATGTGCCT-3'	64.4	-

wtF: wild-type-specific forward primer, wtR: wild-type-specific reverse primer, mtF: mutant-specific forward primer, mtR: mutant-specific reverse primer, wtBL: wild-type-specific blocker

Every oligonucleotide was purchased from the IDT Company in the United States. Thermo Fisher Scientific Inc. (USA) supplied the commercial master mix, nuclease-free water, 6x loading buffers, and dNTPs.

3.3.2 Assessment of cfDNA quality and evaluation of PCR input volume

Using qPCR pre-assessment, the majority of cfDNA samples demonstrated Ct values below 35, confirming adequate quality for mutation analysis. Samples with Ct > 35 were re-extracted from stored plasma to obtain sufficient cfDNA for testing. In addition, we evaluated the potential impact of the cfDNA input volume by performing wild-type–specific PCR reactions on both *ESR1* mutation-negative and mutation-positive samples. The Ct values obtained from these reactions were comparable, indicating that the use of 2 μL cfDNA as PCR input did not introduce

amplification bias and was appropriate for low-concentration cfDNA. These data are summarized in Table 14.

Table 14. Comparison of Ct values from wild-type-specific PCR amplification between *ESR1* mutation–positive and mutation–negative samples

Samples	***ESR1* mutation (Ct value of wild-type-specific PCR amplification)**			
	E380Q	Y537S	Y537N	D538G
Negative (n = 15)	28.44	29.31	28.44	29.38
Positive (n = 15)	30.23	30.30	30.23	31.58
p-value	0.276	0.973	0.679	0.452

3.3.3 To optimize the condition of Asymmetric PCR assays for ESR1 hotspot mutation detection

The ARMS primer was unique to the mutant allele; therefore, it extensively amplified the optimally matched DNA while considerably inhibiting the amplification signal of mismatched target DNA (wild-type DNA). The addition of wild-type-specific oligo clamping that is bound to wild-type sequences improves the ability to restrict false-positive amplification signals while enhancing assay analytical sensitivity (Figure 17).

The experimental conditions were optimized in detail for the annealing temperature, time, and concentration of the primers, concentration of the blockers, and buffer (data not shown). We used synthetic oligonucleotide sequences for each individual *ESR1* mutation as a positive control and gDNA from healthy donors as a wild-type DNA control.

The higher the reaction temperature, the greater the analytical specificity, yet the lower the reaction analytical sensitivity, so the temperature was adjusted to maximize the reaction's analytical specificity while maintaining analytical sensitivity. In mixture with blockers, a number of primer sequences with varying Tm were generated that performed well with primers, and the blocker that most

effectively inhibited wild-type amplification while having minimal effect on mutant amplification was selected (data not shown).

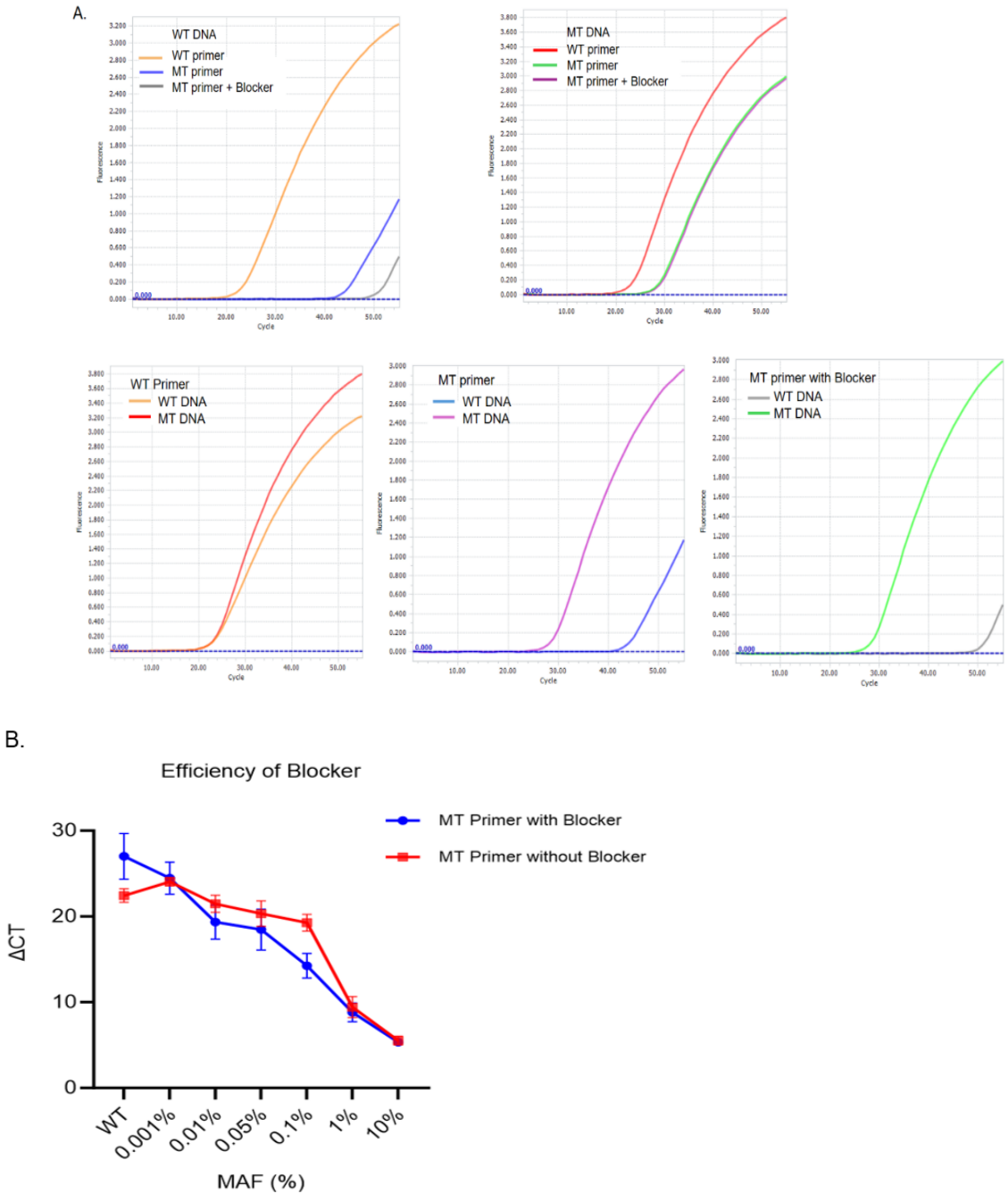

Figure 17. The efficiency of clamping-mediated ARMS PCR assays for *ESR1* mutation detection assays. A. Evaluation of ARMS primer and blocker performance to identify the *ESR1* D538G mutaion. Upper panel: Amplification of the *ESR1* mutant DNA (right) and wild-type DNA (left) under different conditions: wild-type specific primer (WT primer, orange and red lines), mutant specific primer (MT primer, blue and green lines), mutant specific primer with blocker

(MT primer with blocker, grey and purple lines). Lower panel: Amplification of *ESR1* mutant DNA (MT DNA, red line, pink line, green line) versus wild-type DNA (WT DNA, orange line, blue line, grey line) under different conditions: reactions using WT primer (left figure), reactions using MT primer (middle figure), reactions using MT primer with blocker (right figure). B. Evaluation of blocker performance to identify the *ESR1* E380Q mutation with different mutant allele frequencies (MAF). Relative amplification of the clamping-mediated ARMS PCR for detecting the *ESR1* E380Q mutation with different MAFs of 10%, 1%, 0.1%, 0.01%, 0.05%, 0.001%, and 0% was reported as ΔCt. The blue line indicates ΔCt values that were computed as the difference between Ct-1 and Ct-2 (Ct-1 and Ct-2 were values of the analogous target amplification using WT primer or MT primer, respectively). The red line indicates ΔCt values that were computed as the difference between Ct-1 and Ct-3 (Ct-1 and Ct-3 were values of the analogous target amplification using WT primer or MT primer with blocker, respectively).

3.3.4 Real-time PCR amplification and detection of ESR1 mutations

The LightCycler 96 real-time PCR device was used for PCR. Thermal cycle mode: 10 minutes at 95 ℃, followed by 50 cycles of 15 seconds at 95 ℃, 30 seconds at 58-62 ℃, and 15 seconds at 72 ℃. Each PCR reaction was done in a final volume of 10 µl, using 2X Universal PCR Master Mix (no UNG) TM (SYBR™ Green; Applied Biosystems, Thermo Fisher Scientific, USA; Cat. No. 4344463), 2 µl each primer, 2 µl oligo clamping, and 2 µl of input DNA. A SYBR fluorescence signal was detected, and the data were processed using the appropriate software.

3.3.5. Validation of the ESR1 mutation detection assays

In accordance with the manufacturer's instructions, the amplicons were sequenced using a 3130 XL Genetic analyzer (Applied Biosystems) and a Big Dye Terminator v3.1 Cycle Sequencing kit (Applied Biosystems, Thermo Fisher Scientific, USA; Cat. No. 4337455) for additional confirmation. Confirmation of *ESR1* hotspot mutations by Sanger sequencing shown in Figure 18. The amplicons

from 120 bp to 150 bp surrounding the targeted mutant variants were intended to be amplified using sequencing primers (Table 13).

A. D538G (T>C)

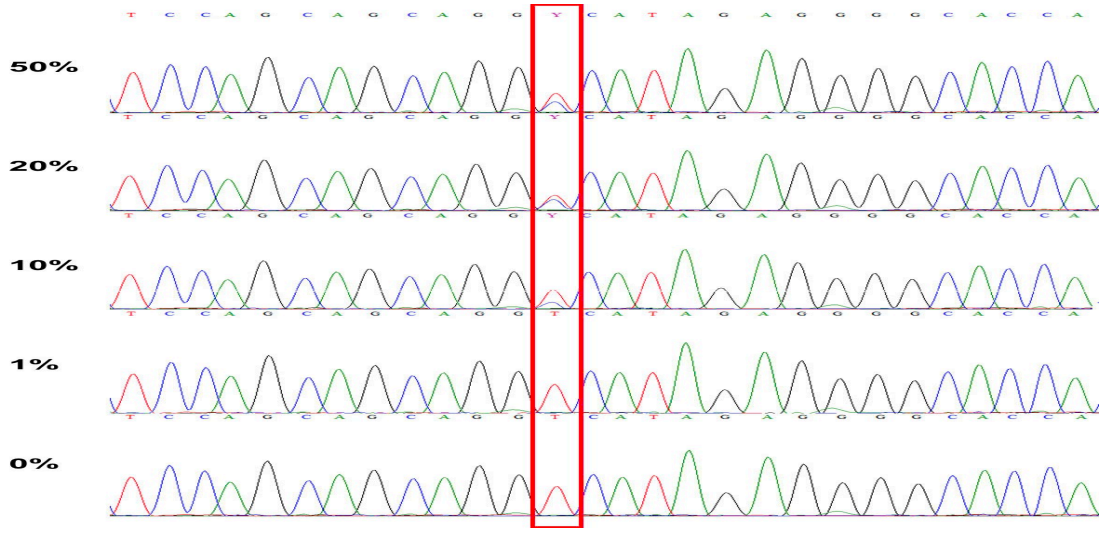

B. E380Q (C>G)

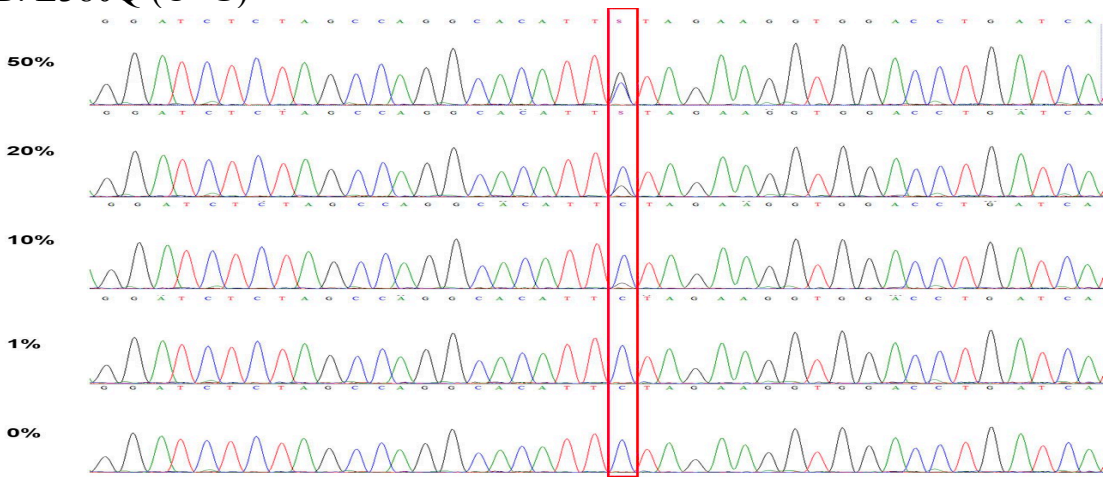

C. Y537S (T>G)

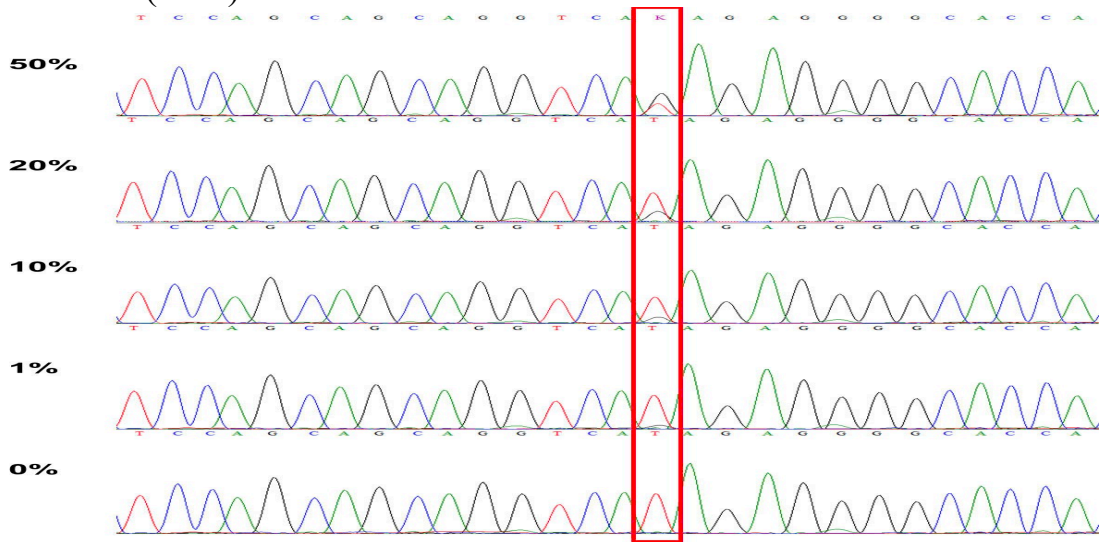

D. Y537N (A>T)

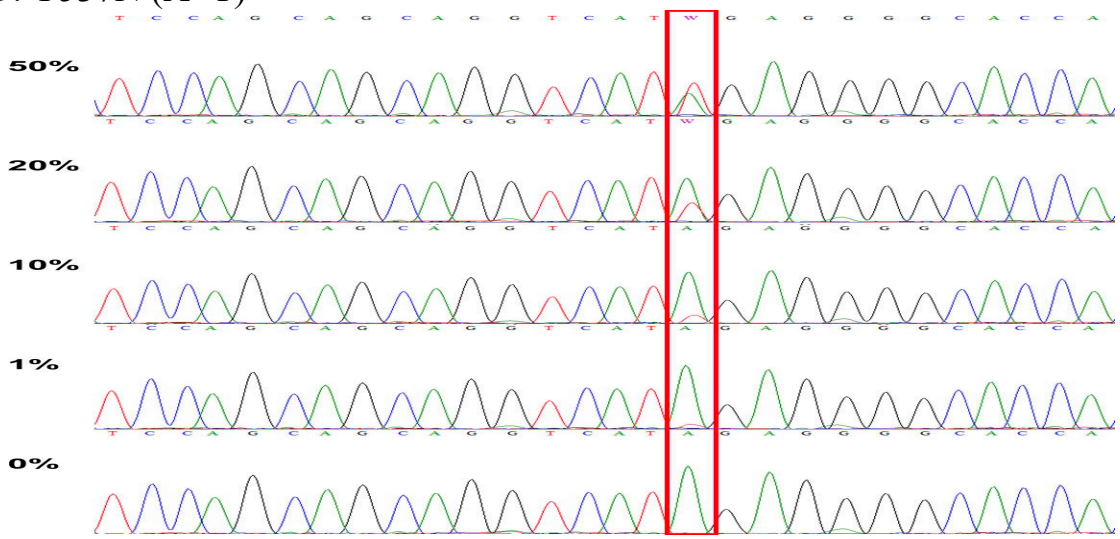

Figure 18. Confirmation of *ESR1* hotspot mutations by Sanger sequencing

(A): Sanger sequencing results of dilution series control samples with D538G (T>C) mutant concentrations of 0%, 1%, 10%, 20%, and 50%. (B): Sanger sequencing results of dilution series control samples with E380Q (C>G) mutant concentrations of 0%, 1%, 10%, 20%, and 50%. (C): Sanger sequencing results of dilution series control samples with Y537S (T>G) mutant concentrations of 0%, 1%, 10%, 20%, and 50%. (D): Sanger sequencing results of dilution series control samples with Y537N (A>T) mutant concentrations of 0%, 1%, 10%, 20%, and 50%.

3.3.6 Statistical analyses

The statistical analysis was carried out using IBM SPSS Statistics version 25.0 (Armonk, NY, USA). We employed chi-square tests and Fisher's tests to analyze the correlation between *ESR1* mutations and clinicopathological characteristics in BC patients. Progression-free survival (PFS) was calculated as the time from enrollment to any local recurrence, or distant metastasis event. The Kaplan-Meier method was used to estimate the PFS, followed by a log-rank or Wilcoxon test for comparison among subgroups; variables associated with PFS were also assessed by Cox proportional hazard model. A p-value of < 0.05 was judged significant. Graphics were created using MS Excel 2010 (Microsoft Corporation, USA), Prism 10.0.0 (GraphPad).

3.4 Results

3.4.1 Detection limit optimization for the ESR1 mutation detection assays

DNA mixtures were prepared through serial dilutions of MT gBlocks in a constant wild-type gDNA background to reach theoretical MAFs of 10%, 1%, 0.1%, 0.01%, 0.05%, 0.001%, and 0% served as input templates of the corresponding real-time PCR experiments (Figure 19). The real-time PCR settings and data evaluation approaches are identical for the identification of all four *ESR1* mutations. Experiments were repeated 15 times to identify each independent positive sample. It was determined that the clamping-mediated ARMS PCR could be identified accurately when the relative amplification of the mutant allele was statistically significantly lower than that of wild-type DNA. Sensitivities of *ESR1* assays were 0.01% for E380Q, 0.05% for D538G, 0.05% for Y537S, and 0.1% for Y537N, as only assays with a p-value < 0.05 are considered statistically significant (Figure 20).

A. E380Q

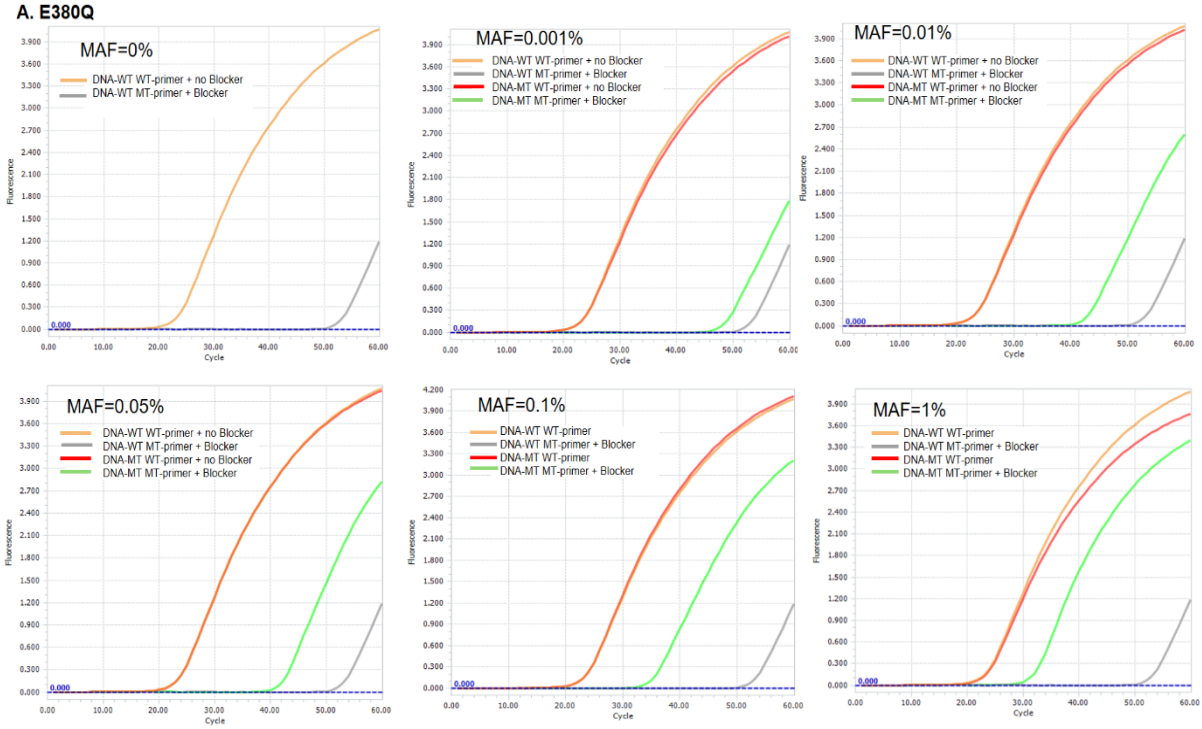

B. Y537N

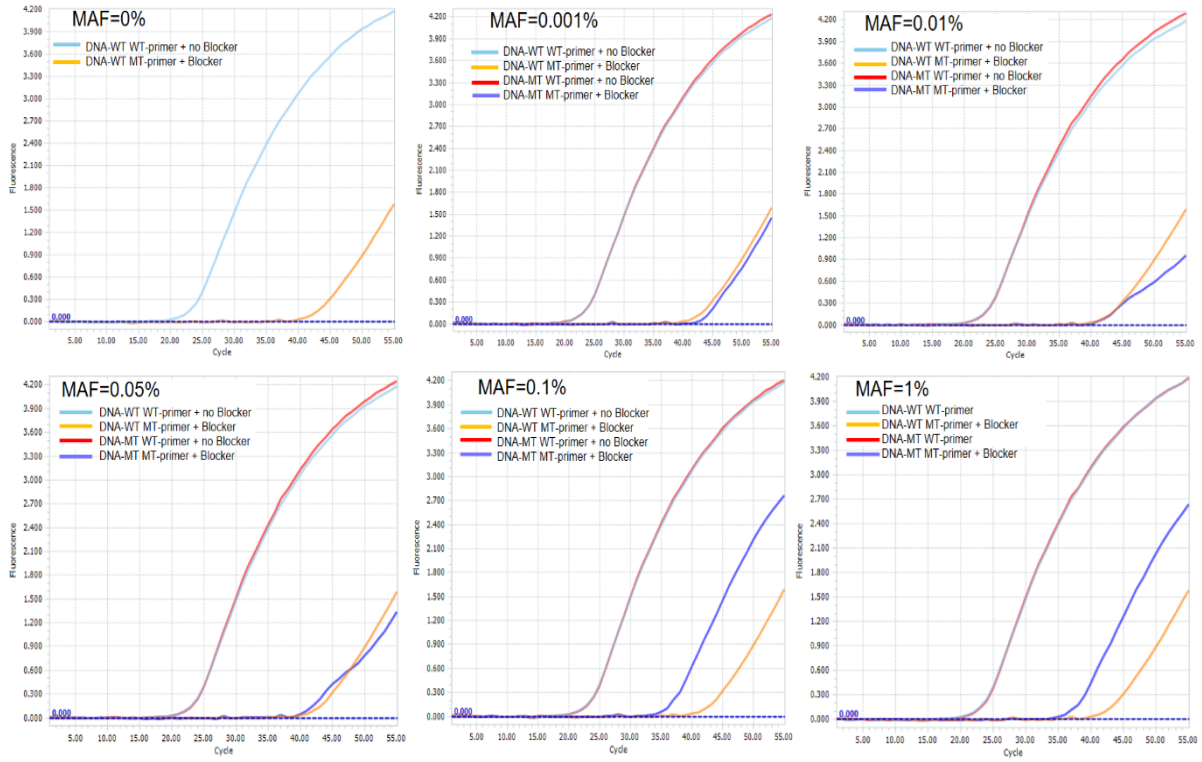

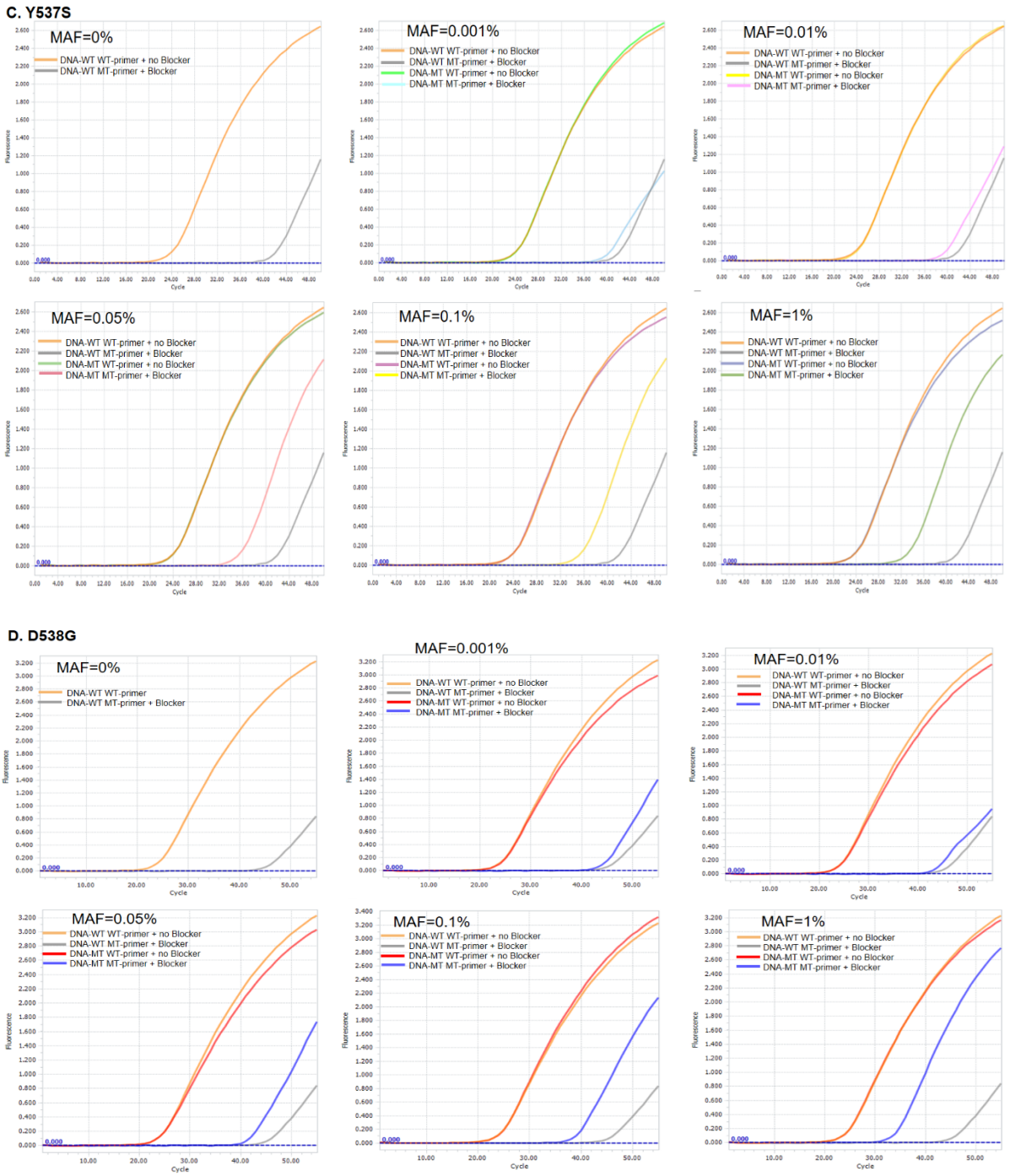

Figure 19. Dilution series of asymmetric PCR curves for the *ESR1* mutation detection. All four *ESR1* mutations (A. E380Q, B. Y537N, C. Y537S, and D. D538G) can be identified using the same real-time PCR conditions and data assessment techniques. The use of wild-type specific primer (WT-primer without blocker) or mutant specific primer and blocker (MT-primer + Blocker) to amplify wild-type DNA (DNA-WT) or various mutant DNA (DNA-MT) at concentrations of 10%, 1%, 0.1%, 0.01%, 0.05%, and 0.001%.

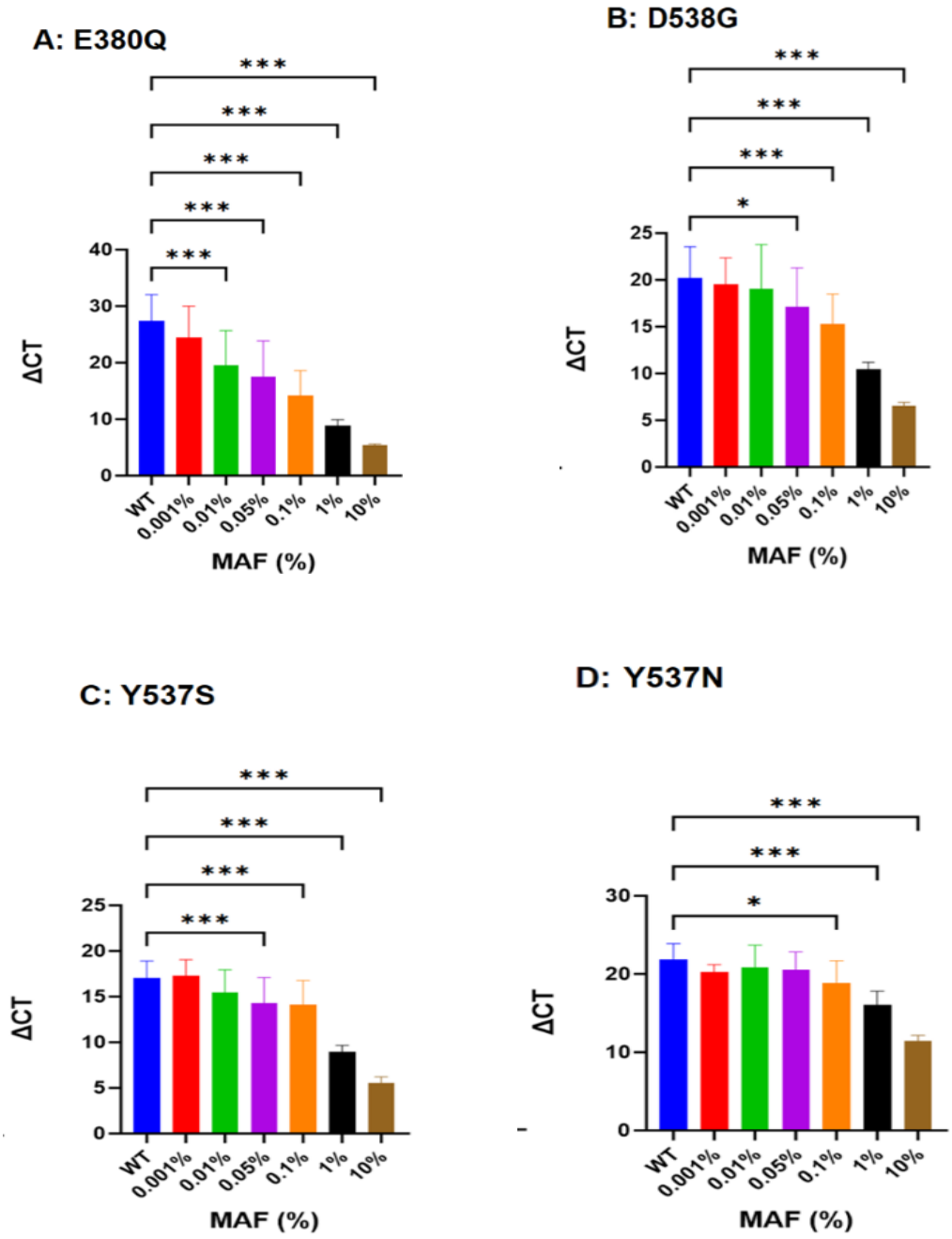

Figure 20. The detection limit of clamping-mediated ARMS-PCR assays for the *ESR1* mutation detection. To get diminishing ratios of mutant (MT) to wild-type (WT) DNA, the pool of mutant DNA carrying the mutation sequence was continuously decreased. MAF: mutant allele frequencies. ΔCt values are defined as Ct values of reaction using MT primer with blocker compared to analogue DNA amplification using WT primer. Reactions were carried out 15 times. ***P < 0.001, **P < 0.01, and *P < 0.05 compared to 0% mutant load (or wild-type DNA).

3.4.2 Application of the ESR1 mutation detection assays on clinical samples

After the optimization and analytical validation, the developed assays were applied in 148 HR-positive BC (66 early BC and 82 advanced BC) plasma samples.

The mean age of the early BC (EBC) group was 53.64 ± 12.78 years. Of these, 81.8% (54/66) had stage II diseases, 18.2% (12/66) had stage I tumors, 21.2% (14/66) had lymph node invasion, and 56.1% (37/66) had HER2-positive tumors (Table 15). Additionally, 18 out of 66 (27.3%) received Tamoxifen (TAM), and 39.4% (26/66) received Aromatase inhibitor (AI), 62 out of 66 (93.9%) received surgery, 13 out of 66 (19.7%) treated with radiation, 60 out of 66 (90.9%) treated with chemotherapy prior to enrollment (Table 15). Eleven patients (16.7%) had *ESR1* hotspot mutations, with Y537S (7/11) having the highest frequency, followed by Y537N (6/11), Y538G (4/11), and E380Q (2/11) (Figure 21). All *ESR1* mutations were found in stage II BC patients and 5 cases had multiple *ESR1* hotspot mutations (Table 15, Figure 21). Furthermore, there was no relationship between the presence of *ESR1* mutations and the clinical features of the patients ($p > 0.05$).

The advanced BC (ABC) group had a mean age of 52.29 ± 14.37 years. Of these, 34.1% (28/82) of patients had recurrence, 51.2% (42/82) were locally ABC, and 48.8% (40/82) were classified as stage IV (Table 16). Additionally, 26 out of 82 (31.7%) received TAM, 25.6% (21/82) received FUL, and 37.8% (31/82) received AI prior to enrollment. *ESR1* hotspot mutations were found in 49 (59.8%) patients (Table 16), with the highest occurrence being Y537S (44/49), followed by Y537N (31/49), Y538G (21/49), and E380Q (14/49) (Figure 20). Thirty-five individuals had multiple *ESR1* mutations (Figure 20). *ESR1* mutations were more common in patients with at least one metastatic site (lymph node, lung, bone, liver, brain, bone) or those treated with endocrine therapy, chemotherapy or radiotherapy. On the other hand, there was no correlation between *ESR1* mutant occurrence and patients' clinial characteristics ($p > 0.05$) (Table 16).

The *ESR1* E538Q mutation was detected at the lowest rate, whereas the *ESR1* Y537S mutation was the most prevalent in both young and old ABC patient groups. The majority of patients with *ESR1* mutations were polyclonal in both the over-50 and under-50 groups (Figure 22). The rate of *ESR1* mutations was higher in ABC patients under 50 with lung, liver, and brain metastases and in ABC patients over 50 years old with lymph node, lung, and brain metastases. However, there was no significant difference in mutation rate between the metastatic and non-metastatic groups (Figure 23).

Table 15. Characteristics of early BC patients with detected-*ESR1* mutant compared to undetected-*ESR1* mutant patients

Characteristic	Total n = 66 (100%)	*ESR1* mutant status		p-value[a]
		Positive n = 11 (16.7%)	Negative n = 55 (83.3%)	
Age ($\bar{X}$±SD, years)	53.64 ± 12.78	52.45 ± 8.2	53.87 ± 13.56	0.74
HER2 - positive	37 (56.1%)	4 (36.4%)	33 (60%)	0.149
Stage				
I	12 (18.2%)	0 (0%)	12 (21.8%)	0.087
II	54 (81.8%)	11 (100%)	43 (78.2%)	
Metastatic sites				
Lymph node	14 (21.2%)	4 (36.4%)	10 (18.2%)	0.178
Received therapy				
Endocrine therapy	40 (60.6%)	5 (45.5%)	35 (63.6%)	0.26
Tamoxifen	18 (27.3%)	1 (9.1%)	17 (30.9%)	0.138
AI	26 (39.4%)	4 (36.4%)	22 (40%)	0.822
Surgery	62 (93.9%)	10 (90.9%)	52 (94.5%)	0.527*
Chemotherapy	60 (90.9%)	10 (90.9%)	50 (90.9%)	1.000
Radiotherapy	13 (19.7%)	4 (36.4%)	9 (16.4%)	0.128
Her2-target therapy	20 (30.3%)	3 (27.3%)	17 (30.9%)	0.811

"*" Fisher's Exact Test; "a" Mutant vs wild-type; AI: aromatase inhibitor

Table 16. Characteristics of advanced BC patients with detected-*ESR1* mutant compared to undetected-*ESR1* mutant patients

Characteristic	Total n = 82 (100%)	*ESR1* mutant status		p-value[a]
		Positive n = 49 (59.8%)	Negative n = 33 (40.2%)	
Age ($\bar{X}$±SD, years)	52.29 ± 14.37	52.63 ± 14.04	55.7 ± 14.21	0.881
Stage				
III	42 (51.2%)	24 (49%)	18 (54.5%)	0.621
IV	40 (48.8%)	25 (51%)	15 (45.5%)	
HER2 status				
Positive	40 (48.8%)	24 (49%)	16 (48.5%)	0.965
Negative	42 (51.2%)	25 (51%)	17 (51.5%)	
Recurrence	28 (34.1%)	17 (34.7%)	11 (33.3%)	0.899
Number of metastatic locations				
1	50 (61%)	23 (46.9%)	23 (69.7%)	0.125
≥2	32 (39%)	23 (46.9%)	9 (27.3%)	
Metastatic sites				
Lymph node	71 (86.6%)	44 (89.8%)	27 (81.8%)	0.299
Lung	16 (19.5%)	12 (24.5%)	4 (12.1%)	0.166
Bone	24 (29.3%)	16 (32.7%)	8 (24.2%)	0.412
Brain	4 (4.9%)	4 (8.2%)	0	0.145*
Liver	6 (7.3%)	4 (8.2%)	2 (6.1%)	1.000*
Received therapy				
ET	66 (80.5%)	40 (60.6%)	26 (39.4%)	0.750
Tamoxifen	26 (31.7%)	16 (32.7%)	10 (30.3%)	0.823
Fulvestrant	21 (25.6%)	13 (26.5%)	8 (24.2%)	0.816
AI	31 (37.8%)	18 (36.7%)	13 (39.4%)	0.808
Chemotherapy	68 (82.9%)	42 (85.7%)	26 (78.8%)	0.414
Radiotherapy	33 (40.2%)	20 (40.8%)	13 (39.4%)	0.898
Her2-targeted	19 (23.2%)	12 (24.5%)	7 (21.2%)	0.730

"*" Fisher's Exact Test; "a" Mutant vs wild-type; ET: endocrine therapy; AI: aromatase inhibitor

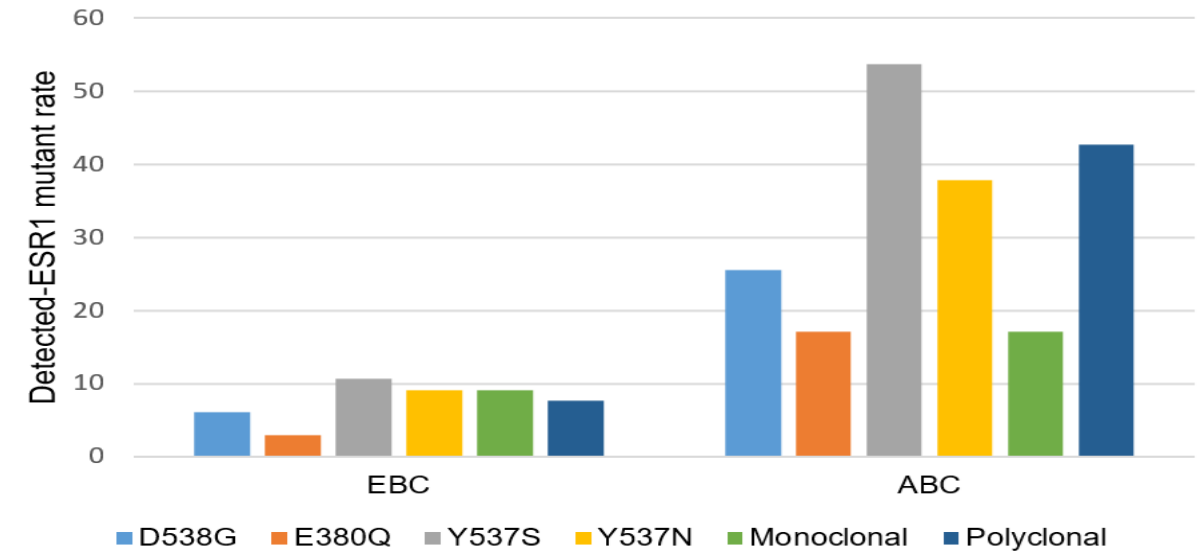

Figure 21. Percentage of detected *ESR1* mutations in HR-positive BC patients.

EBC: early breast cancer, ABC: advanced breast cancer

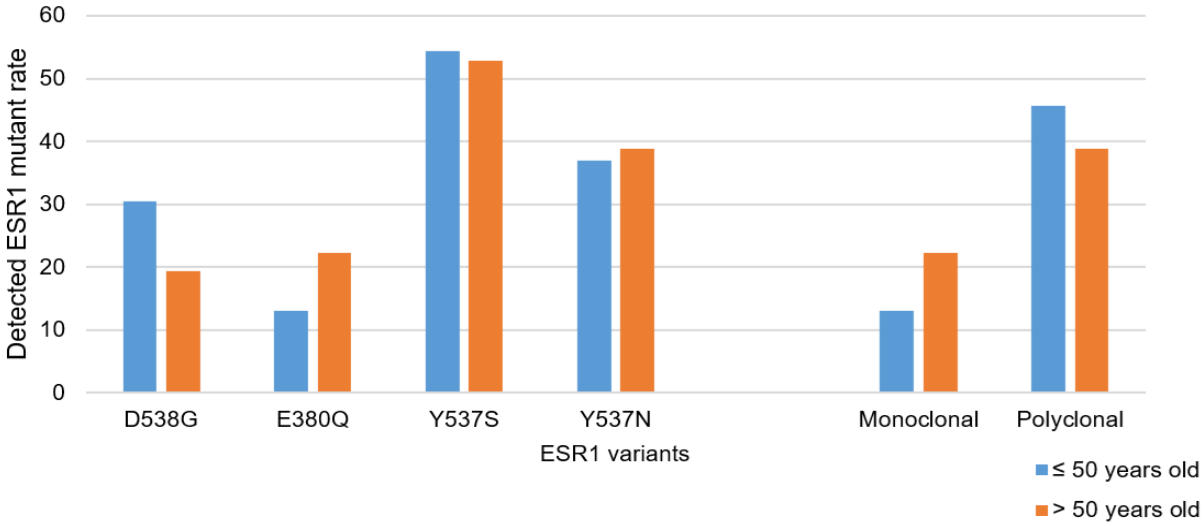

Figure 22. Characteristic of the circulating *ESR1* mutations by age groups.

The *ESR1* mutant frequency in HR-positive ABC patients under 50 years old (blue) and over 50 years old (orange), respectively.

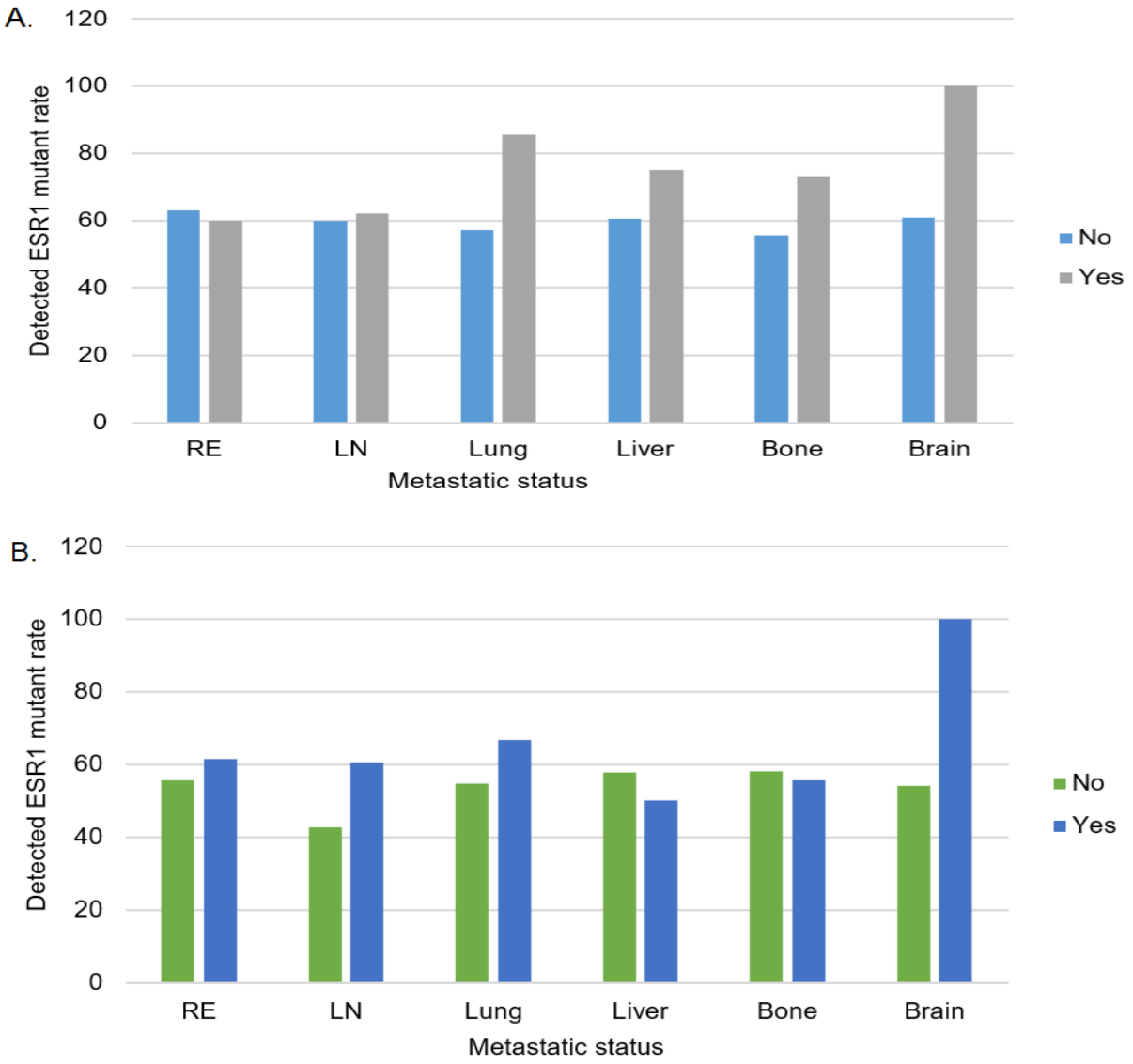

Figure 23. Distribution of the circulating *ESR1* mutations by age groups.

The *ESR1* mutant frequency in ABC patients under 50 years old (A) and over 50 years old (B), respectively. RE: recurrence; LN: lymph node invasion; Lung: lung metastasis; Liver: liver metastasis; Bone: bone metastasis; Brain: brain metastasis. "*" $p < 0.05$. No: non-metastasis, Yes: metastasis.

3.4.3 Circulating ESR1 mutant status and outcomes of HR-positive metastatic breast cancer

3.4.3.1 Association between ESR1 hotspot mutations and HR-positive metastatic breast cancer patients' characteristics

The HR-positive MBC patients' characteristics were summarized in Table 13. *ESR1* mutations were detected in 62.5% (25/40) of HR-positive MBC patients; of these, 5 out of 25 (20%) had a single *ESR1* mutant variant, and 20 out of 25 (80%) had multiple *ESR1* mutations. Only 18 out of 40 *ESR1* positive cases (45%) received AI, 25% and 50% previously or ongoing treated TAM or FUL, respectively (Table 17). Patients undergone endocrine therapy, particularly AI, or those with numerous metastatic sites, as well as those with lung or brain metastases, were more likely to have *ESR1* mutations. However, the presence of the *ESR1* mutations and the mentioned features did not correlate ($p > 0.05$) (Table 17, Figures 24-27).

Table 17. Characteristics metastatic BC patients with detected-*ESR1* mutant compared to undetected-*ESR1* mutant patients

Characteristic	Total n = 40 (100%)	*ESR1* mutant status		p-value[a]
		Positive n = 25 (62.5%)	Negative n = 15 (37.5%)	
Age ($\bar{X}$±SD, years)	53.23 ± 16	52.6 ± 16.43	54.27 ± 15.78	0.754
HER2-positive	22 (55%)	15 (60%)	7 (46.7%)	0.412
Recurrence	25 (65.6%)	16 (64%)	9 (60%)	0.8
Number of metastatic locations				
1	13 (32.5%)	6 (24%)	7 (46.7%)	0.138
≥2	27 (67.5%)	19 (76%)	8 (53.3%)	
Metastatic sites				
Lymph node	35 (87.5%)	22(88%)	13 (86.7%)	1.000*
Lung	16 (40%)	12 (48%)	4 (26.7%)	0.182
Bone	23 (57.5%)	15 (60%)	8 (53.3%)	0.68
Brain	4 (10%)	4 (16%)	0 (0%)	0.278*
Liver	6 (15%)	4 (16%)	2 (13.3%)	1.000*
Received therapy				
ET	39 (97.5%)	25 (100%)	14 (93.3)	0.375
Tamoxifen	10 (25%)	6 (24%)	4 (26.7%)	0.85
Fulvestrant	20 (50%)	12 (48%)	8 (53.3%)	0.744
AI	18 (45%)	12 (48%)	6 (40%)	0.622
Chemotherapy	31 (77.5%)	20 (80%)	11 (73.3%)	0.625
Radiotherapy	15 (37.5%)	9 (36%)	6 (40%)	0.800
Trastuzumab	12 (30%)	9 (36%)	3 (20%)	0.285

"*" Fisher's Exact Test; "a" Mutant vs wild-type; ET: endocrine therapy; AI: aromatase inhibitor

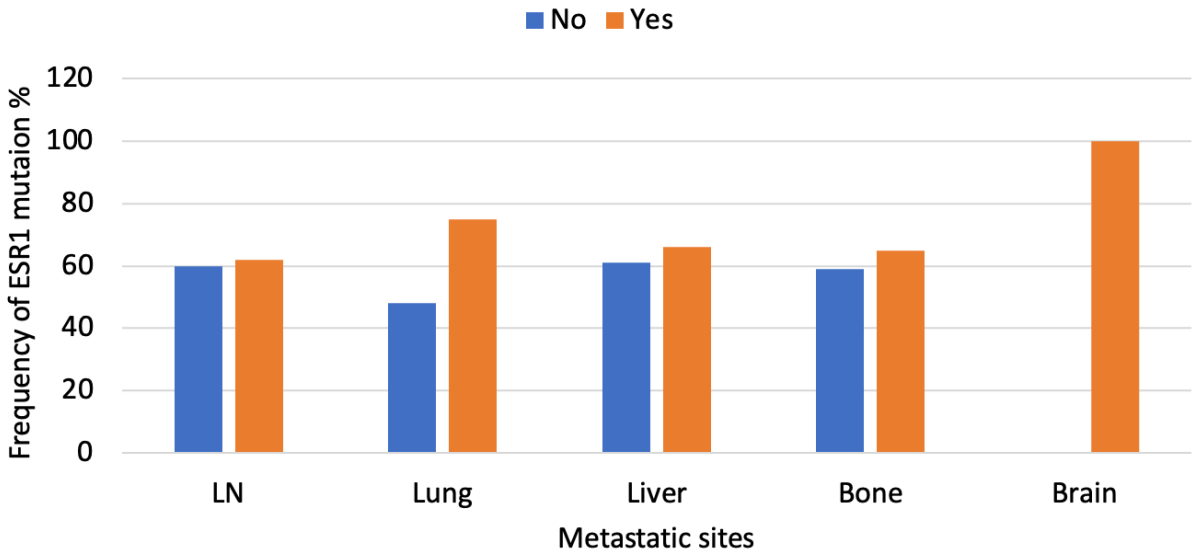

Figure 24. Distribution of *ESR1* mutations in HR-positive MBC patients based on metastatic sites. LN: lymph node invasion; Lung: lung metastasis; Liver: liver metastasis; Bone: bone metastasis; Brain: brain metastasis. No: non-metastasis, Yes: metastasis. "*" $p < 0.05$.

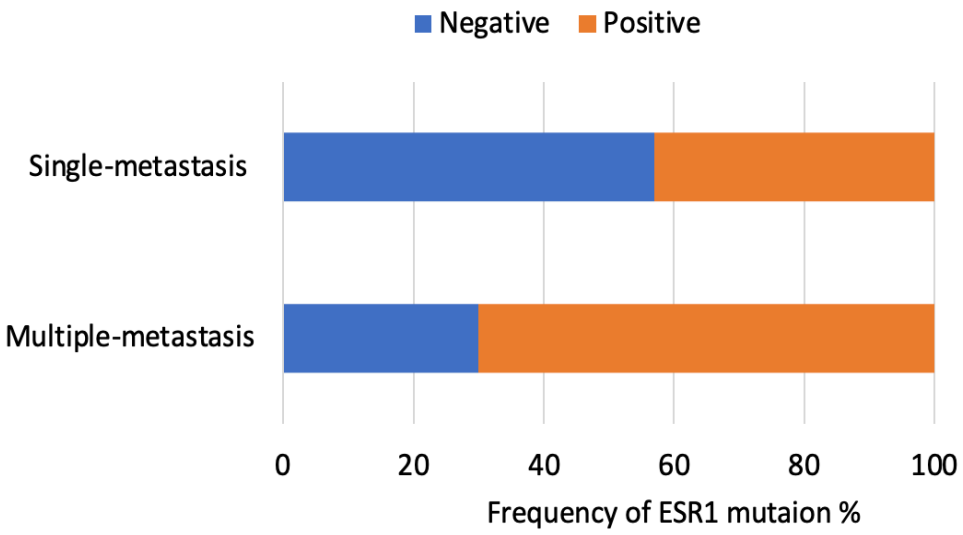

Figure 25. Distribution of *ESR1* mutations in HR-positive MBC patients based on metastatic status.

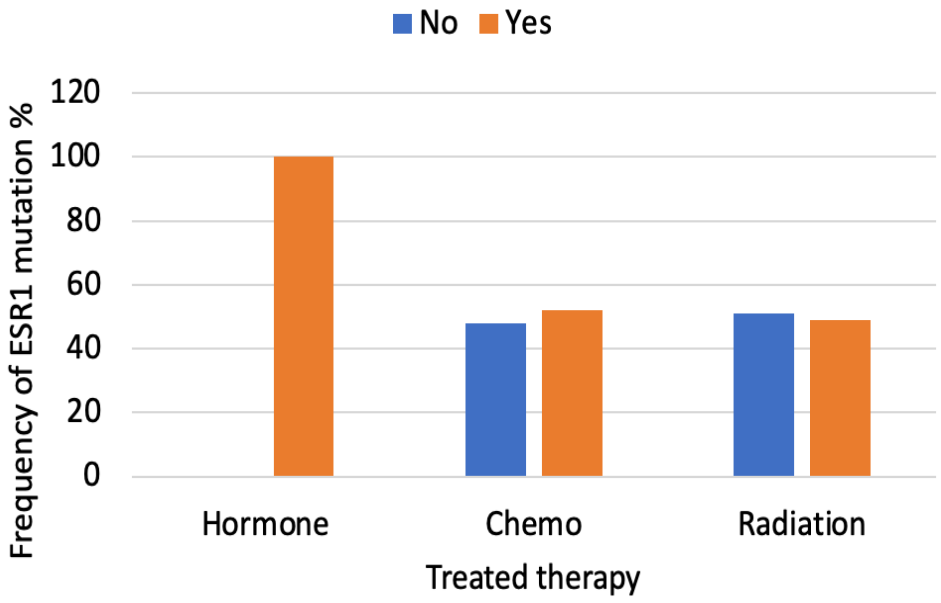

Figure 26. Distribution of *ESR1* mutations based on received therapy. Hormone: endocrine therapy, Chemo: chemotherapy, Radiation: radiotherapy. No: untreated endocrine therapy, Yes: treated endocrine therapy.

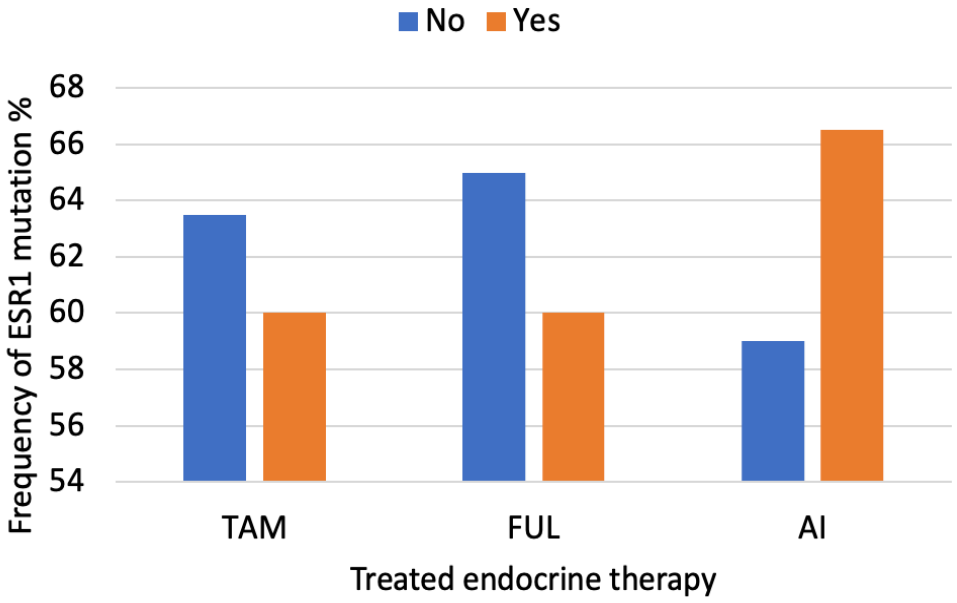

Figure 27. Distribution of *ESR1* mutations based on received endocrine therapy. TAM: tamoxifen, FUL: fulvestrant, AI: aromatase inhibitor. No: untreated endocrine therapy, Yes: treated endocrine therapy.

3.4.3.2 ESR1 mutant status and outcome of HR-positive metastatic breast cancer

We analyzed whether *ESR1* mutations detected in cfDNA were associated with the duration of progression. In the PFS analysis, local recurrences and distant metastases were considered as an event. These were tested by Kaplan-Meier analysis and verified by the log-rank test. At the end of our current study, 16 out of 18 detected *ESR1* mutant cases (88.88%) had progression at a median of 8.1 months. The presence of mutations in *ESR1* was an important predictive factor for shorter PFS ($p < 0.05$). The plotted Kaplan-Meier survival curve of the MBC patients carrying blood circulating *ESR1* mutations (with mean PFS time of 11.8 months (95% CI 8.02–15.58)) was significantly lower than MBC patients without this factor (with mean PFS time of 21.07 months (95% CI 17.28–24.85), p=0.004 (Figure 28A). In more detail, we calculated and plotted the PFS time of sub-grouped MBC patients, and see that MBC patients with multiple *ESR1* mutant variants acquired PFS curve (mean PFS time of 11.05 months (95% CI 6.76-15.34)) lower than those with single *ESR1* mutation (mean PFS time of 14.8 months (95% CI 7.42-22.18)) or free of *ESR1* mutations (mean PFS time of 21.07 months (95% CI 17.28-24.85)), $p = 0.013$. There was a clear tendency for shorter mean PFS as the number of *ESR1* mutations increased ($p < 0.05$) (Figure 28B).

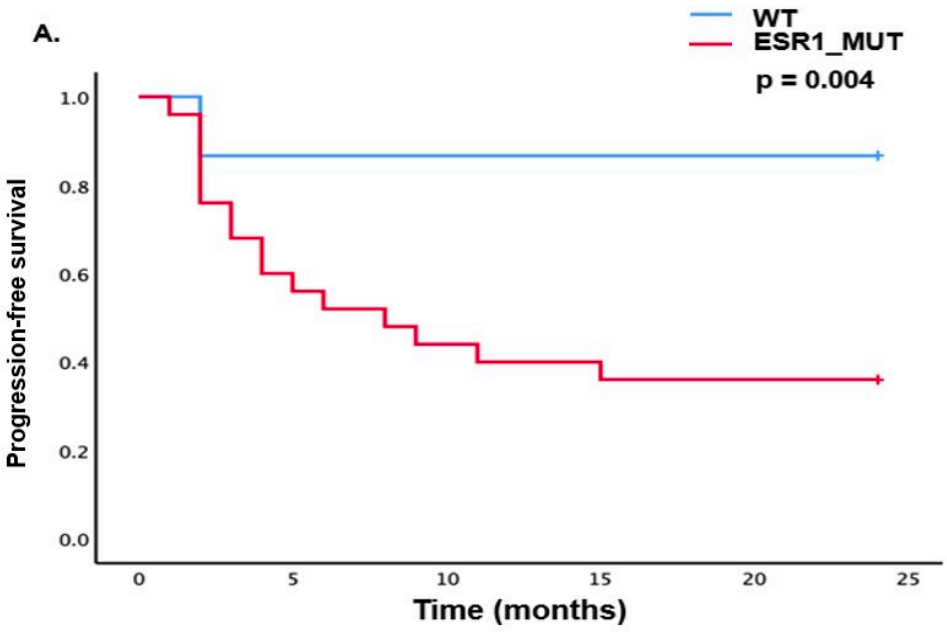

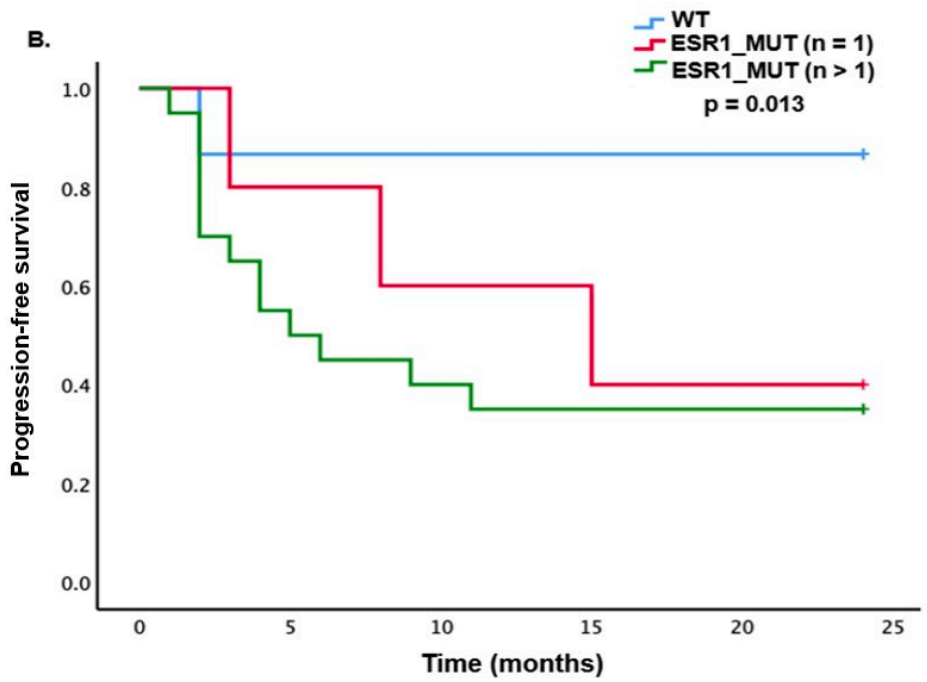

Figure 28. Time to progression after enrollment according to *ESR1* mutational status in HR-positive MBC. (A.) Time to progression after enrollment according to the presence of *ESR1* mutations; (B.) Time to progression after enrollment according to the number of *ESR1* mutant variants, WT: wild-type, ESR1_MUT: *ESR1* gene mutation.

In both univariate and multivariate Cox proportional hazards analyses (Table 18), *ESR1* mutation remained a strong and independent predictor of poor PFS. In the univariate model, *ESR1*-mutated patients had a 6.27-fold higher risk of disease progression compared with wild-type patients (HR = 6.27; 95% CI 1.44–27.43; p = 0.015). After adjusting for age, HER2 status, metastatic burden, and lymph node involvement, the association persisted (HR = 8.82; 95% CI 1.69–45.79; p = 0.01), confirming that *ESR1* mutation independently predicts shorter PFS in HR-positive metastatic BC.

Table 18. Univariate and multivariate Cox proportional hazards analyses identifying predictors of progression-free survival in HR-positive metastatic breast cancer (n = 40)

Variables	Univariate analysis		Multivariate analysis	
	HR (95%CI)	**p-value**	**HR (95%CI)**	**p-value**
ESR1 mutation (mutant vs. wild-type)	6.27 (1.44-27.43)	**0.015**	8.82 (1.69-45.79)	**0.01**
Age (≤ 50 vs. > 50 years)	-	-	1.71 (0.57-5.09)	0.34
HER2 status (positive vs. negative)	-	-	0.27 (0.09-0.81)	**0.02**
Metastatic number (< 2 vs. ≥ 2)	-	-	1.44 (0.24-8.61)	0.69
Lymph node invasion (Yes vs. No)	-	-	0.39 (0.06-2.45)	0.31
Visceral invasion (Yes vs. No)	-	-	- (Complete separation)	**-**
Bone invasion (Yes vs. No)	-	-	4.42 (1.19-16.31)	0.26
Prior ET (Yes vs. No)	-	-	- (Complete separation)	-

Abbreviations: HR, hazard ratios; HER2, human epidermal growth factor receptor-2; Statistically significant values ($p < 0.05$) are shown in bold.

3.4.4 Circulating gene (PIK3CA and/or ESR1) mutant status and outcomes of HR-positive breast cancer

3.4.4.1 Association between gene (PIK3CA and/or ESR1) mutations and HR-positive breast cancer patients' characteristics

Gene (*PIK3CA* and/or *ESR1*) alterations were found in 45.5% (30/66) of HR-positive EBC patients; 3 out of 30 positive cases were stage I BC, and 27 out

of 30 positive cases were stage II BC, as shown in Table 21. Out of the patients with gene mutations, 11 out of 30 received AI, 7 out of 30 received TAM, 15 out of 30 received ET, 27 out of 30 had surgery, 28 out of 30 received chemotherapy, and 8 out of 30 received HER2-target therapy. There was no correlation between the presence of the gene mutations and the aforementioned characteristics ($p > 0.05$). Nonetheless, these alterations in genes were more common in patients who had received radiation therapy ($p = 0.011$) (Table 19).

As stated in table 20, of the HR-positive EBC patients, 19 out of 66 had a *PIK3CA* mutation, 5 out of 66 had an *ESR1* mutation, and 6 out of 66 had both mutations.

Table 19. Characteristics of EBC patients with detected-gene mutant (*PIK3CA* and/or *ESR1*) compared to undetected-gene mutant patients

Characteristic	Total n = 66 (100%)	Gene mutant status		p-value[a]
		Positive n = 30 (45.5%)	Negative n = 36 (54.5%)	
Age ($\bar{X}$±SD, years)	53.64 ± 12.78	53.3 ± 12.07	53.92 ± 13.51	0.847
HER2 - positive	37 (56.1%)	16 (53.3%)	21 (58.3%)	0.684
Stage				
I	12 (18.2%)	3 (10%)	9 (25%)	0.116
II	54 (81.8%)	27 (90%)	27 (75%)	
Metastatic sites				
Lymph node	14 (21.2%)	6 (20%)	8 (22.2%)	0.826
Received therapy				
ET	40 (60.6%)	15 (50%)	25 (69.4%)	0.107
Tamoxifen	18 (27.3%)	7 (23.3%)	11 (30.6%)	0.512
AI	26 (39.4%)	11 (36.7%)	15 (41.7%)	0.679
Surgery	62 (93.9%)	27 (90%)	35 (97.2%)	0.323
Chemotherapy	60 (90.9%)	28 (93.3%)	32 (88.9%)	0.532
Radiotherapy	13 (19.7%)	10 (33.3%)	3 (8.3%)	**0.011**[*]
Trastuzumab	20 (30.3%)	8 (26.7%)	12 (33.3%)	0.557

"*" Fisher's Exact Test; "a" Mutant vs wild-type; AI: aromatase inhibitor; Statistically significant value is shown in bold.

Table 20. Circulating *PIK3CA, ESR1* mutations in 66 HR-positive EBC patients

		***PIK3CA* mutation (n)**		**Total**
		Negative	Positive	
***ESR1* mutation (n)**	Negative	36	19	55
	Positive	5	6	11
Total		41	25	66

Of the 82 HR-positive ABC patients, 17 cases had a *PIK3CA* mutation, 21 had an *ESR1* mutation, and 28 had both gene mutations (Table 21). Table 22 revealed that 80.5% (66/82) of HR-positive ABC patients carried gene (*PIK3CA* and/or *ESR1)* mutations; 30 out of 66 of these patients had stage III BC, and 36 out of 66 had stage IV BC. Of the patients with identified genes, 26 were treated with AI, 21 and 19 were treated with TAM or FUL, 55 out of 66 received ET, 26 received radiation, 56 received chemotherapy, and 14 received HER2-target therapy. There was no correlation between the presence of the gene mutations and those features ($p > 0.05$). Even so, these mutations in genes were more prevalent in individuals with lung invasion, multiple metastatic sites, or recurrence ($p < 0.05$) (Table 22).

Table 21. Circulating *PIK3CA, ESR1* mutations in 82 HR-positive ABC patients

		Number of *PIK3CA* mutation (n)		**Total**
		Negative	Positive	
Number of *ESR1* mutation (n)	Negative	16	17	33
	Positive	21	28	49
Total		37	45	82

Table 22. Characteristics of advanced BC patients with detected-gene mutant (*PIK3CA* and/or *ESR1*) compared to undetected-gene mutant patients

Characteristic	Total n = 82 (100%)	Gene mutant status		p-value[a]
		Positive n = 66 (80.5%)	Negative n = 16 (19.5%)	
Age ($\overline{X}$±SD, years)	52.29 ± 14.37	53.26 ± 14.64	56.38 ± 11.68	0.431
Stage				
III	42 (51.2%)	30 (45.5%)	12 (75%)	**0.034***
IV	40 (48.8%)	36 (54.5%)	4 (25%)	
HER2 status				
Positive	40 (48.8%)	36 (54.5%)	6 (37.5%)	0.221
Negative	42 (51.2%)	30 (45.5%)	10 (62.5%)	
Recurrence	28 (34.1%)	27 (40.9%)	1 (6.2%)	**0.009***
Number of metastatic locations				
1	50 (61%)	35 (53%)	15 (93.8%)	**0.003***
≥2	32 (39%)	31 (47%)	1 (6.2%)	
Metastatic sites				
Lymph node	71 (86.6%)	59 (89.4%)	12 (75%)	0.130
Lung	16 (19.5%)	16 (24.2%)	0 (0%)	**0.028***
Bone	24 (29.3%)	21 (31.8%)	3 (18.8%)	0.303
Brain	4 (4.9%)	4 (6.1%)	0 (0%)	0.581
Liver	6 (7.3%)	6 (9.1%)	0 (0%)	0.592
Received therapy				
Endocrine	66 (80.5%)	55 (83.3%)	11 (68.8%)	0.187
Tamoxifen	26 (31.7%)	21 (31.8%)	5 (31.2%)	0.965
Fulvestrant	21 (25.6%)	19 (28.8%)	2 (12.5%)	0.181
AI	31 (37.8%)	26 (39.4%)	5 (31.2%)	0.547
Chemotherapy	68 (82.9%)	56 (84.8%)	12 (75%)	0.348
Radiotherapy	33 (40.2%)	26 (39.4%)	7 (43.8%)	0.750
Her2-targeted	19 (23.2%)	14 (21.2%)	5 (31.2%)	0.393

"*" Statistically significant value; "a" Mutant vs wild-type

3.4.4.2 Gene (PIK3CA and/or ESR1) mutant status and outcome of HR-positive metastatic breast cancer

Of the 40 HR-positive MBC patients, 36 (90%) had at least one mutation in either the *PIK3CA*, *ESR1*, 26 (65%) had a *PIK3CA* mutation, 25 (62.5%) had an *ESR1* mutation, and 15 (37.5%) had both gene mutations. Additionally, the majority of patients with detected gene mutations were polyclonal (Table 23).

Among 13 monoclonal tumors, 2 cases had *ESR1* mutation, 11 cases had *PIK3CA* mutation. Higher rates of the gene changes were reported by patients who had previously had ET or chemotherapy, developed recurrence, numerous metastases, or LN invasion. Nevertheless, there was no connection between the features of the MBC patients and these gene mutations (data not showed).

As shows in Table 24, the presence of D538G, Y537S, and Y537N was found to correlate with progression status ($p < 0.05$). In addition, there was a correlation between the presence of D538G mutation and bone metastasis ($p = 0.03$).

Table 23. Characteristics of metastatic BC patients with gene mutations

Characteristic	Total n = 40 (100%)
Age ($\overline{X}$±SD, years)	53.23 ± 16
HER2-positive	22 (55%)
Recurrence	25 (65.6%)
Number of metastatic locations	
1	13 (32.5%)
≥2	27 (67.5%)
Metastatic sites	
Lymph node	35 (87.5%)
Lung	16 (40%)
Bone	23 (57.5%)
Brain	4 (10%)
Liver	6 (15%)
Received therapy	
Endocrine therapy	39 (97.5%)
Tamoxifen	10 (25%)
Fulvestrant	20 (50%)
Aromatase inhibitor	18 (45%)
Chemotherapy	31 (77.5%)
Radiotherapy	15 (37.5%)
Her2-target therapy	12 (30%)
Gene mutant status	
Detected gene mutations	36 (90%)
PIK3CA mutations	26 (65%)
ESR1 mutations	25 (62.5%)
Both 2 gene mutations	15 (37.5%)
Monoclonal	13 (32.5%)
Polyclonal	23 (57.5%)

Table 24. Association between *PIK3CA/ESR1* mutant variants and HR-positive metastatic BC patients' characteristics

Characteristic		Positive cases, n (%)					
		E545K	**H1047R**	**D538G**	**E380Q**	**Y537S**	**Y537N**
Recurrence	Yes	3 (12)	15 (60)	9 (36)	5 (20)	13 (52)	12 (48)
	No	4 (26.7)	7 (46.7)	3 (20)	4 (26.7)	9 (60)	4 (26.7)
p1		ns	ns	ns	Ns	ns	ns
Progression	Yes	4 (22.2)	9 (50)	**9 (50)**	6 (33.3)	**13 (72.2)**	**11 (61.1)**
	No	3 (13.6)	13 (59.1)	**3 (13.6)**	3 (13.6)	**9 (40.9)**	**5 (22.7)**
p2		ns	ns	**0.013**	Ns	**0.048**	**0.014**
Lympho node	Yes	7 (20)	20 (57.1)	10 (28.6)	9 (25.7)	19 (54.3)	13 (37.1)
	No	0	2 (40)	2 (40)	0	3 (60)	3 (60)
p3		ns	ns	ns	Ns	ns	ns
Lung	Yes	5 (31.2)	9 (56.2)	5 (31.2)	3 (18.8)	10 (62.5)	9 (56.2)
	No	2 (8.3)	13 (54.2)	7 (29.2)	6 (25)	12 (50)	7 (29.2)
p4		ns	ns	ns	Ns	ns	ns
Live	Yes	1 (16.7)	5 (83.3)	3 (50)	1 (16.7)	3 (50)	4 (66.7)
	No	6 (17.6)	17 (50)	9 (26.5)	8 (23.5)	19 (55.9)	12 (35.3)
p5		ns	ns	ns	Ns	ns	ns
Bone	Yes	5 (21.7)	13 (56.5)	**10 (43.5)**	5 (21.7)	13 (56.5)	9 (39.1)
	No	2 (11.8)	9 (52.9)	**2 (11.8)**	4 (23.5)	9 (52.9)	7 (41.2)
p6		ns	ns	**0.03**	ns	ns	ns
Brain	Yes	1 (25)	2 (50)	2 (50)	2 (50)	3 (75)	3 (75)
	No	6 (16.7)	20 (55.6)	10 (27.8)	7 (19.4)	19 (52.8)	13 (36.1)
p7		ns	ns	ns	ns	ns	ns

p1: Recurrence vs non recurrence; p2: progression vs non progression; p3: lymph node metastasis vs non metastasis; p4: lung metastasis vs non metastasis; p5: live metastasis vs non metastasis; p6: bone metastasis vs non metastasis; p7: brain metastasis vs non metastasis; "ns": not significant

We investigated the impact of *PIK3CA* and/or *ESR1* mutations on the occurrence of MBC progression. Local recurrences and distant metastases were considered as events in the PFS analysis. Kaplan-Meier analysis was used in evaluating these, and the log-rank test was used for verification. At a median of 3.0 months after mutations were identified, 17 of 36 gene-positive cases progressed. There was no difference of PFS between detected-gene-mutation patients and undetected-gene-mutation patients [mean of TTP 15.28 months (95% CI 12.02 – 18.54) vs 15.2 months (95% CI 5.75 – 24.65), p = 0.928] (Figure 29A). Patients who had more gene mutations tended to have a shorter PFS [mean of TTP: 18.5 months (95% CI 9.16 - 27.84) vs. 17.24 months (95% CI 13.35 - 21.13) vs. 11.67 months (95% CI 6.52 - 16.82), p = 0.255 (Figure 29B).

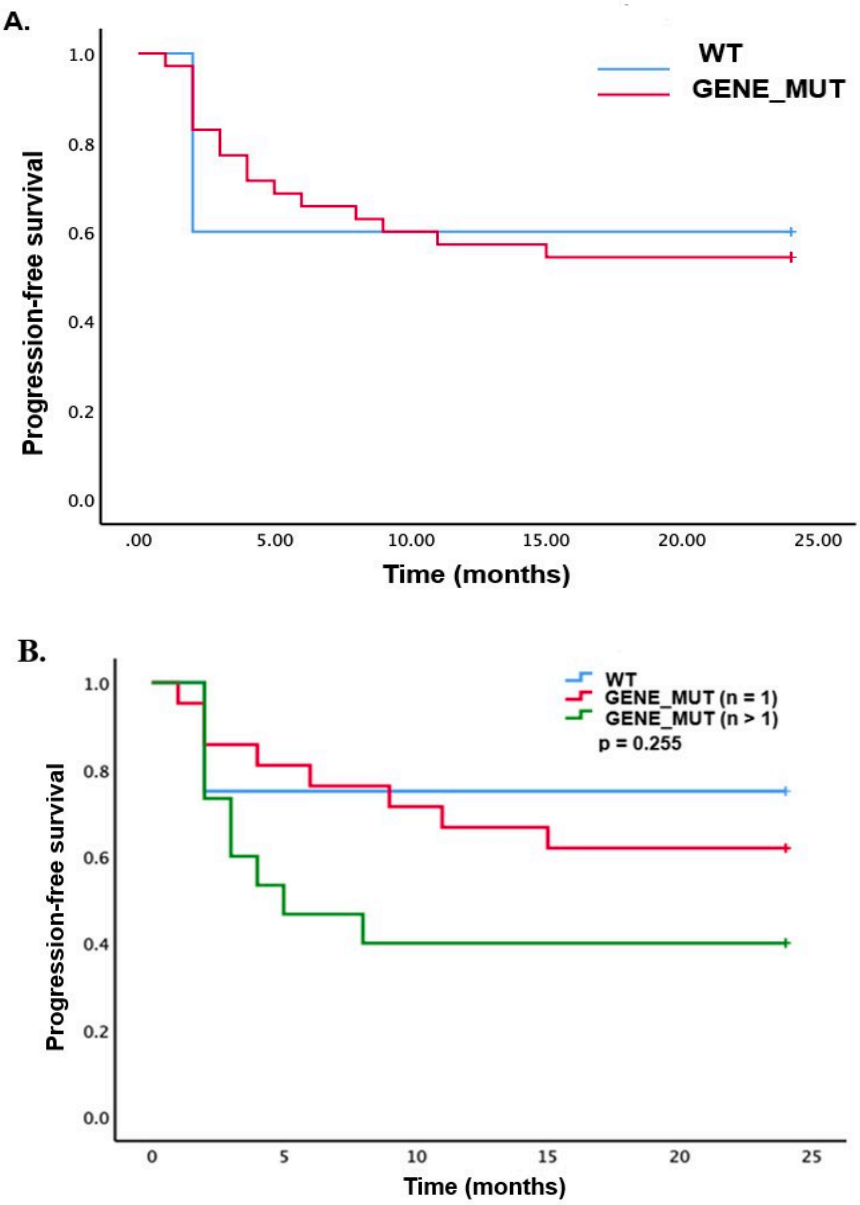

Figure 29. Time to progression after enrollment according to *PIK3CA* and *ESR1* mutational status in HR-positive MBC. Time to progression after enrollment according to the number of gene mutations (*PIK3CA* and/or *ESR1* mutations). WT: wild-type, GENE_MUT: gene (*PIK3CA* and/or *ESR1*) mutation.

3.5 Discussion

Endocrine therapy is the main strategy for HR-positive BC, and the clinical availability of a number of drugs, like AI, TAM, or FUL, has led to substantial improvements in survival outcomes for patients with HR-positive BC [21, 252]. Nevertheless, approximately 20% of patients with early BC experience disease relapse, and most patients with MBC show resistance to treatment [252, 253]. Activating *ESR1* mutations in patients previously exposed to AI or TAM, revealing a possible correlation between hormone therapy resistance and the existence of the mutations [254]. Y537N, the first to identify an *ESR1* mutation, was found in a metastatic ER-positive tumor biopsy by Zhang et al. in 1997 [255]. Subsequently, numerous laboratories have now validated the presence of *ESR1* mutations in MBC biopsy samples using deep sequencing, and combined these investigations have identified a hotspot for *ESR1* mutations within the LBD region using multiple DNA sequencing methods [41, 98, 112, 113]. All *ESR1* resistance mutations reside in the LBD: the most prevalent are D538G and Y537S; others include Y537N, Y537C, L536H, L536P, L536R, S463P, and E380Q [110, 256-258]. Among the two most common mutations, *ESR1* Y537S mutation has stronger resistance to estrogen deprivation, tamoxifen, fulvestrant, and new medicines such as bazedoxifene than *ESR1* D538G mutation, while *ESR1* D538G mutation has a greater metastatic potential [43, 98-100, 102, 256]. These days, CDK4/6 inhibitors and a new generation of SERDs-elacestrant-has showed promising outcomes for treatment of HR-positive MBC harboring *ESR1* mutations [244, 253]. cfDNA analysis could be minimally invasive to gather serial genetic data for evaluating therapy outcomes and guiding targeted medicines [259].

A simple, inexpensive, and minimally invasive blood test is sought for use in clinical practice; thus, highly sensitive assays would be needed to detect a broad variety of gene mutations. In previous research, Super-arms was upgraded from ARMS-PCR for identifying *ESR1* mutations, becoming more specific than ARMS-PCR and efficiently detecting the 0.2% target sequence from BC patients'

plasma cfDNA [136]. Through the modification of allele-specific primers mixing with wild-type-specific blocking reagents in our novel assays for *ESR1* mutation detection that bound specifically to a particular base sequence, only mutant DNA could be enriched while inhibited wild-type DNA replication, allowing them to successfully identify the four most common *ESR1* mutations (Y537S, D538G, Y537N, and E380Q) with higher sensitivity.

Using the developed clamping-mediated ARMS-PCR assays, *ESR1* mutations in cfDNA were detected in 59.8% (49/82) of HR-positive ABC samples, 16.7% (11/66) of HR-positive EBC. Among patients with any detectable *ESR1* mutations, 44 out of 49 ABC cases and 5 out of 11 EBC had two or more mutations. Our mutation rate is higher than the published studies such as PALOMA-3 (25%), BOLERO-2 (29%), FERGI (37%), SOFEA (30%), and MONARCH2 study (59%) [105, 112, 118, 120, 260]. The gene mutations were detected in 16.7% (11/66) stage II BC individuals who previously treated with TAM or AI monotherapy. This is a relatively high percentage in contrast to earlier studies that have remarkable shown undetectable or extremely low allele frequencies of *ESR1* mutations in primary tumors [108, 136, 261, 262]. Stergiopoulou et al, using NAPA assay, detected *ESR1* Y537C mutation in 23% (3/13) of ER+ primary breast tumors [137]. In Hashimoto's study, 12.7% ET-treated ER+ primary BC had *ESR1* mutations [263]. Gelsomino et al. found a prevalence of 12% for Y537N, 5% for Y537S, and 2% for D538G mutation in primary tumors treated with TAM monotherapy [264]. The higher percentage reported in our study could be explained by the high analytical sensitivity of our *ESR1* assays, or a difference in the populations tested and/or in the time of samples' collection (the course of disease, the application of endocrine drugs, or the duration of endocrine treatment).

The reported prevalence of *ESR1* mutations varies widely among studies, reflecting differences in population background, disease stage, sample type, and analytical methodology. Across populations, *ESR1* mutation rates in HR–positive

MBC have been reported in the range of 20–40%, predominantly in cohorts previously exposed to aromatase inhibitors. For instance, Schiavon et al. detected mutations in 36.4% (16/44) of plasma samples [97]; Spoerke et al. reported 37% (57/153) in cfDNA from U.S. patients [105]; Clatot et al. found 31.4% (22/70) in a French cohort [115]; whereas Asian populations such as Japan and China generally reported slightly lower frequencies (15–25%) [123, 124, 125]. In contrast, the prevalence in primary, treatment-naïve tumors remains low (typically 1–7%) [39, 98, 113], confirming that *ESR1* alterations are predominantly acquired mutations emerging after endocrine therapy [97, 113, 123].

Sample source also influences mutation detection. Studies analyzing tissue DNA often report lower mutation rates (5–15%), likely because most archival tumor samples are from pre-treatment stages, whereas plasma cfDNA captures ongoing tumor evolution and yields higher frequencies (20–40%) [97, 105, 113, 115]. This difference underscores the complementary role of cfDNA in identifying treatment-emergent *ESR1* mutations missed by single-site tissue biopsies.

From a methodological perspective, assay analytical sensitivity is another key determinant. *ESR1* mutations can exist at very low variant allele fractions (VAF < 0.1%) in cfDNA; thus, high-sensitivity techniques such as digital droplet PCR (ddPCR) or targeted NGS (LOD 0.01–0.05%) detect a greater number of variants compared with conventional PCR (LOD 0.5–1%) [69, 97, 98, 113, 115]. Indeed, studies employing ddPCR—such as Schiavon et al. [97] and Fribbens et al. [113]—reported detection rates of 30–40%, whereas standard PCR assays usually identified ≤15% of cases.

Additionally, treatment exposure and disease context have a profound effect on *ESR1* mutation prevalence. Mutations are rarely detected in endocrine therapy–naïve patients but rise sharply after AI or SERD exposure. For example, Chandarlapaty et al. reported *ESR1* mutations in 29% of patients progressing on AI therapy [112], and Fribbens et al. found frequencies up to 38% in serial cfDNA

analyses following AI resistance [113]. In our cohort, *ESR1* mutations were enriched in patients with metastatic HR^+ disease previously treated with AIs or SERDs, consistent with the concept of therapy-driven clonal selection that favors ligand-independent receptor activation.

Our findings are consistent with previous reports indicating that *ESR1* mutations are associated with aggressive disease. Several studies have reported the high frequency of mutation detection in cases of liver metastasis [265, 266]; in contrast to our study, *ESR1* mutations were more frequently observed in lung or brain metastasis as well as AI-treated MBC patients (Figure 22, Figure 25). Regrettably, the small sample size restricted us from observing a correlation between the clinical features of the study's patients and the existence of *ESR1* gene alterations.

The SoFEA and EFECT trials assessed for preexisting *ESR1* mutations in cfDNA of individuals with MBC after previous progression on AI [113, 118]. The *ESR1* mutations were detectable at baseline in 39% of SoFEA and 23% of EFECT patients, and it indicated a considerably shorter PFS compared to *ESR1* wild-type of 2.4 months versus 4.8 months, as well as a significantly lesser one-year overall survival rate (62% versus 79%). Additionally, three-month-repeated cfDNA collection revealed that the *ESR*1 mutations emerged months before radiologic development on AI [114]. Of progressed patients, 56% had *ESR1* mutations at progression, while 86% had *ESR1* mutations detectable prior to development at a median of 6.7 months earlier. A comparable discovery from the FMER trial revealed *ESR1* mutations detected in cfDNA prior to progression in 82% of patients, with a median of 3.6 months [115]. This study observed that most detected *ESR1* HR-positive MBC cases (88.88%) had progression after median 8.1 months. HR-positive MBC patients with ctDNA *ESR1* mutations had a shorter PFS than those with *ESR1* wild-type ($p = 0.004$). Additionally, increasing the number of variants in *ESR1* induces a clear tendency for shorter PFS ($p = 0.013$)

(Figures 26A, 26B). Therefore, *ESR1* mutations were an independent predictor of shorter PFS in HR-positive MBC patients.

The present study demonstrated that *ESR1* mutations represent a strong and independent predictor of poor PFS in patients with HR-positive MBC. Even after adjustment for key clinicopathologic variables—including age, HER2 status, number of metastatic sites, and lymph node involvement—*ESR1* mutation remained significantly associated with an increased risk of disease progression. These findings are consistent with previous clinical and molecular studies showing that LBD mutations such as Y537S, D538G, and E380Q confer constitutive, ligand-independent activation of the ER, thereby maintaining tumor proliferation and survival despite estrogen deprivation therapy [98, 110, 108, 109]. These alterations enhance coactivator recruitment, reduce receptor degradation, and lower binding affinity for selective ER modulators, which collectively result in endocrine resistance and shortened survival [106, 107, 113]. Mechanistically, the acquisition of *ESR1* mutations under the selective pressure of AI therapy leads to ligand-independent ER signaling and therapy escape, explaining the shorter PFS observed in our *ESR1*-mutant cohort [111, 112, 114]. These results reinforce the clinical utility of cfDNA-based *ESR1* mutation detection as a minimally invasive biomarker for monitoring disease progression and therapeutic resistance in HR^+ metastatic BC. Furthermore, emerging endocrine therapies such as SERDs—including elacestrant (RAD1901) and SAR439859—have demonstrated potent antitumor efficacy in *ESR1*-mutant BC models [101, 104]. Our findings therefore underscore the importance of integrating *ESR1* mutation profiling into clinical decision-making, particularly for selecting candidates for these novel ER-targeting agents or combination regimens involving PI3K/AKT/mTOR inhibitors. Collectively, these results emphasize that *ESR1* mutation testing provides valuable prognostic and therapeutic information and may assist in personalized treatment planning for HR-positive MBC.

In multivariate Cox proportional hazards analyses, for visceral metastasis and prior endocrine therapy, the models exhibited complete separation, meaning that all patients within these subgroups experienced disease progression during follow-up. This led to extremely large and unstable hazard ratios with undefined confidence intervals, indicating that the Cox model could not estimate a reliable HR due to perfect prediction. While these variables were excluded from the final interpretation for statistical reasons, the finding itself underscores their strong clinical association with poor prognosis—patients with visceral involvement or prior exposure to endocrine therapy are well known to have more aggressive, treatment-resistant disease.

The two most common mutations in BC were *ESR1* and *PIK3CA*, with co-mutations in both genes ranging from 10% to more than 50% [260, 267-269]. *PIK3CA* and *ESR1* mutations have been responsible for ET resistance, and they indicated a poor prognosis and a shorter response to ET. Dempsey et al. observed a trend towards worse OS and shorter duration of treatment with alpelisib and ET in the co-mutation group in comparison to the *PIK3CA* alone group [268]. Sim et al. reported that *ESR1* and *PIK3CA* mutations in cfDNA have been attributed to clinical efficacy of ET in HR+ MBC patients. As *ESR1* mutations increased, the time to progression of the first ET following enrollment (TTP1) reduced dramatically ($p < 0.001$). *PIK3CA* mutations also corresponded with shorter TTP1 (16.2 months vs. 10.9 months), although they were substantially associated with longer TTP in patients undergoing exemestane-everolimus treatment (15.9 months vs. 5.2 months) [269]. Takashi et al. found that *ESR1* mutations were more common in patients who had previously been treated with ET than *PIK3CA* mutations. Both *ESR1* and *PIK3CA* mutation identification were associated with a shorter duration of ET efficacy. Sequential cfDNA analysis revealed that loss of *ESR1* mutations resulted in a prolonged response time, whereas *PIK3CA* mutations did not [210]. In another investigation, the existence of *ESR1* or *PIK3CA* mutations varied among metastatic locations. The concurrent *ESR1* and

PIK3CA mutant analysis revealed that patients with lung, liver, and bone metastases had considerably more *ESR1* mutations, whereas patients with lung and bone metastases had significantly more *PIK3CA* mutations. The eventual identification of *ESR1* or *PIK3CA* mutations had a significantly negative influence on OS, but no differential impact was identified among *ESR1* or *PIK3CA* codon variations [270]. However, in MONARCH 2, patients who received abemaciclib plus fulvestrant experienced an improvement in PFS regardless of *PIK3CA* or *ESR1* status; the degree of benefit was statistically stronger for patients with tumors having *PIK3CA/ESR1* mutations [260].

Our study found that 34 out of 148 HR-positive BC patients had both the *PIK3CA* and *ESR1* gene mutations (28 ABC and 6 EBC patients). The mutations in *PIK3CA* and/or *ESR1* genes were more common in EBC patients who had received radiation therapy ($p = 0.011$). In addition, these alterations in genes were more commonly found in ABC patients with lung disease, multiple metastatic locations, or relapse ($p < 0.05$). Remarkably, in HR+ MBC analysis, there was a correlation between the presence of D538G, Y537S, and Y537N and progression status ($p < 0.05$), and the D538G associated with bone metastases ($p = 0.03$); whereas no relationship was observed between the E545K, H1047R, and E380Q variants and the risk of recurrence, progression, or distant metastasis ($p > 0.05$). MBC patients who have mutations in both the *PIK3CA* and *ESR1* genes appear to have a shorter TTP than patients who have mutation in either *PIK3CA* gene or *ESR1* gene or those who have no mutations (Figure 26C). Unfortunately, the sample size in our study was too small to meet statistical significance. Further observations in a longer period of time involving a larger number of patients are needed to thoroughly comprehend the role of the two genes *PIK3CA* and *ESR1* mutations in BC patients.

The development of the cfDNA PCR assay for *ESR1* mutations provides a practical avenue for real-time detection of endocrine resistance in advanced HR^+ breast cancer. As *ESR1* mutations frequently arise under aromatase inhibitor or

SERD pressure, their early identification can guide therapeutic adjustments—such as switching to elacestrant or other selective estrogen receptor degraders—before overt clinical progression. The ability to monitor these mutations through plasma cfDNA represents an important step toward dynamic, response-guided management of endocrine therapy.

Incorporating this assay into clinical workflows could enhance precision-based follow-up strategies in breast cancer care. In settings where NGS is not routinely available, this PCR-based platform offers a cost-effective and scalable solution for mutation surveillance. Its adaptability to standard qPCR instruments enables implementation in most diagnostic laboratories. Future steps should focus on prospective clinical validation and the establishment of standardized reporting guidelines to facilitate widespread adoption of *ESR1* cfDNA testing as part of routine therapeutic monitoring.

While our study did not include matched plasma–tumor samples for direct cfDNA validation, previous reports have demonstrated strong concordance between plasma- and tissue-based genotyping results in BC [32–34]. Moreover, plasma *ESR1* testing is currently recognized as a clinically reliable approach when tumor tissue is not accessible in MBC [21]. This underscores the clinical relevance of plasma-based assays in detecting resistance-associated mutations. Given that *ESR1* mutations are acquired alterations associated with endocrine resistance, comparative analyses between plasma and metastatic tumor tissues would provide valuable insights into tumor evolution and therapeutic response. Future studies incorporating prospectively paired plasma–tumor cohorts will therefore be essential to further substantiate these findings.

Furthermore, our study has some limitations, including that the novel developed assays are not quantitative; therefore, they cannot be used to determine the mutational burden in plasma. A number of other limitations are also present in this investigation, including a cross-sectional design with a small patient sample, an institution-only design, and the absence of a matched tumor analysis.

The clinical performance of blood-based *ESR1* assays should be studied prospectively in a large number of patients.

3.6. Conclusion

In this study, we developed and validated an enhanced wild-type-blocking ARMS-PCR assay specifically designed for the detection of *ESR1* hotspot mutations (E380Q, Y537S, Y537N, D538G) in plasma cfDNA from patients with HR+ breast cancer. Our assay demonstrated outstanding analytical sensitivity, achieving a limit of detection as low as 0.01%–0.1%, depending on the specific mutation, which markedly surpasses the performance of conventional ARMS-PCR and many existing clinical molecular assays. Through systematic optimization of primer design, blocker oligonucleotide configuration, and reaction conditions, we achieved a robust balance between analytical specificity and analytical sensitivity. The inclusion of a wild-type-specific blocker oligo significantly enhanced discrimination between mutant and wild-type alleles, minimizing false positives while allowing amplification of low-frequency mutant alleles in plasma cfDNA, a challenge in liquid biopsy settings due to the typically low abundance of tumor-derived DNA. Analytical validation using synthetic mutant DNA controls demonstrated consistent performance across replicates, and confirmatory Sanger sequencing of PCR amplicons supported the assay's reliability. This rigorous two-layer validation framework enhances the credibility of the assay for clinical application. We subsequently applied this optimized method to plasma samples from a cohort of 148 HR+ breast cancer patients, including both early-stage and advanced-stage disease. Our findings revealed that *ESR1* hotspot mutations were present in 16.7% of early breast cancer patients and in 59.8% of advanced breast cancer patients, highlighting the strong association between *ESR1* mutations and disease progression or therapeutic resistance. Detailed analysis showed that the Y537S mutation was the most frequent, followed by Y537N, D538G, and E380Q, consistent with patterns reported in large clinical studies. Importantly, *ESR1* mutations were more frequently detected in patients who had received prior endocrine therapy, particularly AI, supporting the

hypothesis that AI treatment exerts selective pressure favoring the emergence of ligand-independent *ESR1* mutations. Our data further confirmed that *ESR1* mutations were associated with metastatic disease sites, particularly lung, liver, and brain metastases, although the statistical significance varied depending on the subgroup. Progression-free survival (PFS) analyses using Kaplan-Meier curves revealed that patients harboring circulating *ESR1* mutations had a shorter median PFS compared to patients without detectable mutations. These results reinforce the clinical relevance of plasma *ESR1* mutation testing as a prognostic biomarker and as a potential tool for therapeutic decision-making.

The key advantages of our assay are manifold: ultra-sensitive detection, non-invasive sampling, cost-effective and accessible technology. However, several limitations should be acknowledged. First, our assay targeted only four of the most common *ESR1* hotspot mutations, potentially missing less frequent but clinically significant variants. Second, although we demonstrated excellent analytical performance, larger-scale prospective studies tracking dynamic changes in *ESR1* mutations during treatment would be essential to fully validate the clinical utility of this assay. Third, the ability to differentiate between polyclonal versus monoclonal *ESR1* mutations could further refine prognostic stratification but was not fully addressed in this study. Moreover, while the presence of *ESR1* mutations was associated with poorer PFS, multivariate analyses adjusting for other clinical and pathological factors (e.g., tumor burden, prior treatments, site of metastasis) would strengthen the interpretation of *ESR1* mutation status as an independent prognostic biomarker. In clinical practice, detecting *ESR1* mutations can have significant therapeutic implications. Patients harboring these mutations may benefit from switching from aromatase inhibitors to SERDs such as fulvestrant or, more recently, to novel oral SERDs like elacestrant. Furthermore, combining SERDs with CDK4/6 inhibitors or PI3K/AKT/mTOR pathway inhibitors could offer enhanced efficacy in *ESR1*-mutated tumors. Therefore, sensitive and cost-effective methods such as the one developed in this chapter could be incorporated into real-time monitoring

protocols to guide dynamic therapeutic adaptations, ultimately aiming to delay disease progression and improve patients' outcomes.

CONCLUSION

The accurate, sensitive detection of somatic mutations in plasma cfDNA is crucial for the personalized management of BC, particularly in HR+ subtypes where endocrine resistance remains a significant therapeutic challenge. In this thesis, we focused on the development, optimization, and clinical application of highly sensitive, cost-effective, and feasible PCR-based assays for detecting two critical categories of genomic alterations associated with BC progression and therapy resistance: *PIK3CA* and *ESR1* hotspot mutations.

Here, we presented comprehensive workflows that spanned assay design, optimization, analytical validation, and preliminary clinical evaluation. Both chapters not only established robust technical platforms but also contributed important clinical insights into the prevalence and prognostic significance of *PIK3CA* and *ESR1* mutations in BC patients. In Chapter 2, we successfully established a novel wild-type-blocking asymmetric PCR assay for the detection of two major *PIK3CA* mutations, H1047R and E545K, in cfDNA. Similarly, in Chapter 3, we optimized a clamping-mediated ARMS-PCR assay targeting four clinically relevant *ESR1* mutations: E380Q, Y537S, Y537N, and D538G. Both assay platforms demonstrated impressive analytical sensitivities: the *PIK3CA*-detected assay achieved LODs of 0.01% for H1047R and 0.1% for E545K, while the *ESR1*-detected assay had LODs ranging from 0.01% to 0.1%, depending on the specific mutation.

Compared with other cfDNA detection platforms, our assays offer multiple strengths, such as high LOD, low complexity, cost-effectiveness, rapid turnaround, and versatility. These sensitivities surpass those typically achieved by conventional Sanger sequencing and rival the performance of more costly methods such as ddPCR or NGS, yet with much simpler laboratory requirements. Optimization steps, including primer design, blocker oligo integration, reaction temperature modification, and concentration balancing, were rigorously carried out, resulting in highly reproducible, specific, and

efficient assays. Analytical validation using synthetic DNA constructs and cell line-derived genomic DNA established the technical robustness of both assays. Further, sequencing of positive samples confirmed the presence of targeted mutations, ensuring specificity and reliability.

Clinical application of these methods to plasma samples from 196 BC patients for *PIK3CA* and 148 HR+ BC patients for *ESR1* revealed significant biological and clinical findings. *PIK3CA* mutations were detected in 42.9% of cases, with H1047R being more prevalent than E545K, whereas *ESR1* mutations were found in 16.7% of Early BC and 59.8% of advanced BC patients. Both mutation types were associated with more advanced disease stages, higher rates of metastasis (particularly to liver and brain), and shorter PFS. In addition, the presence of multiple concurrent ESR1 mutations could predict even poorer outcomes and influence the selection of combination therapies.

The research we conducted provides a snapshot of the molecular portrait in BC patients; therefore, more investigation at different points of treatment is required to provide a deeper comprehension of the existence, mutant allele frequency alterations, and the effect of *PIK3CA/ESR1* gene mutations on BC patient outcomes in real time. The investigation of two common *PIK3CA* and *ESR1* mutations in cfDNA from Vietnamese female BC patients is reported for the first time, revealing genetic variations that may contribute to knowledge of genetic alterations by geographical and ethnic communities. The study offers insights into the pathological characteristics of BC from a single center in Vietnam, emphasizing the necessity for broader prospective clinical research with multicenter populations.

REFERENCES

1. Kim J, H.A., McCormack V. et al, *Global patterns and trends in breast cancer incidence and mortality across 185 countries.* Nature Medicine, 2025. **31**(4): p. 1154-1162.
2. Bray F, L.M., Sung H, Ferlay J, Siegel RL, Soerjomataram I, Jemal A, *Global cancer statistics 2022: GLOBOCAN estimates of incidence and mortality worldwide for 36 cancers in 185 countries.* CA Cancer J Clin, 2024. **74(3)**(1542-4863 (Electronic)): p. 229-263.
3. Corben, A.D., *Pathology of invasive breast disease.* Surg Clin North Am, 2013. **93(2)**(1558-3171 (Electronic)): p. 363-92.
4. Carey LA, P.C., Livasy CA, Dressler LG, Cowan D, Conway K, et al., *Race, breast cancer subtypes, and survival in the Carolina Breast Cancer Study.* JAMA, 2006. **295(21)**(1538-3598 (Electronic)): p. 2492-502.
5. Clusan L, L.G.P., Flouriot G, Pakdel F *A Closer Look at Estrogen Receptor Mutations in Breast Cancer and Their Implications for Estrogen and Antiestrogen Responses.* Int J Mol Sci, 2021. **22(2)**(1422-0067 (Electronic)): p. 756.
6. Hammond ME, H.D., Dowsett M, Allred DC, Hagerty KL, Badve S, et al., *American Society of Clinical Oncology/College Of American Pathologists guideline recommendations for immunohistochemical testing of estrogen and progesterone receptors in breast cancer.* J Clin Oncol, 2010. **28(16)**(1527-7755 (Electronic)): p. 2784-95.
7. Dwivedi S, P.P., Misra R, Lingeswaran M, Vishnoi JR, Pareek P, Misra S, Sharma P, *Single Cell Omics of Breast Cancer: An Update on Characterization and Diagnosis.* Indian J Clin Biochem, 2019. **34(1)**(0970-1915 (Print)): p. 3-18.
8. Zhu H, D.B., *American Joint Committee on Cancer's Staging System for Breast Cancer, Eighth Edition: Summary for Clinicians.* Eur J Breast Health, 2021. **17(3)**(2587-0831 (Print)): p. 234-238.
9. Van Dooijeweert C, V.D.P., Ellis IO, *Grading of invasive breast carcinoma: the way forward.* Virchows Arch, 2022. **480(1)**(1432-2307 (Electronic)): p. 33-43.
10. Gradishar WJ, M.M., Abraham J, Abramson V, Aft R, Agnese D, et al., *Breast Cancer, Version 3.2024, NCCN Clinical Practice Guidelines in Oncology.* J Natl Compr Canc Netw, 2024. **22(5)**(1540-1413 (Electronic)): p. 331-357.
11. Ring A, D.M., *Mechanisms of tamoxifen resistance.* Endocr Relat Cancer, 2004. **11(4)**(1351-0088 (Print)): p. 643-58.
12. Osborne CK, S.R., *Mechanisms of endocrine resistance in breast cancer.* Annu Rev Med, 2011. **62**(1545-326X (Electronic)): p. 233-47.

13. Schiff R, M.S., Shou J, Bharwani L, Mohsin SK, Osborne CK, *Cross-talk between estrogen receptor and growth factor pathways as a molecular target for overcoming endocrine resistance.* Clin Cancer Res, 2004. **10**(1078-0432 (Print)): p. 331S-6S.
14. Braicu C, B.M., Busuioc C, Drula R, Gulei D, Raduly L, et al, *A Comprehensive Review on MAPK: A Promising Therapeutic Target in Cancer. LID - 10.3390/cancers11101618 [doi] LID - 1618.* Cancers (Basel), 2019. **10(11)**(2072-6694 (Print)): p. 1618.
15. Jordan, V.C., *Chemoprevention of breast cancer with selective oestrogen-receptor modulators.* Nat Rev Cancer, 2007. **7(1)**(1474-175X (Print)): p. 46-53.
16. Wardell SE, M.J., McDonnell DP, *The turnover of estrogen receptor α by the selective estrogen receptor degrader (SERD) fulvestrant is a saturable process that is not required for antagonist efficacy.* Biochem Pharmacol, 2011. **82(2)**(1873-2968 (Electronic)): p. 122-30.
17. Osborne CK, W.A., Nicholson RI, *Fulvestrant: an oestrogen receptor antagonist with a novel mechanism of action.* Br J Cancer, 2004. **90**(0007-0920 (Print)): p. S2-6.
18. Guan J, Z.W., Hafner M, Blake RA, Chalouni C, Chen I, et al., *Therapeutic Ligands Antagonize Estrogen Receptor Function by Impairing Its Mobility.* Cell, 2019. **178(4)**(1097-4172 (Electronic)): p. 949-963.e18.
19. Brueggemeier, R.W., *Update on the use of aromatase inhibitors in breast cancer.* Expert Opin Pharmacother, 2006. **7(14)**(1744-7666 (Electronic)): p. 1919-30.
20. Chan HJ, P.K., Chen S, *Structural and functional characterization of aromatase, estrogen receptor, and their genes in endocrine-responsive and -resistant breast cancer cells.* J Steroid Biochem Mol Biol, 2016. **161**(1879-1220 (Electronic)): p. 73-83.
21. Pan H, G.R., Braybrooke J, Davies C, Taylor C, McGale P, et al., *20-Year Risks of Breast-Cancer Recurrence after Stopping Endocrine Therapy at 5 Years.* N Engl J Med, 2017. **377(19)**(1533-4406 (Electronic)).
22. Lewis JS, J.V., *Selective estrogen receptor modulators (SERMs): mechanisms of anticarcinogenesis and drug resistance.* Mutat Res, 2005. **591**(0027-5107 (Print)): p. 247-263.
23. Early Breast Cancer Trialists' Collaborative Group (EBCTCG); Davies C, G.J., Gray R, Clarke M, Cutter D, et al., *Aromatase inhibitors versus tamoxifen in early breast cancer: patient-level meta-analysis of the randomised trials.* Lancet, 2015. **386(10001)**(1474-547X (Electronic)): p. 1341-1352.

24. McDonnell, D.P., *The molecular determinants of estrogen receptor pharmacology.* Maturitas, 2004. **48**(0378-5122 (Print)): p. S7-12.
25. Paech K, W.P., Kuiper GG, Nilsson S, Gustafsson J, Kushner PJ, Scanlan TS *Differential ligand activation of estrogen receptors ERalpha and ERbeta at AP1 sites.* Science, 1997. **277(5331)**(0036-8075 (Print)): p. 1508-10.
26. Zou A, M.K., Arnold KE, Berger EM, Fitzgerald P, Mais DE, Allegretto EA, *Estrogen receptor beta activates the human retinoic acid receptor alpha-1 promoter in response to tamoxifen and other estrogen receptor antagonists, but not in response to estrogen.* Mol Endocrinol, 1999. **13(3)**(0888-8809 (Print)): p. 418-30.
27. Smith CL, O.M.B., *Coregulator function: a key to understanding tissue specificity of selective receptor modulators.* Endocr Rev, 2004. **25(1)**(0163-769X (Print)): p. 45-71.
28. Hall JM, M.D., *Coregulators in nuclear estrogen receptor action: from concept to therapeutic targeting.* Mol Interv, 2005. **5(6)**(1534-0384 (Print)): p. 343-57.
29. Kumar R, G.A., Vadlamudi RK, Rayala SK, *The clinical relevance of steroid hormone receptor corepressors.* Clin Cancer Res, 2005. **11(8)**(1078-0432 (Print)): p. 2822-31.
30. Clarke R, L.F., Welch JN, Skaar TC, *Cellular and molecular pharmacology of antiestrogen action and resistance.* Pharmacol Rev, 2001. **53(1)**(0031-6997 (Print)): p. 25-71.
31. Stendahl M, R.L., Nordenskjöld B, Jönsson PE, Landberg G, Jirström K, *High progesterone receptor expression correlates to the effect of adjuvant tamoxifen in premenopausal breast cancer patients.* Clin Cancer Res, 2006. **12(15)**(1078-0432 (Print)): p. 4614-8.
32. Ottaviano YL, I.J., Parl FF, Smith HS, Baylin SB, Davidson NE, *Methylation of the estrogen receptor gene CpG island marks loss of estrogen receptor expression in human breast cancer cells.* Cancer Res, 1994. **54(10)**(0008-5472 (Print)): p. 2552-5.
33. Roodi N, B.L., Kao WY, Verrier CS, Yee CJ, Dupont WD, Parl FF *Estrogen receptor gene analysis in estrogen receptor-positive and receptor-negative primary breast cancer.* Cancer Inst, 1995. **87(6)**(0027-8874 (Print)): p. 446-51.
34. Van Den Berg HW, L.M., Martin J, Nelson J, Dickson GR, Crockard AD, *Characterisation of a tamoxifen-resistant variant of the ZR-75-1 human breast cancer cell line (ZR-75-9a1) and ability of the resistant phenotype.* Br J Cancer, 1989. **59(4)**(0007-0920 (Print)): p. 522-6.
35. Sommer A, H.J., Lichtner RB, Schneider MR, Parczyk K, *Studies on the development of resistance to the pure antiestrogen Faslodex in three human*

breast cancer cell lines. Biochem Mol Biol, 2003. **85(1)**(0960-0760 (Print)): p. 33-47.
36. Brünner N, B.B., Jirus S, Skaar TC, Holst-Hansen C, et al., *MCF7/LCC9: an antiestrogen-resistant MCF-7 variant in which acquired resistance to the steroidal antiestrogen ICI 182,780 confers an early cross-resistance to the nonsteroidal antiestrogen tamoxifen.* Cancer Res, 1997. **57(16)**(0008-5472 (Print)): p. 3486-93.
37. Howell, A., *Fulvestrant ('Faslodex'): current and future role in breast cancer management.* Crit Rev Oncol Hematol, 2005. **57(3)**(1040-8428 (Print)): p. 265-73.
38. Ma CX, R.T., Chmielewska I, Ellis MJ, *Mechanisms of aromatase inhibitor resistance.* Nat Rev Cancer, 2015. **15(5)**(1474-1768 (Electronic)): p. 261-75.
39. Jeselsohn R, Y.R., Buchwalter G, Frampton G, Meric-Bernstam F, Gonzalez-Angulo AM, et al., *Emergence of constitutively active estrogen receptor-α mutations in pretreated advanced estrogen receptor-positive breast cancer.* Clin Cancer Res, 2014. **20(7)**(1557-3265 (Electronic)): p. 1757-1767.
40. Fanning SW, M.C., Dharmarajan V, Carlson KE, Martin TA, Novick SJ, et al., *Estrogen receptor alpha somatic mutations Y537S and D538G confer breast cancer endocrine resistance by stabilizing the activating function-2 binding conformation. LID - 10.7554/eLife.12792 [doi] LID - e12792.* Elife, 2016. **5**(2050-084X (Electronic)): p. e12792.
41. Robinson DR, W.Y., Vats P, Su F, Lonigro RJ, Cao X, et al., *Activating ESR1 mutations in hormone-resistant metastatic breast cancer.* Nat Genet, 2013. **45(12)**(1546-1718 (Electronic)): p. 1446-51.
42. Arnesen S, B.Z., Williams MM, Berrett KC, Li Z, Oesterreich S, et al., *Estrogen Receptor Alpha Mutations in Breast Cancer Cells Cause Gene Expression Changes through Constant Activity and Secondary Effects.* Cancer Res, 2021. **81(3)**(1538-7445 (Electronic)): p. 539-551.
43. Jeselsohn R, B.J., Pun M, Cornwell M, Liu W, Nardone A, et al, *Allele-Specific Chromatin Recruitment and Therapeutic Vulnerabilities of ESR1 Activating Mutations.* Cancer cell, 2018. **33(2)**(1878-3686 (Electronic)): p. 173-186.
44. Nayar U, C.O., Kapstad C, Cuoco MS, Waks AG, Wander SA, et al., *Acquired HER2 mutations in ER(+) metastatic breast cancer confer resistance to estrogen receptor-directed therapies.* Nat Genet, 2019. **51(2)**(1546-1718 (Electronic)): p. 207-216.
45. Gutierrez MC, D.S., Johnston S, Mohsin SK, Shou J, Allred DC, Schiff R, Osborne CK, Dowsett M *Molecular changes in tamoxifen-resistant breast cancer: relationship between estrogen receptor, HER-2, and p38 mitogen-*

activated protein kinase. J Clin Oncol, 2005. **23(11)**(0732-183X (Print)): p. 2469-76.
46. Massarweh S, O.C., Creighton CJ, Qin L, Tsimelzon A, Huang S, Weiss H, Rimawi M, Schiff R, *Tamoxifen resistance in breast tumors is driven by growth factor receptor signaling with repression of classic estrogen receptor genomic function.* Cancer Res, 2008. **68(3)**(1538-7445 (Electronic)): p. 826-33.
47. Mao P, C.O., Kowalski KJ, Kusiel JG, Buendia-Buendia JE, et al., *Acquired FGFR and FGF Alterations Confer Resistance to Estrogen Receptor (ER) Targeted Therapy in ER(+) Metastatic Breast Cancer.* Clin Cancer Res, 2020. **26(22)**(1557-3265 (Electronic)): p. 5974-5989.
48. Razavi P, C.M., Xu G, Bandlamudi C, Ross DS, Vasan N, et al., *The Genomic Landscape of Endocrine-Resistant Advanced Breast Cancers.* Cancer Cell, 2018. **34(3)**(1878-3686 (Electronic)): p. 427-438.e6.
49. Miller TW, H.B., González-Angulo AM, Fox EM, Mills GB, Chen H, Higham C, et al., *Hyperactivation of phosphatidylinositol-3 kinase promotes escape from hormone dependence in estrogen receptor-positive human breast cancer.* J Clin Invest, 2010. **120(7)**(1558-8238 (Electronic)): p. 2406-13.
50. Campbell RA, B.-N.P., Patel NM, Constantinidou D, Ali S, Nakshatri H, *Phosphatidylinositol 3-kinase/AKT-mediated activation of estrogen receptor alpha: a new model for anti-estrogen resistance.* J Biol Chem, 2001. **276(13)**(0021-9258 (Print)): p. 9817-24.
51. Duong BN, E.S., Frigo DE, Melnik LI, Vanhoy L, Tomchuck S, et al. , *AKT regulation of estrogen receptor beta transcriptional activity in breast cancer.* Cancer Res, 2006. **66(17)**(1538-7445 (Electronic)): p. 8373-81.
52. Angus L, S.M., Wilting SM, van Riet J, Van Hoeck A, Nguyen L, et al., *The genomic landscape of metastatic breast cancer highlights changes in mutation and signature frequencies.* Nat Genet, 2019. **51(10)**(1546-1718 (Electronic)): p. 1450-1458.
53. Liang J, S.J., *Multiple roles of the PI3K/PKB (Akt) pathway in cell cycle progression.* Cell Cycle, 2003. **2(4)**(1538-4101 (Print)): p. 339-45.
54. Abukhdeir AM, P.B., *P21 and p27: roles in carcinogenesis and drug resistance.* Expert Rev Mol Med, 2008. **10**(1462-3994 (Electronic)): p. e19.
55. Shoman N, K.S., McFadden A, Bickis MG, Torlakovic E, Chibbar R., *Reduced PTEN expression predicts relapse in patients with breast carcinoma treated by tamoxifen.* Mod Pathol, 2005. **18(2)**(0893-3952 (Print)): p. 250-9.
56. Lloyd MR, W.S., Hamilton E, Razavi P, Bardia A, *Next-generation selective estrogen receptor degraders and other novel endocrine therapies for management of metastatic hormone receptor-positive breast cancer: current*

and emerging role. Ther Adv Med Oncol, 2020. **14**(1758-8340 (Print)): p. 17588359221113694.
57. Fruman DA, C.H., Hopkins BD, Bagrodia S, Cantley LC, Abraham RT, *The PI3K Pathway in Human Disease.* Cell, 2017. **170(4)**(1097-4172 (Electronic)): p. 605-635.
58. Janku F, Y.T., Meric-Bernstam F, *Targeting the PI3K pathway in cancer: are we making headway?* Nat Rev Clin Oncol, 2018. **15(5)**(1759-4782 (Electronic)): p. 273-291.
59. Chalhoub N, B.S., *PTEN and the PI3-kinase pathway in cancer.* Annu Rev Pathol., 2009. **4**(1553-4014 (Electronic)): p. 127-50.
60. Martini M, D.S.M., Braccini L, Gulluni F, Hirsch E, *PI3K/AKT signaling pathway and cancer: an updated review.* Ann Med, 2014. **46(6)**(1365-2060 (Electronic)): p. 372-83.
61. Huang D, T.L., Yang F, Jin J, Guan X, et al., *PIK3CA mutations contribute to fulvestrant resistance in ER-positive breast cancer.* Am J Transl Res 2019. **11**(9): p. 6055-6065.
62. Rasti AR, G.-Y.A., Datko F, Borges VF, Aisner DL, Shagisultanova E, *PIK3CA Mutations Drive Therapeutic Resistance in Human Epidermal Growth Factor Receptor 2-Positive Breast Cancer.* JCO Precis Oncol, 2022. **6**(2473-4284 (Electronic)): p. e2100370.
63. Karakas B, B.K., Park BH, *Mutation of the PIK3CA oncogene in human cancers.* Br J Cancer, 2006. **94(4)**(0007-0920 (Print)): p. 455-9.
64. Miricescu, D., Totan, A., Stanescu, Spinu, II, Badoiu, S. C., Stefani, C., Greabu, M., *PI3K/AKT/mTOR Signaling Pathway in Breast Cancer: From Molecular Landscape to Clinical Aspects.* Int J Mol Sci, 2020. **22**(1).
65. Reinhardt, K., Stuckrath, K., Hartung, C., Kaufhold, S., Uleer, C., Hanf, V. Lantzsch, T., Peschel, S., John, J., Pohler, M., Bauer, M., Burrig, F. K., Weigert, E., Buchmann, J., Kantelhardt, E. J., Thomssen, C., Vetter, M., *PIK3CA-mutations in breast cancer.* Breast Cancer Res Treat, 2022. **196**(3): p. 483-493.
66. Corne, J., Le Du, F., Quillien, V., Godey, F., Robert, L., Bourien, H., Brunot, A., Crouzet, L., Perrin, C., Lefeuvre-Plesse, C., Dieras, V., De la Motte Rouge, T., *Development of multiplex digital PCR assays for the detection of PIK3CA mutations in the plasma of metastatic breast cancer patients.* Sci Rep, 2021. **11**(1): p. 17316.
67. Harle, A., Lion, M., Lozano, N., Husson, M., Harter, V., Genin, P., Merlin, J. L., *Analysis of PIK3CA exon 9 and 20 mutations in breast cancers using PCR-HRM and PCR-ARMS: correlation with clinicopathological criteria.* Oncol Rep, 2013. **29**(3): p. 1043-52.

68. Ruth E. Board, N.J.T., Paul F., Ravetto, Stephen Little, Malcolm Ranson, Caroline Dive, Andrew Hughes, David Whitcombe, *Multiplexed Assays for Detection of Mutations in PIK3CA.* Clinical Chemistry 2008. **54:4**: p. 757-760.
69. Oshiro, C., Kagara, N., Naoi, Y., Shimoda, M., Shimomura, A., Maruyama, N., Shimazu, K., Kim, S., Noguchi, S., *PIK3CA mutations in serum DNA are predictive of recurrence in primary breast cancer patients.* Breast Cancer Research and Treatment, 2015. **150**(2): p. 299-307.
70. Keraite, I., Alvarez-Garcia, V., Garcia-Murillas, I., Beaney, M., Turner, N. C., Bartos, C., Oikonomidou, O., Kersaudy-Kerhoas, M., Leslie, N. R., *PIK3CA mutation enrichment and quantitation from blood and tissue.* Sci Rep, 2020. **10**(1): p. 17082.
71. Yi, Z., Ma, F., Liu, B., Guan, X., Li, L., Li, C., Qian, H., Xu, B., *Everolimus in hormone receptor-positive metastatic breast cancer: PIK3CA mutation H1047R was a potential efficacy biomarker in a retrospective study.* BMC Cancer, 2019. **19**(1): p. 442.
72. Suppan, C., Graf, R., Jahn, S., Zhou, Q., Klocker, E. V., Bartsch, R., Terbuch, A., Kashofer, K., Regitnig, P., Lindenmann, J., Posch, F., Gerritsmann, H., Jost, P. J., Heitzer, E., Dandachi, N., Balic, M., *Sensitive and robust liquid biopsy-based detection of PIK3CA mutations in hormone-receptor-positive metastatic breast cancer patients.* Br J Cancer, 2022. **126**(3): p. 456-463.
73. Fan, C., Liu, S., Fan, S., Yang, Z., Ye, N., Wang, K., *Comprehensive multigene mutation spectra of breast cancer patients from Northeast China obtained using the Ion Torrent sequencing platform.* ONCOLOGY REPORTS, 2019. **42**: p. 1580-1588.
74. Takashi Takeshita, Y.Y., Mutsuko Yamamoto-Ibusuki, Toko Inao, Aiko Sueta, Saori Fujiwara, Yoko Omoto and Hirotaka Iwase, *Prognostic role of PIK3CA mutations of cell-free DNA in early-stage triple negative breast cancer.* Cancer Sci 2015. **106**: p. 1582–1589.
75. Ikenoue T, K.F., Hikiba Y, Obata T, Tanaka Y, Imamura J, et al., *Functional analysis of PIK3CA gene mutations in human colorectal cancer.* Cancer Res, 2005. **65(11)**(0008-5472 (Print)): p. 4562-7.
76. Jiang W, H.T., Liu S, Zheng Y, Xiang L, Pei X, et al., *The PIK3CA E542K and E545K mutations promote glycolysis and proliferation via induction of the β-catenin/SIRT3 signaling pathway in cervical cancer.* J Hematol Oncol, 2018. **11(1)**(1756-8722 (Electronic)): p. 139.
77. Zhao L, V.P., *Helical domain and kinase domain mutations in p110alpha of phosphatidylinositol 3-kinase induce gain of function by different mechanisms.* Proc Natl Acad Sci U S A, 2008. **105(7)**(1091-6490 (Electronic)): p. 2652-7.

78. Martínez-Sáez, O., Chic, N., Pascual, T., Adamo, B., Vidal, M., González-Farré, B., Sanfeliu, E., Schettini, F., Conte, B., Brasó-Maristany, F., Rodríguez, A., Martínez, D., Galván, P., Rodríguez, A. P., Martinez, A., Muñoz, M., Prat, A., *Frequency and spectrum of PIK3CA somatic mutations in breast cancer.* Breast Cancer Research, 2020. **22**.
79. Stemke-Hale K, G.-A.A., Lluch A, Neve RM, Kuo WL, Davies M, et al., *An integrative genomic and proteomic analysis of PIK3CA, PTEN, and AKT mutations in breast cancer.* Cancer Res, 2008. **68(15)**(1538-7445 (Electronic)): p. 6084-91.
80. Zardavas D, T.M.L., Milne RL, Fumagalli D, Fountzilas G, Kotoula V, et al., *Tumor PIK3CA Genotype and Prognosis in Early-Stage Breast Cancer: A Pooled Analysis of Individual Patient Data.* J Clin Oncol, 2018. **36(10)**(1527-7755 (Electronic)): p. 981-990.
81. Deng L, Z.X., Sun Y, Wang J, Zhong X, Li J, et al., *Prevalence and Prognostic Role of PIK3CA/AKT1 Mutations in Chinese Breast Cancer Patients.* Cancer Res Treat, 2019. **51(1)**(2005-9256 (Electronic)): p. 128-140.
82. Li SY, R.M., Grieu F, Iacopetta B, *PIK3CA mutations in breast cancer are associated with poor outcome.* Breast Cancer Res Treat, 2006. **96(1)**(0167-6806 (Print)): p. 91-5.
83. Dieci MV, M.F., Griguolo G, Guarneri V, *Biomarkers for HER2-positive metastatic breast cancer: Beyond hormone receptors.* Cancer Treat Rev, 2020. **88**(1532-1967 (Electronic)): p. 102064.
84. Mosele F, S.B., Lusque A, Tran Dien A, Garberis I, Droin N, et al., *Outcome and molecular landscape of patients with PIK3CA-mutated metastatic breast cancer.* Ann Oncol, 2020. **31(3)**(1569-8041 (Electronic)): p. 377-386.
85. Jensen JD, K.A., Laenkholm AV, Grauslund M, Jensen MB, Santoni-Rugiu E, et al., *PIK3CA mutations, PTEN, and pHER2 expression and impact on outcome in HER2-positive early-stage breast cancer patients treated with adjuvant chemotherapy and trastuzumab.* Ann Oncol, 2012. **23(8)**(1569-8041 (Electronic)): p. 2034-2042.
86. Baselga J, C.J., Im SA, Clark E, Ross G, Kiermaier A, Swain SM, *Biomarker analyses in CLEOPATRA: a phase III, placebo-controlled study of pertuzumab in human epidermal growth factor receptor 2-positive, first-line metastatic breast cancer.* J Clin Oncol, 2014. **32(33)**(1527-7755 (Electronic)): p. 3753-61.
87. Araki K, M.Y., *Mechanism of resistance to endocrine therapy in breast cancer: the important role of PI3K/Akt/mTOR in estrogen receptor-positive, HER2-negative breast cancer.* Breast Cancer, 2018. **25(4)**(1880-4233 (Electronic)): p. 392-401.

88. Vitale SR, M.F., Stella S, Motta G, Inzerilli N, Massimino M, et al., *PI3K inhibition in breast cancer: Identifying and overcoming different flavors of resistance.* Crit Rev Oncol Hematol, 2021. **162**(1879-0461 (Electronic)): p. 103334.
89. Fusco N, M.U., Fassan M, Marchiò C, Buglioni S, Zupo S, et al., *PIK3CA Mutations as a Molecular Target for Hormone Receptor-Positive, HER2-Negative Metastatic Breast Cancer.* Front Oncol, 2021. **11**(2234-943X (Print)): p. 644737.
90. Andre, F., Ciruelos, E., Rubovszky, G., Campone, M., Loibl, S., Rugo, H. S., Iwata, H., Conte, P., Mayer, I. A., Kaufman, B., Yamashita, T., Lu, Y. S., Inoue, K., Takahashi, M., Papai, Z., Longin, A. S., Mills, D., Wilke, C., Hirawat, S., Juric, D, Solar- Study Group, *Alpelisib for PIK3CA-Mutated, Hormone Receptor-Positive Advanced Breast Cancer.* N Engl J Med, 2019. **380**(20): p. 1929-1940.
91. André, F., et al., *Alpelisib plus fulvestrant for PIK3CA-mutated, hormone receptor-positive, human epidermal growth factor receptor-2-negative advanced breast cancer: final overall survival results from SOLAR-1.* Ann Oncol., 2021. **32(2)**(1569-8041 (Electronic)): p. 208-217.
92. Turner NC, O.M., Howell SJ, Dalenc F, Cortes J, Gomez Moreno HL, et al., *Capivasertib in Hormone Receptor-Positive Advanced Breast Cancer.* N Engl J Med, 2023. **388(22)**(1533-4406 (Electronic)): p. 2058-2070.
93. Alvarez-Garcia, V., Bartos, C., Keraite, I., Trivedi, U., Brennan, P. M., Kersaudy-Kerhoas, M., Gharbi, K., Oikonomidou, O., Leslie, N. R., *A simple and robust real-time qPCR method for the detection of PIK3CA mutations.* Sci Rep, 2018. **8**(1): p. 4290.
94. Park, J., Abbas, N., Park, Y., Park, K. H., Kim, Y. H., Shin, S., *Ultrasensitive and highly selective detection of PIK3CA single point mutations in cell-free DNA with LNA-modified hairpin-shaped probe.* Sensors and Actuators B: Chemical, 2022. **355**.
95. Ang, D., O'Gara, R., Schilling, A., Beadling, C., Warrick, A., Troxell, M. L., Corless, C. L., *Novel method for PIK3CA mutation analysis: locked nucleic acid--PCR sequencing.* J Mol Diagn, 2013. **15**(3): p. 312-8.
96. Patel JM, J.R., *Estrogen Receptor Alpha and ESR1 Mutations in Breast Cancer.* Adv Exp Med Biol, 2022. **1390**(0065-2598 (Print)): p. 171-194.
97. Schiavon G, H.S., Garcia-Murillas I, Cutts RJ, Pearson A, Tarazona N, et al., *Analysis of ESR1 mutation in circulating tumor DNA demonstrates evolution during therapy for metastatic breast cancer.* Sci Transl Med, 2015. **7(313)**(1946-6242 (Electronic)): p. 313ra182.

98. Toy W, S.Y., Won H, Green B, Sakr RA, Will M, et al., *ESR1 ligand-binding domain mutations in hormone-resistant breast cancer.* Nat Genet, 2013. **45(12)**(1546-1718 (Electronic)): p. 1439-45.
99. Merenbakh-Lamin K, B.-B.N., Yeheskel A, Dvir A, Soussan-Gutman L, Jeselsohn R, et al., *D538G mutation in estrogen receptor-α: A novel mechanism for acquired endocrine resistance in breast cancer.* Cancer Res, 2013. **73(23)**(1538-7445 (Electronic)): p. 6856-64.
100. Fanning SW, J.R., Dharmarajan V, Mayne CG, Karimi M, Buchwalter G, et al., *The SERM/SERD bazedoxifene disrupts ESR1 helix 12 to overcome acquired hormone resistance in breast cancer cells. LID - 10.7554/eLife.37161 [doi] LID - e37161.* Elife, 2018. **7**(2050-084X (Electronic)): p. e37161.
101. Puyang X, F.C., Zheng GZ, Wu ZJ, Banka D, Aithal K, et al., *Discovery of Selective Estrogen Receptor Covalent Antagonists for the Treatment of ERα(WT) and ERα(MUT) Breast Cancer.* Cancer Discov, 2018(2159-8290 (Electronic)): p. 1176-1193.
102. Bahreini A, L.Z., Wang P, Levine KM, Tasdemir N, Cao L, et al, *Mutation site and context dependent effects of ESR1 mutation in genome-edited breast cancer cell models.* Breast Cancer Res, 2017. **19(1)**(1465-542X (Electronic)): p. 60.
103. Martin LA, R.R., Simigdala N, et al., *Discovery of naturally occurring ESR1 mutations in breast cancer cell lines modelling endocrine resistance.* Nature Communications, 2017. **8**(1): p. 1865.
104. Shomali M, C.J., Sun F, Koundinya M, Guo Z, Hebert AT, et al., *SAR439859, a Novel Selective Estrogen Receptor Degrader (SERD), Demonstrates Effective and Broad Antitumor Activity in Wild-Type and Mutant ER-Positive Breast Cancer Models.* Mol Cancer Ther, 2021. **20(2)**(1538-8514 (Electronic)): p. 250-262.
105. Spoerke JM, G.S., Walter K, Qiu J, Wilson TR, Savage H, et al., *Heterogeneity and clinical significance of ESR1 mutations in ER-positive metastatic breast cancer patients receiving fulvestrant.* Nat Commun, 2016. **7**(2041-1723 (Electronic)): p. 11579.
106. Clatot F, P.A., Augusto L, Beaussire L, Delacour J, Calbrix C, et al., *Kinetics, prognostic and predictive values of ESR1 circulating mutations in metastatic breast cancer patients progressing on aromatase inhibitor.* Oncotarget, 2016. **7(46)**(1949-2553 (Electronic)): p. 74448-74459.
107. Lefebvre C, B.T., Filleron T, Pedrero M, Campone M, Soria JC, et al., *Mutational Profile of Metastatic Breast Cancers: A Retrospective Analysis.* PLoS Med, 2016. **13(12)**(1549-1676 (Electronic)): p. e1002201.

108. Wang, P., Bahreini, A, Gyanchandani, R, Lucas, P. C, Hartmaier, R. J, Watters, R. J, et al., *Sensitive Detection of Mono- and Polyclonal ESR1 Mutations in Primary Tumors, Metastatic Lesions, and Cell-Free DNA of Breast Cancer Patients.* Clin Cancer Res, 2016. **22**(5): p. 1130-7.
109. Zundelevich A, D.M., Kahana-Edwin S, Itay A, Sella T, Gadot M, et al., *ESR1 mutations are frequent in newly diagnosed metastatic and loco-regional recurrence of endocrine-treated breast cancer and carry worse prognosis.* Breast Cancer Res, 2020. **22(1)**(1465-542X (Electronic)): p. 16.
110. Jeselsohn R, B.G., De Angelis C, Brown M, Schiff R, *ESR1 mutations—a mechanism for acquired endocrine resistance in breast cancer.* Nat Rev Clin Oncol, 2015. **12(10)**(1759-4782 (Electronic)): p. 573-83.
111. Takeshita, T., Yamamoto, Y., Yamamoto-Ibusuki, M., Tomiguchi, M., Sueta, A., Murakami, K., Omoto, Y., Iwase, H., *Analysis of ESR1 and PIK3CA mutations in plasma cell-free DNA from ER-positive breast cancer patients.* Oncotarget., 2017. **8**(32): p. 52142-52155.
112. Chandarlapaty S, C.D., He W, Sung P, Samoila A, You D, et al., *Prevalence of ESR1 Mutations in Cell-Free DNA and Outcomes in Metastatic Breast Cancer: A Secondary Analysis of the BOLERO-2 Clinical Trial.* JAMA Oncol, 2016. **2(10)**(2374-2445 (Electronic)): p. 1310-1315.
113. Fribbens C, O.L.B., Kilburn L, Hrebien S, Garcia-Murillas I, Beaney M, Cristofanilli M, et al., *Plasma ESR1 Mutations and the Treatment of Estrogen Receptor-Positive Advanced Breast Cancer.* J Clin Oncol, 2016. **34(25)**(1527-7755 (Electronic)): p. 2961-8.
114. Fribbens C, G.M.I., Beaney M, Hrebien S, O'Leary B, Kilburn L, et al., *Tracking evolution of aromatase inhibitor resistance with circulating tumour DNA analysis in metastatic breast cancer.* Ann Oncol, 2018. **29(1)**(1569-8041 (Electronic)): p. 145-153.
115. Clatot F, P.A., Beaussire L, Lequesne J, Lévy C, Emile G, et al., *Risk of early progression according to circulating ESR1 mutation, CA-15.3 and cfDNA increases under first-line anti-aromatase treatment in metastatic breast cancer.* Breast Cancer Res, 2020. **22(1)**(1465-542X (Electronic)): p. 56.
116. Franken A, H.E., Reinhardt F, Meier-Stiegen F, Yang L, Jaschinski S, et al., *Detection of ESR1 Mutations in Single Circulating Tumor Cells on Estrogen Deprivation Therapy but Not in Primary Tumors from Metastatic Luminal Breast Cancer Patients.* J Mol Diagn, 2020. **22(1)**(1943-7811 (Electronic)): p. 111-121.
117. Jeannot E, D.L., Michel M, Stern MH, Pierga JY, et al., *A single droplet digital PCR for ESR1 activating mutations detection in plasma.* Oncogene, 2020. **39 (14)**(1476-5594 (Electronic)): p. 2987-2995.

118. Turner NC, S.C., Kilburn L, Fribbens C, Beaney M, Garcia-Murillas I, et al., *ESR1 Mutations and Overall Survival on Fulvestrant versus Exemestane in Advanced Hormone Receptor-Positive Breast Cancer: A Combined Analysis of the Phase III SoFEA and EFECT Trials.* Clin Cancer Res, 2020. **26(19)**(1557-3265 (Electronic)): p. 5172-5177.
119. Turner NC, K.B., Kilburn LS, Kernaghan S, Wardley AM, Macpherson IR, et al., *Circulating tumour DNA analysis to direct therapy in advanced breast cancer (plasmaMATCH): a multicentre, multicohort, phase 2a, platform trial.* Lancet Oncol, 2020. **21(10)**(1474-5488 (Electronic)): p. 1296-1308.
120. O'Leary B, C.R., Liu Y, Hrebien S, Huang X, Fenwick K, et al., *The Genetic Landscape and Clonal Evolution of Breast Cancer Resistance to Palbociclib plus Fulvestrant in the PALOMA-3 Trial.* Cancer Discov, 2018. **8(11)**(2159-8290 (Electronic)): p. 1390-1403.
121. Lok SW, W.J., Vaillant F, Teh CE, Lo LL, Policheni AN, et al., *A Phase Ib Dose-Escalation and Expansion Study of the BCL2 Inhibitor Venetoclax Combined with Tamoxifen in ER and BCL2-Positive Metastatic Breast Cancer.* Cancer Discov, 2019. **9(3)**(2159-8290 (Electronic)): p. 354-369.
122. Moore HM, S.H., O'Brien C, Zhou W, Sokol ES, Goldberg ME, et al., *Predictive and Pharmacodynamic Biomarkers of Response to the Phosphatidylinositol 3-Kinase Inhibitor Taselisib in Breast Cancer Preclinical Models.* Mol Cancer Ther, 2020. **19(1)**(1538-8514 (Electronic)): p. 292-303.
123. Kuang Y, S.B., Hu J, Pun M, Cornwell M, Buchwalter G, et al., *Unraveling the clinicopathological features driving the emergence of ESR1 mutations in metastatic breast cancer.* Breast Cancer, 2018. **4**(2374-4677 (Print)): p. 22.
124. Leal MF, H.B., Schuster E, Yeo B, Afentakis M, Zabaglo L, et al., *Early Enrichment of ESR1 Mutations and the Impact on Gene Expression in Presurgical Primary Breast Cancer Treated with Aromatase Inhibitors.* Cancer Res, 2019. **25(24)**(1557-3265 (Electronic)): p. 7485-7496.
125. Anne Pradines, C.C., Aurélia Doussine, Ivan Bièche, Jérôme Lemonnier, et al., *Abstract CT189: Characterization of ESR1 mutations at metastatic relapse and outcome under first line aromatase inhibitor and palbociclib in the PADA-1 trial*. Vol. 81. 2021, Cancer Research. CT189-CT189.
126. Hortobagyi GN, S.S., Burris HA, Yap YS, Sonke GS, Paluch-Shimon S, et al., *Ribociclib as First-Line Therapy for HR-Positive, Advanced Breast Cancer.* N Engl J Med, 2016. **375(18)**(1533-4406 (Electronic)): p. 1738-1748.
127. Finn RS, M.M., Rugo HS, Jones S, Im SA, Gelmon K, et al., *Palbociclib and Letrozole in Advanced Breast Cancer.* N Engl J Med, 2016. **375(20**(1533-4406 (Electronic)): p. 1925-1936.

128. Goetz MP, T.M., Campone M, Sohn J, Paluch-Shimon S, Huober J, et al., *MONARCH 3: Abemaciclib As Initial Therapy for Advanced Breast Cancer.* J Clin Oncol, 2017. **35(32)**(1527-7755 (Electronic)): p. 3638-3646.
129. Slamon DJ, N.P., Chia S, Fasching PA, De Laurentiis M, Im SA, et al., *Phase III Randomized Study of Ribociclib and Fulvestrant in Hormone Receptor-Positive, Human Epidermal Growth Factor Receptor 2-Negative Advanced Breast Cancer: MONALEESA-3.* J Clin Oncol, 2018. **36(24)**(1527-7755 (Electronic)): p. 2465-2472.
130. Sledge GW Jr, T.M., Neven P, Sohn J, Inoue K, Pivot X, et al., *MONARCH 2: Abemaciclib in Combination With Fulvestrant in Women With HR+/HER2- Advanced Breast Cancer Who Had Progressed While Receiving Endocrine Therapy.* J Clin Oncol, 2017. **35(25)**(1527-7755 (Electronic)): p. 2875-2884.
131. Turner NC, R.J., André F, Loi S, Verma S, Iwata H, et al., *Palbociclib in Hormone-Receptor-Positive Advanced Breast Cancer.* N Engl J Med, 2015. **373(3)**(1533-4406 (Electronic)): p. 209-19.
132. Bihani T, P.H., Arlt H, Tao N, Jiang H, Brown JL, et al., *Elacestrant (RAD1901), a Selective Estrogen Receptor Degrader (SERD), Has Antitumor Activity in Multiple ER(+) Breast Cancer Patient-derived Xenograft Models.* Clin Cancer Res, 2017. **23(16)**(1557-3265 (Electronic)): p. 4793-4804.
133. Garner F, S.M., Paquin D, Lyttle CR, Hattersley G, *RAD1901: a novel, orally bioavailable selective estrogen receptor degrader that demonstrates antitumor activity in breast cancer xenograft models.* Anticancer Drugs, 2015. **26(9)**(1473-5741 (Electronic)): p. 948-56.
134. Patel HK, T.N., Lee KM, Huerta M, Arlt H, Mullarkey T, et al., *Elacestrant (RAD1901) exhibits anti-tumor activity in multiple ER+ breast cancer models resistant to CDK4/6 inhibitors.* Breast Cancer Res, 2019. **21(1)**(1465-542X (Electronic)): p. 146.
135. Francois-Clement Bidard, V.G.K., Patrick Neven, Guillermo Streich, Alberto J. Montero, Fred´eric Forget et al., *Elacestrant (oral selective estrogen receptor degrader) Versus Standard Endocrine Therapy for Estrogen Receptor–Positive, Human Epidermal Growth Factor Receptor 2–Negative Advanced Breast Cancer: Results From the Randomized Phase III EMERALD Trial.* Journal of Clinical Oncology, 2022. **40**(28).
136. Chen Y, Z.X., Wang L, Wu F, Zhang X, Wu H, et al., *Super-ARMS: A new method for plasma ESR1 mutation detection.* Clin Chim Acta, 2021. **520**: p. 23-28.
137. Stergiopoulou D, M.A., Tzanikou E, Ladas I, Makrigiorgos GM, Georgoulias V, et al., *ESR1 NAPA Assay: Development and Analytical Validation of a Highly Sensitive and Specific Blood-Based Assay for the Detection of ESR1 Mutations in Liquid Biopsies.* Cancers (Basel), 2021. **13**(3).

138. Kojima Y, N.E., Yoshino T, Yagishita S, Yazaki S, Okuma HS, et al., *Development of a Detection System for ESR1 Mutations in Circulating Tumour DNA Using PNA-LNA-Mediated PCR Clamping.* Diagnostics (Basel), 2023. **13**(12).
139. Newman, A.M., Bratman, S. V., To, J., Wynne, J. F., Eclov, N. C., Modlin, L. A., et al., *An ultrasensitive method for quantitating circulating tumor DNA with broad patient coverage.* Nat Med, 2014. **20 (5)**(1546-170X (Electronic)): p. 548-54.
140. Frank Diehl, M.L., Devin Dressman, Yiping He, Dong Shen, Steve Szabo, Luis A. Diaz, Jr., Steven N. Goodman, Kerstin A. David, Hartmut Juhl, Kenneth W. Kinzler, Bert Vogelstein, *Detection and quantification of mutations in the plasma of patients with colorectal tumors.* PNAS, 2005. **105**(45): p. 16368–16373.
141. Hirahata T, U.Q.R., Quraish AU, Ul Quraish S, Naz M, Razzaq MA, *Liquid Biopsy: A Distinctive Approach to the Diagnosis and Prognosis of Cancer.* Cancer Inform, 2022. **21**(1176-9351 (Print)): p. 11769351221076062.
142. Adashek, J.J., F. Janku, and R. Kurzrock, *Signed in Blood: Circulating Tumor DNA in Cancer Diagnosis, Treatment and Screening.* Cancers (Basel), 2021. **13**(14).
143. Alfonso Alba-Bernal, R.L.-V., María Emilia Domínguez-Recio, *Challenges and achievements of liquid biopsy technologies employed in early breast cancer.* EBioMedicine, 2020. **62**: p. 103100.
144. Thierry AR, E.M.S., Gahan PB, Anker P, Stroun M, *Origins, structures, and functions of circulating DNA in oncology.* Cancer Metastasis Rev, 2016. **35(3)**(1573-7233 (Electronic)): p. 347-76.
145. Stroun M, A.P., Maurice P, Lyautey J, Lederrey C, Beljanski M, *Neoplastic characteristics of the DNA found in the plasma of cancer patients.* Oncology, 1989. **46(5)**(0030-2414 (Print)): p. 318-22.
146. Caputo V, C.F., Corte CMD, Martini G, Troiani T, Napolitano S, *Diagnostic value of liquid biopsy in the era of precision medicine: 10 years of clinical evidence in cancer.* Explor Target Antitumor Ther, 2023. **4**(1): p. 102-138.
147. Ignatiadis M, S.G., Jeffrey SS, *Liquid biopsy enters the clinic - implementation issues and future challenges.* Nat Rev Clin Oncol, 2021. **18(5)**(1759-4782 (Electronic)): p. 297-312.
148. Ungerer V, B.A., Holdenrieder S, *Preanalytical variables that affect the outcome of cell-free DNA measurements.* Crit Rev Clin Lab Sci, 2020. **57(7)**(1549-781X (Electronic)): p. 484-507.
149. Aucamp J, B.A., Badenhorst CPS, Pretorius PJ, *The diverse origins of circulating cell-free DNA in the human body: a critical re-evaluation of the*

literature. Biol Rev Camb Philos Soc, 2018. **93(3)**(1469-185X (Electronic)): p. 1649-1683.
150. Lin SY, L.Y., Marshall MM, Johnson BJ, Park SR, Wang Z, Su YH, *A New Method for Improving Extraction Efficiency and Purity of Urine and Plasma Cell-Free DNA.* . Diagnostics (Basel), 2021. **11(4)**(2075-4418 (Print)): p. 650.
151. Aw WC, T.S., Melvin RG, Youngson NA, Garvin MR, Hu Y, et al, *Genotype to phenotype: Diet-by-mitochondrial DNA haplotype interactions drive metabolic flexibility and organismal fitness.* PLoS Genet, 2018. **14(11)**(1553-7404 (Electronic)).
152. Drag MH, K.T., *Cell-free DNA and RNA-measurement and applications in clinical diagnostics with focus on metabolic disorders.* Physiol Genomics, 2021. **53(1)**(1531-2267 (Electronic)): p. 33-46.
153. Trumpff C, M.A., Sloan RP, Kaufman BA, Picard M, *Predictors of ccf-mtDNA reactivity to acute psychological stress identified using machine learning classifiers: A proof-of-concept.* Psychoneuroendocrinology, 2019. **107**(1873-3360 (Electronic)): p. 82-92.
154. Fatouros IG, J.A., Nikolaidis MG, Destouni A, Michailidis Y, Vrettou C, et al., *Time of sampling is crucial for measurement of cell-free plasma DNA following acute aseptic inflammation induced by exercise.* Clin Biochem, 2010. **43(16-17)**(1873-2933 (Electronic)): p. 1368-70.
155. Bronkhorst AJ, U.V., Holdenrieder S, *Early detection of cancer using circulating tumor DNA: biological, physiological and analytical considerations.* Crit Rev Clin Lab Sci, 2019. **57(4)**(1549-781X (Electronic)): p. 253-269.
156. Müller Bark J, K.A., Chua B, Day BW, Punyadeera C, *Circulating biomarkers in patients with glioblastoma.* Br J Cancer, 2020. **122(3)**(1532-1827 (Electronic)): p. 295-305.
157. Oellerich M, S.K., Keown P, Schütz E, Beck J, Stegbauer J, et al., *Liquid biopsies: donor-derived cell-free DNA for the detection of kidney allograft injury.* Nat Rev Nephrol, 2021. **17(9)**(1759-507X (Electronic)): p. 591-603.
158. Markus H, C.-C.T., Farooq M, Liang WS, Borad MJ, Sivakumar S, et al., *Evaluation of pre-analytical factors affecting plasma DNA analysis.* Sci Rep, 2018. **8(1)**(2045-2322 (Electronic)): p. 7375.
159. Fujihara J, T.Y., Kawai Y, Kimura-Kataoka K, Takeshita H, *Comparison of serum cell-free DNA between postmortem and living samples.* Clin Chim Acta, 2021. **519**(1873-3492 (Electronic)): p. 255-259.
160. Fernando MR, J.C., Krzyzanowski GD, Ryan WL, *New evidence that a large proportion of human blood plasma cell-free DNA is localized in exosomes.* PLoS One, 2017. **12(8)**(1932-6203 (Electronic)): p. e0183915.

161. Martignano, F., *Cell-Free DNA: An Overview of Sample Types and Isolation Procedures.* Methods Mol Biol, 2019. **1909**(1940-6029 (Electronic)): p. 13-27.
162. Pittella-Silva F, C.Y., Chan HT, Nagayama S, Miyauchi E, Low SK, *Plasma or Serum: Which Is Preferable for Mutation Detection in Liquid Biopsy?* Clin Chem, 2020. **66(7)**(1530-8561 (Electronic)): p. 946-957.
163. Huang Y, M.J., Qi L, Ge W, Fang X, Song Y, et al, *Diverse fragment lengths dismiss size selection for serum cell-free DNA: a comparative study of serum and plasma samples.* Clin Chem Lab Med, 2020. **58(9)**(1437-4331 (Electronic)): p. 1451-1459.
164. Wong FC, S.K., Jiang P, Cheng YK, Chan KC, Leung TY, et al., *Cell-free DNA in maternal plasma and serum: A comparison of quantity, quality and tissue origin using genomic and epigenomic approaches.* Clin Biochem, 2016. **49(18)**(1873-2933 (Electronic)): p. 1379-1386.
165. Luo J, W.S., Zhang S, He Y, Li S, Han J, Xu M, et al., *Performance of ImproGene Cell-Free DNA Tubes for Stabilization and Analysis of cfDNA in Blood Samples.* Fetal Pediatr Pathol, 2022. **41(5)**(1551-3823 (Electronic)): p. 771-780.
166. Barra GB, S.R.T., de Almeida Vasques J, Chianca CF, Nery LF, Santana Soares Costa S, *EDTA-mediated inhibition of DNases protects circulating cell-free DNA from ex vivo degradation in blood samples.* Clin Biochem, 2015. **48(15)**(1873-2933 (Electronic)): p. 976-81.
167. Lam NY, R.T., Chiu RW, Lo YM, *EDTA is a better anticoagulant than heparin or citrate for delayed blood processing for plasma DNA analysis.* Clin Chem, 2004. **50(1)**(0009-9147 (Print)): p. 256-7.
168. Kang Q, H.N., Paoletti C, Jiang H, Vats P, Chinnaiyan AM, et al., *Comparative analysis of circulating tumor DNA stability In K(3)EDTA, Streck, and CellSave blood collection tubes.* Clin Biochem, 2016. **49(18)**(1873-2933 (Electronic)): p. 1354-1360.
169. Sorber L, Z.K., Jacobs J, De Winne K, Goethals S, Reclusa P, et al., *Circulating Cell-Free DNA and RNA Analysis as Liquid Biopsy: Optimal Centrifugation Protocol. LID - 10.3390/cancers11040458 [doi] LID - 458.* Cancers (Basel), 2019. **11(4)**(2072-6694 (Print)): p. 458.
170. Nesic M, B.J., Terp SK, Dybkær K, *Optimization of Preanalytical Variables for cfDNA Processing and Detection of ctDNA in Archival Plasma Samples.* Biomed Res Int, 2021. **2021**(2314-6141 (Electronic)): p. 5585148.
171. Deger T, B.R., de Weerd V, Angus L, van der Put MMJ, et al., *High-throughput and affordable genome-wide methylation profiling of circulating cell-free DNA by methylated DNA sequencing (MeD-seq) of LpnPI digested fragments.* Clin Epigenetics, 2021. **13(1)**(1868-7083 (Electronic)): p. 196.

172. Zhao Y, L.Y., Chen P, Li S, Luo J, Xia H, *Performance comparison of blood collection tubes as liquid biopsy storage system for minimizing cfDNA contamination from genomic DNA.* J Clin Lab Anal, 2019. **33(2)**(1098-2825 (Electronic)): p. e22670.
173. El Messaoudi S, R.F., Mouliere F, Thierry AR, *Circulating cell free DNA: Preanalytical considerations.* Clin Chim Acta, 2013(1873-3492 (Electronic)).
174. Bronkhorst AJ, A.J., Pretorius PJ, *Cell-free DNA: Preanalytical variables.* Clin Chim Acta, 2015. **450**(1873-3492 (Electronic)): p. 243-53.
175. Diao ZL, Z.R., Li JM, *[Analysis of the methods and quality assurance of metagenomic next-generation sequencing to detect the microbial cfDNA from blood samples in China].* Zhonghua Yi Xue Za Zhi, 2022. **102(15)**(0376-2491 (Print)): p. 1114-1118.
176. Meddeb R, P.E., Thierry AR, *Guidelines for the Preanalytical Conditions for Analyzing Circulating Cell-Free DNA.* Clin Chem, 2019. **65(5)**(1530-8561 (Electronic)): p. 623-633.
177. Shin S, W.H., Kim JW, M D YK, Lee KA, *Clinical Practice Guidelines for Pre-Analytical Procedures of Plasma Epidermal Growth Factor Receptor Variant Testing.* Ann Lab Med, 2022. **42(2)**(2234-3814 (Electronic)): p. 141-149.
178. Shao W, K.S., Kopp WC, *Characterization of effect of repeated freeze and thaw cycles on stability of genomic DNA using pulsed field gel electrophoresis.* Biopreserv Biobank, 2012. **10(1)**(1947-5535 (Print)): p. 4-11.
179. Janku F, H.H., Pereira DY, Kobayashi M, Chiu CH, Call SG, et al., *A novel method for liquid-phase extraction of cell-free DNA for detection of circulating tumor DNA.* Sci Rep, 2021. **11(1)**(2045-2322 (Electronic)): p. 19653.
180. Liu Y, C.L., Wang G, Lv J, He Y, Shao PL, et al., *A nano-magnetic size selective cfDNA extraction platform for liquid biopsy with enhanced precision.* J Chromatogr B Analyt Technol Biomed Life Sci, 2022. **1199**(1873-376X (Electronic)): p. 123236.
181. Diefenbach RJ, L.J., Kefford RF, Rizos H, *Evaluation of commercial kits for purification of circulating free DNA.* Cancer Genet, 2018. **228-229**(2210-7762 (Print)): p. 21-27.
182. Kemp BM, W.M., Monroe C, Barta JL, *How much DNA is lost? Measuring DNA loss of short-tandem-repeat length fragments targeted by the PowerPlex 16® system using the Qiagen MinElute Purification Kit.* Hum Biol, 2014. **86(4)**(1534-6617 (Electronic)): p. 313-29.
183. Bai Y, W.Z., Liu Z, Liang G, Gu W, Ge Q, *Technical progress in circulating tumor DNA analysis using next generation sequencing.* Mol Cell Probes, 2020. **49**(1096-1194 (Electronic)): p. 101480.

184. Lin C, L.X., Zheng B, Ke R, Tzeng CM, *Liquid Biopsy, ctDNA Diagnosis through NGS.* Life (Basel), 2021. **11(9)**(2075-1729 (Print)): p. 890.
185. Forshew T, M.M., Parkinson C, Gale D, Tsui DW, Kaper F, et al, *Noninvasive identification and monitoring of cancer mutations by targeted deep sequencing of plasma DNA.* Sci Transl Med, 2012. **4(136)**(1946-6242 (Electronic)): p. 136ra68.
186. Gale D, L.A., Howarth K, Madi M, Durham B, Smalley S, et al., *Development of a highly sensitive liquid biopsy platform to detect clinically-relevant cancer mutations at low allele fractions in cell-free DNA.* PLoS One, 2018(1932-6203 (Electronic)).
187. Cohen JD, L.L., Wang Y, Thoburn C, Afsari B, Danilova L, et al., *Detection and localization of surgically resectable cancers with a multi-analyte blood test.* Science, 2018. **359**: p. 26–930.
188. Chen M, Z.H., *Next-generation sequencing in liquid biopsy: cancer screening and early detection.* Hum Genomics, 2019. **13(1)**(1479-7364 (Electronic)): p. 34.
189. Sykes PJ, N.S., Brisco MJ, Hughes E, Condon J, Morley AA., *Quantitation of targets for PCR by use of limiting dilution.* Biotechniques, 1992. **13(3)**(0736-6205 (Print)): p.:444-9.
190. Gezer U, B.A., Holdenrieder S, *The Clinical Utility of Droplet Digital PCR for Profiling Circulating Tumor DNA in Breast Cancer Patients.* . Diagnostics (Basel), 2022. **12(12)**(2075-4418 (Print)): p. 3042.
191. Day E, D.P., McCaughan F, *Digital PCR strategies in the development and analysis of molecular biomarkers for personalized medicine.* Methods, 2013. **59(1)**(1095-9130 (Electronic)): p. 101-7.
192. Nixon G, G.J., Grant P, Nastouli E, Foy CA, Huggett JF., *Comparative study of sensitivity, linearity, and resistance to inhibition of digital and nondigital polymerase chain reaction and loop mediated isothermal amplification assays for quantification of human cytomegalovirus.* Anal Chem, 2014. **86(9)**(1520-6882 (Electronic)): p. 4387-94.
193. Bohers E, V.P., Jardin F, *cfDNA Sequencing: Technological Approaches and Bioinformatic Issues. LID - 10.3390/ph14060596 [doi] LID - 596.* Pharmaceuticals (Basel), 2021. **14(6)**(1424-8247 (Print)): p. 596.
194. Morlan, J., Baker, J., Sinicropi, D., *Mutation detection by real-time PCR: a simple, robust and highly selective method.* PLoS One, 2009. **4**(2): p. e4584.
195. Aung KL, D.E., Ellison G, Bujac S, Fletcher L, Cantarini M, et al, *Analytical validation of BRAF mutation testing from circulating free DNA using the amplification refractory mutation testing system.* J Mol Diagn, 2014. **16(3)**(1943-7811 (Electronic)): p. 343-9.

196. Zhang X, C.N., Yang G, Zhang Y, Ye M, Cao J, et al, *A comparison of ARMS-Plus and droplet digital PCR for detecting EGFR activating mutations in plasma.* Oncotarget, 2017. **8(67)**(1949-2553 (Electronic)): p. 112014-112023.
197. Lung, J., Hung, M. S., Lin, Y. C., Jiang, Y. Y., Fang, Y. H., Lu, M. S., Hsieh, C. C., Wang, C. S. et al., *A highly sensitive and specific real-time quantitative PCR for BRAF V600E/K mutation screening.* Sci Rep, 2020. **10(1)**(2045-2322 (Electronic)).
198. Itonaga, M., et al., *Novel Methodology for Rapid Detection of KRAS Mutation Using PNA-LNA Mediated Loop-Mediated Isothermal Amplification.* PLoS One, 2016. **11**(3): p. e0151654.
199. Oh, J.E., Lim, H. S., An, C. H., Jeong, E. G., Han, J. Y., Lee, S. H., Yoo, N. J., *Detection of low-level KRAS mutations using PNA-mediated asymmetric PCR clamping and melting curve analysis with unlabeled probes.* J Mol Diagn, 2010. **12**(4): p. 418-24.
200. Zeng, Q., Xie, L., Zhou, N., Liu, M., Song, X., *Detection of PIK3CA Mutations in Plasma DNA of Colorectal Cancer Patients by an Ultra-Sensitive PNA-Mediated PCR.* Mol Diagn Ther, 2017. **21**(4): p. 443-451.
201. Watanabe K, F.T., Tsukita Y, Morita M, Suzuki A, et al, *EGFR Mutation Analysis of Circulating Tumor DNA Using an Improved PNA-LNA PCR Clamp Method.* Can Respir J, 2016. **2016**(1916-7245 (Electronic)): p. 5297329.
202. Milbury CA, L.J., Liu P, Makrigiorgos GM, *COLD-PCR: improving the sensitivity of molecular diagnostics assays.* Expert Rev Mol Diagn, 2011. **11(2)**(1744-8352 (Electronic)): p. 159-69.
203. Markou, A., Farkona, S., Schiza, C., Efstathiou, T., Kounelis, S., Malamos, N., Georgoulias, V., Lianidou, E., *PIK3CA mutational status in circulating tumor cells can change during disease recurrence or progression in patients with breast cancer.* Clin Cancer Res, 2014. **20**(22): p. 5823-34.
204. Dahiru, T., *P - value, a true test of statistical significance? A cautionary note.* Ann Ib Postgrad Med, 2008. **6 (1)**(1597-1627 (Print)): p. 21-6.
205. Giada V Zapparoli, R.N.J., Chelsee A Hewitt, Michelle McBean, David A Westerman, Alexander Dobrovic, *Quantitative threefold allele-specific PCR (QuanTAS-PCR) for highly sensitive JAK2V617F mutant allele detection.* BMC Cancer, 2013. **13**(206).
206. Miyazawa, H., Tanaka, T., Nagai, Y., Matsuoka, M., Huqun., Sutani, A., Udagawa, K., Zhang, J., Hirama, T., Murayama, Y., Koyama, N., Ikebuchi, K., Nagata, M., Kanazawa, M., Nukiwa, T., Takenoshita, S., Kobayashi, K., Hagiwara, K., *Peptide nucleic acid-locked nucleic acid polymerase chain reaction clamp-based detection test for gefitinib-refractory T790M epidermal growth factor receptor mutation.* Cancer Sci, 2008. **99**(3): p. 595-600.

207. Pellestor F, P.P., *The peptide nucleic acids (PNAs), powerful tools for molecular genetics and cytogenetics.* Eur J Hum Genet, 2004. **12(9)**(1018-4813 (Print)): p. 694-700.
208. Ishige T, I.S., Matsushita K, *Locked Nucleic Acid Technology for Highly Sensitive Detection of Somatic Mutations in Cancer.* Adv Clin Chem, 2018. **83**(0065-2423 (Print)): p. 53-72.
209. Allouchery V, P.A., Calbrix C, Berghian A, Lequesne J, Fontanilles M, et al., *Circulating PIK3CA mutation detection at diagnosis in non-metastatic inflammatory breast cancer patients.* Sci Rep, 2021. **11**(1): p. 24041.
210. Takashi Takeshita, Y.Y., Mutsuko Yamamoto-Ibusuki, Mai Tomiguchi, Aiko Sueta, Keiichi Murakami, Yoko Omoto and Hirotaka Iwase, *Analysis of ESR1 and PIK3CA mutations in plasma cell-free DNA from ER-positive breast cancer patients.* Oncotarget., 2017. **8**(32): p. 52142-52155.
211. Ben Rekaya M, S.F., Saied E, Bel Haj Kacem L, Mansouri N, Zarrouk S, et al, *PIK3CA mutations in breast cancer: A Tunisian series.* PLoS One, 2023. **18(5)**(1932-6203 (Electronic)): p. e0285413.
212. Arthur LM, T.A., Renshaw L, Keys J, Thomas JS, Wilson TR, et al., *Changes in PIK3CA mutation status are not associated with recurrence, metastatic disease or progression in endocrine-treated breast cancer.* Breast Cancer Res Treat, 2014. **147(1)**(1573-7217 (Electronic)): p. 211-9.
213. William Jacot, F.D., Evelyne Lopez-Crapez, Leonor Chaltiel , Anna Durigova, Nathalie Gros, Nicolas Lozano, Jean-Louis Lacaze, Stéphane Pouderoux, Laurence Gladieff, Gilles Romieu, Henri Roché, Thomas Filleron, Pierre-Jean Lamy, *PIK3CA mutations early persistence in cell-free tumor DNA as a negative prognostic factor in metastatic breast cancer patients treated with hormonal therapy.* Breast Cancer Research and Treatment, 2019. **2019**.
214. Waks AG, K.D., Jain E, Snow C, Kirkner GJ, Rosenberg SM, et al., *Somatic and Germline Genomic Alterations in Very Young Women with Breast Cancer.* Clin Cancer Res, 2022. **28(11)**(1557-3265 (Electronic)): p. 2339-2348.
215. Mealey NE, O.S.D., Pader J et al., *Mutational landscape differences between young-onset and older-onset breast cancer patients.* BMC Cancer, 2020. **20**(1): p. 212.
216. Luen SJ, V.G., Nik-Zainal S, Savas P, Kammler R, Dell'Orto P et al., *Genomic characterisation of hormone receptor-positive breast cancer arising in very young women.* Annals of Oncology, 2023. **34**(4): p. 397-409.
217. Nagy TR, M.S., Encinas G, Katayama MLH, Pereira GFL, Gaburo-Júnior N, et al., *Germline and Somatic mutations in postmenopausal breast cancer patients.* Clinics (Sao Paulo), 2021. **76**(1980-5322 (Electronic)): p. e2837.
218. Berns K, H.H., Bryan T, Hennessy BFM, Mandy, Madiredjo MFH, et al., *A functional genetic approach identifies the PI3K pathway as a major*

determinant of trastuzumab resistance in breast cancer. Cancer Cell, 2007. **12 (4)**(1535-6108 (Print)): p. 395-402.
219. Miller TW, R.B., Garrett JT, Arteaga C, *Mutations in the phosphatidylinositol 3-kinase pathway: role in tumor progression and therapeutic implications in breast cancer.* Breast Cancer Res, 2011. **13(6)**(1465-542X (Electronic)): p. 224.
220. Kalinsky K, J.L., Heguy A, Patil S, Drobnjak M, Bhanot UK, et al., *PIK3CA mutation associates with improved outcome in breast cancer.* Clin Cancer Res, 2009. **15(16)**(1557-3265 (Electronic)): p. 5049-59.
221. Mayer IA, A.V., Formisano L, Balko JM, Estrada MV, Sanders ME, et al., *A Phase Ib Study of Alpelisib (BYL719), a PI3Kα-Specific Inhibitor, with Letrozole in ER+/HER2- Metastatic Breast Cancer.* Clin Cancer Res, 2017. **23(1)**(1557-3265 (Electronic)): p. 26-34.
222. Vasan N, R.P., Johnson JL, Shao H, Shah H, Antoine A, et al, *Double PIK3CA mutations in cis increase oncogenicity and sensitivity to PI3Kα inhibitors.* Science, 2019. **366(6466)**(1095-9203 (Electronic)): p. 714-723.
223. Barbareschi M, B.F., Felicioni L, Cotrupi S, Barassi F, Del Grammastro M, et al, *Different prognostic roles of mutations in the helical and kinase domains of the PIK3CA gene in breast carcinomas.* Clin Cancer Res, 2007. **13(20)**(1078-0432 (Print)): p. 6064-9.
224. Cizkova M, S.A., Vacher S et al., *PIK3CAmutation impact on survival in breast cancer patients and in ERα, PR and ERBB2-based subgroups.* Breast Cancer Research, 2012. **14**(1): p. R28.
225. Turner NC, I.S., Saura C, Juric D, Loibl S, Kalinsky K, et al., *Inavolisib-Based Therapy in PIK3CA-Mutated Advanced Breast Cancer.* N Engl J Med, 2024. **391(17)**(1533-4406 (Electronic)): p. 1584-1596.
226. Kim JW, L.A., You JY, Lee JH, Song SE, Lee NK, Jung SP, Cho KR, Kim CY, Park KH, et al., *PIK3CA Mutation is Associated with Poor Response to HER2-Targeted Therapy in Breast Cancer Patients.* Cancer Res Treat, 2023. **55**(2): p. 531-541.
227. Cho YA, K.S., Suh YJ, Kim S, Park JH, Park HR, et al., *PIK3CA Mutation as Potential Poor Prognostic Marker in Asian Female Breast Cancer Patients Who Received Adjuvant Chemotherapy.* Curr Oncol, 2022. **29(5)**(1718-7729 (Electronic)): p. 2895-2908.
228. Flavia RM, I.G., Sibeli S, Erika M, Maria AN, et al., *PIK3CA exon 20 mutations are associated with poor prognosis in breast cancer patients.* CLINICAL SCIENCE, 2012. **67(11)**: p. 1285-1290.
229. Loi S, H.-K.B., Majjaj S, Lallemand F, Durbecq V, Larsimont D, et al., *PIK3CA mutations associated with gene signature of low mTORC1 signaling*

and better outcomes in estrogen receptor-positive breast cancer. Proc Natl Acad Sci U S A, 2010. **107(22)**(1091-6490 (Electronic)): p. 10208-13.
230. Martínez-Nava GA, U.-J.L., Lira-Albarrán S, Gómez HL, Ruiz-García E, Nieto-Coronel MT, et al. *Somatic Mutations in Latin American Breast Cancer Patients: A Systematic Review and Meta-Analysis*. Diagnostics, 2024. **14**, 287 DOI: 10.3390/diagnostics14030287.
231. Avivar-Valderas A, M.R., Taheri-Ghahfarokhi A, Carnevalli LS, Hardaker EL, et al, *Functional significance of co-occurring mutations in PIK3CA and MAP3K1 in breast cancer.* Oncotarget, 2018. **9(30)**(1949-2553 (Electronic)): p. 21444-21458.
232. Chen X, G.Y., Ouyang T, Li J, Wang T, Fan Z, et al, *Co-mutation of TP53 and PIK3CA in residual disease after neoadjuvant chemotherapy is associated with poor survival in breast cancer.* Cancer Res Clin Oncol, 2019. **145(5)**(1432-1335 (Electronic)): p. 1235-1242.
233. Lin XY, G.L., Lin X, Wang Y, Zhang G, *Concomitant PIK3CA and TP53 Mutations in Breast Cancer: An Analysis of Clinicopathologic and Mutational Features, Neoadjuvant Therapeutic Response, and Prognosis.* J Breast Cancer, 2023. **26(4)**(1738-6756 (Print)): p. 363-377.
234. Kotoula V, K.V., Zagouri F, Kouvatseas G, Giannoulatou E, Gogas H, et al., *Effects of TP53 and PIK3CA mutations in early breast cancer: a matter of co-mutation and tumor-infiltrating lymphocytes.* Breast Cancer Res Treat, 2016. **158(2)**(1573-7217 (Electronic)): p. 307-21.
235. Deng L, C.J., Zhong XR, Luo T, Wang YP, Huang HF, et al., *Correlation between activation of PI3K/AKT/mTOR pathway and prognosis of breast cancer in Chinese women.* PLoS One, 2015. **10(3)**(1932-6203 (Electronic)): p. e0120511.
236. Takeshita T, Y.Y., Yamamoto-Ibusuki M, Tomiguchi M, Sueta A, Murakami K, et al., *Clinical significance of plasma cell-free DNA mutations in PIK3CA, AKT1, and ESR1 gene according to treatment lines in ER-positive breast cancer.* Mol Cancer, 2018. **17(1)**(1476-4598 (Electronic)): p. 67.
237. Saal LH, H.K., Maurer M, Memeo L, Su T, Wang X, et al., *PIK3CA mutations correlate with hormone receptors, node metastasis, and ERBB2, and are mutually exclusive with PTEN loss in human breast carcinoma.* Cancer Res, 2005. **65(7)**(0008-5472 (Print)): p. 2554-9.
238. Razis E, B.M., Kotoula V, Eleftheraki AG, Kalofonos HP, Pavlakis K, et al, *Evaluation of the association of PIK3CA mutations and PTEN loss with efficacy of trastuzumab therapy in metastatic breast cancer.* Breast Cancer Res Treat, 2011. **128(2)**(1573-7217 (Electronic)): p. 447-56.
239. Pérez-Tenorio G, A.L., Olsson B, Waltersson MA, Nordenskjöld B, Rutqvist LE, et al., *PIK3CA mutations and PTEN loss correlate with similar prognostic*

factors and are not mutually exclusive in breast cancer. Clin Cancer Res, 2007. **13(12)**(1078-0432 (Print)): p. 3577-84.
240. Pereira B, C.S., Rueda O, et al., *The somatic mutation profiles of 2,433 breast cancers refine their genomic and transcriptomic landscapes.* Nature Communications, 2016. **7**(1): p. 11479.
241. Barakeh DH, A.R., Bashawri Y, Almutairi A, Alqubaishi F, Alnamnakani M, et al., *Landscape of somatic mutations in breast cancer: new opportunities for targeted therapies in Saudi Arabian patients.* Oncotarget, 2021. **12(7)**(1949-2553 (Electronic)): p. 686-697.
242. Clusan L, F., Flouriot, Pakdel, *A Basic Review on Estrogen Receptor Signaling Pathways in Breast Cancer.* Int J Mol Sci, 2023. **24(7)**(1422-0067 (Electronic)).
243. Riggins, R.B., Schrecengost, R. S., Guerrero, M. S., Bouton, A. H., *Pathways to tamoxifen resistance.* Cancer Lett, 2007. **256**(1): p. 1-24.
244. Bidard FC, K.V., Neven P, Streich G, Montero AJ, Forget F, et al., *Elacestrant (oral selective estrogen receptor degrader)Versus Standard Endocrine Therapy for Estrogen Receptor-Positive, Human Epidermal Growth Factor Receptor 2-Negative Advanced Breast Cancer: Results From the Randomized Phase III EMERALD Trial.* J Clin Oncol, 2022. **40(28)**(1527-7755 (Electronic)): p. 3246-3256.
245. Brett, J.O., Spring, L. M., Bardia, A., Wander, S. A., *ESR1 mutation as an emerging clinical biomarker in metastatic hormone receptor-positive breast cancer.* Breast Cancer Res, 2021. **23**(1): p. 85.
246. Sefrioui, D., Perdrix, A, Sarafan-Vasseur, N, Dolfus, C, Dujon, A, Picquenot, J. M, et al., *Short report: Monitoring ESR1 mutations by circulating tumor DNA in aromatase inhibitor resistant metastatic breast cancer.* Int J Cancer, 2015. **137**(10): p. 2513-9.
247. Wang P, B.A., Gyanchandani R, Lucas PC, Hartmaier RJ, Watters RJ, et al., *Sensitive Detection of Mono- and Polyclonal ESR1 Mutations in Primary Tumors, Metastatic Lesions, and Cell-Free DNA of Breast Cancer Patients.* Clin Cancer Res, 2016. **22(5)**(1557-3265 (Electronic)): p. 1130-7.
248. Chung, J.H., Pavlick, D, Hartmaier, R, Schrock, A. B, Young, L, Forcier, B et al., *Hybrid capture-based genomic profiling of circulating tumor DNA from patients with estrogen receptor-positive metastatic breast cancer.* Ann Oncol, 2017. **28(11)**(1569-8041 (Electronic)): p. 2866-2873.
249. Yanagawa, T., Kagara, N, Miyake, T, Tanei, T, Naoi, Y, Shimoda, M, et al., *Detection of ESR1 mutations in plasma and tumors from metastatic breast cancer patients using next-generation sequencing.* Breast Cancer Res Treat, 2017. **163(2)**(1573-7217 (Electronic)): p. 231-240.

250. Masunaga, N., Kagara, Motooka, D, Nakamura, S, Miyake, T, Tanei, T, Naoi, Y, et al., *Highly sensitive detection of ESR1 mutations in cell-free DNA from patients with metastatic breast cancer using molecular barcode sequencing.* Breast Cancer Res Treat, 2018. **167(1)**(1573-7217 (Electronic)): p. 49-58.
251. Dustin, D., Gu, G., Fuqua, S. A. W., *ESR1 mutations in breast cancer.* Cancer, 2019. **125(21)**(1097-0142 (Electronic)): p. 3714-3728.
252. Early Breast Cancer Trialists' Collaborative Group (EBCTCG); Davies C, G.J., Gray R, Clarke M, Cutter D, et al., *Relevance of breast cancer hormone receptors and other factors to the efficacy of adjuvant tamoxifen: patient-level meta-analysis of randomised trials.* Lancet, 2011. **378(9793)**(1474-547X (Electronic)): p. 771-84.
253. Rossi V, B.P., Giannarelli D, Nisticò C, Ferretti G, Gasparro S, et al., *Should All Patients With HR-Positive HER2-Negative Metastatic Breast Cancer Receive CDK 4/6 Inhibitor As First-Line Based Therapy? A Network Meta-Analysis of Data from the PALOMA 2, MONALEESA 2, MONALEESA 7, MONARCH 3, FALCON, SWOG and FACT Trials. LID - 10.3390/cancers11111661 [doi] LID - 1661.* Cancers (Basel), 2019. **11(11)**(2072-6694 (Print)): p. 1661.
254. Najim O, H.M., Papadimitriou K, Trinh XB, Pauwels P, Goethals S, et al., *The prevalence of estrogen receptor-1 mutation in advanced breast cancer: The estrogen receptor one study (EROS1).* Cancer Treat Res Commun, 2019. **19**(2468-2942 (Electronic)): p. 100123.
255. Zhang QX, B.A., Wolf DM, Oesterreich S, Fuqua SA, *An estrogen receptor mutant with strong hormone-independent activity from a metastatic breast cancer.* Cancer Res, 1997. **57(7)**(0008-5472 (Print)): p. 1244-9.
256. Toy W, W.H., Razavi P, Lawson M, Goeppert AU, Mazzola AM, et al, *Activating ESR1 Mutations Differentially Affect the Efficacy of ER Antagonists.* Cancer Discov, 2017. **7(3)**(2159-8290 (Electronic)): p. 277-287.
257. Jeselsohn R, D.A.C., Brown M, Schiff R, *The Evolving Role of the Estrogen Receptor Mutations in Endocrine Therapy-Resistant Breast Cancer.* Curr Oncol Rep, 2017. **19(5)**(1534-6269 (Electronic)): p. 35.
258. De Santo I, M.A., Migliaccio I, Di Leo A, Malorni L, *The Emerging Role of ESR1 Mutations in Luminal Breast Cancer as a Prognostic and Predictive Biomarker of Response to Endocrine Therapy. .* Cancers (Basel), 2019. **11(12)**(2072-6694 (Print)): p. 1984.
259. Addanki, S., et al., *Applications of Circulating Tumor Cells and Circulating Tumor DNA in Precision Oncology for Breast Cancers.* Int J Mol Sci, 2022. **23**(14).
260. Tolaney SM, T.M., Neven P, Sohn J, Grischke EM, Llombart-Cussac A, et al., *Clinical Significance of PIK3CA and ESR1 Mutations in Circulating*

Tumor DNA: Analysis from the MONARCH 2 Study of Abemaciclib plus Fulvestrant. Clin Cancer Res, 2022. **28(8)**(1557-3265 (Electronic)): p. 1500-1506.
261. Dahlgren M, G.A., Brueffer C, Gladchuk S, Chen Y, Vallon-Christersson J, et al., *Preexisting Somatic Mutations of Estrogen Receptor Alpha (ESR1) in Early-Stage Primary Breast Cancer. LID - 10.1093/jncics/pkab028 [doi] LID - pkab028.* JNCI Cancer Spectr, 2021. **5(2)**(2515-5091 (Electronic)): p. pkab028.
262. Takeshita T, Y.Y., Yamamoto-Ibusuki M, Inao T, Sueta A, Fujiwara S, et al., *Droplet digital polymerase chain reaction assay for screening of ESR1 mutations in 325 breast cancer specimens.* Transl Res, 2015. **166(6)**(1878-1810 (Electronic)): p. 540-553.
263. Hashimoto, Y., Masunaga, N., Kagara, N., Abe, K., Yoshinami, Tsukabe, M., et al., *Detection of Ultra-Rare ESR1 Mutations in Primary Breast Cancer Using LNA-Clamp ddPCR.* Cancers (Basel), 2023. **15**(9).
264. Gelsomino L, G.G., Rechoum Y, Beyer AR, Pejerrey SM, Tsimelzon A, et al., *ESR1 mutations affect anti proliferative responses to tamoxifen through enhanced cross-talk with IGF signaling.* Breast Cancer Res Treat, 2016. **157(2)**(1573-7217 (Electronic)): p. 253-265.
265. Cha S, L.E., Won HH., *Comprehensive characterization of distinct genetic alterations in metastatic breast cancer across various metastatic sites.* NPJ Breast Cancer, 2021. **7(1)**(2374-4677 (Print)): p. 93.
266. Corné J, Q.V., Callens C, Portois P, Bidard FC, Jeannot E, et al., *Development of sensitive and robust multiplex digital PCR assays for the detection of ESR1 mutations in the plasma of metastatic breast cancer patients.* Clin Chim Acta, 2023. **545**(1873-3492 (Electronic)): p. 117366.
267. Dempsey N, C.Y., Tolman D, et al, *Incidence and outcomes among patients with HR+/HER2- metastatic breast cancer (mBC) with co-occurring ESR1 and PIK3CA mutations detected by ctDNA and treated with alpelisib: A retrospective review.* Journal of Clinical Oncology, 2023. **41(16)**.
268. Dempsey N, B.P., Lewis C, Tolman D, Chamorro Y, et al, *Co-occurrence of ESR1 and PIK3CA mutations in HR+/HER2- metastatic breast cancer: Incidence and outcomes with targeted therapy.* Journal of Clinical Oncology, 2024. **42(16)**.
269. Sim SH, Y.H., Jeon SY et al., *Mutation analysis using cell-free DNA for endocrine therapy in patients with HR+ metastatic breast cancer.* Scientific Reports, 2021. **11**(1): p. 5566.
270. Gerratana L, D.A., Velimirovic M, Clifton K, Hensing WL, Shah AN, et al., *Interplay between ESR1/PIK3CA codon variants, oncogenic pathway alterations and clinical phenotype in patients with metastatic breast cancer*

(MBC): comprehensive circulating tumor DNA (ctDNA) analysis. Breast Cancer Res, 2023. **25(1)**(1465-542X (Electronic)): p. 112.

Appendices

Appendix 1: IRB approvals

Appendix 2: Published journals

MINISTRY OF NATIONAL DEFENSE
108 MILITARY CENTRAL HOSPITAL
No. 2527/A-EC
Approval of the Ethical issues
in Biomedical Research

SOCIALIST REPUBLIC OF VIETNAM
Independence – Freedom – Happiness
Hanoi, May 21st, 2021

APPROVAL OF THE MEDICAL ETHICS COMMITTEE IN BIOMEDICAL RESEARCH

Pursuant to Decision No. 2661/QD-BV by the Director of 108 Military Central Hospital on June 15th, 2020, on the Ethics Committee in Biomedical Research establishment from 2010 to 2025.

Pursuant to the research proposal and an interpretation from the principal investigator.

In reference to ethical aspects, the 108 Military Central Hospital's Ethics Committee in Biomedical Research consents to the research proposal: "**Identifying PIK3CA, ESR1 gene mutations and their relationship with clinical outcome of breast cancer**".

• Principal investigator: Thao Thi Dinh, MD

• Institution in charge: 108 Military Central Hospital

• Research venue: 108 Military Central Hospital

• Research in frame: from June 2021 to June 2024.

The 108 Military Central Hospital's Ethics Committee in Biomedical Research agrees to endorse the research proposal and accompanying documents, committing to guiding the investigators to follow the principles of the International Conference on Harmonization (ICH), Good Clinical Practice (GCP) guidelines, and ongoing Vietnamese regulations.

Recipients:
- PI
- Saved in: DD, MSD, K06b

ON BE HALF OF CHAIRMAN
OF THE ETHICS COMMITTEE
DEPUTY CHAIRMAN

(Signed)

DEPUTY DIRECTOR
ASSOC.PROF. LAM KHANH

BỘ QUỐC PHÒNG
BỆNH VIỆN TWQĐ 108

Số: 2527 /CN-HĐĐĐ
V/v chấp thuận vấn đề ĐĐNCYSH

CỘNG HÒA XÃ HỘI CHỦ NGHĨA VIỆT NAM
Độc lập – Tự do – Hạnh phúc

Hà Nội, ngày 21 tháng 05 năm 2021

CHỨNG NHẬN CHẤP THUẬN CỦA HỘI ĐỒNG ĐẠO ĐỨC TRONG NGHIÊN CỨU Y SINH HỌC

Căn cứ Quyết định số 2661/QĐ-BV ngày 15/6/2020 của Giám đốc Bệnh viện TWQĐ 108 về việc Thành lập Hội đồng Đạo đức trong nghiên cứu Y sinh học nhiệm kỳ 2020-2025. Trên cơ sở xem xét đề cương nghiên cứu và giải trình của chủ nhiệm đề tài.

Hội đồng Đạo đức trong nghiên cứu Y sinh học Bệnh viện TWQĐ 108 chấp thuận về các khía cạnh đạo đức trong nghiên cứu đối với đề tài nghiên cứu: "*Nghiên cứu xác định đột biến gen PIK3CA, ESR1 và mối liên quan với kết quả điều trị ung thư vú*".

Chủ nhiệm đề tài: ThS.BS Đinh Thị Thảo.

Cơ quan chủ trì: Bệnh viện Trung ương Quân đội 108.

Địa điểm nghiên cứu: Bệnh viện Trung ương Quân đội 108.

Thời gian nghiên cứu: Từ tháng 06/2021 đến tháng 06/2024.

Hội đồng Đạo đức trong nghiên cứu Y sinh học - Bệnh viện TWQĐ 108 đồng ý thông qua thuyết minh đề cương nghiên cứu và các tài liệu khác kèm theo; cam kết chỉ đạo nhóm nghiên cứu tuân thủ các nguyên tắc của Hội nghị hài hòa quốc tế và sử dụng dược phẩm trên người (ICH), các hướng dẫn thực hành lâm sàng tốt (GCP) và các quy định hiện hành của Việt Nam./.

Nơi nhận:
- CNĐT;
- Lưu: VT, KHQS, K06b.

KT. CHỦ TỊCH HỘI ĐỒNG
PHÓ CHỦ TỊCH HỘI ĐỒNG

PHÓ GIÁM ĐỐC
PGS.TS. Lâm Khánh

INVESTIGATION OF EXON20 PIK3CA GENE MUTATION IN PLASMA OF HORMONE RECEPTOR POSITIVE BREAST CANCER PATIENTS

Dinh Thi Thao[1,2], Nguyen Phu Thanh[1], Dong Van Quyen[2,3], Ly Tuan Khai[1], Le Huu Song[1], Ngo Tat Trung[1]

ABSTRACT

Objective*:** To determine the frequency of H1047R mutation on exon 20 *PIK3CA* gene in the plasma of hormone recepter positive (HR+) breast cancer (BC) women and its relationship with clinical characteristics of these patients. *Subjects*: Plasma was separated from venous blood of 141 female HR+ BC patients, have been treating at 108 Military Central Hospital from June 2021 to June 2023. ***Method*:** Circulating free DNA (cfDNA) was isolated from plasma by magnetic beads (Thermo Fisher Scientific). The H1047R hotspot mutation on exon 20 *PIK3CA* gene was detected in 141 plasma samples by an in-house Realtime PCR assay using a wild-type allele-specific blocker. ***Results*:** 47/141 samples (33,3 %) had the H1047R mutation. The H1047R mutation was present in all disease stages, both in metastatic and non-metastatic cases. Although, the rates of gene mutation in late-stage, metastatic cancer patients were higher than those in the early-stage, non-metastatic cancer group, there was no statistically significant difference between the two groups ($p > 0.05$). Whereas it was not linked to other clinical traits of patients with HR+BC, the H1047R mutation was more common in those with liver metastases and in those received Fulvestrant ($p < 0.05$). ***Conclusion: Peripheral blood from patients with HR+BC in all stages contained the H1047R mutation on exon 20 of the PIK3CA gene. This mutation frequently developed in patients received Fulvestrant treatment and has been related to liver metastases.

Keyword: *breast cancer, PIK3CA gene, plasma, mutation, circulating free DNA*

[1] *108 Military Center Hospital*
[2] *University of Science and Technology of Hanoi*
[3] *Institute of Biotechnology, Vietnam Academy of Science and Technology*
Responsible person: Dinh Thi Thao
Email: thaodinh3883@gmail.com
Date of receipt: 11/9/2023
Date of scientific judgment: 9/10/2023
Reviewed date: 16/10/2023

I. INTRODUCTION

Breast cancer (BC) is the most frequent malignant disease in both sexes and the major cause of cancer-related deaths in women, according to Globocan data in 2020 [1]. With the advancement of diagnostic technologies, most women are diagnosed in the early stages; yet, more than 20% of patients undergo recurrence and metastasis each year [2]. Endocrine inhibitor therapy is the initial choice for individuals with hormone receptor-positive breast cancer (HR+BC), which accounts for more than 70% of cases. However, clinicians continue to face obstacles such as treatment resistance, relapse, and disease progression. In recent years, identifying somatic gene mutations has provided significant information to targeted therapy to assist improve treatment quality and lengthen life for cancer patients [3].

PIK3CA is an oncogene that encodes the protein p110, a structural component of the PI3K signaling pathway, and is the second most frequently mutated gene in BC tumors. Up to 80% of this gene mutations occur in E545K (exon 9) and H1047R (exon 20) positions which are seen in 20-50% of BC patients and increase PI3K signaling pathway activation [4]. As a result, blocking the PI3K

signaling pathway is critical in BC treatment. Many clinical trials have focused on this topic in recent years, and Alpelisib has been approved by the US FDA to treat patients with metastatic BC who have HR+HER2- and PIK3CA gene mutations [5]. Identifying PIK3CA gene mutations facilitates in the selection of specific therapy regimens for individuals with advanced-stage HR+BC [3]. The relevance of PIK3CA gene variants, particularly exon 20 mutations, is currently debated in research. Some researchers discovered that PIK3CA gene mutations were frequently associated with a poor prognosis and patients with a shorter overall survival [6, 7]. Takashi Takeshitaa's research, on the other hand, demonstrates that patients with exon 20 mutations had a better prognosis than patients without mutations [8].

Somatic mutations have recently been identified not only on DNA molecules isolated from biopsy tumor tissues, but also on DNA molecules generated from tumors that circulate freely in the peripheral blood (circulating tumor DNA-ctDNA), which aids in the testing process because it is less invasive and can be substituted in cases where tissue samples are unavailable or unsuitable for molecular biological testing methods [9].

Thus, this research was conducted to determine the prevalence of the H1047R mutation in exon 20 of the PIK3CA gene in the plasma of HR+BC patients and to analyze the link between this mutation and the clinical characteristics of HR +BC patients.

II. SUBJECTS AND METHODS

2.1. Clinical samples

From June 2021 to June 2023, 141 HR+BC patients have been treated at the Cancer Institute, 108 Military Central Hospital. The patients had agreement to participate in the study and had adequate clinical and histological data.

2.2. Methods

*** cfDNA extration method from plasma:** Within 4 hours of blood collection, peripheral venous blood samples will be centrifuged at 4000g for 10 minutes to separate plasma from blood cells, and the plasma will be stored in a freezer at – 80 ^{0}C until analysis. CfDNA was extracted from plasma samples using Thermo Fisher Scientific magnetic beads. The cfDNA isolation method was carried out in accordance with the manufacturer's instructions. cfDNA samples are utilized to detect genetic changes, while the rest are kept in a freezer at – 80 ^{0}C.

*** H1047R mutation detection method:** The H1047R mutation was discovered using an in-house Realtime PCR process that combined primers intended to specifically couple with the mutant allele and a blocker designed to specifically pair with the wild-type allele. Blocker is an oligonuclotide fragment with a phosphorylated 3' end, thus in the wild-type sample reaction, this substance partners particularly with the wild-type sequence, inhibiting the polymerization reaction. In the case of a mutant DNA sample, the blocker does not couple with the mutated nucleotide; instead, the particular primer pairs with the altered nucleotide, kicking off the amplification and synthesis of the DNA chain. Figure 1 depicts the reaction principle.

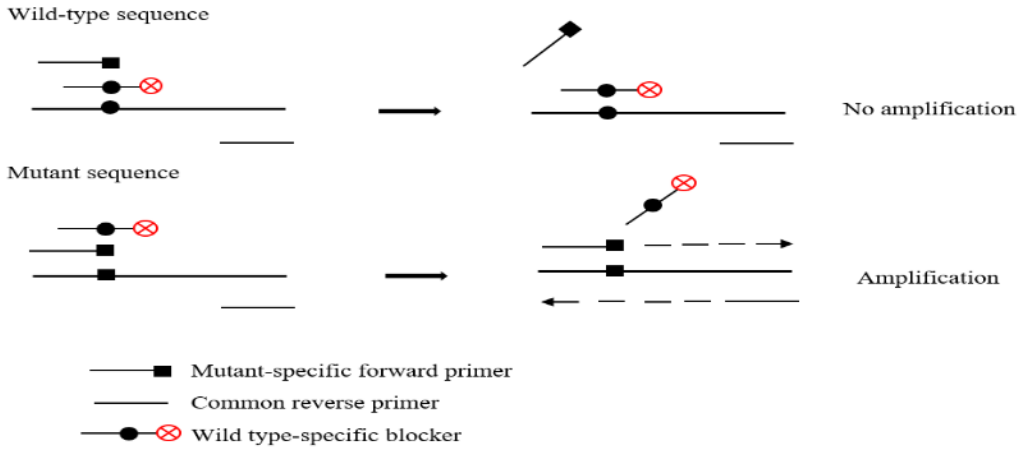

Figure 1. ***The principle of a real-time PCR process to identify the H1047R mutation.***

The final Realtime PCR assay was carried out in a reaction volume of up to 10 µl, using 2X Universal PCR Master Mix (no UNG)TM (Applied Biosystems, Foster City, CA), 40 nM of each primer, 1.2 µM blocker, 2 µl cfDNA or DNA of control samples. The following thermocycling conditions were utilized for the realtime PCR assay: 10 min. at 95°C, 50 cycles of 15 sec. at 95°C, 20 sec. at 55 °C and 20 sec at 72°C.

The comparative cycle threshold (Ct) approach was utilized to investigate fold amplification shifts. Ct values were recorded for each allele-specific experiment, and ΔCt values were computed as the difference in Ct of the same allele amplification with and without blocker. The sample was considered to have the mutation when the ΔCt values of the relative amplification were significantly lower than the ΔCt values of a wild-type control sample (figure2).

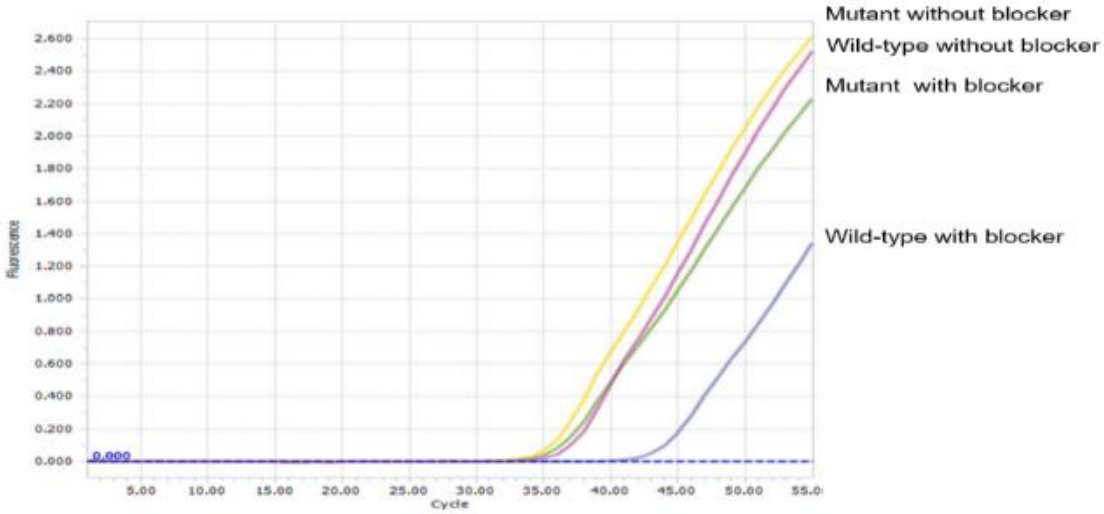

Figure 2: ***DNA amplification of negative control (wild-type DNA) and positive control (mutant DNA) samples, PCR procedure with and without blocker.***

*** Data analysis approaches**: Data was calculated using medical statistical techniques on Spss 20.00 software. Compare the difference between two proportions using the Chi-square test.

III. RESULTS

3.1. Characteristics of HR+BC patients

	Characteristics of study'population, n (%)	
Age (years)	$\overline{X} \pm SD$ (range)	51,5 ± 12,64 (26 - 81)
	< 50	72 (51,1)
	≥ 50	69 (48,9)
Family history	yes	29 (20,6)
Menopausal status	Post-menopausal	74 (52,5)
Tumor histology	Ductal	136 (96,5)
	Lobular	5 (3,5)
Stages	Early	78 (55,3)
	Late	63 (44,7)
Relapse	yes	27 (19,1)
Metastatic status	Any sites	76 (53,9)
	Lymph nodes	68 (48,2)
	Liver	5 (3,5)
	Lung	15 (10,6)
	Bone	23 (16,3)
The number of metastasis lesion	0	65 (46,1)
	≤ 2	63 (44,7)
	≥ 3	13 (9,2)
Treatment	Surgery	116 (82,3)
	Chemotherapy	125 (88,7)
	Endocrine therapy	93 (66,0)
	Radiotherapy	48 (34,0)
	Immunotherapy	50 (35,5)
H1047R mutation	yes	47 (33,3)

Comment: The participants'age ranged from 26 to 81 years old, with an average age of 51.5±12.64 years. 52.5% of the women were postmenopausal, had early stage cancer, and had ductal carcinoma. Recurrence occurred in 19.1% of patients, and metastasis occurred in 53.9% of cases, including lymph nodes, lung, liver, and bone metastases. The majority of patients (82.3%) underwent total mastectomy, axillary lymph node dissection (Patey), and chemotherapy (88.7%). Patients received endocrine therapy, radiation, immunotherapy that accounted for 66%, 34%, 35.5%, respectively . H1047R mutation was found in 47/141 plasma samples from HR+BC patients, accounting for 33.3%.

3.2. The relationship between the H1047 mutation and clinical features of HR+BC patients

Table 2. *Association between H1047R mutation and clinical features of HR+BC patients*

Patients' clinical features		H1047 R mutation status		p-value
		No n = 94 (66,7%)	**Yes n = 47 (33,3%)**	
Age (years)	< 50 ≥ 50	46 (48,9) 48 (51,1)	26 (55,3) **21 (44,7)**	0,592
Family history	No Yes	76 (80,9) 18 (19,1)	36 (76,6) 11 (23,4)	0,659
Menopausal status	Pre-menopausal Post-menopausal	42 (44,7) 52 (55,3)	25 (53,2) **22 (46,8)**	0,375
Tumor histology	Ductal Lobular	89 (94,7) 5 (5,3)	**47 (100)** 0 (0)	0,169
Stages	Early Late	56 (59,6) 38 (40,4)	22 (46,8) **25 (53,2)**	0,151
Relapse	No Yes	80 (85,1) 14 (14,9)	34 (72,3) 13 (27,7)	0,110
Metastasis	No Yes	47 (50) 47 (50)	18 (38,3) **29 (61,7)**	0,213
Lymph nodes invasion	No Yes	53 (56,4) 41 (43,6)	20 (42,6) 27 (47,4)	0,153
Liver metastasis	No Yes	93 (98,9) 1 (1,1)	43 (91,5) 4 (8,5)	**0,042***
Lung metastasis	No Yes	85 (90,4) 9 (9,6)	41 (87,2) 6 (12,8)	0,572
Bone metastasis	No Yes	81 (86,2) 13 (13,8)	37 (78,7) 10 (21,3)	0,334
The number of metastasis lesion	0 ≤2 ≥ 3	47 (50) 41 (43,6) 6 (6,4)	18 (38,3) 22 (46,8) 7 (14,9)	0,177
Received therapy				
Surgical therapy	No Yes	15 (16) 79 (84)	10 (21,3) **37 (78,7)**	0,486
Chemotherapy	No Yes	13 (13,8) 81 (86,2)	3 (6,4) **44 (93,6)**	0,263
Hormone therapy	No Yes	32 (34) 62 (66)	16 (34) **31 (66)**	1.000
Radio therapy	No Yes	67 (71,3) 27 (28,7)	26 (55,3) 21 (44,7)	0,089
Immunotherapy	No Yes	61 (64,9) 33 (35,1)	30 (63,8) 17 (36,2)	1,000

Comment: The H1047R mutation has been found in the peripheral blood of BC women at all stages of the disease, both metastatic and non-metastatic. This mutation was only discovered in ductal BC patients' blood and not in lobular group. Mutations in exon 20 of the PIK3CA gene were more common in patients under 50 years old, pre-menopausal, with metastases, and who have received surgery, chemotherapy, or endocrine therapy, but the difference of mutation rates among these groups was not statistically significant ($p > 0.05$). The H1047R mutation, on the other hand, is more prevalent in liver metastatic BC individuals ($p < 0.05$).

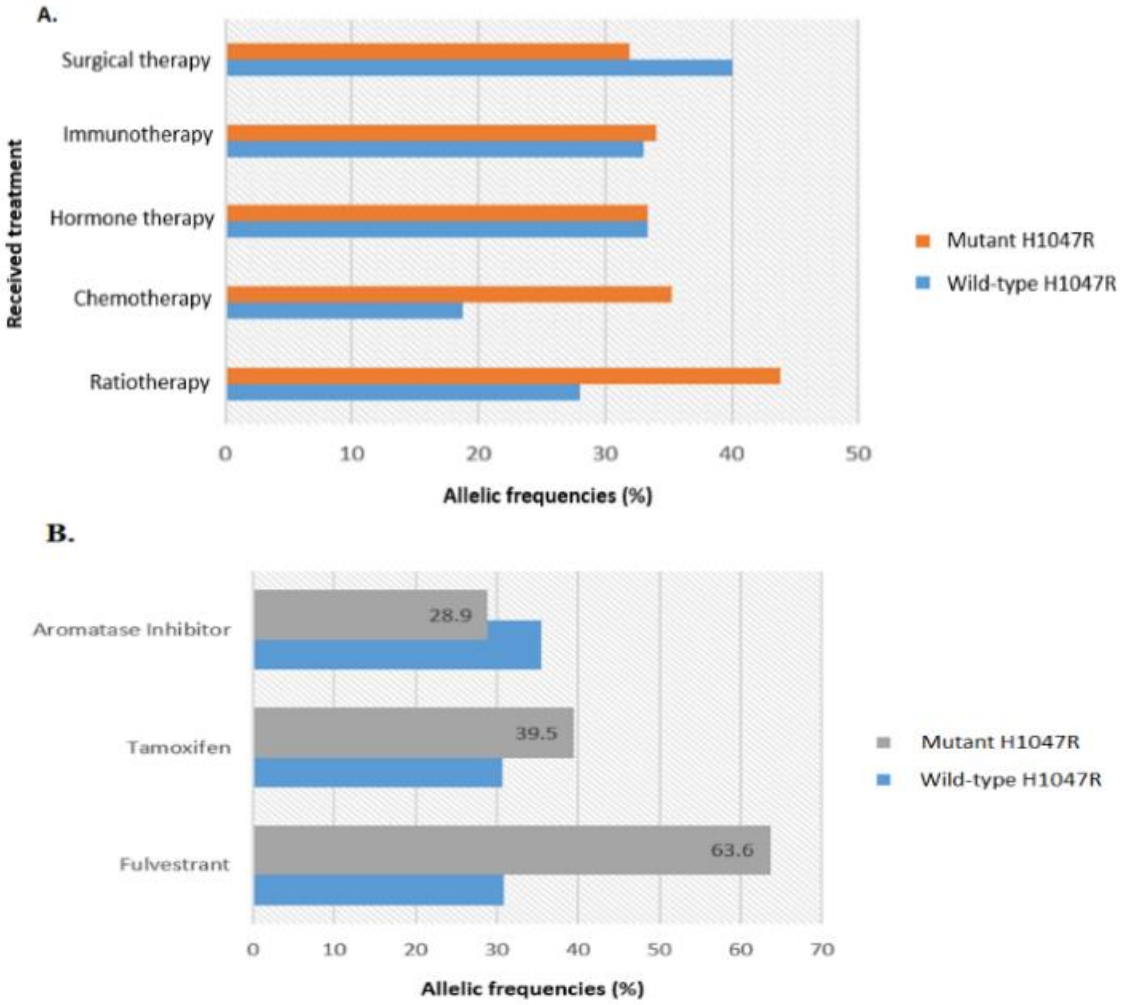

Figure 3. ***Distribution of H1047R mutation rates by treatment regimen (A) and endocrine therapy regimen (B).***

Comment: The H1047R mutation was more common in individuals who had not undergone surgery and have received chemotherapy, radiation, Tamoxifen, or Fulvestrant. Exon 20 PIK3CA gene mutation was found in a significantly higher proportion of HR+ BC patients treated with Fulvestrant than in the non-treated group ($p < 0.05$).

IV. DISCUSSION

The study's participants had an average age of 51.5 ± 12.64 years, with 48.9% being over 50 years old, 52.5% being menopausal, and 20.6% having a personal or relative history of prior malignancy. According to data in 2022, 83% of invasive BC diagnoses in the United States are above the age of 50, the average age at BC diagnosis was 62, and more than half of cases are diagnosed with early stage BC [10]. Thus, the average age of disease in the research group is younger, and the proportion of BC patients under 50 in the study is also greater than the above statistical data, nevertheless the proportion of early stage cases is similar to previously reported data [10, 11].

Published studies reported that PIK3CA gene mutations account for 20-50% of breast cancer tumors; the majority of hot spot

mutations of this gene occur in exon 20 and exon 9, with the most common frequency being H1047R, E545K, E542R, and H1047L [4, 12]. In recent years, researchers have contributed a large amount of evidence demonstrating the presence of freely circulating DNA fragments in the blood (cfDNA) originating from tumors (ctDNA), promising to become a potential tool called "Liquid Biopsy" that can replace biopsy tumor tissue because analysis of molecular abnormalities on cfDNA allows to reveal genetic information of primary and metastatic tumors, genetic changes over time of tumor development, and predict treatment response [13]. In the present research, 33.3% of HR+ BC patients had the hotspot mutation H1047R exon 20 in their blood. Our study's mutation rate is quite similar to other authors' investigations on tissue and peripheral blood samples [14]. Furthermore, several observation revealed a higher percentage of H1047R mutation than our finding, presumably due to the fact that our study population only included HR+breast cancer women [12]. The H1047R mutation was found at all stages of the disease, with the frequency the mutation increasing with disease stages. The mutation was only found in the ductal carcinoma group, not the lobular carcinoma group. On the other hand, previous researches found that PIK3CA gene mutations were present at varying frequencies in early and late stage BC, as well as in all BC subtypes [8, 11]. This disparity can be explained by the fact that our study had a smaller sample size, as HR-negative breast cancer patients were excluded from the study. The major difficulty in analyzing liquid biopsies is that the amount of ctDNA is often very low in the large number of wild-type DNA background, is greatly reduced in the blood under the influence of therapeutic interventions on the patient, and has a short half-life, requiring cfDNA isolation and analysis to be performed as soon as possible after blood collection, and at the same time it is necessary to use a sensitive testing method. So, in addition to differences in the research population, the time and mutation analysis method also greatly affect the frequency of mutations in researches [9].

Exon 20 mutation was also more common in patients with recurrence, having bone, lung, or liver metastasis; the occurrence of this mutation is more frequently encountered in people with severe disease stages and more metastatic sites. The data demonstrated that the appearance of the H1047R mutation might indicate the disease progression, especially since the difference in the rate of gene mutations between patients with liver invasion and the non affected group was statistically significant ($p < 0.05$). So, prospective research data on a larger population is required to evaluate the prognosis role of this mutation of BC patients in Vietnam.

The association between exon 20 mutations and clinical features of BC patients has been observed to differ greatly amongst studies. Mosele and colleagues discovered that PIK3CA gene mutations were more prevalent in HR+HER2- BC patients under the age of 65 who had received endocrine therapy ($p < 0.01$) [11]. Exon 20 mutation was also more common in females under the age of 55, as well as in late-stage cancer patients, postmenopausal women, and patients with lymph node metastases, although this mutation was not appeared to connect with other clinical features ($p > 0.05$) [6].

In our finding, the rate of exon 20 mutation was higher in patients who did not have surgery, chemotherapy, or radiotherapy, but the difference was not statistically significant when compared to the non-treated groups ($p > 0.05$) (Figure 3A). Furthermore,

when assessing the group of HR+ BC patients who underwent endocrine therapy, the H1047R mutation showed at a considerably greater rate in the Fulvestrant – received group compared to the non-Fulvestrant-treated group (p = 0.042) (Figure 3B).

Drug resistance to endocrine therapy has previously been observed in HR+ BC patients with PIK3CA gene mutations [15]. As a result, several targeted medicines that inhibit the PI3K signaling pathway have been studied and developed to treat endocrine-resistant individuals with PI3K mutations. Among them, when coupled with fulvestrant, Alpelisib has been demonstrated to dramatically improve disease-free survival in HR+HER2- advanced post-menopausal patients who had PIK3CA mutations [5]. It can be shown that assessing whether BC patients have PIK3CA gene mutations would assist physicians in making a prognosis and guiding the selection of appropriate treatment regimens for the patients.

V. CONCLUSION

H1047R mutation on exon 20 of the PIK3CA gene in peripheral blood of HR+ BC patients at all stages. The mutation was related with liver metastases and developed at a high rate in individuals treated with Fulvestrant.

REFERENCES

1. **Arnold, M., et al.,** Current and future burden of breast cancer: Global statistics for 2020 and 2040. Breast, 2022. 66: p. 15-23.
2. **Pan, H., et al.,** 20-Year Risks of Breast-Cancer Recurrence after Stopping Endocrine Therapy at 5 Years. N Engl J Med, 2017. 377(19): p. 1836-1846.
3. **Lau, K.H., Tan, A. M., Shi, Y.,** New and Emerging Targeted Therapies for Advanced Breast Cancer. Int J Mol Sci, 2022. 23(4).
4. **Anderson, E.J., Mollon, L. E., Dean, J. L., Warholak, T. L., Aizer, A., Platt., E. A., Tang, D. H., Davis, L. E.,** A Systematic Review of the Prevalence and Diagnostic Workup of PIK3CA Mutations in HR+/HER2- Metastatic Breast Cancer. Int J Breast Cancer, 2020. 2020: p. 3759179.
5. **André, F., et al.,** Alpelisib plus fulvestrant for PIK3CA-mutated, hormone receptor-positive, human epidermal growth factor receptor-2-negative advanced breast cancer: final overall survival results from SOLAR-1. Ann Oncol., 2021. 32(2)(1569-8041 (Electronic)): p. 208-217.
6. **Flavia R. Mangone, I.G.B., Sibeli Salaorni, Erika Manuli, Maria A. Nagai,** PIK3CA exon 20 mutations are associated with poor prognosis in breast cancer patients. CLINICAL SCIENCE, 2012. 67(11): p. 1285-1290.
7. **Takashi Takeshita, Y.Y., Mutsuko Yamamoto-Ibusuki, Mai Tomiguchi, Aiko Sueta, Keiichi Murakami, Yoko Omoto and Hirotaka Iwase,** Analysis of ESR1 and PIK3CA mutations in plasma cell-free DNA from ER-positive breast cancer patients. Oncotarget., 2017. 8(32): p. 52142-52155.
8. **Takashi Takeshita, Y.Y., Mutsuko Yamamoto-Ibusuki, Toko Inao, Aiko Sueta, Saori Fujiwara, Yoko Omoto and Hirotaka Iwase,** Prognostic role of PIK3CA mutations of cell-free DNA in early-stage triple negative breast cancer. Cancer Sci 2015. 106: p. 1582–1589.
9. **Alfonso Alba-Bernal, R.L.-V., María Emilia Domínguez-Recio,** Challenges and achievements of liquid biopsy technologies employed in early breast cancer. EBioMedicine, 2020. 62: p. 103100.
10. **Giaquinto, A.N., Sung, H, Miller, K. D, Kramer, J. L, Newman, L. A, Minihan, A, Jemal, A, Siegel, R. L.,** Breast Cancer Statistics, 2022. CA Cancer J Clin, 2022. 72(6): p. 524-541.
11. **Mosele, F., et al.,** Outcome and molecular landscape of patients with PIK3CA-mutated metastatic breast cancer. Ann Oncol, 2020. 31(3): p. 377-386.

12. **Martínez-Sáez, O., Chic, N., Pascual, T., Adamo, B., Vidal, M., González-Farré, B., Sanfeliu, E., Schettini, F., Conte, B., Brasó-Maristany, F., Rodríguez, A., Martínez, D., Galván, P., Rodríguez, A. P., Martinez, A., Muñoz, M., Prat, A.,** Frequency and spectrum of PIK3CA somatic mutations in breast cancer. Breast Cancer Research, 2020. 22.
13. **Addanki, S., et al.,** Applications of Circulating Tumor Cells and Circulating Tumor DNA in Precision Oncology for Breast Cancers. Int J Mol Sci, 2022. 23(14).
14. **Takashi Takeshitaa, Y.Y., Mutsuko Yamamoto-Ibusukib, Mai Tomiguchia, Aiko Suetaa and Hirotaka Iwase,** ESR1 and PIK3CA mutational status in serum and plasma from metastatic breast cancer patients: A comparative study. Cancer Biomarkers, 2018. 8: p. 48.
15. **William Jacot, F.D., Evelyne Lopez-Crapez, Leonor Chaltiel , Anna Durigova, Nathalie Gros, Nicolas Lozano, Jean-Louis Lacaze, Stéphane Pouderoux, Laurence Gladieff, Gilles Romieu, Henri Roché, Thomas Filleron, Pierre-Jean Lamy,** PIK3CA mutations early persistence in cell-free tumor DNA as a negative prognostic factor in metastatic breast cancer patients treated with hormonal therapy. Breast Cancer Research and Treatment, 2019. 2019.

PLOS ONE

RESEARCH ARTICLE

Identification of breast cancer-associated PIK3CA H1047R mutation in blood circulation using an asymmetric PCR assay

Dinh Thi Thao[1,2]*, Nguyen Phu Thanh[1], Dong Van Quyen[2,3], Ly Tuan Khai[4], Le Huu Song[5], Ngo Tat Trung[1,5]*

1 Center for Genetic Consultation and Cancer Screening, 108 Military Center Hospital, Hai Ba Trung, Hanoi, Vietnam, **2** University of Science and Technology of Hanoi, Cau Giay, Hanoi, Vietnam, **3** Institute of Biotechnology, Vietnam Academy of Science and Technology, Cau Giay, Hanoi, Vietnam, **4** Department of Hematology, Laboratory Center, 108 Military Center Hospital, Hai Ba Trung, Hanoi, Vietnam, **5** Vietnamese-German Center for Medical Research, 108 Military Center Hospital, Hai Ba Trung Hanoi, Vietnam

* tatrungngo@gmail.com (NTT); thaodinh3883@gmail.com (DTT)

OPEN ACCESS

Citation: Thao DT, Thanh NP, Quyen DV, Khai LT, Song LH, Trung NT (2024) Identification of breast cancer-associated PIK3CA H1047R mutation in blood circulation using an asymmetric PCR assay. PLoS ONE 19(8): e0309209. https://doi.org/10.1371/journal.pone.0309209

Editor: Avaniyapuram Kannan Murugan, King Faisal Specialist Hospital and Research Center, SAUDI ARABIA

Received: January 26, 2024

Accepted: August 8, 2024

Published: August 28, 2024

Data Availability Statement: All relevant data are within the manuscript.

Funding: This study was financially supported by the VIN group Innovation Foundation (VINIF) under the grant number VINIF.2021.TS.161, and the National Foundation for Science and Technology Development (NAFOSTED) under the grant number 108.06-2020.10. The authors state that the funders had no role in study design, data collection and

Abstract

Purpose

To establish a highly sensitive and specific approach for the detection of circulating *PIK3CA* H1047R mutation in breast cancer (BC) patients and to investigate the association between the prevalence of *PIK3CA* H1047R mutation and clinical presentations.

Methods

A proper blocker was designed in an allele-specific manner and optimized for PCR-based identification of the *PIK3CA* H1047R mutation. The established technique was validated in cell-free DNA samples from 196 recruited BC patients.

Results

The allele-specific PCR assay with a properly designed blocker was able to detect the H1047R mutant variant with 0.01%. By applying the newly established assay, 62 cases (31.6% of the total recruited cases) were found to carry a blood-circulating H1047R mutant. Wherein, the detected mutant rates increased with disease stages from 2/18 (11.1%) of stage I to 17/71 (23.9%) of stage II, 20/53 (37.7%) of stage III, and 23/31 (42.6%) of stage IV ($p = 0.025$), respectively. Higher frequencies of H1047R mutation were associated with late-stage ($p = 0.033$) or recurrence ($p = 0.045$) or metastatic patients ($p = 0.049$) as well as radiation-treated human epidermal growth factor receptor 2 (HER2) positive BC ($p = 0.004$). *PIK3CA* mutant carriers were frequently observed in patients under the age of 50 who had liver-metastasized or brain metastases or lymph node-invaded ($p < 0.05$).

Conclusion

A novel allele-specific PCR assay with high sensitivity was established successfully for the detection of the *PIK3CA* H1047R mutation in clinical practice.

analysis, decision to publish, or preparation of the manuscript.

Competing interests: The authors have declared that no competing interests exist.

Introduction

Breast cancer (BC) is the most women-specific malignant disease, in which 70% of the disease is hormone receptor positive (HR-positive) tumours are indicated endocrine-based therapies as standard treatment [1]. However, about 20% of patients acquire resistance to their initial endocrine based regimen, leading to recurrence, metastasis, or even mortality [2]. The disease is specified by stimulation of the PI3K/Akt/mTOR signalling [3–8]. Previous studies have demonstrated that genetic lesions of the *PIK3CA* gene drive such consecutive activation of the PI3K/Akt/mTOR pathway that not only sustain the in the tumor cells' survival, proliferation and metastasis but also trigger the breast cancer cells to become resistant to the conventional endocrine therapy [9]. Therefore, blocking the PI3K/Akt/mTOR pathway in *PIK3CA*-mutated BC would logically sensitize the *PIK3CA*-mutation carriers to the conventional endocrine regimen [10]. Alpelisib, a PI3K inhibitor, has been approved for the treatment of HR-positive/HER2-negative, *PIK3CA*-mutated, metastatic BC patients [11]. Screening for *PIK3CA* mutations is mandatorily recommended when considering patient candidates for PI3K inhibitor-targeted therapy, especially for cancers with endocrine resistance [12]. *PIK3CA* mutations occur frequently in exons 9 and 20, notably at positions H1047R, E545K, and E542K, which account for 70–80% of *PIK3CA* mutated cases in breast cancer [13]. So, most effort reported so far was to optimize diagnostic assays to identify the mentioned hotspots: H1047R, E545K, and E542K [14–22].

Tumour tissues are traditionally the main sources for DNA extraction and downstream genetic analysis. However, if patients carry tiny tumour masses or relapse with distant metastases, the repeat of tumour biopsy would be a challenge, and the information encoded in tumour tissues is a snap-shot of a given pathological stage, thus it is not suitable for determining the clinical kinetics during patients' treatments. In these cases, such body fluids as peripheral blood would be an alternative source for DNA analysis; additionally, the analysis of cell-free DNA (cfDNA) from the mentioned biopsy can also be used to monitor the disease progression, tumour burden loads, or patients' responses to the indicated therapy at a real-time level [23]. One challenge that thwarts the use of liquid biopsy for the identification of clinically relevant genetic lesions is that the amount of extractable cfDNA and the ratio of detectable mutation load are pretty low, even lower than 0.1% of total extractable cfDNA from patients' plasma [24, 25].

The Sanger sequencing technique can hardly detect mutations with allelic variants lower than 10%; hence, it is rarely used in searching for mutations in plasma samples [26]. Whereas next-generation sequencing (NGS) and digital PCR are examples of current advanced technologies that can be customized to detect a specific panel of somatic mutations, such as the *PIK3CA* gene, with an extremely deep sensitivity [22, 24], the accompanying consumables and equipment cost are high and are unlikely to be widely utilized for routine diagnostics in low-income communities [23].

Asymmetric PCR is an analogue of conventional PCR-based methods wherein the amplification of undesirable or wild-type alleles is blocked by the presence of molecular peptide clamps or oligonucleotide blockers [27]. This art of techniques was optimized for targeted amplification and synchronous detection of either point mutations for instant *KRAS*, *BRAF*, or *JAK2* genes or even mutational hotspots, provided that the mutation hotspots are focused in narrow domains similar to an instant *EGFR* gene [27–30]. In the case of *PIK3CA*, the appearance of the gene mutations in a narrow frame at codons 542, 545, and 1047 allows to utilise asymmetric PCR for detecting these alterations. However, the recently published asymmetric PCR assays hardly acquired a technical sensitivity of about 0.1% (Table 1), which is inadequate

Table 1. Sensitivity of various asymmetric PCR approaches for detecting the *PIK3CA* H1047R mutation.

Methods	Sensitivity (%)	Sample types	Tumour types	Mutation frequency (%)	Authors (Year)
An amplification refractory mutation system (ARMS) PCR	0.1%	Tissue	Breast cancer	15/49 (30.6%)	Ruth E. Board et al. (2008) [17]
Lock Nucleic Acid (LNA) PCR Sequencing	1.3%	Tissue	Breast cancer	30/60 (50%)	Daphne Ang et al. (2012) [21]
An amplification refractory mutation system (ARMS-PCR) using allele-specific scorpion primers	0.5%	Tissue	Breast cancer	15/102 (14.7%)	Alexandre Harlé et al. (2013) [20]
The combination of allele-specific, melting analysis and asymmetric rapid PCR	0.05%	Plasma	Breast cancer	14/76 (18.4%)	Athina Markou et al. (2014) [15]
Peptide Nucleic Acid (PNA) PCR Sequencing	0.2%	Plasma	Colorectal carcinoma	29/128 (22.65%)	Qian Zeng et al. (2017) [31]
Allele-specific competitive blocker-PCR	5%	Tissue	Breast cancer	2/22 (9.1%)	Virginia Alvarez-Garcia et al. (2018) [16]
The nuclease-assisted minor-allele enrichment PCR assay with overlapping probes	0.3%	Plasma	Breast cancer	4/25 (16%)	Leva Keraite et al. (2020) [18]
LNA-modified hairpin-shaped primers	0.1%	Plasma	Colorectal carcinoma	1/2 (50%)	Junsoo Park et al. (2022) [32]

https://doi.org/10.1371/journal.pone.0309209.t001

to identify the H1047R point mutation in real clinical settings, especially to detect *PIK3CA* mutations in blood.

In this study, we proposed an optimized blocker-mediated asymmetric PCR assay integrated with an allele-specific (AS) primer to almost completely inhibit the amplification of a wild-type allele while specifically enriching the signal of a mutant target to get such an ultra-sensitive detection limit of 0.01%. Therefore, our newly established method can be exploited for the identification of the H1047R point mutation from BC patients' peripheral blood samples.

Materials and methods

Clinical samples, sample preparation and DNA extraction

196 over-18-year-old female breast cancer patients (stages I-IV) were recruited from 108 Military Central Hospital (MCH) between June 2021 and June 2023 for this study. Right after hospitalization, written consents to the study were given to individual patients; blood samples, clinical and paraclinical parameters were also collected.

Among the studied cohort, 43 cases (21.9%) suffered recurrence, 54 out of 196 (27.6%) patients were classified as stage IV, and 116 out of 196 (59.2%) patients bear at least one invasive location, either lymph nodes and/or metatases to other organs, as summarized in Table 4 (the patients' characteristics).

EDTA K_2-processed peripheral blood samples were centrifuged at 2,000 g for 10 minutes at room temperature, then the separated plasma fractions were collected and frozen until DNA was further used. 500 μL aliquots of plasma were input for individual cfDNA preparation using the MagMAX™ Cell-Free DNA Isolation Kit (Thermo Fisher Scientific, USA). The isolated cfDNA samples were stored at -80˚C until further utilization.

The human T-47D breast cancer cell line was purchased from Thermo Fisher Scientific Inc. T-47D cells were maintained in RPMI 1640 medium (Invitrogen, Carlsbad, CA) with phenol red and supplemented with 7.5% fetal bovine serum (FBS) plus 100 units/ml penicillin-streptomycin (Sigma-Aldrich). Cells were cultured and grown in an air-carbon dioxide (95:5) atmosphere at 37˚C. Genomic DNA was extracted from the T-47D cells and healthy donors' white

blood cells using the genomic DNA purification kit (Thermo Fisher Scientific) following the manufacturer's protocol in an elution volume of 100 μl. The extracted DNA was aliquoted and stored at -20˚C until use.

A given T-47D cell line number (that contains 50% *PIK3CA* mutant allele [18]) was mixed with white blood cells of healthy donors to formulate a so-called positive cell line dilution series that bears 10%, 1%, 0.1%, 0.01%, 0.001%, and 0% of T-47D cells. These positive cell line dilution series were then input for total genomic DNA extraction. The genomic DNA extracted from the positive dilution series was later used as positive and negative controls for further assay optimization.

Ethical considerations

The study and its accompanying methods of consent were submitted for regulatory approval to the Institutional Review Board of the 108 Military Central Hospital in Hanoi, Vietnam, and were approved. The Ethical Committee of the 108 Military Central Hospital, Hanoi, provided ethical approval for the study (No. 2527/CN-HDDD). Informed written consent was obtained from all study participants or from their parents or guardians if the study participant was in an unconscious condition. The patients were completely anonymous.

Primers and oligonucleotides

Primers were designed to amplify amplicons of 86 bp flanking around the studied H1047R mutant, whereas blocker was selected to bone-fine complementarily clamp and inhibit the amplification of wild-type allele (detailed sequences of primers and blocker are listed in Table 2). All oligonucleotides were obtained from the IDT Company (USA). Commercial master mix, nuclease-free water, 6 x loading buffer, and dNTPs were purchased from Thermo Fisher Scientific Inc (USA).

Amplification of the *PIK3CA* H1047R point mutation

Allele-specific amplification targeting the *PIK3CA* H1047R point mutation was performed using a real-time PCR system (LightCycler 96, Roche, Switzerland). Primers, blocker, and 2 μl DNA sample were mixed with 2X Universal PCR Master Mix (no UNG) TM (Applied Biosystems, Foster City, CA) in a reaction volume of up to 10 μl. Standard real-time PCR assay thermocycling conditions were used: 10 min. at 95˚C, 50 cycles of 15 sec. at 95˚C, 20 sec. at 55˚C, and 20 sec. at 72˚C.

Statistical analysis

Statistical analysis was performed via SPSS version 20.0 (IBM SPSS Statistics, Armonk, NY, USA). The $\chi 2$ and Fisher's tests were used to determine associations between *PIK3CA* gene mutation and clinicopathological features of BC patients. A p-value ≤ 0.05 was considered to

Table 2. Oligonucleotides for the real-time PCR assay.

Primer name	Sequence (5'-3')	Tm (˚C)	Final concentration
PIK3CA H1047R mt F	ACAAATGAATGATGCACG	58.5	40 nM
PIK3CA H1047R R	CAGTTCAATGCATGCTGTTTAATT	64.1	40 nM
PIK3CA H1047R wt BL	TGATGCACATCATGG TG/PO4	59	1.2 μM

mt F: mutant specific forward primer; R: common reverse primer; wt BL: wild-type specific blocker.

https://doi.org/10.1371/journal.pone.0309209.t002

be significant. Graphics were generated with MS Excel 2010 (Microsoft Corporation, Seattle, WA, USA).

Results

Assay optimization

The blocker-mediated PCR clamping system is schematically presented in Fig 1A. A forward primer (mutant-specific primer) is perfectly matched to the mutant allele, while a 3′ phosphorylated, un-extended oligonucleotide sequence (wild-type blocker) that is perfectly complementary to the wild-type sequence on the same strand was used as the blocker to inhibit the polymerase-mediated amplification of the wild-type allele. Various blocker concentrations (0, 0.8 μM, 1.2 μM, 1.6 μM) were tested to evaluate the clamping effect on the amplification of wild-type versus mutant alleles. At a concentration of 1.2 μM, the blocker acquires its sharpest inhibitory effect on the amplification of the wild-type allele while keeping the mutant allele almost intact. Hence, 1.2 μM of the blocker was selected as the optimized parameter for further downstream analysis (Fig 1B and 1C).

Detection limit optimization for identifying the *PIK3CA* H1047R mutation

The total genomic DNA extracted from T-47D positive cell line (known to carry 50% H1047R [18]) was mixed with an equal amount of total genomic DNA extracted from healthy donors' white blood cells to form dilution series that bear 10%, 1%, 0.1%, 0.01%, 0.001%, and 0% of H1047R. These dilution series were used as input templates for validating the technical sensitivity and the specificity of the designed real-time PCR assay. At each dilution point, the real-time PCR was performed in four conditions: (i) wild-type template without blocker (blocker-free); (ii) wild-type template with blocker; (iii) mutant template (0.001%, 0.01%, 0,1%, 1%, 10%) without blocker; and (iv) mutant template (0.001%, 0.01%, 0,1%, 1%, 10%) with blocker, and was repeated 15 times to determine the assay's technical sensitivity (the limit of detection, LOD). At the lowest concentration of the mutant allele (0.001%), the acquired ΔCt value distance is 5.19 ($p = 0.714$), and the ΔCt distance linearly decreases to 1.22 ($p = 0.001$) at the highest dilution point of the 10% mutant allele (Fig 2 and Table 3). Because only assays with a p-value lower than 0.05 are considered statistically significant [33], the 0.01% mutant allele is concluded to be the LOD of our newly established technique, and the assay's accuracy was maintained at 0.01% or higher H1047R mutation.

PIK3CA mutation determined in BC patients' plasma samples

By applying the newly established assay to 196 institutionally recruited BC patients' plasma samples, 62 cases (31.6% of total recruited cases) harboured the H1047R mutant (Table 4); the detected mutant rates increased with disease stages from 2/18 (11.1%) of stage I to 17/71 (23.9%) of stage II, 20/53 (37.7%) of stage III, and 23/31 (42.6%) of stage IV ($p = 0.025$), respectively (Table 4 and S1A Fig). However, there was no relationship between the H1047R mutation and the patient's age, family history, menopausal status, HR or HER2 expressions, or tumour histopathology (Table 4). On the other hand, patients with recurrence, metastasis, visceral metastasis, bone metastases, and patients with multiple metastatic sites have a higher incidence of *PIK3CA* gene mutations (S1B and S1C Fig). Our data also revealed that individuals with late-stage cancer ($p = 0.033$), recurrence ($p = 0.045$), metastasis ($p = 0.049$), or liver metastatic disease ($p = 0.034$) or brain metastases ($p = 0.009$), as well as radiation-treated HER2 positive BC ($p = 0.004$) were more likely to have the H1047R mutation (Table 4, S1 and S2B Figs); HR-positive/HER2-negative advanced BC patients who were treated selective

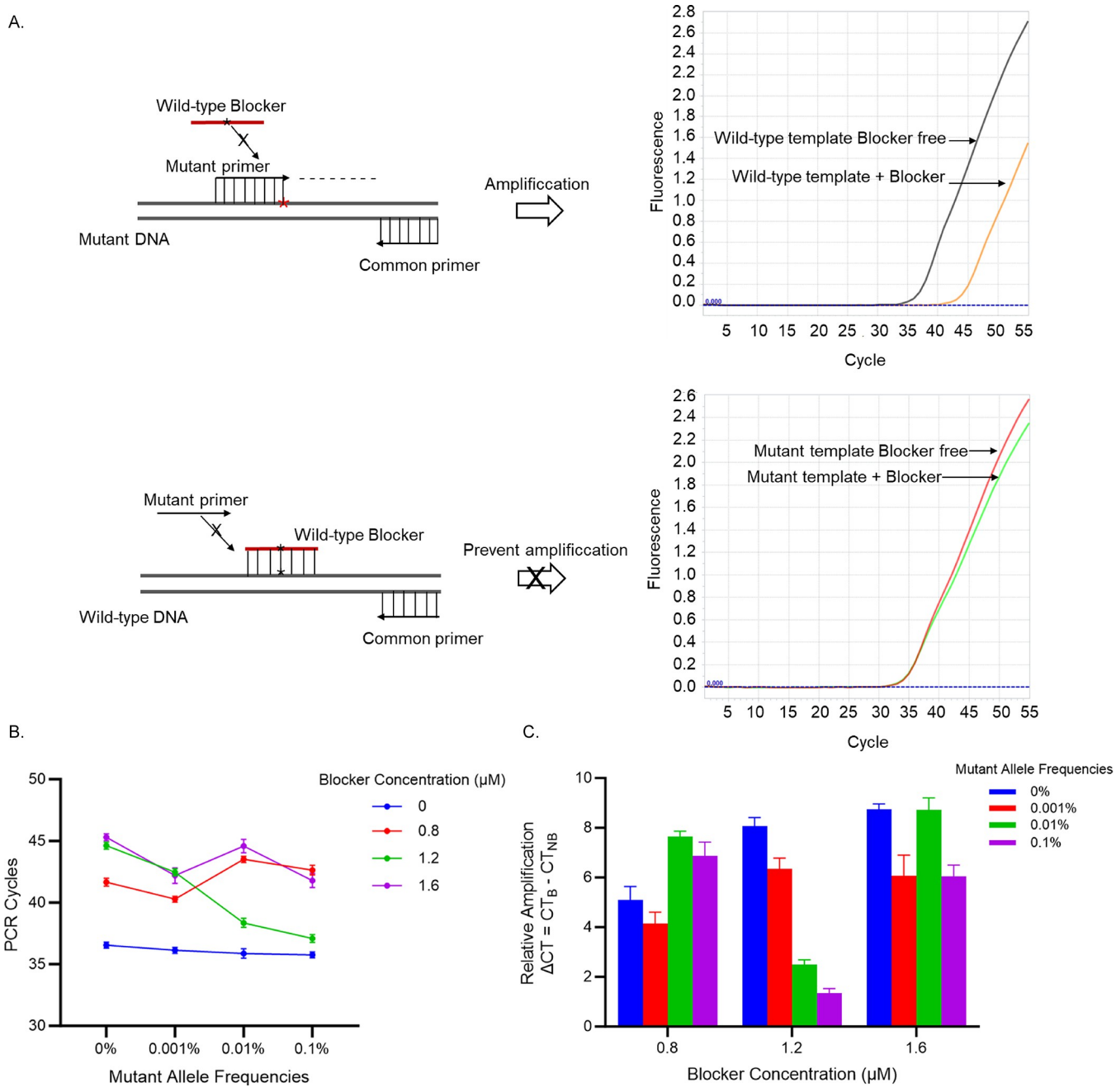

Fig 1. Blocker effect on the polymerase-mediated amplification of targeted amplicons. Upper panel (A): The blocker oligomer was designed to perfectly match the wild-type allele, while the forward primer partially overlapped the blocker binding site, and its 3' end exactly matched the H1047R mutation site. During the PCR reaction, a perfect blocker/wild-type allele hybrid thwarts the forward primer from annealing to its target, hence suppressing the amplification of the wild-type sequence. On the other hand, the designed blocker bears a mismatched nucleotide to the mutant allele; therefore, a blocker/mutant allele hybrid is weakly formed and hardly prevents the mutant allele's amplification. Lower panel (B, C): Various blocker concentrations were tested to evaluate the clamping effect on the amplification of wild-type versus mutant alleles. Real-time PCR reactions were performed in triplicate at given blocker concentrations (0, 0.8μM, 1.2μM, 1.6μM); cycle threshold–Ct values (Fig B) were recorded, and ΔCt values (Fig C) were computed as the difference in Ct of the analogous target assays with and without blocker (CT_B, CT_{NB}), respectively. The 1.2μM blocker was selected as the best-optimized parameter for further downstream analysis.

https://doi.org/10.1371/journal.pone.0309209.g001

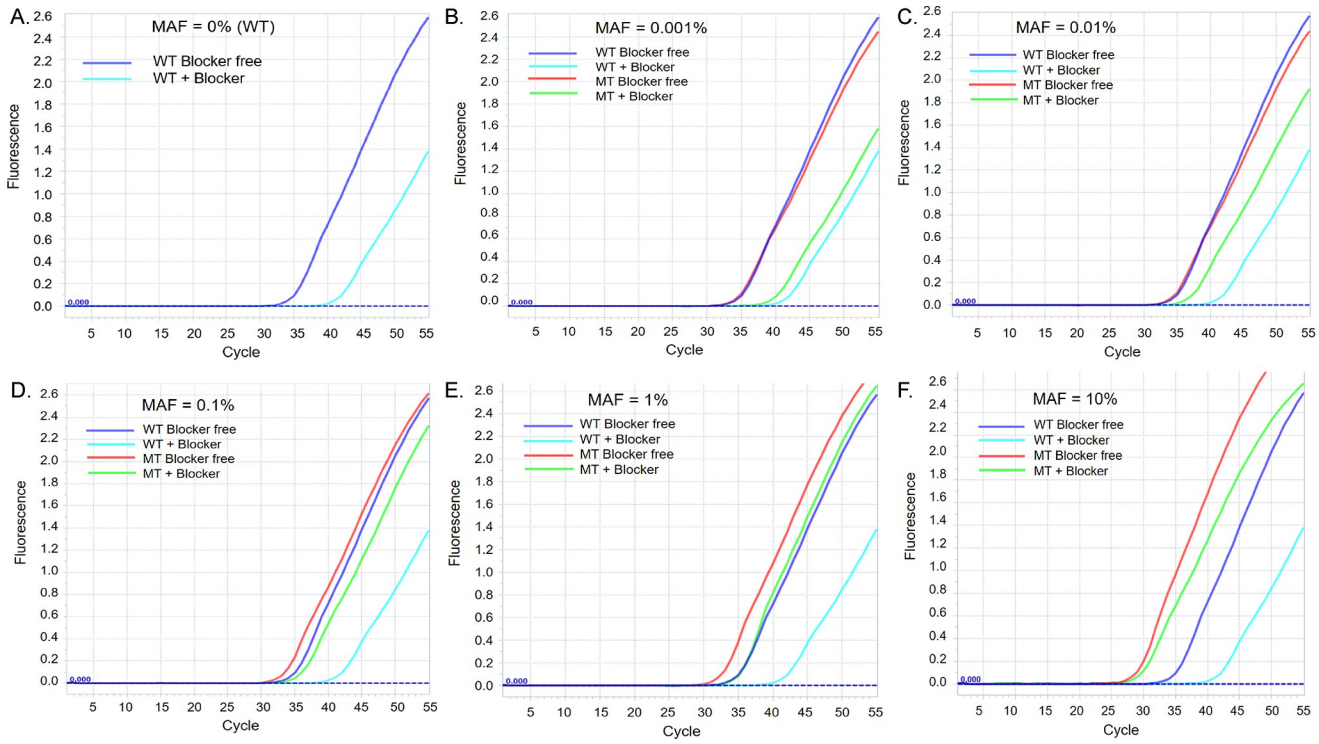

Fig 2. Real-time PCR assays to optimize the LOD for identifying the *PIK3CA* H1047R mutation. The total genomic DNA extracted from T-47D cell positive cell line dilution series that bear mutant allele frequency (MAF) of 10%, 1%, 0.1%, 0.01%, 0.001%, and 0% were used as input templates for corresponding real-time PCR assays. At each dilution point, the real-time PCR was performed in four conditions: (i) wild-type template without blocker (blocker-free); (ii) wild-type template with blocker; (iii) mutant template (0.001%, 0.01%, 0,1%, 1%, 10%) without blocker; and (iv) mutant template (0.001%, 0.01%, 0,1%, 1%, 10%) with blocker.

https://doi.org/10.1371/journal.pone.0309209.g002

estrogen receptor modulators (SERMs, 45.5%) or selective estrogen receptor degraders (SERDs, 36.4%) had a higher percentage of the *PIK3CA* H1047R mutation than those who were free of SERMs or SERDs treatment (36.4% and 13.6%, respectively), and no AI-recipients carried the mutation (S2A Fig). There is no significant association found between SERMs/SERDs and the *PIK3CA* H1047R mutation ($p > 0.05$) (S2A Fig). Especially, *PIK3CA* mutant carriers were strongly associated with patients under the age of 50 who had liver-metastasized or brain metastases or lymph node-invaded ($p < 0.05$) (S3 Fig).

Table 3. Assay reproducibility and LOD.

Repeated optimal assays (n = 15)	Mutant allele frequency (%)					
	0% (WT)	**0.001%**	**0.01%**	**0.1%**	**1%**	**10%**
Ct (no blocker)	39.71	38.19	37.68	37.00	35.10	30.76
Ct (blocker)	45.28	43.38	41.77	38.83	36.51	31.98
Δ Ct	5.57	5.19	4.09	1.83	1.41	1.22
p-value		0.714	**0.041***	**0.003***	**0.003***	**0.001***

*Statistically significant value, $p < 0.05$

p-value: mutant H1047R versus wild-type H1047R

Real-time PCR assays with or without blocker were performed fifteen times on dilution series of 10%, 1%, 0.1%, 0.01%, 0.001%, and 0% mutant. ΔCt values were computed as the difference in Ct of the analogous target assays with and without blocker.

https://doi.org/10.1371/journal.pone.0309209.t003

Table 4. Characteristics of the study population according to circulating *PIK3CA* H1047R mutation status.

Variable	Total n = 196 (100%)	H1047R		p-value[#]
		Mutant n = 62 (31.6%)	Wild-type n = 134 (68.4%)	
Age at diagnosis	52.43 ± 12.38	50.32±11.97	53.41±12.49	0.105
Family history				
Yes	38 (19.4)	11 (17.7)	27 (20.1)	0.846
No	158 (80.6)	51 (82.3)	107 (79.9)	
Disease stages				
I	18 (9.2)	2 (3.2)	16 (11.9)	**0.025***
II	71 (36.2)	17 (27.4)	54 (40.3)	
III	53 (27)	20 (32.3)	33 (24.6)	
IV	54 (27.6)	23 (37.1)	31 (23.1)	
Tumour histology				
Ductal	191 (97.4)	62 (100)	129 (96.3)	0.181
Lobular	5 (2.6)	0 (0)	5 (3.7)	
Grade				
1	12 (6.1)	3 (6.1)	9 (6.7)	0.797
2	108 (55.1)	36 (58.1)	72 (53.7)	
3	76 (38.8)	23 (37.1)	53 (39.6)	
Menopausal status				
Post-menopausal	109 (55.6)	31 (50)	78 (58.2)	0.354
HR status				
Positive	148 (75.5)	50 (80.6)	98 (73.1)	0.255
Negative	48 (24.5)	12 (19.4)	36 (26.9)	
HER2 status				
Positive	120 (61.2)	42 (67.7)	78 (58.2)	0.212
Negative	76 (38.8)	20 (32.3)	56 (41.8)	
Recurrence				
Yes	43 (21.9)	19 (30.6)	24 (17.9)	**0.045***
No	153 (78.1)	43 (69.4)	110 (82.1)	
Metastatic disease				
Yes	116 (59.2)	43 (69.4)	73 (54.5)	**0.049***
No	80 (40.8)	19 (30.6)	61 (45.5)	
The number of metastasis lesion				
0	80 (40.8)	19 (30.6)	61 (45.5)	0.131
≤ 2	94 (48)	34 (54.8)	60 (44.8)	
≥ 3	22 (11.2)	9 (14.5)	13 (9.7)	
Metastatic sites				
Lymph nodes	104 (53.1)	38 (61.3)	66 (49.3)	0.126
Lung	26 (13.3)	9 (14.5)	17 (12.7)	0.821
Liver	7 (3.6)	5 (8.1)	2 (1.5)	**0.034***[a]
Brain	4 (2.0)	4 (6.5)	0 (0)	**0.009***[a]
Bone	29 (14.8)	12 (19.4)	17 (12.7)	0.279
Treatment				
Surgical therapy	161 (82.1)	49 (79)	112 (83.6)	0.431
Hormone therapy	98 (50)	32 (51.6)	66 (49.3)	0.878
Chemotherapy	175 (89.3)	57 (91.9)	118 (88.1)	0.469

(*Continued*)

Table 4. (Continued)

Variable	Total n = 196 (100%)	H1047R		p-value[#]
		Mutant n = 62 (31.6%)	Wild-type n = 134 (68.4%)	
Radiotherapy	60 (30.6)	25 (40.3)	35 (26.1)	**0.045**[*]

[*]Statistically significant value, $p < 0.05$

p-value[#]: mutant versus wild-type

a: Fisher's Exact Test

HER2: human epidermal growth factor receptor-2; HR: hormone receptor.

https://doi.org/10.1371/journal.pone.0309209.t004

Discussion

Clinical samples are normally heterogeneous in terms of having both tumour and normal cells, or both wild-type and mutant DNA alleles. The mutation load may occasionally be below the detection threshold of diagnostic tools when the disease is at an early stage. Therefore, it is necessary to establish high-sensitivity diagnostic tools suitable for deployment in routine diagnostic conditions, especially for patient samples with low DNA quantities obtained from plasma.

Asymmetric PCR is one of the methods available for identifying gene mutations, including allele-specific priming in combination with competitive oligonucleotides to block the amplification of wild-type alleles that have been deployed for the detection of various mutation targets [27–29]. However, in some cases, the blocking of wild-type alleles is not specific enough to generate a significant signal amplification difference between the targets and unwanted alleles. In the case of the H1047R mutation model, most of the previously reported asymmetric PCR assays hardly acquired enough sensitivity to be robustly implemented in routine clinical diagnostics, especially to detect circulating H1047R in patients' blood samples. We tactfully designed an AS-PCR assay with an optimized blocker to weakly inhibit the PCR signal of the mutant target while strongly clamping amplification of wild-type sequences, hence leading to the acquisition of a 0.01% mutant allele detection limit (LOD) in a DNA cell line model. Most earlier studies did not reveal any methods that were superior to the novel technique mentioned here (Table 1).

With the use of the newly established assay, we identified 31.6% (62/196) of recruited BC's plasma carrying the *PIK3CA* H1047R mutation. This mutation rate is in accordance with previous findings from other ethnicities [13, 17, 34]. In our study cohort, the *PIK3CA* mutation was related to disease progression or worse illness in patients, which is consistent with prior research [18, 25–37]. Metastatic BC patients with *PIK3CA*-mutated HR-positive/HER2-negative tumours exhibit a poor prognosis and hormone resistance [36, 38, 39]. Our data also revealed that the H1047R mutation was considerably more common in SERMs/SERDs-received HR-positive /HER2-negative advanced BC patients or in radiotherapy-treated HER2 positive individuals, which strengthens the potential utility of cfDNA *PIK3CA* mutations as a tumour marker to guide treatment selection.

On the other hand, the current study embeds a number of limitations, such as a cross-sectional design with a limited patient size, being a single-institution study, and no matching-tumor analysis. Additionally, we only tested for the *PIK3CA* H1047R hotspot mutation, and the method does not provide a quantitative evaluation of initial mutant allele frequency, which is important for quantitative monitoring of patients' responses during a given treatment.

Conclusion

A novel allele-specific PCR assay was established for the detection of the *PIK3CA* H1047R mutation from the patients' plasma in the clinical setting. The H1047R mutation is more

common in advanced Vietnamese BC patients, especially those with liver invasion or brain metastases, or HER2-positive BC who are treated with radiation.

Supporting information

S1 Fig. Clinical data on the detected *PIK3CA* H1047R mutation. Prevalence of the circulating *PIK3CA* H1047R mutation in different stages of breast cancer (A), in groups based on recurrence and metastatic status (B), and the number of metastatic lesions (C). * $p < 0.05$. RE: recurrence; MS: metastatic disease; VS: visceral metastasis; Liver: liver metastasis; Lung: lung metastasis; Brain: brain metastasis; LN: lymph node invasion; Bone: bone metastasis.
(TIF)

S2 Fig. Distribution of the circulating *PIK3CA* H1047R mutation in subgroups with different therapies. Prevalence of the circulating *PIK3CA* H1047R mutation in HR-positive/HER2-negative advances breast cancer (HR+/HER2- ABC) with different endocrine regimens (A) and in HER2-positive breast cancer (HER2+ BC) with different treatments (B). SERMs: selective estrogen receptor modulators; SERDs: selective estrogen receptor degraders; AI: Aromatase inhibitors. * $p < 0.05$.
(TIF)

S3 Fig. Distribution of the circulating H1047R mutation by age groups. The *PIK3CA* H1047R mutant frequency in groups $\leq$ 50 years old (A) and $>$ 50 years old (B), respectively. RC: recurrence; MS: metastatic disease; LN: lymph node invasion; Liver: liver metastasis; Lung: lung metastasis; Brain: brain metastasis; Bone: bone metastasis. * $p < 0.05$.
(TIF)

Acknowledgments

The authors would like to thank Assoc. Prof. Hoang Van Tong for his painstaking proofreading of the manuscript.

Author Contributions

Conceptualization: Dinh Thi Thao, Dong Van Quyen, Le Huu Song, Ngo Tat Trung.

Data curation: Dinh Thi Thao, Nguyen Phu Thanh, Ly Tuan Khai.

Formal analysis: Dinh Thi Thao, Nguyen Phu Thanh, Le Huu Song.

Funding acquisition: Dinh Thi Thao, Ngo Tat Trung.

Investigation: Dinh Thi Thao, Nguyen Phu Thanh, Ngo Tat Trung.

Methodology: Dinh Thi Thao, Le Huu Song, Ngo Tat Trung.

Project administration: Dinh Thi Thao, Ngo Tat Trung.

Resources: Dinh Thi Thao, Ly Tuan Khai, Le Huu Song.

Software: Dinh Thi Thao, Nguyen Phu Thanh.

Supervision: Dong Van Quyen, Le Huu Song, Ngo Tat Trung.

Validation: Dinh Thi Thao, Nguyen Phu Thanh.

Visualization: Dinh Thi Thao, Ngo Tat Trung.

Writing – original draft: Dinh Thi Thao, Ngo Tat Trung.

Writing – review & editing: Dinh Thi Thao, Dong Van Quyen, Ly Tuan Khai, Le Huu Song, Ngo Tat Trung.

References

1. Bray F, Laversanne M, Sung H, Ferlay J, Siegel RL, Soerjomataram I, et al. Global cancer statistics 2022: GLOBOCAN estimates of incidence and mortality worldwide for 36 cancers in 185 countries. CA Cancer J Clin. 2024 May-Jun; 74(3):229–263. https://doi.org/10.3322/caac.21834 Epub 2024 Apr 4. PMID: 38572751.
2. Huppert LA, Gumusay O, Idossa D, Rugo HS. Systemic therapy for hormone receptor-positive/human epidermal growth factor receptor 2-negative early stage and metastatic breast cancer. CA Cancer J Clin. 2023; 73(5):480–515. https://doi.org/10.3322/caac.21777 Epub 2023 Mar 20. PMID: 36939293.
3. Murugan AK, Munirajan AK, Tsuchida N. Genetic deregulation of the PIK3CA oncogene in oral cancer. Cancer Lett. 2013 Sep 28; 338(2):193–203. https://doi.org/10.1016/j.canlet.2013.04.005 Epub 2013 Apr 15. PMID: 23597702.
4. Rose MM, Dhamodharan S, Revathidevi S, Chakkarappan SR, Jagadeesan MG, Subbiah S, et al. High incidence of PI3K pathway gene mutations in South Indian cervical cancers. Cancer Genet. 2022 Jun; 264–265:100–108. https://doi.org/10.1016/j.cancergen.2022.05.002 Epub 2022 May 8. PMID: 35568000.
5. Murugan AK, Hong NT, Fukui Y, Munirajan AK, Tsuchida N. Oncogenic mutations of the PIK3CA gene in head and neck squamous cell carcinomas. Int J Oncol. 2008 Jan; 32(1):101–11. PMID: 18097548.
6. Murugan AK. mTOR: Role in cancer, metastasis and drug resistance. Semin Cancer Biol. 2019 Dec; 59:92–111. https://doi.org/10.1016/j.semcancer.2019.07.003 Epub 2019 Aug 10. PMID: 31408724.
7. Paplomata EO'Regan RThe PI3K/AKT/mTOR pathway in breast cancer: targets, trials and biomarkers. Ther Adv Med Oncol. 2014 Jul; 6(4):154–66. https://doi.org/10.1177/1758834014530023 PMID: 25057302; PMCID: PMC4107712.
8. Leiphrakpam PD, Are C. PI3K/Akt/mTOR Signaling Pathway as a Target for Colorectal Cancer Treatment. Int. J. Mol. Sci. 2024; 25: 3178. https://doi.org/10.3390/ijms25063178 PMID: 38542151
9. Tufail M, Hu JJ, Liang J. et al. Predictive, preventive, and personalized medicine in breast cancer: targeting the PI3K pathway. J Transl Med. 2024; 22(15):37. https://doi.org/10.1186/s12967-023-04841-w PMID: 38172946
10. Lau KH, Tan AM, Shi Y. New and Emerging Targeted Therapies for Advanced Breast Cancer. Int J Mol Sci. 2022; 23(4):2288. https://doi.org/10.3390/ijms23042288 PMID: 35216405; PMCID: PMC8874375.
11. The U.S Food and Drug Administration (FDA). Resources for Information Approved Drugs [Internet]. FDA approves alpelisib for metastatic breast cancer; c2019 [cited 2023 June 15]. Available from: https://www.fda.gov/drugs/resources-information-approved-drugs/fda-approves-alpelisib-metastatic-breast-cancer.
12. National Comprehensive Cancer Network (NCCN). NCCN Guidelines [Internet]. NCCN Guidelines for Breast Cancer V. 1.2021; c2021 [cited 2023 June 15]. Available from: https://www.nccn.org/guidelines/guidelines-process/transparency-process-and-recommendations/GetFileFromFileManagerGuid?FileManagerGuidId=c28eedc5-9a5a-4161-b791-89d7f3b73cfc.
13. Martínez-Sáez O, Chic N, Pascual T, et al. Frequency and spectrum of PIK3CA somatic mutations in breast cancer. Breast Cancer Research: BCR. 2020; 22(1):45. https://doi.org/10.1186/s13058-020-01284-9 PMID: 32404150; PMCID: PMC7222307.
14. Shimoi T, Hamada A, Yamagishi M, Hirai M, Yoshida M, Nishikawa T, et al. PIK3CA mutation profiling in patients with breast cancer, using a highly sensitive detection system. Cancer Sci. 2018; 109 (8):2558–2566. https://doi.org/10.1111/cas.13696 PMID: 29906308; PMCID: PMC6113507.
15. Markou A, Farkona S, Schiza C, Efstathiou T, Kounelis S, Malamos N, et al. PIK3CA mutational status in circulating tumor cells can change during disease recurrence or progression in patients with breast cancer. Clin Cancer Res. 2014; 20(22):5823–34. https://doi.org/10.1158/1078-0432.CCR-14-0149 PMID: 25398847.
16. Alvarez-Garcia V, Bartos C, Keraite I, Trivedi U, Brennan PM, et al. A simple and robust real-time qPCR method for the detection of PIK3CA mutations. Sci Rep. 2018 Mar 9; 8(1):4290. https://doi.org/10.1038/s41598-018-22473-9 PMID: 29523855; PMCID: PMC5844869.
17. Board RE, Thelwell NJ, Ravetto PF, Little S, Ranson M, Dive C, et al. Multiplexed assays for detection of mutations in PIK3CA. Clin Chem. 2008; 54(4):757–60. https://doi.org/10.1373/clinchem.2007.098376 PMID: 18375489.

18. Keraite I, Alvarez-Garcia V, Garcia-Murillas I, Beaney M, Turner NC, Bartos C, et al. PIK3CA mutation enrichment and quantitation from blood and tissue. Sci Rep. 2020 Oct 13; 10(1):17082. https://doi.org/10.1038/s41598-020-74086-w PMID: 33051521; PMCID: PMC7555501.

19. Corné J, Le Du F, Quillien V, Godey F, Robert L, Bourien H, et al. Development of multiplex digital PCR assays for the detection of PIK3CA mutations in the plasma of metastatic breast cancer patients. Sci Rep. 2021; 11(1):17316. https://doi.org/10.1038/s41598-021-96644-6 PMID: 34453076; PMCID: PMC8397758.

20. Harlé A, Lion M, Lozano N, Husson M, Harter V, et al. Analysis of PIK3CA exon 9 and 20 mutations in breast cancers using PCR-HRM and PCR-ARMS: correlation with clinicopathological criteria. Oncol Rep. 2013; 29(3):1043–52. https://doi.org/10.3892/or.2013.2229 PMID: 23314198.

21. Ang DO'Gara R, Schilling A, Beadling C, Warrick A, et al. Novel method for PIK3CA mutation analysis: locked nucleic acid—PCR sequencing. J Mol Diagn. 2013; 15(3):312–8. https://doi.org/10.1016/j.jmoldx.2012.12.005 PMID: 23541593.

22. Oshiro C, Kagara N, Naoi Y, Shimoda M, Shimomura A, et al. PIK3CA mutations in serum DNA are predictive of recurrence in primary breast cancer patients. Breast Cancer Res Treat. 2015; 150(2):299–307. https://doi.org/10.1007/s10549-015-3322-6 PMID: 25736040.

23. Elazezy M, Joosse SA. Techniques of using circulating tumor DNA as a liquid biopsy component in cancer management. Comput Struct Biotechnol J. 2018; 16:370–378. https://doi.org/10.1016/j.csbj.2018.10.002 PMID: 30364656; PMCID: PMC6197739.

24. Newman AM, Bratman SV, To J, Wynne JF, Eclov NC, Modlin LA, et al. An ultrasensitive method for quantitating circulating tumor DNA with broad patient coverage. Nat Med. 2014 May; 20(5):548–54. https://doi.org/10.1038/nm.3519 Epub 2014 Apr 6. PMID: 24705333; PMCID: PMC4016134.

25. Diehl F, Li M, Dressman D, He Y, Shen D, Szabo S, et al. Detection and quantification of mutations in the plasma of patients with colorectal tumors. Proc Natl Acad Sci U S A. 2005 Nov 8; 102(45):16368–73. https://doi.org/10.1073/pnas.0507904102 Epub 2005 Oct 28. PMID: 16258065; PMCID: PMC1283450.

26. Rohlin A, Wernersson J, Engwall Y, Wiklund L, Björk J, Nordling M. Parallel sequencing used in detection of mosaic mutations: comparison with four diagnostic DNA screening techniques. Hum Mutat. 2009; 30(6):1012–20. https://doi.org/10.1002/humu.20980 PMID: 19347965.

27. Oh JE, Lim HS, An CH, Jeong EG, Han JY, et al. Detection of low-level KRAS mutations using PNA-mediated asymmetric PCR clamping and melting curve analysis with unlabeled probes. J Mol Diagn. 2010; 12(4):418–24. https://doi.org/10.2353/jmoldx.2010.090146 PMID: 20413678; PMCID: PMC2893625.

28. Zapparoli GV, Jorissen RN, Hewitt CA, et al. Quantitative threefold allele-specific PCR (QuanTAS-PCR) for highly sensitive JAK2V617F mutant allele detection. BMC Cancer. 2013; 13:206. https://doi.org/10.1186/1471-2407-13-206 PMID: 23617802; PMCID: PMC3658971.

29. Miyazawa H, Tanaka T, Nagai Y, Matsuoka M, Huqun, Sutani A, et al. Peptide nucleic acid-locked nucleic acid polymerase chain reaction clamp-based detection test for gefitinib-refractory T790M epidermal growth factor receptor mutation. Cancer Sci. 2008; 99(3):595–600. https://doi.org/10.1111/j.1349-7006.2007.00706.x PMID: 18271876.

30. Lung J, Hung MS, Lin YC, Jiang YY, Fang YH, Lu MS, et al. A highly sensitive and specific real-time quantitative PCR for BRAF V600E/K mutation screening. Sci Rep. 2020; 10(1):16943. https://doi.org/10.1038/s41598-020-72809-7 PMID: 33037234; PMCID: PMC7547094.

31. Zeng Q, Xie L, Zhou N, Liu M, Song X. Detection of PIK3CA Mutations in Plasma DNA of Colorectal Cancer Patients by an Ultra-Sensitive PNA-Mediated PCR. Mol Diagn Ther. 2017 Aug; 21(4):443–451. https://doi.org/10.1007/s40291-017-0269-9 PMID: 28247181.

32. Park J, Abbas N, Park Y, Park KH, Kim YH, Shin S. Ultrasensitive and highly selective detection of PIK3CA single point mutations in cell-free DNA with LNA-modified hairpin-shaped probe. Sensors and Actuators B: Chemical, 2022. 355. https://doi.org/10.1016/j.snb.2021.131309

33. Dahiru T. P—value, a true test of statistical significance? A cautionary note. Ann Ib Postgrad Med. 2008 Jun; 6(1):21–6. https://doi.org/10.4314/aipm.v6i1.64038 PMID: 25161440; PMCID: PMC4111019.

34. Suppan C, Graf R, Jahn S, et al. Sensitive and robust liquid biopsy-based detection of PIK3CA mutations in hormone-receptor-positive metastatic breast cancer patients. British Journal of Cancer. 2022 Feb; 126(3):456–463. https://doi.org/10.1038/s41416-021-01601-9 PMID: 34754095; PMCID: PMC8810831.

35. Jacot W, Lopez-Crapez E, Chaltiel L, Durigova A, Gros N, et al. PIK3CA mutations early persistence in cell-free tumor DNA as a negative prognostic factor in metastatic breast cancer patients treated with hormonal therapy. Breast Cancer Res Treat, 2019; 177(3):659–667. https://doi.org/10.1007/s10549-019-05349-y PMID: 31297647.

36. Mosele F, Stefanovska B, Lusque A, Tran Dien A, Garberis I, Droin N, et al. Outcome and molecular landscape of patients with PIK3CA-mutated metastatic breast cancer. Ann Oncol. 2020; 31(3):377–386. https://doi.org/10.1016/j.annonc.2019.11.006 PMID: 32067679.

37. Mangone FR, Bobrovnitchaia IG, Salaorni S, Manuli E, Nagai MA. PIK3CA exon 20 mutations are associated with poor prognosis in breast cancer patients. Clinics (Sao Paulo). 2012 Nov; 67(11):1285–90. https://doi.org/10.6061/clinics/2012(11)11 PMID: 23184205; PMCID: PMC3488987.

38. Huang D, Tang L, Yang F, Jin J, Guan X. *PIK3CA* mutations contribute to fulvestrant resistance in ER-positive breast cancer. Am J Transl Res. 2019 Sep 15; 11(9):6055–6065. PMID: 31632573; PMCID: PMC6789267.

39. Reinhardt K, Stückrath K, Hartung C, et al. PIK3CA-mutations in breast cancer. Breast Cancer Res Treat. 2022 Dec; 196(3):483–493. https://doi.org/10.1007/s10549-022-06637-w PMID: 36279023; PMCID: PMC9633529.

Subtype-specific prognostic implications of plasma-detected *PIK3CA* mutations in Vietnamese breast cancer patients

Dinh Thi Thao[1,3*], Dong Van Quyen[3,4], Le Huu Song[2], and Ngo Tat Trung[2, 5*]

[1] Center for Genetic Consultation and Cancer Screening, 108 Military Center Hospital, 1 Tran Hung Dao, Hai Ba Trung, Hanoi, Vietnam
[2] Vietnamese-German Center for Medical Research, 108 Military Center Hospital, 1 Tran Hung Dao, Hai Ba Trung, Hanoi, Vietnam
[3] University of Science and Technology of Hanoi, 18 Hoang Quoc Viet, Cau Giay, Hanoi, Vietnam
[4] Institute of Biotechnology, Vietnam Academy of Science and Technology, 18 Hoang Quoc Viet, Cau Giay, Hanoi, Vietnam
[5] Department of Molecular Biology, Laboratory Center, 108 Military Central Hospital, 1 Tran Hung Dao, Hai Ba Trung, Hanoi, Vietnam

*** Correspondence:**
Corresponding Author: Ngo Tat Trung, Dinh Thi Thao
email: tatrungngo@gmail.com, thaodinh3883@gmail.com

Keywords: Breast cancer, circulating tumor DNA, cell-free DNA, mutation analysis, liquid biopsy, *PIK3CA* mutation, prognostic biomarker.

Abstract

Background: *PIK3CA* mutations are among the most frequent genomic alterations in breast cancer (BC), contributing to disease progression and therapeutic resistance. Non-invasive blood assays can reveal tumor-specific DNA alterations, enhancing personalized oncology.

Aim: This study aims to investigate the clinical relevance of plasma-detected *PIK3CA* mutations in Vietnamese breast cancer patients, with a focus on subtype-specific outcomes.

Methods: *PIK3CA* hotspot mutations (H1047R and E545K) were detected in plasma from 196 BC patients. Associations with clinicopathological features and progression-free survival (PFS) were assessed.

Results: *PIK3CA* mutations were identified in 42.9% of patients with H1047R (31.6%) more prevalent than E545K (15.3%). Mutation rates were highest in HR+ subtypes and elevated in advanced or irradiated patients ($p = 0.009$). E545K was enriched in HR+ cases, while H1047R was more frequent in HER2+ tumors following radiotherapy. Among metastatic BC patients, those with *PIK3CA* mutations had shorter PFS (median, 7.0 vs. 15.0 months; $p = 0.022$), and univariate Cox regression showed increased progression risk (HR = 2.16), although not significant after multivariate adjustment. E545K was associated with lung ($p = 0.047$) and bone metastases ($p = 0.012$) and H1047R was enriched in brain metastases ($p = 0.028$).

Conclusion: Plasma-detected *PIK3CA* mutations, particularly E545K and H1047R, exhibited subtype-specific associations with clinical outcomes, indicating that plasma analysis may provide complementary information for prognostic assessment in metastatic BC.

1 Introduction

Breast cancer (BC) is a molecularly heterogeneous disease and remains the most frequently diagnosed malignancy among women globally. According to the Global Cancer Observatory (GLOBOCAN 2022), BC accounted for over 2.3 million new cases, with a growing burden in low- and middle-income countries, including Vietnam (1). Despite advances in early detection and targeted therapies, disease recurrence, metastasis, and treatment resistance remain major challenges in clinical management. Among molecular subtypes, hormone receptor-positive (HR+), HER2-negative (HER2-) BC accounts for the majority of cases and is primarily treated with endocrine therapy. Despite initial responsiveness, roughly 20% of patients experience disease progression or recurrence or distant metastasis due to acquired resistance to endocrine agents (2). Aberrant activation of the phosphoinositide 3-kinase (PI3K)/Akt/mTOR signaling pathway has been recognized as a key mechanism implicated in this treatment resistance (3).

Somatic mutations in the *PIK3CA* gene, which encodes the p110α catalytic subunit of the PI3Kα complex, are the most frequent genetic alterations observed in HR+/HER2− BC, occurring in approximately 20% to 40% of patients. These mutations, particularly those at hotspots in exon 9 (E545K) and exon 20 (H1047R), result in constitutive pathway activation and contribute to tumor progression, and therapeutic resistance (3). While the prognostic and predictive roles of *PIK3CA* mutations have been explored in various populations, data remain limited and inconsistent, particularly in underrepresented cohorts. The mutations have been correlated with improved prognosis in early-stage BC (4, 5); however, emerging evidence suggests an association between these mutations and reduced treatment efficacy, including resistance to endocrine and chemotherapeutic therapies, as well as unfavorable outcomes (6-12). Conversely, several studies have failed to demonstrate a consistent predictive or prognostic role for *PIK3CA* mutations (13-16).

Recent advances in targeted therapy have led to the development of PI3Kα inhibitors such as alpelisib and inavolisib, which have shown clinical benefit and are approved for the treatment of *PIK3CA*-mutated HR+/HER2− advanced BC when combined with fulvestrant (17, 18). Furthermore, capivasertib, an AKT inhibitor, has demonstrated efficacy in HR+/HER2− BC patients harboring *PIK3CA*, *AKT1*, or *PTEN* alterations following disease progression on standard adjuvant therapies (19). In recent years, liquid biopsy techniques, particularly plasma-derived circulating tumor DNA (ctDNA) analysis, have been known as a minimally invasive approach for detecting relevant mutations and guiding treatment decisions in real time. Liquid biopsy is particularly advantageous in patients with inaccessible metastatic lesions or for longitudinal monitoring of tumor evolution (20). Consequently, *PIK3CA* mutation testing via liquid biopsy is increasingly recommended when evaluating patients who are candidates for PI3K-targeted therapies or AKT inhibitors, especially in cases of endocrine-resistant disease (21).

Most prior investigations have focused on tissue-based profiling, which may not fully capture spatial and temporal tumor heterogeneity, particularly in the metastatic setting. The increasing clinical adoption of circulating tumor DNA (ctDNA) analysis provides a minimally invasive approach to real-time tumor monitoring; however, the clinical relevance of plasma-detected *PIK3CA* mutations—especially in relation to specific molecular subtypes and treatment outcomes—remains insufficiently characterized. Moreover, despite emerging evidence suggesting distinct biological behaviors and therapeutic implications of individual *PIK3CA* variants, such as E545K and H1047R, comparative analyses of their prognostic impact remain limited. These gaps underscore the need for more detailed, variant-specific investigations using liquid biopsy–based approaches to inform personalized management strategies in BC.

In this research, we utilized a recently developed blocker-mediated asymmetric PCR assay (22) designed to investigate the frequency and subtype-specific prognostic implications of *PIK3CA* mutations (H1047R and E545K) in plasma-derived cell-free DNA (cfDNA) from BC patients. This study aims to evaluate the association between plasma *PIK3CA* mutation status and clinical outcomes, with the goal of clarifying its potential relevance as a prognostic biomarker and contribution to individualized treatment strategies.

2 Materials and methods

2.1 Patients and sample collection

A total of 196 patients diagnosed with BC were enrolled at the 108 Military Central Hospital (MCH), Vietnam, between June 2021 and June 2023. All participants provided written informed consent prior to inclusion in the study. Patient information was completely anonymous. All procedures were approved by the institutional ethics and scientific committees. The study protocol received ethical approval from the Medical Ethics Committee of the 108 MCH, Hanoi, Vietnam (Aprroval number: 2527/21-5-2021). Venous blood samples and relevant clinical data were collected at the time of enrollment.

Progression-free survival (PFS) was defined as the duration from the date of blood collection to the first confirmed local recurrence or distant metastasis, based on the RECIST guideline (23). Disease progression was assessed by the attending physicians using clinical and/or radiographic evidence, and findings were documented in patients' medical records.

2.2 Sample preparation

Whole blood was drawn into EDTA tubes and centrifuged at 2,000 × g for 10 minutes at room temperature within 2 hours of collection. Plasma was separated, aliquoted, and stored at −80 °C. cfDNA was extracted from 500 µL of plasma using the MagMAX™ Cell-Free DNA Isolation Kit (Thermo Fisher Scientific, Waltham, MA, USA), following the manufacturer's instructions. The extracted cfDNA was stored at −80 °C until further use.

2.3 Control samples: positive and negative genomic DNA

Breast cancer cell lines MCF7 and T-47D (Thermo Fisher Scientific, USA) were cultured in RPMI 1640 medium (Invitrogen, Carlsbad, CA, USA) supplemented with 7.5% fetal bovine serum and 100 U/mL penicillin-streptomycin (Sigma-Aldrich, USA), and maintained at 37 °C in a humidified atmosphere with 5% CO_2. Genomic DNA was isolated from MCF7, T-47D, and peripheral white blood cells of healthy donors using the Genomic DNA Purification Kit (Thermo Fisher Scientific), with elution in 100 µL of buffer. Extracted DNA was aliquoted and stored at −20 °C. To generate sample controls, MCF7 cells (carrying ~30% E545K mutant allele) or T-47D cells (carrying ~50% H1047R mutant allele) were mixed with healthy donor cells to achieve mutant allele frequencies of 10% and 0%. DNA extracted from these mixtures was used as a positive control (10%) and a negative control (0%) during cfDNA analysis.

2.4 Detection of *PIK3CA* mutations using asymmetric PCR

Blocker-mediated asymmetric PCR was used to detect *PIK3CA* hotspot mutations (H1047R and E545K). Reactions were performed on the LightCycler 96 real-time PCR system (Roche Diagnostics,

Mannheim, Germany). The thermal cycling protocol included: initial denaturation at 95 °C for 10 minutes, followed by 50 cycles at 95 °C for 15 seconds, 55 °C for 20 seconds, and 72 °C for 20 seconds.

Each 20 μL reaction mixture contained 10 μL of 2× Universal PCR Master Mix (no UNG; Applied Biosystems, Foster City, CA, USA), 0.8 μL each of forward and reverse primers, 1.6–2.4 μL of allele-specific blocker oligonucleotides, and 4 μL of cfDNA template. SYBR Green fluorescence was monitored in real time, and data were analyzed using the accompanying software.

2.5 Oligonucleotides and PCR reagents

Primers and blockers were designed based on recommendations from a previous study (24). Detailed sequences of the primers and blockers, as well as the limit of detection values of the asymmetric PCR assays, are provided in the Supplementary Materials (Table S1). All oligonucleotides were synthesized by Integrated DNA Technologies (IDT, Coralville, IA, USA). Additional reagents, including the PCR master mix, nuclease-free water, deoxynucleotide triphosphates (dNTPs), and loading buffer, were obtained from Thermo Fisher Scientific (Waltham, MA, USA).

2.6 Immunohistochemical analysis

Pathological assessment was performed by certified pathologists at the Department of Pathology, Laboratory Center, 108 MCH. Estrogen receptor (ER) and progesterone receptor (PR) expression was assessed via immunohistochemistry (IHC), with ≥1% nuclear staining considered positive (25). HER2 status was determined by IHC or confirmed by fluorescence in situ hybridization (FISH) for equivocal (2+) cases. A HER2 IHC score of 3+ or a positive FISH result was considered HER2-positive (26).

2.7 Statistical analysis

Statistical analyses were performed using IBM SPSS Statistics version 25.0 (IBM Corp., Armonk, NY, USA). Associations between *PIK3CA* mutations and clinicopathological characteristics were evaluated using the chi-square test or Fisher's exact test as appropriate. PFS was estimated using the Kaplan–Meier method, and differences between groups were assessed using the log-rank test. The median follow-up duration was 24.0 months (95% CI, 22.7–25.3). Univariate and multivariate Cox regression analyses estimated Hazard ratios (HRs) and 95% confidence intervals (CIs) for PFS, adjusting for relevant clinical covariates. A p-value < 0.05 was considered statistically significant. No correction for multiple comparisons (e.g., Bonferroni or false discovery rate) was applied given the exploratory nature of the study and limited sample size; therefore, all subgroup analyses were interpreted as hypothesis-generating. Graphs were generated using Microsoft Excel 2010.

3 Results

3.1 Circulating *PIK3CA* mutations in breast cancer patients

Using a blocker-mediated asymmetric PCR assay, we analyzed plasma samples from 196 BC patients. Circulating hotspot mutations in the *PIK3CA* gene (E545K and/or H1047R) were detected in 84 patients (42.9%). Notably, 8 patients (4.1%) harbored both mutations concurrently, while 112 patients (57.1%) tested negative for both (Figure 1). The H1047R mutation was more frequently observed than E545K, and most patients carried only one hotspot mutation regardless of the disease stages (Figure 1, Figure 2). Mutation frequencies differed across molecular subtypes. The HR+/HER2+ group had the

highest prevalence (48.8%), followed by HR+/HER2− (45.2%), HR−/HER2+ (32.4%), and triple-negative (21.4%) subtypes (Table 1).

Of the total cohort, 43 patients (21.9%) experienced disease recurrence, 54 (27.6%) were classified as stage IV, and 116 (59.2%) presented with at least one site of invasion-either nodal or distant metastases (Table 2). The prevalence of *PIK3CA* mutations significantly increased with disease stage: 4.8% in stage I, 28.6% in stage II, 33.3% in stage III, and 33.3% in stage IV (p = 0.024). No statistically significant associations were observed between *PIK3CA* mutation status and age, menopausal status, or tumor histopathology (Table 2). However, mutation rates were significantly higher in patients with metastatic disease (p = 0.032), particularly in those with multiple metastatic sites (p = 0.032).

Furthermore, *PIK3CA* mutations were significantly associated with patients who had received radiotherapy (p = 0.009) (Table 2). Stratified analysis revealed mutation subtype-specific enrichment in distinct treatment subgroups: the E545K variant was more frequent in radiotherapy-treated HR+ BC patients (OR = 2.72; 95% CI, 1.13–6.55; p = 0.022), while the H1047R mutation was enriched in HER2+ BC patients who had undergone radiotherapy (OR = 3.45; 95% CI, 1.47–8.13; p = 0.004; Figure 3, Supplementary Table S2).

3.2 Association between plasma-detected *PIK3CA* mutations and prognosis in metastatic breast cancer

A focused analysis of the 54 patients with metastatic BC (detailed characteristics presented in Supplementary Table S3-S4) revealed no significant association between overall *PIK3CA* mutation status and metastatic distribution. However, variant-specific analysis demonstrated that the E545K mutation was significantly associated with lung (OR = 8.1; 95% CI, 0.9–71.1; p = 0.047) and bone metastases (OR = 17.0; 95% CI, 0.9–315.6; p = 0.012), while H1047R mutations were more frequently observed in patients with brain metastases (OR = 14.5; 95% CI, 0.7–285.1; p = 0.028; Figure 4, Supplementary Table S5).

Furthermore, there was a significant association between *PIK3CA* mutations and disease progression (OR = 3.67; 95% CI, 1.10 – 12.0; p = 0.028; Table 3). PFS analysis using the Kaplan–Meier method and log-rank test demonstrated that metastatic BC patients harboring *PIK3CA* mutations had significantly shorter PFS than those without (median, 7 months; 95% CI, 5.0–9.0 vs. 15 months; 95% CI, 7.35–22.64; p = 0.022). In contrast, no significant difference in PFS was observed when patients were stratified by individual mutation subtype (E545K or H1047R; Figure 5, Supplementary Table S6). In univariate Cox regression, *PIK3CA* mutation was associated with an increased risk of progression (HR = 2.16; 95% CI, 1.07–4.35; p = 0.031); however, this association did not remain statistically significant after multivariate adjustment (HR = 1.58; 95% CI, 0.73–3.43; p = 0.245; Table 4).

4 Discussion

This study investigated the prevalence and potential prognostic significance of plasma-detected *PIK3CA* hotspot mutations (E545K and H1047R) across distinct molecular subtypes of BC in a Vietnamese cohort. These two variants are among the most predominant *PIK3CA* hotspots, together accounting for approximately 60–70% of all clinically relevant mutations reported in BC (3, 9, 10, 15, 17, 21). Our findings suggest the clinical utility of liquid biopsy in capturing tumor-derived genetic alterations and indicate that *PIK3CA* mutations are not uniformly distributed across subtypes, nor do they confer identical prognostic implications.

Consistent with prior literature, the overall frequency of plasma-detected *PIK3CA* mutations in our cohort (42.9%) falls within previously reported ranges (30% to 50%) based on tissue or liquid biopsy analyses in Western and Asian populations (3-5, 9). Notably, H1047R mutation was more prevalent than E545K, and co-occurrence of both mutations was rare, corroborating the mutually exclusive nature of most *PIK3CA* alterations (9-11, 15, 16). At the subtype level, the high prevalence of *PIK3CA* mutations in HR+/HER2− and HR+/HER2+ subtypes of our cohort aligns with prior studies (6, 13). Slight differences in mutation frequency across studies may reflect variations in assay sensitivity, sample types (tissue vs. plasma), and underlying population-specific genetic heterogeneity (3-6, 9, 10).

Beyond overall prevalence, our data also revealed an enrichment of *PIK3CA* mutations among patients who had received radiotherapy, suggesting a possible interplay between PI3K pathway activation and radiation sensitivity. Mechanistically, activation of the PI3K/Akt/mTOR pathway has been implicated in radioresistance, primarily through enhanced DNA repair and inhibition of apoptosis (27). Conversely, in some clinical cohorts, tumors harboring *PIK3CA* mutations have shown improved local control and longer recurrence-free survival following radiotherapy (28, 29). This inconsistency underscores the need for prospective, subtype-specific studies to clarify the predictive role of *PIK3CA* mutations in radiotherapy response.

Moreover, our study highlights the subtype-specific prognostic relevance of circulating *PIK3CA* mutations in the metastatic setting. In particular, the presence of the E545K mutation was significantly associated with lung and bone metastases, while H1047R was linked to brain metastasis. These trends, which are comparable to previous clinical observations (30), suggest that distinct mutations may influence could be linked to differences in metastatic tropism through variations in downstream PI3K/AKT/mTOR signaling or tumor–microenvironment interactions. At the molecular level, the helical-domain E545K and kinase-domain H1047R mutations activate the PI3K/AKT/mTOR pathway through distinct mechanisms—RAS-dependent and p85-dependent, respectively (13, 14, 31). These mechanistic differences previously demonstrated in experimental studies may help contextualize the mutation–site-related metastatic patterns observed in our cohort.

Importantly, *PIK3CA* mutations were significantly associated with disease progression and shorter PFS, but this effect was not retained after multivariate adjustment, suggesting that their prognostic impact may be confounded by tumor subtype and related prognostic covariates. Although previous studies have also reported correlations between *PIK3CA* status and patient outcomes (6–12, 5, 14), multivariate analyses were often not clearly described, limiting definitive interpretation. Collectively, the prognostic significance of *PIK3CA* mutations remains uncertain and warrants validation in larger, well-controlled studies.

Building on these data, cfDNA testing enables minimally invasive detection of *PIK3CA* mutation patterns across BC subtypes, providing molecular insights that may refine prognostic evaluation and guide individualized treatment. In Vietnam, where access to NGS-based genotyping remains limited, cfDNA PCR-based testing offers a feasible complementary approach for identifying actionable alterations and assessing therapeutic eligibility, thereby facilitating the clinical application of targeted therapies in resource-limited settings. In this context, the blocker-mediated asymmetric PCR used in our study offers a practical option with acceptable analytical sensitivity (limit of detection 0.01–0.1%; Table S1), reasonable cost, and broad instrument availability, making it potentially applicable for cfDNA analysis in routine laboratories.

The lack of matched plasma–tumor comparisons limits direct validation of cfDNA testing as a surrogate. Even so, previous studies have shown high concordance between plasma- and tissue-based

genotyping in BC (32-34), and plasma–based *PIK3CA* testing is now recognized as a clinically supported option when tumor tissue is unavailable (21). Nonetheless, further validation in prospectively paired plasma–tumor cohorts remains necessary.

In addition, several other limitations should be acknowledged. First, our cohort was recruited from a single tertiary center, and detailed treatment data were not consistently available, which together may not fully capture the genetic diversity among Vietnamese BC patients. Second, the relatively small number of patients with metastatic disease may reduce the robustness of subgroup analyses. Third, potential competing risks, such as treatment crossover or non–cancer-related death, were not accounted for in this analysis and may have influenced time-to-event estimates. Accordingly, the findings should be interpreted with caution as exploratory and hypothesis-generating.

Despite certain limitations, this study provides comprehensive evidence on plasma-detected *PIK3CA* mutations in Vietnamese BC and supports the integration of liquid biopsy into clinical management for mutation profiling, risk stratification, and treatment selection.

5 Conclusion

Our data suggest that *PIK3CA* mutations are frequent in Vietnamese BC patients and show a trend toward prognostic relevance depending on molecular subtypes and mutation variants. Plasma-based detection represents a feasible approach for assessing tumor heterogeneity and may assist in predicting disease progression in the metastatic setting. Future prospective studies are warranted to validate these findings and to explore the predictive utility of *PIK3CA* mutations in guiding personalized therapies.

Data availability statement

The original contributions presented in the study are included in the article/supplementary material. Further inquiries can be directed to the corresponding authors.

Ethics statement

The study was conducted in accordance with the Declaration of Helsinki, and approved by the Medical Ethics Committee of the 108 Military Central Hospital, Ha Noi, Viet Nam (Approval number: 2527/ 21-5-2021). Informed consent was obtained from all subjects involved in the study.

Author contributions

DTT: methodology, software, validation, formal analysis, investigation, resources, data curation, writing—original draft preparation, writing—review and editing, visualization. DVQ: software, visualization, supervision, writing—review and editing. LHS: Conceptualization, resources, project administration, writing—review and editing. NTT: Conceptualization, methodology, validation, formal analysis, investigation, writing—original draft preparation, writing—review and editing, supervision, project administration.

Funding

The authors declare that no financial support was received for the research and/or publication of this article.

Acknowledgments

The authors would like to thank Assoc. Prof. Dr. Ly Tuan Khai, head of the Department of Hematology, Laboratory Center, 108 Military Center Hospital, Hanoi, Vietnam, for providing the blood samples in which ctDNA analysis could be determined. We are grateful to MD. Nguyen Phu Thanh, researcher in the Molecular Department at the Laboratory Center, 108 Military Center Hospital, Hanoi, Vietnam, for technical support.

Conflict of interest

The author(s) declare that the research was conducted in the absence of any commercial or financial relationships that could be construed as a potential conflict of interest.

Generative AI statement

The author(s) declare that no Generative AI was used in the creation of this manuscript

References

1. Bray F, Laversanne M, Sung H, Ferlay J, Siegel RL, Soerjomataram I, Jemal A. Global cancer statistics 2022: GLOBOCAN estimates of incidence and mortality worldwide for 36 cancers in 185 countries. *CA Cancer J Clin.* (2024) 74:229-263. doi: 10.3322/caac.21834.

2. Waks AG, Winer EP. Breast Cancer Treatment: A Review. *JAMA*. (2019) 321:288-300. doi: 10.1001/jama.2018.19323.

3. Miricescu D, Totan A, Stanescu-Spinu II, Badoiu SC, Stefani C, Greabu M. PI3K/AKT/mTOR Signaling Pathway in Breast Cancer: From Molecular Landscape to Clinical Aspects. *Int J Mol Sci*. (2020) 22:173. doi: 10.3390/ijms22010173.

4. Zardavas D, Te Marvelde L, Milne RL, Fumagalli D, Fountzilas G, Kotoula V, et al. Tumor PIK3CA Genotype and Prognosis in Early-Stage Breast Cancer: A Pooled Analysis of Individual Patient Data. *J Clin Oncol*. (2018) 36:981-990. doi: 10.1200/JCO.2017.74.8301.

5. Kalinsky K, Jacks LM, Heguy A, Patil S, Drobnjak M, Bhanot UK, et al. PIK3CA mutation associates with improved outcome in breast cancer. *Clin Cancer Res*. (2009) 15:5049-59. doi: 10.1158/1078-0432.CCR-09-0632.

6. Mosele F, Stefanovska B, Lusque A, Tran Dien A, Garberis I, Droin N, et al. Outcome and molecular landscape of patients with PIK3CA-mutated metastatic breast cancer. *Ann Oncol*. (2020) 31:377-386. doi: 10.1016/j.annonc.2019.11.006.

7. Jensen JD, Knoop A, Laenkholm AV, Grauslund M, Jensen MB, Santoni-Rugiu E, et al. PIK3CA mutations, PTEN, and pHER2 expression and impact on outcome in HER2-positive early-stage breast cancer patients treated with adjuvant chemotherapy and trastuzumab. *Ann Oncol*. (2012) 23:2034-2042. doi: 10.1093/annonc/mdr546.

8. Mangone FR, Bobrovnitchaia IG, Salaorni S, Manuli E, Nagai MA. PIK3CA exon 20 mutations are associated with poor prognosis in breast cancer patients. *Clinics (Sao Paulo).* (2012) 67:1285-90. doi: 10.6061/clinics/2012(11)11.

9. Oshiro C, Kagara N, Naoi Y, Shimoda M, Shimomura A, Maruyama N, et al. PIK3CA mutations in serum DNA are predictive of recurrence in primary breast cancer patients. *Breast Cancer Res Treat*. (2015) 150:299-307. doi: 10.1007/s10549-015-3322-6.

10. Takeshita T, Yamamoto Y, Yamamoto-Ibusuki M, Tomiguchi M, Sueta A, Murakami K, et al. Analysis of *ESR1* and *PIK3CA* mutations in plasma cell-free DNA from ER-positive breast cancer patients. *Oncotarget*. (2017) 8:52142-52155. doi: 10.18632/oncotarget.18479.

11. Jacot W, Dalenc F, Lopez-Crapez E, Chaltiel L, Durigova A, Gros N, et al. PIK3CA mutations early persistence in cell-free tumor DNA as a negative prognostic factor in metastatic breast cancer patients treated with hormonal therapy. *Breast Cancer Res Treat*. (2019) 177:659-667. doi: 10.1007/s10549-019-05349-y.

12. Huang D, Tang L, Yang F, Jin J, Guan X. *PIK3CA*mutations contribute to fulvestrant resistance in ER-positive breast cancer. *Am J Transl Res*. (2019) 11:6055-6065.

13. Stemke-Hale K, Gonzalez-Angulo AM, Lluch A, Neve RM, Kuo WL, Davies M, et al. An integrative genomic and proteomic analysis of PIK3CA, PTEN, and AKT mutations in breast cancer. *Cancer Res*. (2008) 68:6084-91. doi: 10.1158/0008-5472.CAN-07-6854.

14. Loi S, Haibe-Kains B, Majjaj S, Lallemand F, Durbecq V, Larsimont D, et al. PIK3CA mutations associated with gene signature of low mTORC1 signaling and better outcomes in estrogen receptor-positive breast cancer. *Proc Natl Acad Sci U S A*. (2010) 107:10208-13. doi: 10.1073/pnas.0907011107.

15. Allouchery V, Perdrix A, Calbrix C, Berghian A, Lequesne J, Fontanilles M, et al. Circulating PIK3CA mutation detection at diagnosis in non-metastatic inflammatory breast cancer patients. *Sci Rep*. (2021) 11:24041. doi: 10.1038/s41598-021-02643-y.

16. Arthur LM, Turnbull AK, Renshaw L, Keys J, Thomas JS, Wilson TR, et al. Changes in PIK3CA mutation status are not associated with recurrence, metastatic disease or progression in endocrine-treated breast cancer. *Breast Cancer Res Treat*. (2014) 147:211-9. doi: 10.1007/s10549-014-3080-x.

17. André F, Ciruelos E, Rubovszky G, Campone M, Loibl S, Rugo HS, et al. Alpelisib for *PIK3CA*-Mutated, Hormone Receptor-Positive Advanced Breast Cancer. *N Engl J Med*. (2019) 380:1929-1940. doi: 10.1056/NEJMoa1813904.

18. Turner NC, Im SA, Saura C, Juric D, Loibl S, Kalinsky K, et al. Inavolisib-Based Therapy in *PIK3CA*-Mutated Advanced Breast Cancer. *N Engl J Med*. (2024) 391:1584-1596. doi: 10.1056/NEJMoa2404625.

19. Turner NC, Oliveira M, Howell SJ, Dalenc F, Cortes J, Gomez Moreno HL, et al. Capivasertib in Hormone Receptor-Positive Advanced Breast Cancer. *N Engl J Med*. (2023) 388:2058-2070. doi: 10.1056/NEJMoa2214131.

20. Adashek JJ, Janku F, Kurzrock R. Signed in Blood: Circulating Tumor DNA in Cancer Diagnosis, Treatment and Screening. *Cancers (Basel).* (2021) 13:3600. doi: 10.3390/cancers13143600.

21. Gradishar WJ, Moran MS, Abraham J, Abramson V, Aft R, Agnese D, et al. Breast Cancer, Version 3.2024, NCCN Clinical Practice Guidelines in Oncology. *J Natl Compr Canc Netw*. (2024) 22:331-357. doi: 10.6004/jnccn.2024.0035.

22. Thao DT, Thanh NP, Quyen DV, Khai LT, Song LH, Trung NT. Identification of breast cancer-associated PIK3CA H1047R mutation in blood circulation using an asymmetric PCR assay. *PLoS One*. (2024) 19:e0309209. doi: 10.1371/journal.pone.0309209.

23. Eisenhauer EA, Therasse P, Bogaerts J, Schwartz LH, Sargent D, Ford R, et al. New response evaluation criteria in solid tumours: revised RECIST guideline (version 1.1). *Eur J Cancer*. (2009) 45:228-47. doi: 10.1016/j.ejca.2008.10.026.

24. Morlan J, Baker J, Sinicropi D. Mutation detection by real-time PCR: a simple, robust and highly selective method. *PLoS One*. (2009) 4:e4584. doi: 10.1371/journal.pone.0004584.

25. Hammond ME, Hayes DF, Dowsett M, Allred DC, Hagerty KL, Badve S, et al. American Society of Clinical Oncology/College of American Pathologists guideline recommendations for immunohistochemical testing of estrogen and progesterone receptors in breast cancer (unabridged version). *Arch Pathol Lab Med*. (2010) 134:e48-72. doi: 10.5858/134.7.e48.

26. Wolff AC, Hammond ME, Hicks DG, Dowsett M, McShane LM, Allison KH, et al. Recommendations for human epidermal growth factor receptor 2 testing in breast cancer: American Society of Clinical Oncology/College of American Pathologists clinical practice guideline update. *Arch Pathol Lab Med*. (2014) 138:241-56. doi: 10.5858/arpa.2013-0953-SA.

27. Mageau E, Derbowka R, Dickinson N, Lefort N, Kovala AT, Boreham DR, et al. Molecular Mechanisms of Radiation Resistance in Breast Cancer: A Systematic Review of Radiosensitization Strategies. *Curr. Issues Mol. Biol.* (2025) 47: 589. https://doi.org/10.3390/cimb47080589

28. Bernichon E, Vallard A, Wang Q, Attignon V, Pissaloux D, Bachelot T, et al. Genomic alterations and radioresistance in breast cancer: an analysis of the ProfiLER protocol. *Ann Oncol.* (2017) 28:2773-2779. doi: 10.1093/annonc/mdx488.

29. Pérez-Tenorio G, Alkhori L, Olsson B, Waltersson MA, Nordenskjöld B, Rutqvist LE, et al. PIK3CA mutations and PTEN loss correlate with similar prognostic factors and are not mutually exclusive in breast cancer. *Clin Cancer Res*. (2007) 13:3577-84. doi: 10.1158/1078-0432.CCR-06-1609.

30. Barbareschi M, Buttitta F, Felicioni L, Cotrupi S, Barassi F, Del Grammastro M, et al. Different prognostic roles of mutations in the helical and kinase domains of the PIK3CA gene in breast carcinomas. *Clin Cancer Res*. (2007) 13:6064-9. doi: 10.1158/1078-0432.CCR-07-0266.

31. Zhao L, Vogt PK. Helical domain and kinase domain mutations in p110alpha of phosphatidylinositol 3-kinase induce gain of function by different mechanisms. *Proc Natl Acad Sci U S A*. (2008) 105:2652-7. doi: 10.1073/pnas.0712169105.

32. Takeshita T, Yamamoto Y, Yamamoto-Ibusuki M, Tomiguchi M, Sueta A, Murakami K, et al. Comparison of ESR1 Mutations in Tumor Tissue and Matched Plasma Samples from Metastatic Breast Cancer Patients. *Transl Oncol.* (2017) 10:766-771. doi: 10.1016/j.tranon.2017.07.004.

33. Schiavon G, Hrebien S, Garcia-Murillas I, Cutts RJ, Pearson A, Tarazona N, et al. Analysis of ESR1 mutation in circulating tumor DNA demonstrates evolution during therapy for metastatic breast cancer. *Sci Transl Med.* (2015). 7:313ra182. doi: 10.1126/scitranslmed.aac7551.

34. Beaver JA, Jelovac D, Balukrishna S, Cochran R, Croessmann S, Zabransky DJ, et al. Detection of cancer DNA in plasma of patients with early-stage breast cancer. *Clin Cancer Res.* (2014) 20:2643-2650. doi: 10.1158/1078-0432.CCR-13-2933.

Figures

Figure 1. Distribution of plasma-detected *PIK3CA* hotspot mutations (H1047R and E545K) in 196 breast cancer patients. The Venn diagram displays the distribution of *PIK3CA* hotspot mutations (H1047R and E545K) and their overlap, indicating multiple mutant variants in plasma from 196 breast cancer patients.

Figure 2. Distribution of *PIK3CA* mutation profiles and clonality across breast cancer stages. Bar chart shows the distribution of *PIK3CA* hotspot mutations and clonality patterns across clinical stages of breast cancer. EBC: early breast cancer (stage I–II, blue), ABC: advanced breast cancer (stage III, orange), MBC: metastatic breast cancer (stage IV, grey). Mutation subtypes include E545K and H1047R. Clonality status was categorized as monoclonal or polyclonal based on mutation patterns detected.

Figure 3. Subtype-specific association of *PIK3CA* mutations with radiotherapy among HR+ (A) and HER2+ (B) breast cancer. Bar charts depict the distribution of circulating *PIK3CA*, E545K, and H1047R mutations according to radiotherapy exposure, stratified by receptor subtype. (A) In HR+ BC patients, the frequency of *PIK3CA* and E545K mutations was significantly higher in those who received radiotherapy compared to those who did not ($p < 0.05$). (B) Among HER2+ BC patients, *PIK3CA* and H1047R mutations were significantly more common in the radiotherapy group ($p < 0.05$). "*": statistically significant differences ($p < 0.05$).

Figure 4. Distribution of metastatic sites according to plasma-detected *PIK3CA* mutation status. The percentage of patients with metastases to specific organs—including lymph nodes, liver, lung, brain, and bone—is shown for each genetic subgroup: E545K-positive (E545K (+)), H1047R-positive (H1047R (+)), any *PIK3CA* mutation-positive (*PIK3CA* (+)), and wild-type. Notably, E545K mutations were associated with higher rates of lung (85.7%) and bone (100%) metastases, whereas H1047R mutations were more frequently detected in patients with brain metastases (17.4%). Wild-type patients exhibited lower rates of visceral and bone metastases compared to those with *PIK3CA* mutations.

Figure 5. Shorter Progression-Free Survival in metastatic breast cancer patients with circulating *PIK3CA* mutations. Kaplan–Meier survival analysis comparing progression-free survival (PFS) in metastatic breast cancer patients based on plasma *PIK3CA* mutation status. Patients with detectable *PIK3CA* mutations in circulating cell-free DNA (*PIK3CA* Mut, red curve) had significantly shorter PFS compared to those without mutations (*PIK3CA* No_Mut or wild-type, blue curve), log-rank test, $p = 0.022$.

433 **Tables**

434 **Table 1.** *PIK3CA* mutation spectrum stratified by molecular subtypes of breast cancer (n= 196)

Breast cancer subtypes, n(%)	***PIK3CA* (+) 84 (42.9%)**	**E545K (+) 22 (11.2%)**	**H1047R (+) 54 (27.6%)**	**Dual mutations 8 (4.1%)**
HR+/HER2- (n= 62)	28 (45.2%)	12 (19.4%)	17 (27.4%)	1 (1.6%)
HR+/HER2+ (n = 86)	42 (48.8%)	13 (15.1%)	34 (39.5%)	5 (5.8%)
HR-/HER2+ (n= 34)	11 (32.4%)	5 (14.7%)	8 (23.5%)	2 (5.9%)
Triple negative (n=14)	3 (21.4%)	0 (0%)	3 (21.4%)	0 (0%)

435 Abbreviations: *PIK3CA*/E545K/H1047R (+): mutation positive; HER2: human epidermal growth
436 factor receptor-2; HR: hormone receptor.

437

438 **Table 2.** Characteristics of the study population according to circulating *PIK3CA* mutation status

Variables	**Total n = 196 (100%)**	***PIK3CA* mutant status**		**P-value[#]**
		Positive n = 84 (42.9%)	**Negative n = 112 (57.1%)**	
Age ($\bar{X}$±SD, years)	52.43 ± 12.38	50.45 ± 12.46	53.92 ± 12.16	0.052
Disease stages				
I	18 (9.2)	4 (4.8)	14 (12.5)	**0.024**
II	71 (36.2)	24 (28.6)	47 (42.0)	
III	53 (27)	28 (33.3)	25 (22.3)	
IV	54 (27.6)	28 (33.3)	26 (23.2)	
Tumor histology				
Ductal	191 (97.4)	83 (98.8)	109 (96.4)	0.394
Lobular	5 (2.6)	1.0 (1.2)	4 (3.6)	
Grade				
1	12 (6.1)	3.0 (3.6)	9 (8.0)	0.395
2	108 (55.1)	49 (58.3)	59 (52.7)	
3	76 (38.8)	32 (38.1)	44 (39.3)	
Menopausal status				
Post-menopausal	109 (55.6)	41 (48.8)	68 (60.7)	0.111
Recurrence				
Yes	43 (21.9)	24 (28.6)	19 (17.0)	0.052

Variables	Total n = 196 (100%)	*PIK3CA* mutant status		P-value[#]
		Positive n = 84 (42.9%)	Negative n = 112 (57.1%)	
No	153 (78.1)	60 (71.4)	93 (83.0)	
Metastatic disease				
Yes	116 (59.2)	57 (67.9)	59 (52.7)	**0.032**
No	80 (40.8)	27 (32.1)	53 (47.3)	
The number of metastasis lesion				
0	80 (40.8)	27 (32.1)	53 (47.3)	**0.032**
≤ 2	94 (48)	43 (51.2)	51 (45.5)	
≥ 3	22 (11.2)	14 (16.7)	8 (7.1)	
Metastatic sites				
Lymph nodes	104 (53.1)	50 (59.5)	54 (48.2)	0.148
Viscera	34 (17.3)	19 (22.6)	15 (13.4)	0.091
Bone	29 (14.8)	17 (20.2)	12 (10.7)	0.063
Treatment				
Surgical therapy	161 (82.1)	49 (79)	112 (83.6)	0.431
Hormone therapy	98 (50)	43 (51.2)	55 (49.1)	0.885
Chemotherapy	175 (89.3)	78 (92.9)	97 (86.6)	0.243
Radiotherapy	60 (30.6)	34 (40.5)	26 (23.2)	**0.009**

Abbreviations: Statistically significant values ($p < 0.05$) are shown in bold; p-value[#] Mutation versus wild-type; HER2: human epidermal growth factor receptor-2; HR: hormone receptor.

Table 3. Association between *PIK3CA* mutation status and disease progression in the metastatic breast cancer patients (n = 54).

Mutation		Progression		p-value	OR (95%CI)
		Yes	No		
PIK3CA (overall)	MT	22 (78.6%)	6 (21.4%)	**0.028**	3.67 (1.10- 12.0)
	WT	13 (50%)	13 (50%)		
E545K	MT	6 (85.7%)	1 (14.3%)	0.40*	3.72 (0.40 - 33.5)
	WT	29 (61.7%)	18 (38.3%)		
H1047R	MT	18 (78.3%)	5 (21.7%)	0.075	2.96 (0.87 – 10.0)
	WT	17 (54.8%)	14 (45.2%)		

Abbreviations: OR, odds ratio; "*", p-values obtained by Fisher's exact test (two-sided). Statistically significant value ($p < 0.05$) is shown in bold. WT: wild-type, MT: mutation.

Table 4. Univariate and multivariate Cox proportional hazards regression analysis for progression-free survival in the metastatic breast cancer cohort (n = 54)

Variables	Univariate analysis		Multivariate analysis	
	HR (95%CI)	**p-value**	**HR (95%CI)**	**p-value**
PIK3CA mutation (mutant vs. wild-type)	2.16 (1.07 – 4.35)	**0.031**	1.58 (0.73 – 3.43)	0.245
Age (≤ 50 vs. > 50 years)	-	-	0.95 (0.41 – 2.18)	0.895
HER2 status (positive vs. negative)	-	-	0.86 (0.41 – 1.85)	0.709
Metastatic number (< 2 vs. ≥ 2)	-	-	0.55 (0.14 – 2.15)	0.387
Lymph node invasion (Yes vs. No)	-	-	1.58 (0.47 – 5.27)	0.458
Visceral invasion (Yes vs. No)	-	-	3.59 (1.36 – 9.51)	**0.010**
Bone invasion (Yes vs. No)	-	-	1.94 (1.79 – 4.77)	0.150

Abbreviations: HR, hazard ratios; HER2, human epidermal growth factor receptor-2; Statistically significant values ($p < 0.05$) are shown in bold.